Reservoir Simulation of Primary Production in the Zenith Field, Stafford and Reno Counties in Kansas

by

Kent A. Adams III

B.S. Pet. Eng. University of Kansas, 1989

Submitted to the Department of Chemical and Petroleum Engineering and the Faculty of the Graduate School of the University of Kansas in partial fulfillment of the requirements for the degree of Master of Science.

8/22/91
Date Thesis Accepted

Abstract

The Zenith Field is a large reservoir with production coming from four formations, namely 1) Misener Limestone, 2) Misener Sandstone, 3) Maquoketa Dolomite, and 4) Viola Limestone. Initial oil in place was estimated to be 100 million barrels. Recovery from primary production was approximately 20 million barrels, with an additional one million barrels recovered through waterflooding. A large quantity of mobile oil is believed to still exist in the field.

The purpose of this project was to simulate primary recovery in the Zenith Field using a mathematical reservoir model. Limited data were available for the simulation and included formation thicknesses, porosity measurements, a single PVT analysis, four core reports, and production history of the field. The complex geology and fluid flow in the field involved communication between formations, the presence of an aquifer, and indications of natural fractures in the carbonate formations. The long production history and the lack of data also added to the challenge of simulating the behavior of this field.

Grids for each formation were input into the model along with available rock and fluid properties. Where no data were available, correlations were used. The best data were available for the Misener formations, and a match of actual field pressures, water cuts, and field gas-oil ratio was obtained for the initial two years of production from the Misener formations. It was discovered through the simulation that the Maquoketa and Viola contributed to production during these first two years, even though these formations had not been discovered at the time.

A history match of the remaining primary production was not achieved due to the limited amount of data available. Data not available that would have helped in the simulation were more core reports, additional field tests, and production data (pressures, oil, gas, and water) on individual wells. It is recommended from this work that if an attempt to simulate a field as large as the Zenith Field is made in the future, there should be much more data than that which was available for the Zenith Field.

Acknowledgements

The author would like thank Dr. Don Green and Dr. Paul Willhite for their assistance during the course of this study and also Dr. Ken Bishop for his participation as a committee member. The input and assistance provided by Lanny Schoeling is especially appreciated, as is the informal idea exchanges with Gary Gould.

The financial assistance provided by the Tertiary Oil Recovery Project and Phillips Petroleum is greatly appreciated. Thanks goes to Western Atlas' Integrated Technologies for donating the simulator used in this study.

A special thanks goes to Rodney and Giana Reynolds for their hospitality during the final weeks of this project. I would also like to thank Laura Shellady for her patience and understanding during rough times encountered while working on this thesis. This thesis is dedicated to her for her indirect participation in its completion.

Table of Contents

List of Figures

List of Tables

Chapter 1 Introduction

The Zenith Field, located in Stafford and Reno Counties in Kansas, is a large oil field with approximately 100 million stock tank barrels (STB) of original oil in place. Production comes from four major geological formations. In order of increasing depth these formations are, 1) Misener Limestone, 2) Misener Sandstone, 3) Maquoketa Dolomite, and 4) Viola Limestone.

The Zenith Field was discovered in 1937. Oil recovery from primary production totaled approximately 20 MMSTB. Production was commingled between the formations. A water aquifer located on the southern edge of the field provided moderate pressure maintenance during primary production. Proration was placed on the field with wells given an allowable production based on the wells potential to produce. More than 300 wells were drilled into the field during primary production. Many of these were plugged in the late 1940's to early 1950's as the field became uneconomical to produce.

Two attempts to waterflood the reservoir were made. The first was implemented in the mid-1960's. This flood resulted in only 500,000 STB of oil recovery. Another attempt at secondary recovery was made in the mid-1980's. This again resulted in only 500,000 STB of additional oil production. Because of the large amount of initial oil in

place and the poor response from waterfloods, it is believed that a large quantity of mobile oil still exists in the reservoir.

A team of engineers and geologists from the Tertiary Oil Recovery Project and the Kansas Geological Survey at the University of Kansas was formed to perform an in- depth study of the Zenith Field and to make recommendations on ways to produce additional oil from the field. The study was completed with the results presented to the Kansas Corporation Commission in 1991. Included in the report was an extensive geological study of the reservoir, a summary of past production history, a volumetric analysis of all of the reservoirs in the field, and recommendations on potential ways to produce more oil.

The simulation study presented in this thesis was a part of that in-depth study. The objective of this thesis was to utilize data made available from the TORP-KGS study in order to simulate primary production in the Zenith Field. The results from this project will be used in another project to simulate secondary recovery and eventually to aid in making recommendations on where the remaining mobile oil may be located and how to get it out of the ground.

The simulation was to be performed on the University of Kansas' VAX 9000. Western Atlas' Integrated Technologies donated their "VIP" simulator to be used in

this project. It is a three-phase, three-dimensional, black-oil simulator with dual-porosity capability.

Data available for the simulation were limited. Input data included tops and bottoms of formations for every well in the field, approximately fifty gamma ray and porosity logs, four core reports, and several transient tests.

The procedure used to simulate the Zenith Field was to input oil production and then match pressures, water cuts, and field gas-oil ratio. Data available for history matching included contour maps of field pressure, water cuts at six-month intervals, and plots of gas-oil ratio and cumulative water production versus time.

Chapter 2. Literature Review

This chapter will discuss previous work done that is relevant to this study. It includes a discussion of previous studies performed on the Zenith Field and an introduction to dual-porosity simulators.

2.1 Zenith Field Studies

The most current, and probably the most intensive study performed on the Zenith Field, was an investigation performed by a project team of engineers and geologists from the Tertiary Oil Recovery Project and the Kansas Geological Survey at the University of Kansas. The results were published in a report submitted to the Kansas Corporation Commission. (TORP-KGS, 1991) The purpose of the study was to gather all available data on the Zenith Field and evaluate it in order to make recommendations on how to get additional oil recovery from the field. The study included a detailed geological analysis of the field, along with an analysis of production history and the current operating status of the field. Much of the data used in this simulation came from the results of that study.

Several waterflood feasibility studies have been performed on the Zenith Field. The first was performed by

G. L. Yates and Associates in 1965. Another was performed by Questa Engineering Corporation in 1984 with an update presented in 1986. Both reports recommend that the field should be waterflooded. They both predict an additional five to six million barrels of oil recovery through implementation of a waterflood. In actuality, the waterflood started after Yates' 1965 report only produced 500,000 STB of oil and the waterflood initiated after Questa's 1984 report only produced another 500,000 STB of oil. Because waterflood response was so poor along with a volumetric study that indicates an initial oil in place of around 100 MMSTB, (Schoeling, 1990) a substantial amount of mobile oil is believed to be present. This simulation study was the initial phase of a study aimed at modeling primary and secondary recovery in the Zenith Field. The simulations are to be used in an attempt to discover where remaining oil is located and to determine the best possible ways to get it out of the ground.

The earliest engineering study was performed by an engineering committee established by the Kansas Corporation Commission in 1942. This report was found in a barn just outside of the town of Zenith, Kansas. Much of the writing has been rendered illegible from years of weathering and mouse infestation. However, most of the data used when history matching this field was found in that report. This data includes production history plots, contour maps of

water cuts at six-month intervals, and contour maps of field pressures at six-month intervals. This report also contained the PVT data that were available for use in the simulation.

2.2 Dual-Porosity Simulators

As will be discussed, it is believed that the Viola Limestone is fractured. Because of this, a literature search was conducted to determine how to simulate formations that are naturally fractured. This search turned up the use of dual-porosity simulators.

Dual-porosity simulators model fluid flow in fractures. The key paper that most simulators are based on was presented by Warren and Root. (1963) The technique they introduced involves dividing simulator grid blocks into smaller matrix blocks which are modeled by finite difference formulations. These matrix blocks are then surrounded by fractures. Fluid flows through the fractures and the matrix blocks act as source or sink terms to the fractures.

The simulator used in this study uses the technique of Gilman and Kazemi (1983) to model fluid flow in a fractured reservoir. Their technique not only allows dual-porosity modeling, but also has a dual-porosity/dual-permeability option. This means that fluid flow is occurring in both

the matrix and the fracture. According to the VIP Manual, a dual-porosity/dual-permeability simulator is required if part of the reservoir is fractured and another part is not.

A paper was found comparing the results of the simulation of a naturally fractured reservoir with an ordinary single porosity simulator, a simulator with dual-porosity capability, and a simulator with dual-porosity/dual-permeability capability. (Dean et. al., 1988) The authors report that dual-porosity and dual-porosity/dual-permeability simulators give similar results when modeling primary depletion. They report that trying to model a fractured reservoir with a single porosity simulator will lead to erroneous results. They also indicate that the dual-porosity/dual-permeability simulator is much more computationally intensive than the dual-porosity simulator. Therefore, in modeling primary depletion one should use a dual-porosity simulator whenever possible. Because some of the formations in the Zenith Field are fractured while others are not, a dual-porosity/dual-permeability simulator had to be used.

Chapter 3 Zenith Field Geology

An intensive geological study was performed on the Zenith Field. (KGS & TORP, 1991) This chapter provides a summary of this study with emphasis on geologic properties of the reservoir that affect fluid flow and reservoir performance.

3.1 Introduction

The Zenith Field, located in Stafford and Reno Counties in Kansas, is a complex reservoir with oil production from four major producing formations. These formations are, in order of increasing depth, Misener Limestone, Lower Misener Sandstone, Maquoketa Dolomite, and Viola Limestone Pay 1. Another porous interval in the Viola Limestone may have had some original oil. However, through simulation studies that will be discussed later, it is believed that the Viola Limestone Pay 2 contributed very little to oil production in the field. The reservoir covers approximately sixteen square miles and is estimated to have an initial oil in place of approximately 100 MMSTB. (Schoeling, 1990)

3.2 Regional and Local Geology

The Zenith Field is part of the Zenith - Peace Creek reservoir system, lying to the southwest of the Peace Creek Field. The relationship between the two fields can be seen in Figure 3.1. A barrier is believed to exist between the two fields prohibiting fluid flow between them. The fields lie on the southwestern plunging anticlinal fold off the Central Kansas Uplift. (TORP-KGS, 1991)

The Zenith Field is classified as a stratigraphic trap. To the north, lower Paleozoic carbonates and sandstones pinch out unconformably under impermeable shales and conglomerates. (Imbt, 1941) To the east the reservoir terminates against the down-thrown side of a vertical fault that runs north-northeast to south-southwest. (Berendsen and Blair, 1986) The westward limits of the field are due to a stratigraphic pinch-out or a reduction in porosity/permeability of the reservoir units. (TORP-KGS, 1991)

3.3 Reservoir Geology

The Zenith Field is composed of four major producing formations with another formation, the Viola Limestone Pay 2, believed to contribute only slightly to oil production in the field. In order of increasing depth these

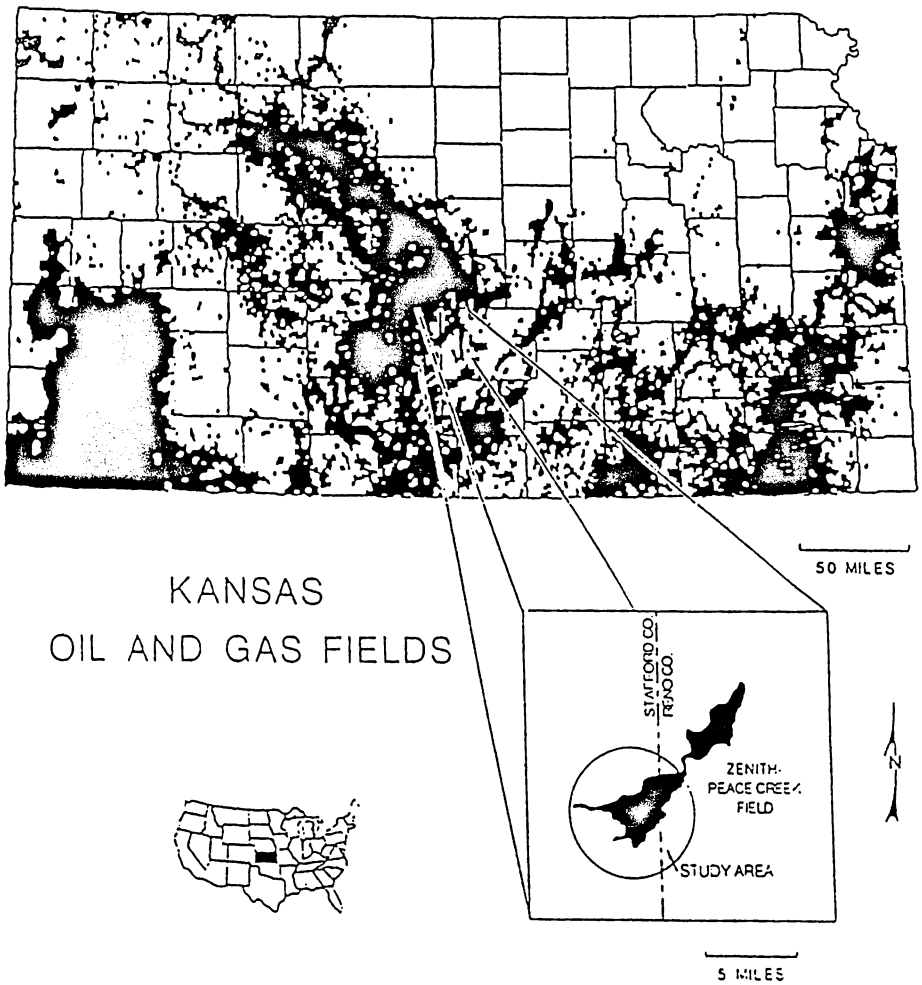

Figure 3.1 Location of the Zenith Field in Kansas and its Relationship with the Peace Creek Field. (TORP-KGS, 1991)

formations are 1) Misener Limestone, 2) Lower Misener Sandstone, 3) Maquoketa Dolomite, 4) Viola Limestone Pay 1, and 5) Viola Limestone Pay 2. The relationship between the layers is shown in Figure 3.2. A labeled type log showing typical log response of each layer is shown in Figure 3.3. These reservoirs are lower to middle Ordovician. There is an Upper Misener Sandstone, but it is of limited extent in the Zenith Field and does not contain a substantial amount of oil. There is also a Viola Limestone Pay 3. Most of it is below the water-oil contact, so it had a negligible amount of original oil in place. The water-oil contact is believed to be at -2019 feet sub-sea over most of the field.

3.3.1 Viola Limestone Pay 1 and 2

The entire Viola Limestone interval averages 115 feet thick. The main reservoir body in the Viola section is the Viola Limestone Pay 1. The Viola Limestone Pay 2 is believed to have some initial oil present. However, through simulation studies that will be discussed in a subsequent chapter, the Viola Limestone Pay 2 is felt to have contributed very little to total field production. It is not included in the model and is only mentioned here for completeness of the geological description. A third porous interval lies below the water-oil contact and will not be

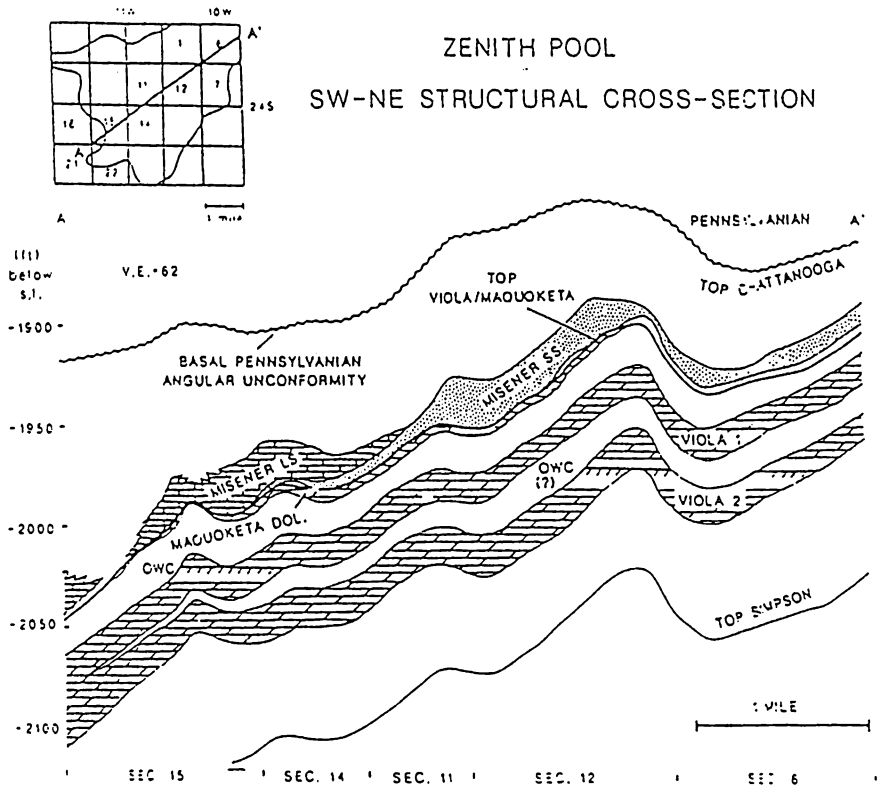

Figure 3.2 Southwest-Northeast Cross-Section of Zenith Field Showing Relationship Between Formations. (TORP-KGS, 1991)

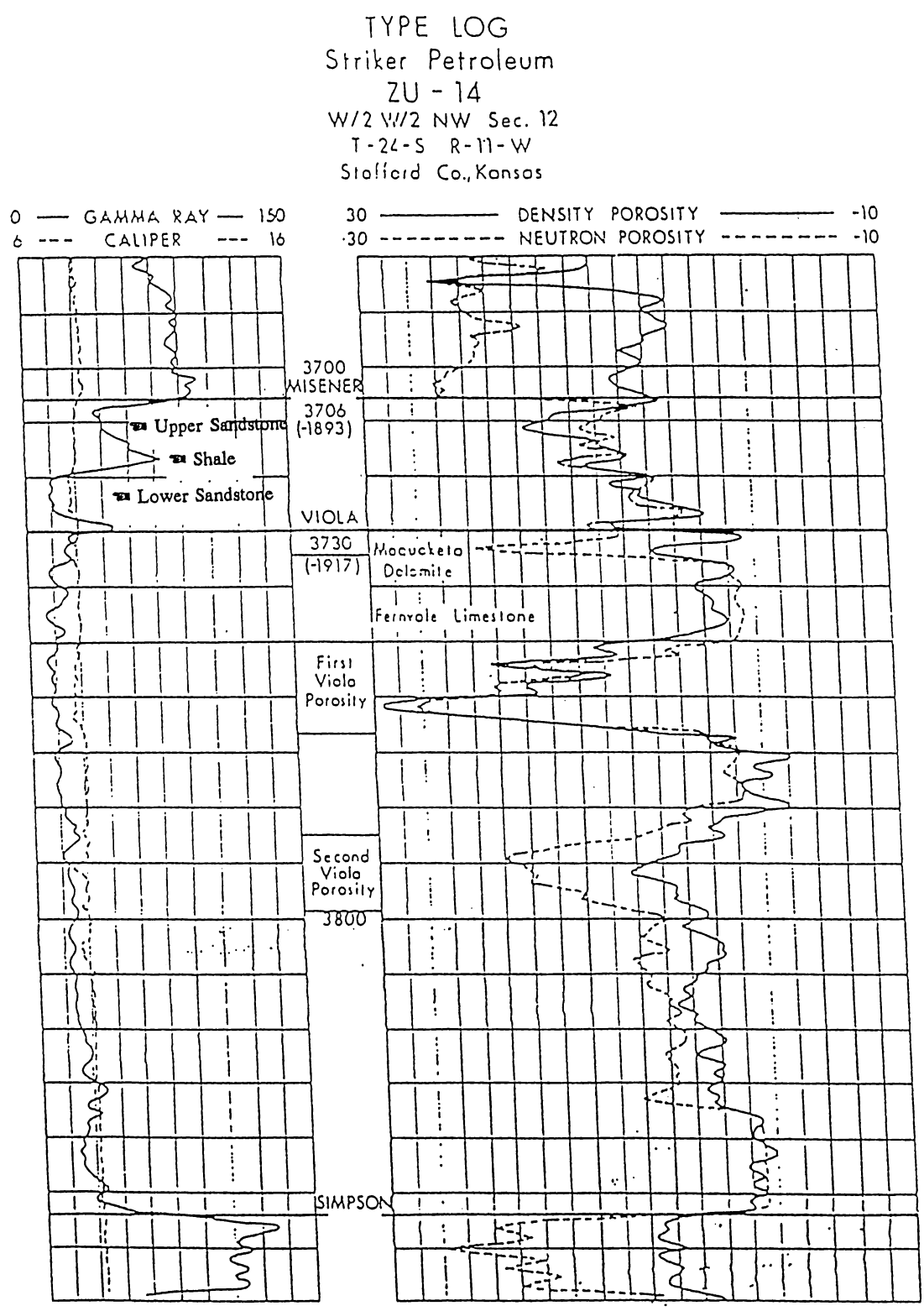

Figure 3.3 Typical Log Response for Formations in the Zenith Field. (TORP-KGS, 1991)

discussed further. Dense, impermeable limestone lies above the first Viola pay zone and separates the other porous intervals.

The two Viola Pay intervals have good thickness consistency as shown in the gross thickness maps presented in Figures 3.4 and 3.5. Viola Pay 1 varies between eleven and twenty-six feet. The thickness of Viola Pay 2 ranges between thirteen and twenty-three feet. The porosity of the pay zones is mainly secondary consisting of vuggy, intercrystalline, and moldic porosity. Average porosity of Viola Pay 1 is 10.8 percent and for Viola Pay 2 is 10.6 percent. (Schoeling, 1990)

Four core reports were available on wells in the Zenith Field. These reports are summarized in Appendix I. The location of the wells that were cored is shown in Figure 3.6. These analyses report that the matrix permeability of the Viola Limestone was typically less than 10 millidarcies. References to vertical fractures in the Viola Limestone are indicated to some degree in all of the cores for which analysis was available. The permeability of the plugs that contain vertical fractures is typically greater than 50 millidarcies. A fractured core plug from ZU-3 was reported to have a permeability of 3,000 millidarcies.

Initial production potentials of wells drilled into the Viola interval varied from less than 300 STB/day in

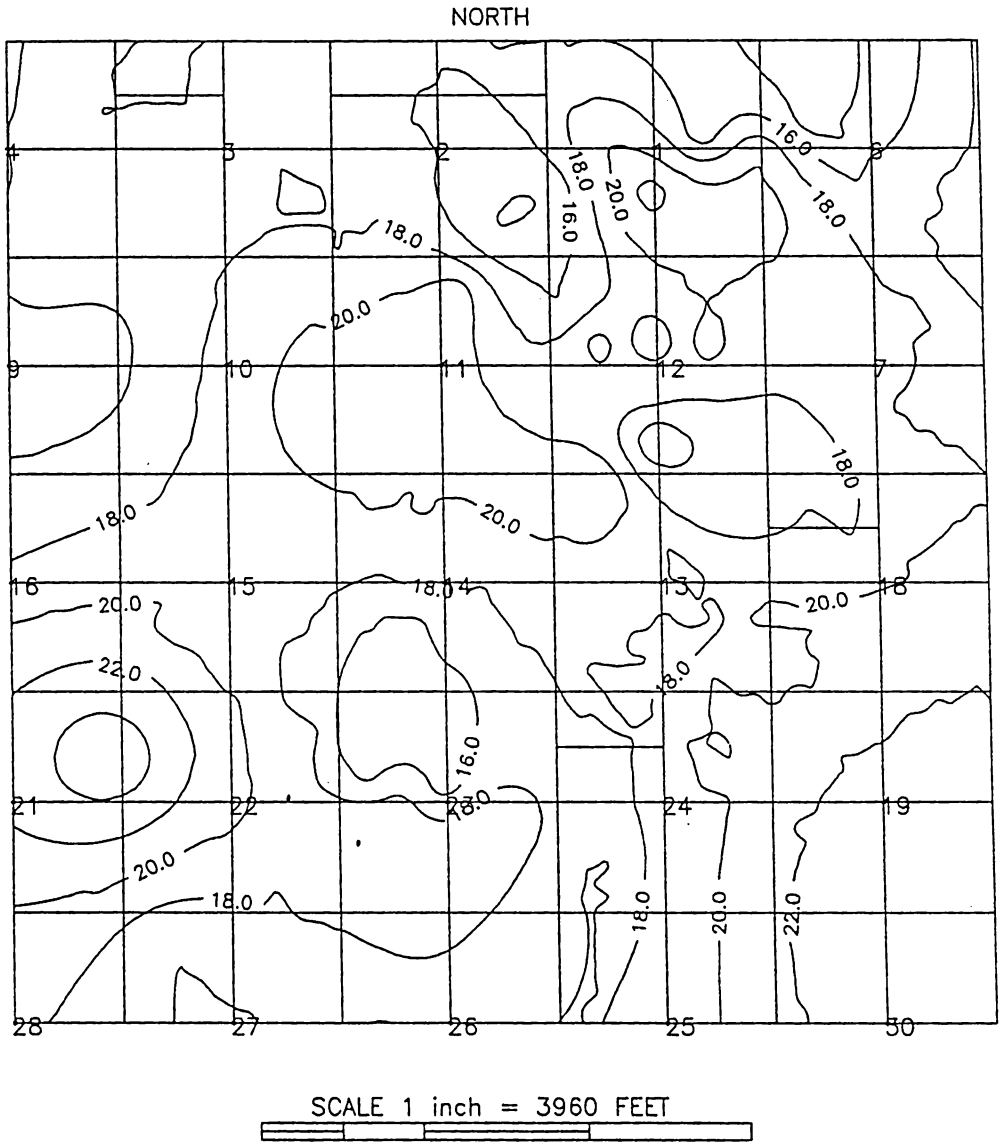

Figure 3.4 Gross Thickness Map of Viola Limestone Pay 2.

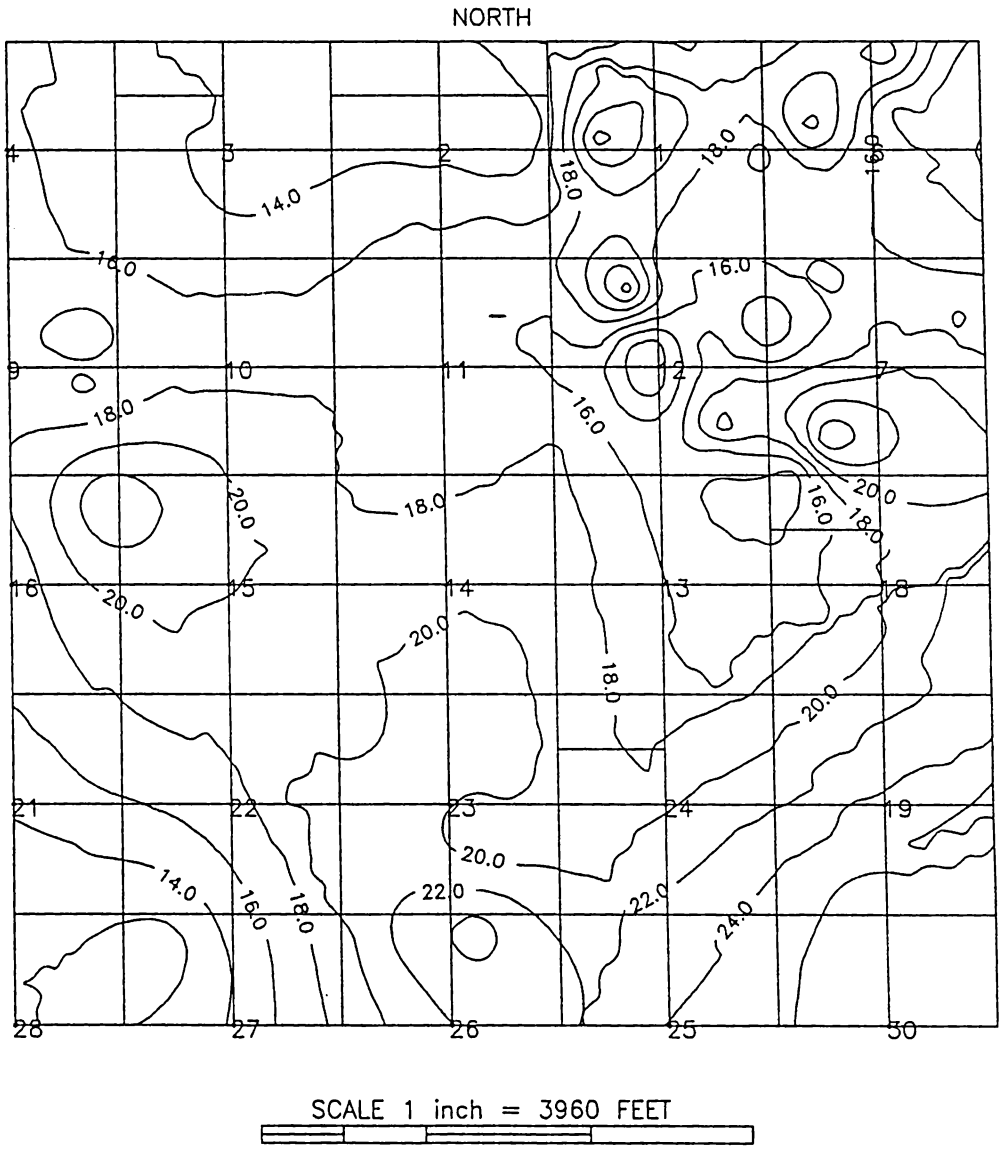

Figure 3.5 Gross Thickness Map of Viola Limestone Pay 1.

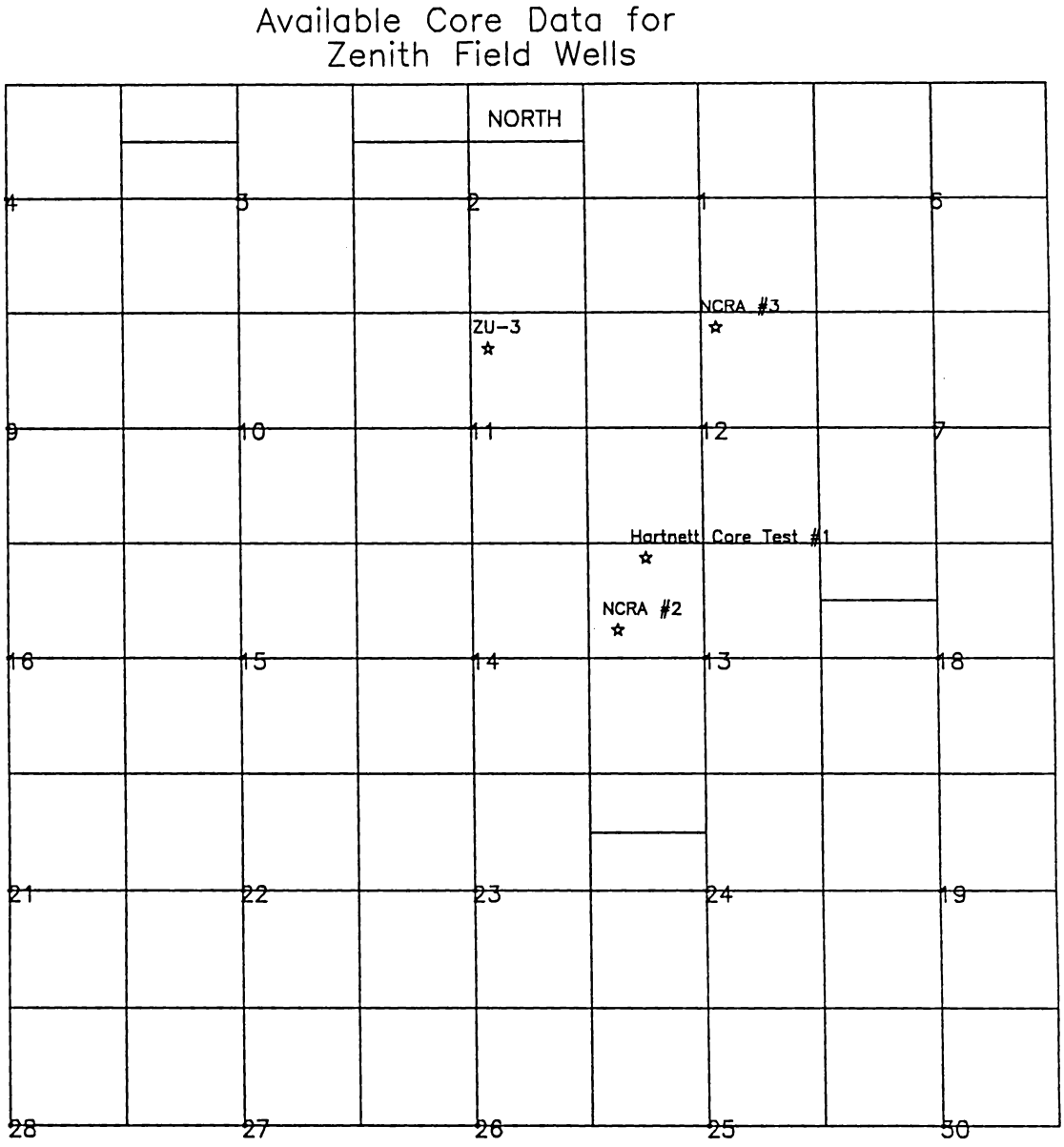

Figure 3.6 Location of Wells in the Zenith Field With Core Analyses Available

some areas of the field to more than 30,000 STB/day in other areas. Initial potentials as high as some that were reported would not be possible for a reservoir with the low matrix permeabilities reported in the core analyses. The high initial potentials in parts of the field and the reference to vertical fractures in the core reports leads one to conclude the Viola Limestone is naturally fractured in certain areas.

The upper fifteen to twenty feet of the Viola interval consists of a dense limestone named the Fernvale member. Analysis of cores and logs indicates that the Fernvale is impermeable and has little porosity. It is therefore not considered to be a reservoir rock. The Fernvale may provide a communication barrier between the upper Viola pay zone and the reservoirs overlying the Viola. It is possible that the Fernvale may be fractured and therefore fluid communication may be possible from the Viola Limestone Pay 1.

The two Viola pay intervals are separated by approximately fifteen feet of dense limestone similar to the Fernvale. This dense limestone thins westward to a pinch-out where Viola Pay 1 and Viola Pay 2 lie in direct contact with one another.

3.3.2 Maquoketa Dolomite

The Maquoketa is an Ordovician aged dolomitic limestone and dolomite. It lies over the Fernvale member of the Viola Limestone in the north-central part of the field. An isopach map is shown in Figure 3.7. The Maquoketa Dolomite is made up of two lobes, the larger being in the central portion of the field with a thickness of up to seventeen feet. The smaller lobe is only a few feet thick and is located in Section 24. Data suggest that the Maquoketa is extremely vuggy with a average porosity of 8.3%. It is in direct contact with the Fernvale below and in some areas with the Misener Sandstone above. Again, if the Fernvale is fractured, this could be a path for fluid movement between the Viola and Misener Formations.

3.3.3 Misener Sandstone

The Misener Sandstone is a major reservoir unit present over the eastern half of the Zenith Field. Figure 3.8 shows an isopach map for the entire Misener Sandstone interval estimated from driller's logs. It is a Mississippian-Devonian aged sandstone with a maximum thickness of 32 feet. In general, the Misener Sandstone is thicker in the southern part of the field, and the east edge thins less abruptly than the western edge. The

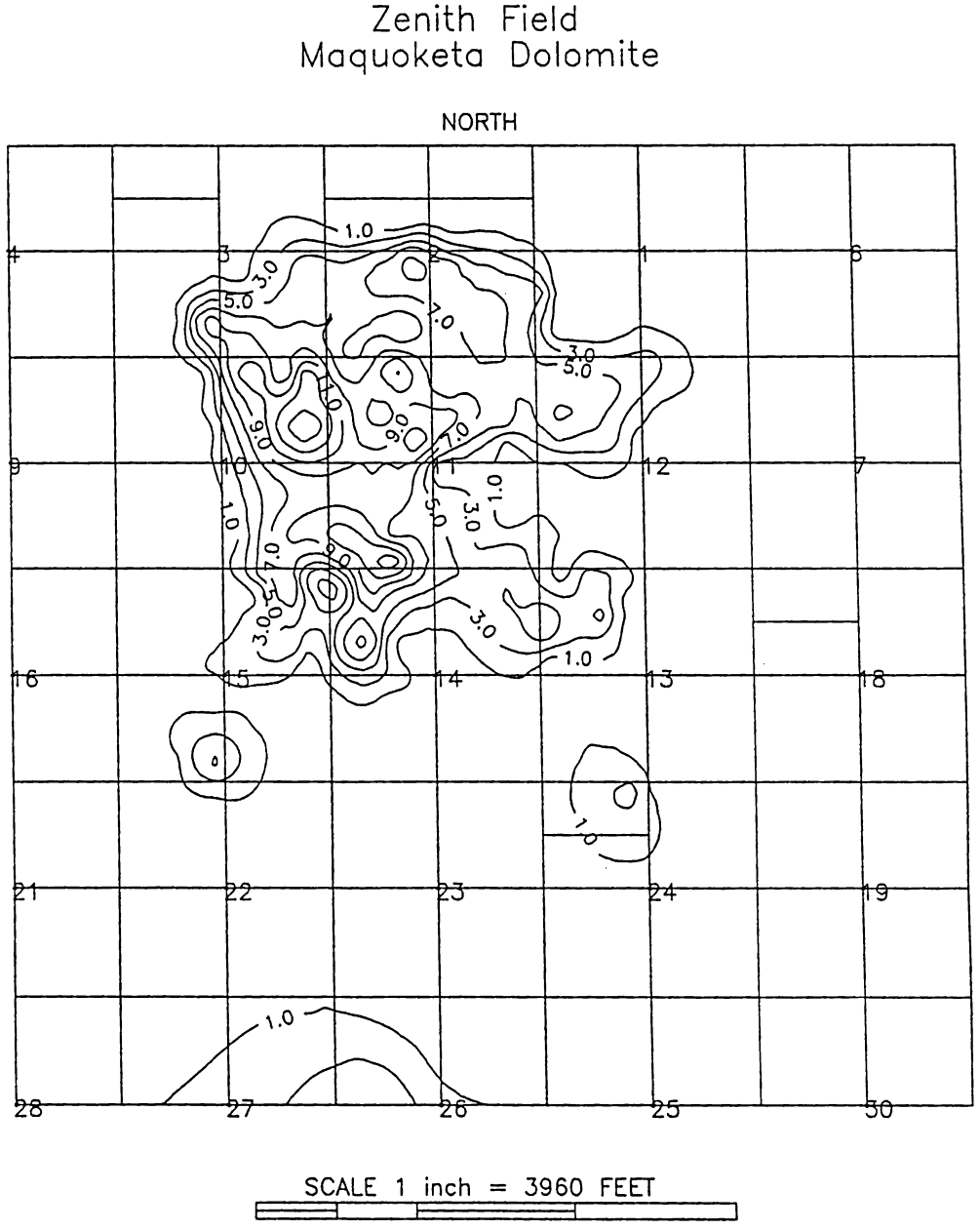

Figure 3.7 Gross-Thickness Map of Maquoketa Dolomite

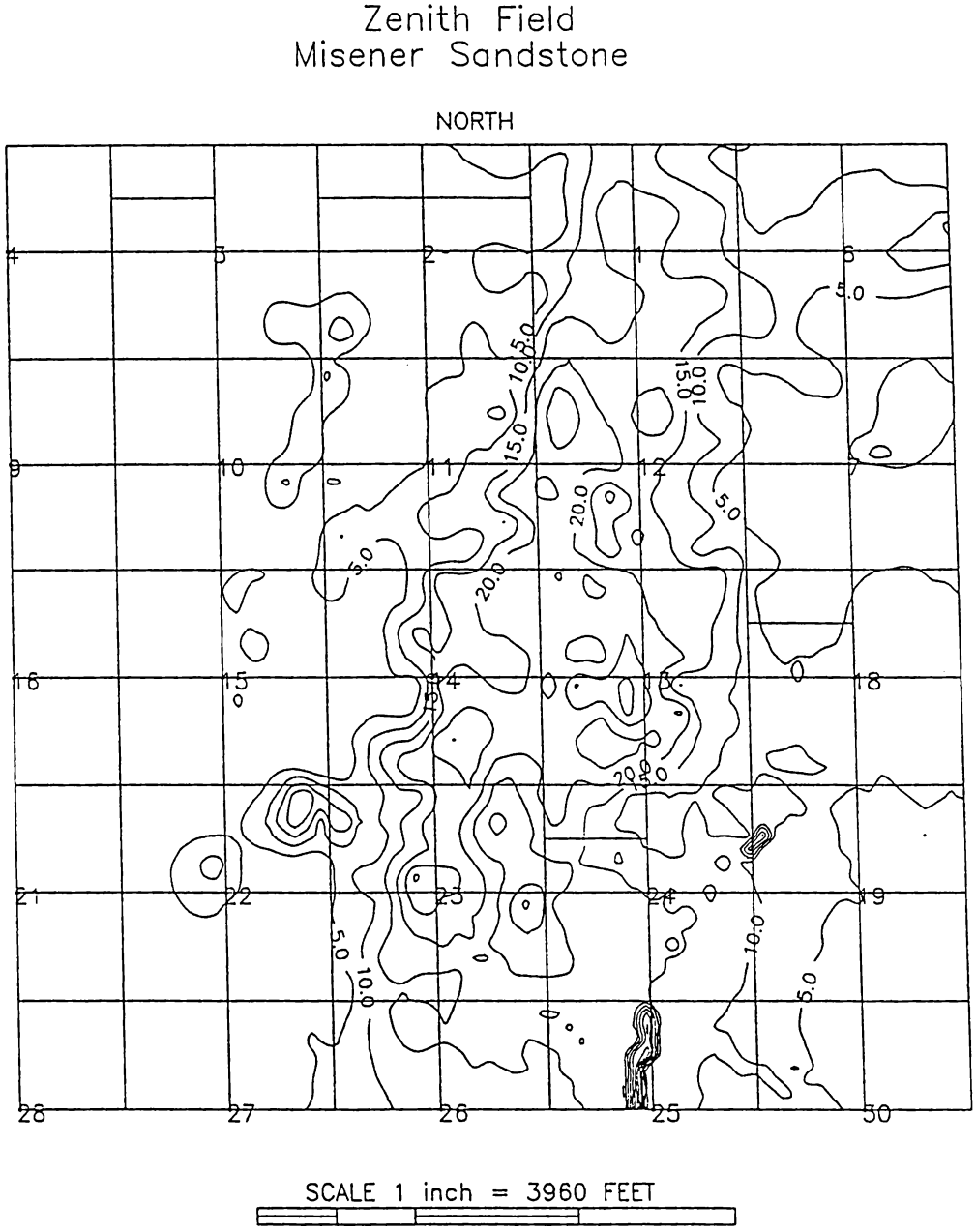

Figure 3.8 Gross-Thickness Map of Misener Sandstone Interval Obtained from Driller's Logs

sandstone is medium to coarse grained, with local conglomerate development at the base of the interval. The average porosity of the Misener Sandstone is 10.9 percent.

There are three distinct zones present in the Misener Sandstone which are important to fluid movement. These consist of an upper sandstone zone (layer 1), a middle shaly member, and a lower sandstone zone (layer 2). The zones were discovered upon the analysis of a core report from the NCRA Core Hole #2. (See Appendix I) This core report indicates that a very shaly sand is present in the middle of the Misener section. This interval had a permeability of less than 2 millidarcies. The core was then correlated with log data, and the distinct beds were found to be distinguishable on a gamma-ray log. Figure 3.3 shows the distinction between the zones for ZU-14. (The location of ZU-14 can be found on the map of current wells in the field in Figure 5.3.) The remainder of the logs that were available in the Zenith Field were analyzed, and the Misener Sandstone zones were mapped. These maps are located in Figures 3.9 through 3.11.

As the type log shows, the lower sandstone bed has a lower gamma ray reading, which indicates that it is less shaly than the upper sandstone bed. The lower sandstone bed is thought to be coarser grained and better sorted than the upper bed. For these reasons, it is believed that the lower bed of the Misener Sandstone is a better quality

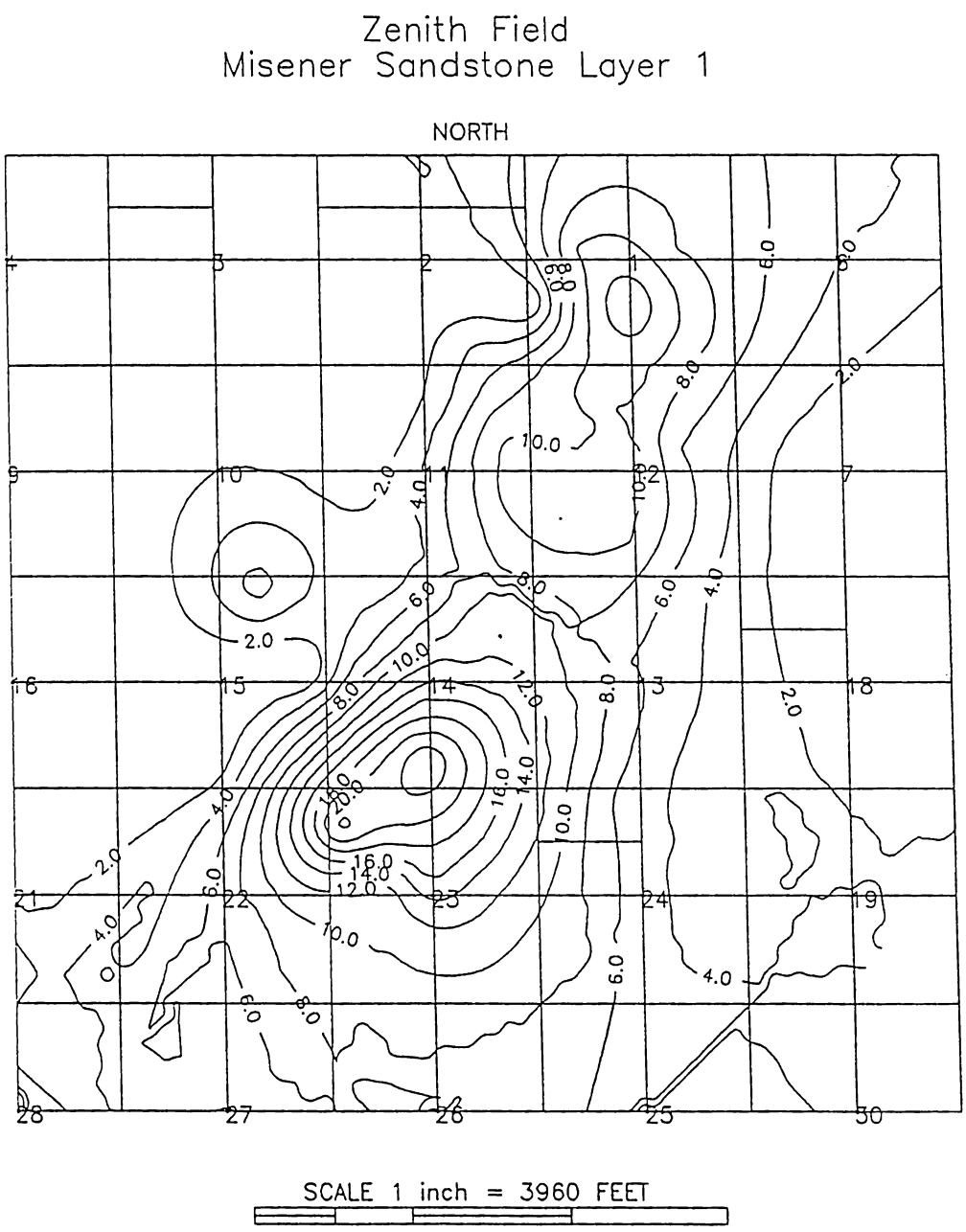

Figure 3.9 Gross-Thickness Map of Upper Misener Sandstone Interval Obtained from Electric Logs

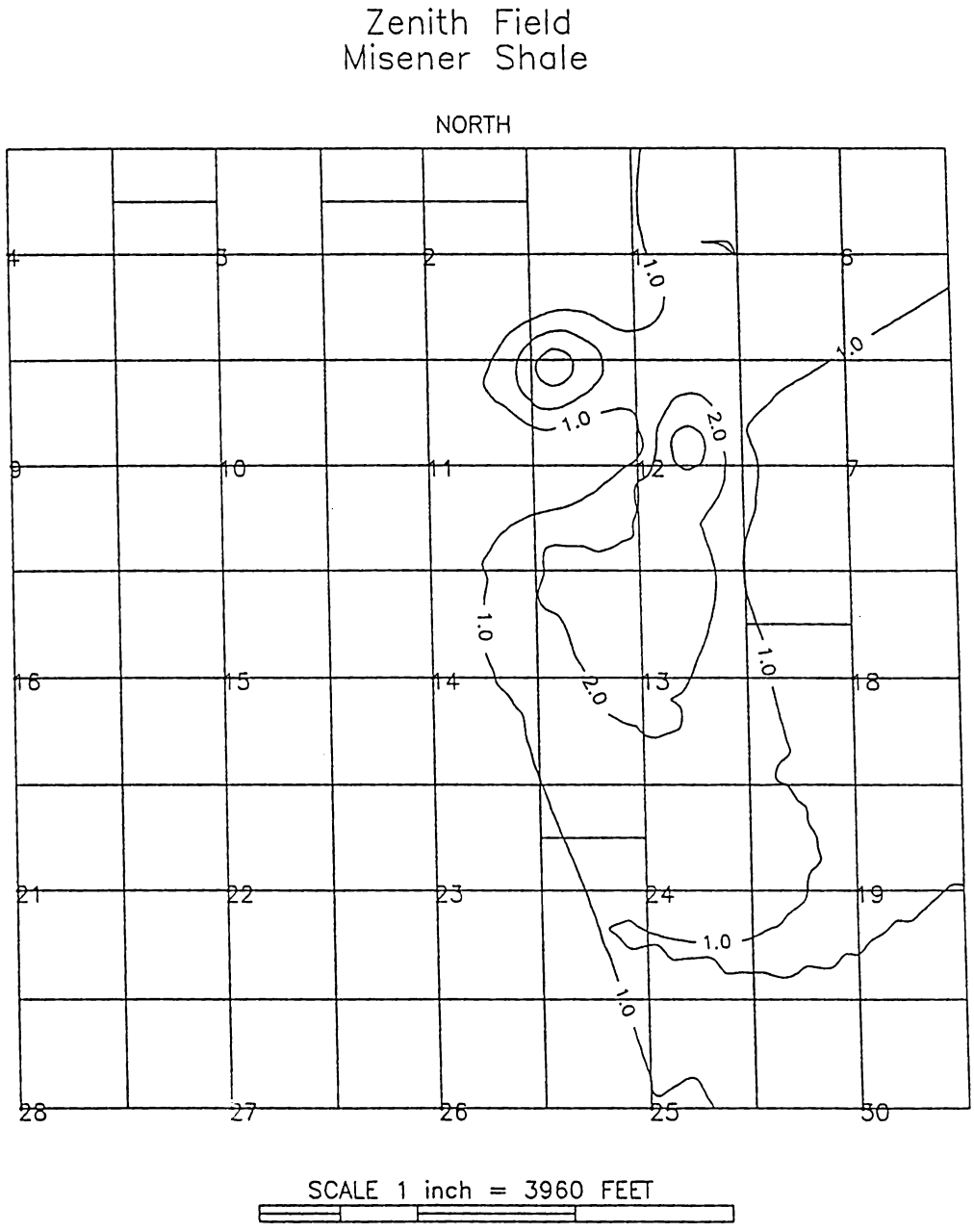

Figure 3.10 Gross-Thickness Map of Misener Shale, Obtained from Electric Logs

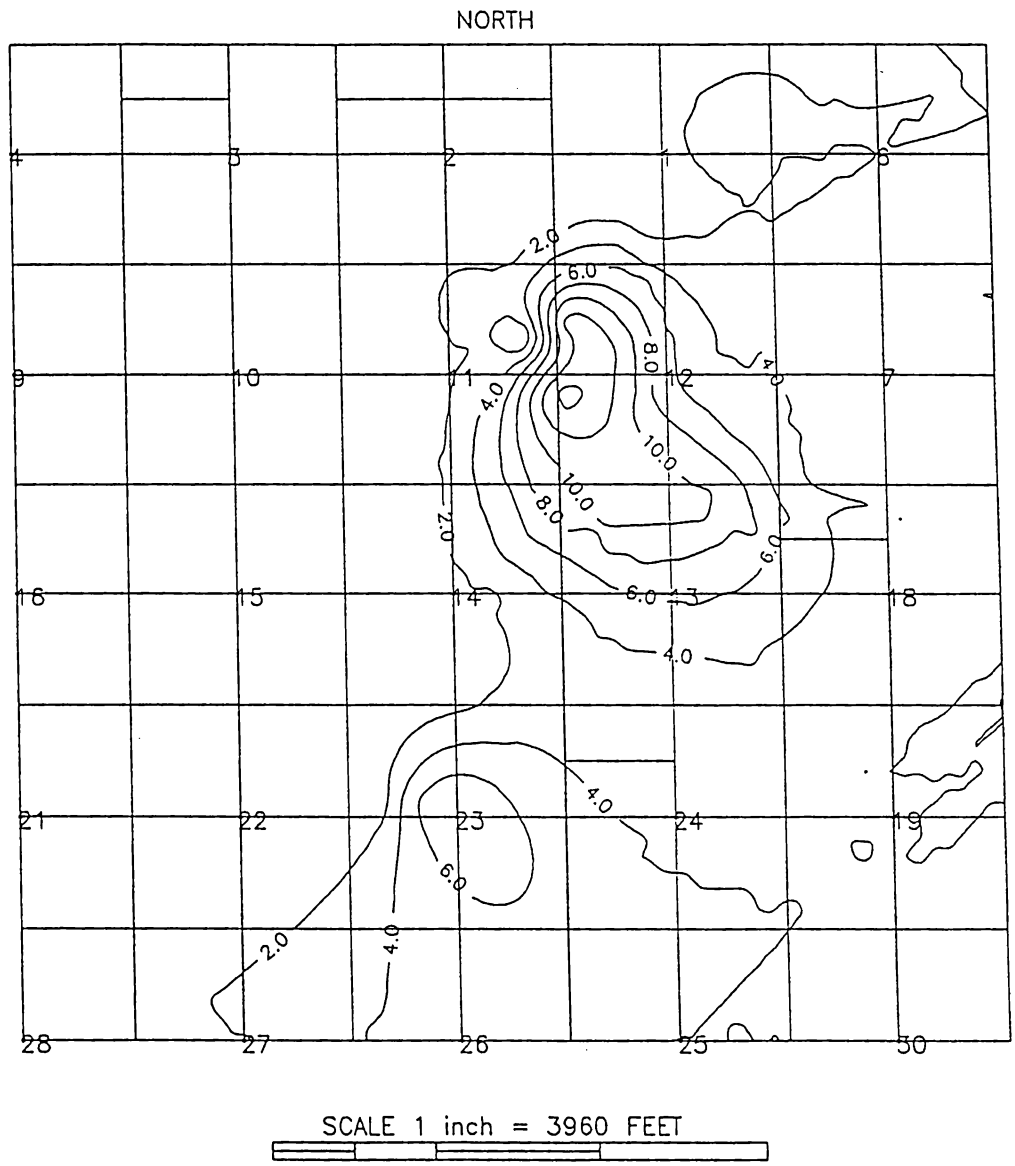

Figure 3.11 Gross-Thickness Map of Lower Misener Sandstone Interval Obtained from Electric Logs

reservoir rock than the upper bed. Well tests performed on the Zenith Field indicate that the lower bed has a permeability on the order of 150 to 300 millidarcies, while the upper bed has a permeability of around 50 millidarcies.

By analyzing porosity logs in the Zenith Field, it was found that no significant difference was found in the porosity of the two sandstone beds. In some instances the porosity of the lower sandstone bed was higher than the porosity of the upper sandstone bed. In others, this trend was reversed. The type log shown indicates that the lower bed is less porous than the upper sandstone bed in the area of ZU-14. The lack of distinction in porosity between the beds is further substantiated in the plot of core permeability versus core porosity for the Misener Sandstone shown in Figure 3.12. It is clear from this figure that the lower sandstone bed has a larger permeability than the upper sandstone bed. However, the figure indicates that there is no substantial difference in porosity between the two beds.

The middle spike in the gamma ray log is believed to be a shale or a very shaly sandstone separating the upper and lower beds. This shale was only detected in the eastern portion of the field. However, because of the limitation a gamma ray log has in distinguishing beds less than one foot thick, the shale may be present over more of the field and may act as a barrier to fluid movement

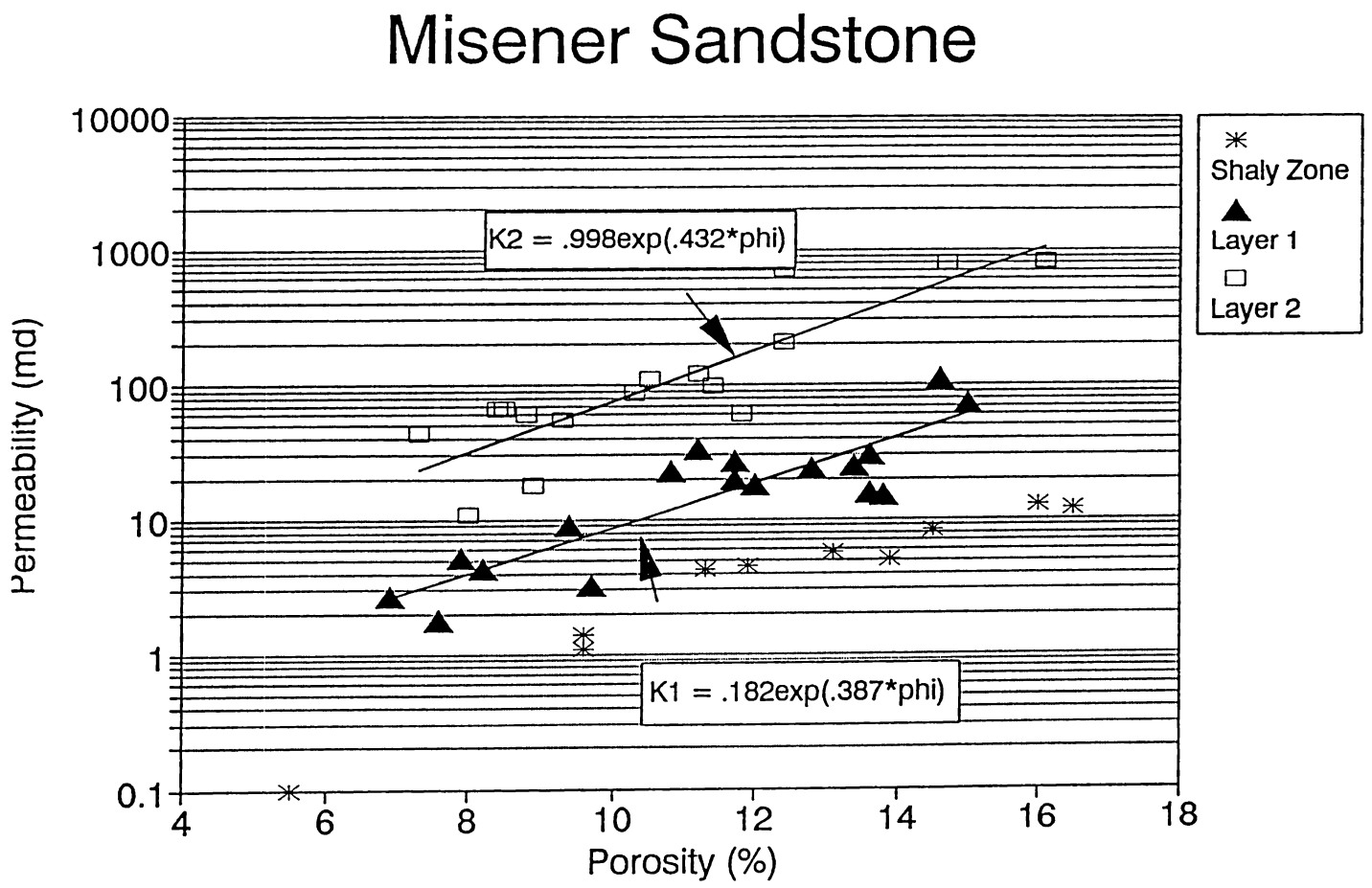

Figure 3.12 Plot of Permeability Versus Porosity for the Misener Sandstone

between the upper and lower beds of the Misener Sandstone.

Aerially, the upper sandstone bed thins to the east where only the lower sandstone bed is present. Likewise the lower bed thins to the west where the upper bed is the only member present. The lower sandstone bed is in direct communication with the Maquoketa Dolomite and Fernvale in the central to southern part of the field, which may allow communication between these reservoir units.

3.3.4 Misener Limestone

The Misener Limestone overlies the Misener Sandstone in the central portion of the field as shown in the gross thickness map presented in Figure 3.13. It has a maximum thickness of 40 feet and an average porosity of 11.3 percent. The Misener Limestone thins toward the center of the field to where it overlies the Misener Sandstone in section eleven and the west half of section fourteen.

The lithology of the Misener Limestone is carbonate, chert and in rare cases shale. In the western edge of the limestone, chert is very abundant. The chert disappears to the east where there is only limestone present. The chert combined with the limestone makes a better reservoir rock than does limestone alone. The porosity in the western edge of the formation is believed to be higher than in the eastern edge.

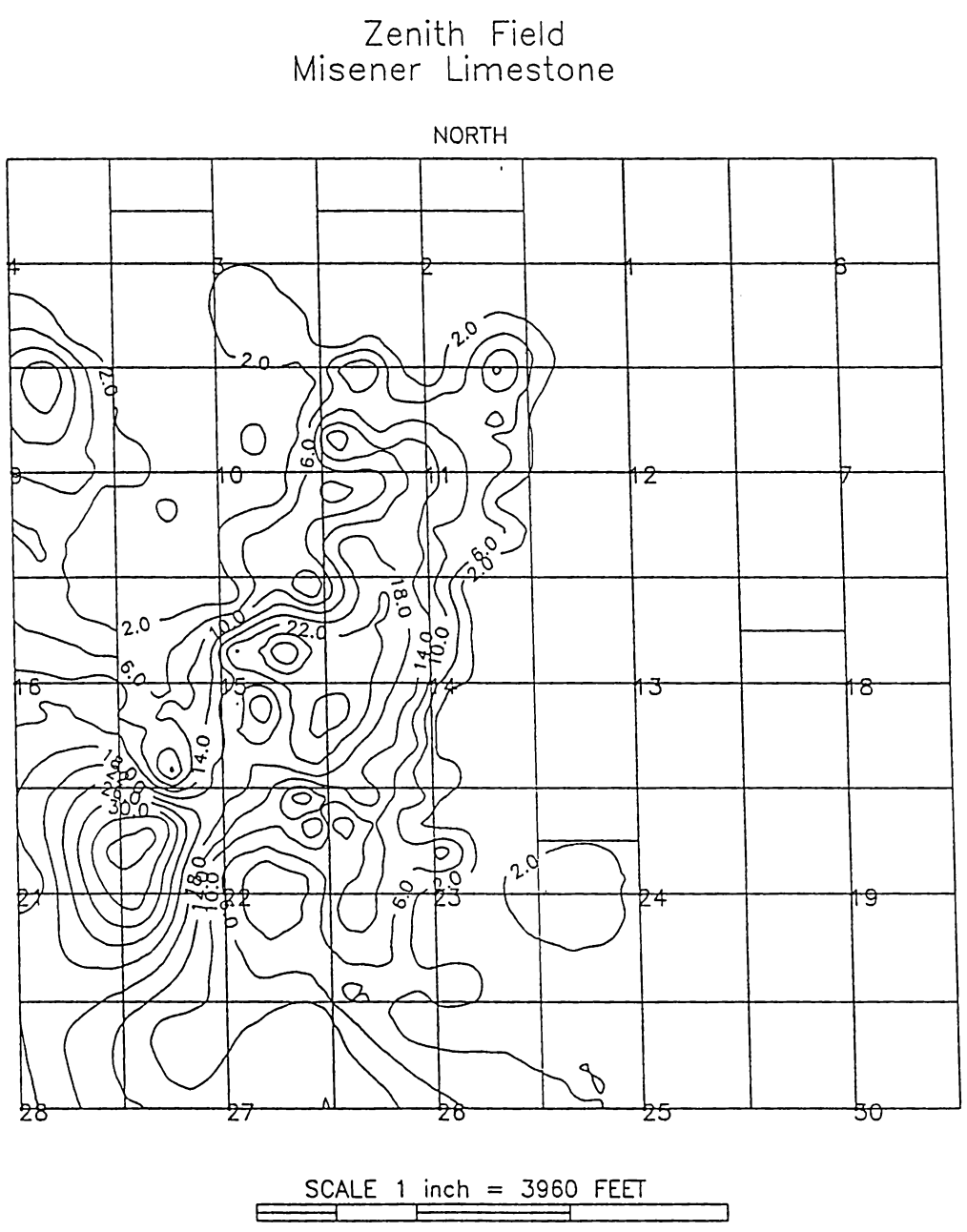

Figure 3.13 Gross-Thickness Map of Misener Limestone

Communication between the Misener Limestone and the Misener Sandstone is likely where the limestone overlays the sandstone. There are also localized areas where the limestone is in direct communication with Maquoketa Dolomite or the Fernvale.

Chapter 4 Production History of the Zenith Field

This chapter will describe the history of primary production in the Zenith Field. It will begin with a description of the field's discovery, completion techniques and development. Primary production characteristics will be presented next with an emphasis on oil, gas and water production relevant to the simulation study performed.

4.1 Discovery and Development

The Zenith Field was discovered in September, 1937 with a completion in the Misener Sandstone in NW-NW-SE Sec. 23-T24S-R11W of Stafford County, Kansas. Development of the Misener Sandstone occurred rapidly on ten to twenty acre tracts. Approximately 300 oil wells were drilled during primary production. The field was placed on proration with each well given an allowable production based on the well's potential to produce. When the Viola Limestone was discovered, many of the previously drilled wells were deepened to increase their allowable.

Initial completion of the wells was done by rotary drilling to the top of the pay zone followed by setting of production casing. The holes were then completed open-hole by deepening the well through the pay zone with cable tools. Early in production, most of the wells were completed with 7 inch production casing, while in later

stages of development, 5 1/2 inch production casing was used.

Initially, the wells were produced naturally without stimulation. Later, in an attempt to gain a higher allowable, large quantities of acid were used to stimulate the wells.

4.2 Primary Production History

During primary production, the Zenith Field produced over 19 million barrels of 42 degree API gravity oil. (Yates, 1965) Maximum daily production occurred in 1942 when the field was making in excess of 10,000 STB/day. The largest yearly production also occurred during 1942 when more than three million barrels of oil were produced. Table 4.1 shows the distribution of the original oil in place calculated from a volumetric study of the Zenith Field. (Schoeling, 1990)

The principal source of reservoir energy during primary production was solution-gas drive. Initial pressure of the field was 1300 psi at a sub-sea datum of -1900 feet. The bubble point of the oil was 1100 psi with an initial gas in solution of approximately 345 SCF/STB.

A producing gas/oil ratio (GOR) limit of 1,000 SCF/STB was placed on the field in 1941 by the Kansas Corporation Commission in order to minimize gas-cap production and preserve reservoir energy. It was believed the gas was

Table 4.1 Original Oil in Place of the Zenith Field

Formation	OOIP (MMSTB)
Misener Limestone	25.06
Misener Sandstone	34.11
Maquoketa Dolomite	5.82
Viola Limestone Pay 1	40.05
Total	105.04

migrating north while the oil migrated south. This clearly was an advantage to oil producers in the center of the field, and the limiting GOR was raised to 2,000 SCF/STB in 1943. In April, 1946, oil and gas proration was dropped due to declining production.

A limited water aquifer is located on the south edge of the field, providing some pressure maintenance. Water encroachment is shown in "iso-water cut" maps constructed by an engineering committee formed by the Kansas Corporation Commission in 1942. (see Appendix II) These maps represent the water cut in the Zenith Field at approximately six-month intervals. The maps for July 1939 and January 1940 show water cuts before the Viola was discovered and therefore indicate water encroachment into the Misener Sandstone.

Iso-baric maps were also constructed by the engineering committee in 1942 and are given in six-month intervals. (see Appendix II) The maps show that initially

pressure decline was greatest in the southeast and decreased to the northwest. However, later in primary production, the trend reverses due to pressure maintenance provided by the water aquifer, and an increased withdrawal to the northwest. One of the last pressure maps available during primary production is for July, 1944. This map shows that the reservoir pressure had been drawn down to less than 50 psi in the west to northwest part of the field and to 500 psi in the south-east corner.

After gas proration ceased, production declined rapidly until the field was uneconomical to produce. By 1950 nearly all of the wells (300+) drilled during primary production were plugged. A waterflood was started on the field in 1966, but evaluation of the flood is beyond the scope of this study.

Chapter 5. Transient Testing in the Zenith Field

5.1 Introduction

Transient testing was performed on wells in the Zenith Field in order to obtain a better understanding of reservoir permeability, fluid movement, and the extent of wellbore damage. Because of the limited amount of money available for these tests, build-up and fall-off tests were conducted by using a fluid level measuring device called an "Echometer." An interference test was conducted with the use of sensitive quartz pressure bombs.

This chapter presents the analysis and a discussion of the results obtained from the transient tests. It also discusses the use of the "Echometer" in obtaining bottom-hole pressure data, as well as general guidelines for performing transient tests with this device.

5.2 Build-up and Fall-off Tests

5.2.1 Use of "Echometer" in Determining Bottom-Hole Pressure

An "Echometer" is a device that uses sonic waves to record the depth of the fluid level in a wellbore. The "Echometer" consists of a gas "gun" which initiates a pressure pulse, a sensor that detects pressure pulses, and

a recording device.

The principle behind the "Echometer" is that sound will reflect off of any abrupt change in diameter inside the wellbore, such as tubing collars and the gas/liquid interface. The "Echometer" sends a high-pressure pulse down the annulus between the casing and the tubing. This pulse is reflected off of tubing collars and the fluid interface and recorded at the surface. Figure 5.1 shows a recorder strip from the "Echometer." As the figure shows, the reflection off tubing collars is clearly discernable from the reflection off of the liquid interface. In order to calculate the depth to the fluid level, the number of joints of tubing above the fluid level are counted and multiplied times the average length of a joint obtained from a recent tubing tally. If the signal dampens out so that tubing collars cannot be seen past a certain point, it is best to extrapolate the tubing to the fluid level using the reflections obtained further up the hole.

In the case of the Zenith Field, injection occurs straight down the production casing, and thus there are no tubing collars to reflect the pressure pulse. In this case, the travel time of the pressure pulse and an estimate of the speed of sound are used to calculate the depth to the fluid level. The "Echometer" records every second as a mark on the recorder strip. These marks can be seen in Figure 5.1. To calculate the depth to the fluid level, the

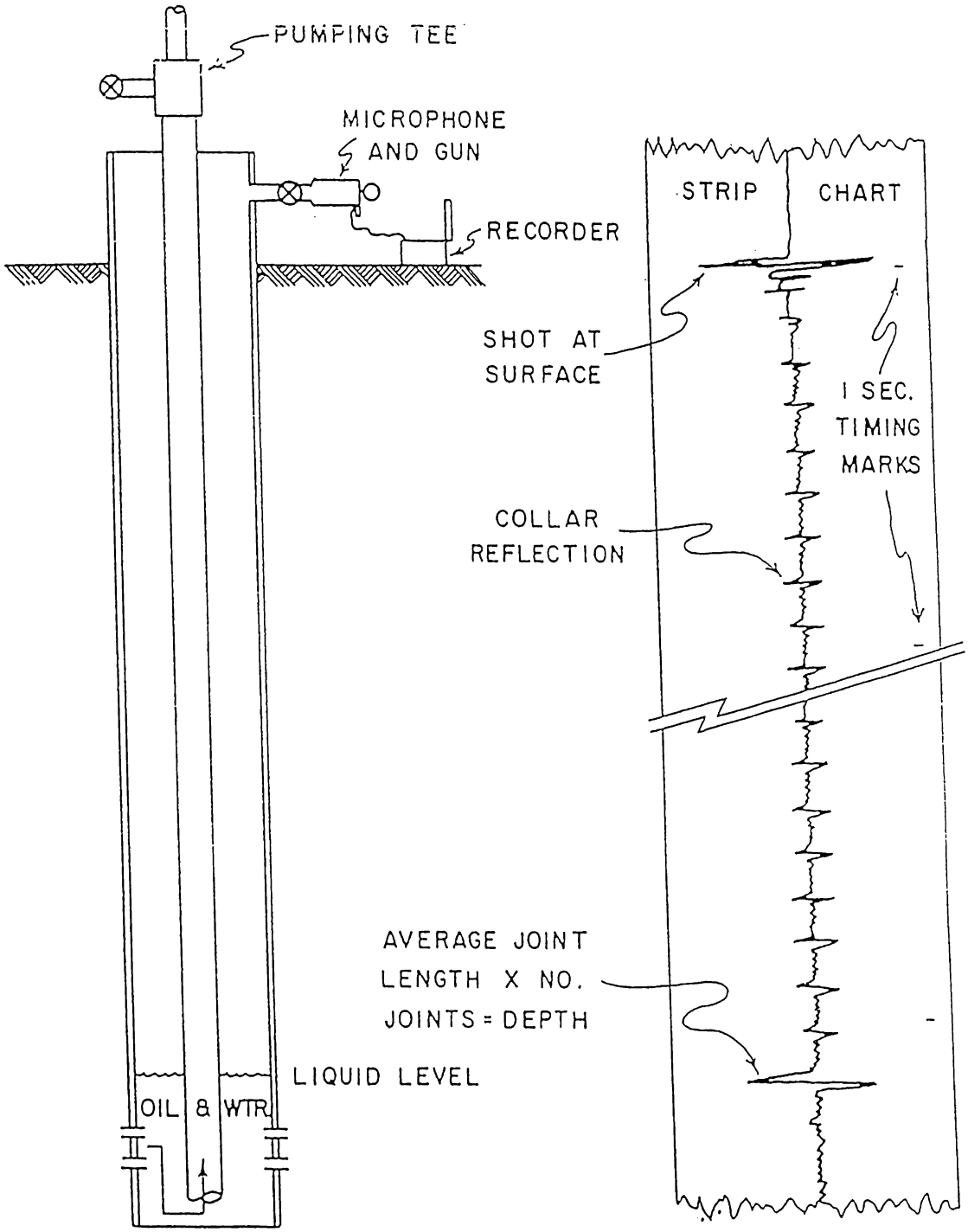

Figure 5.1 Example Recorder Strip from "Echometer" (McCoy et al. ,1985)

travel time is cut in half since the time recorded by the "Echometer" is the travel time to the fluid level and back. This time was then multiplied by the speed of sound to get the depth to the fluid level. The speed of sound is a function of the composition of the gas the sound is traveling through and the temperature and pressure of the gas. A value of 1175 ft/sec, which is approximately the speed of sound in air, was used in the Zenith Field.

Once the depth to the fluid level is calculated, it is subtracted from the depth to the formation in order to get the height of the fluid column. This is then multiplied by an appropriate fluid gradient which takes into account the density of the oil and water, and the ratio of oil and water in the fluid column. Most of the wells produce more than 98 percent water, and thus it was felt that the amount of oil in the fluid column was negligible. Therefore, a value of 0.48 psi/ft was used for these tests, which is the pressure gradient for brine.

5.2.2 Check of Validity of Transient Tests Performed with an "Echometer"

To ensure that the build-up and fall-off tests performed with an "Echometer" were valid, a fall-off test was conducted on ZU-13 with both sensitive quartz crystal pressure bombs and the "Echometer." A comparison of bottom-hole pressure from both of these tools is shown in

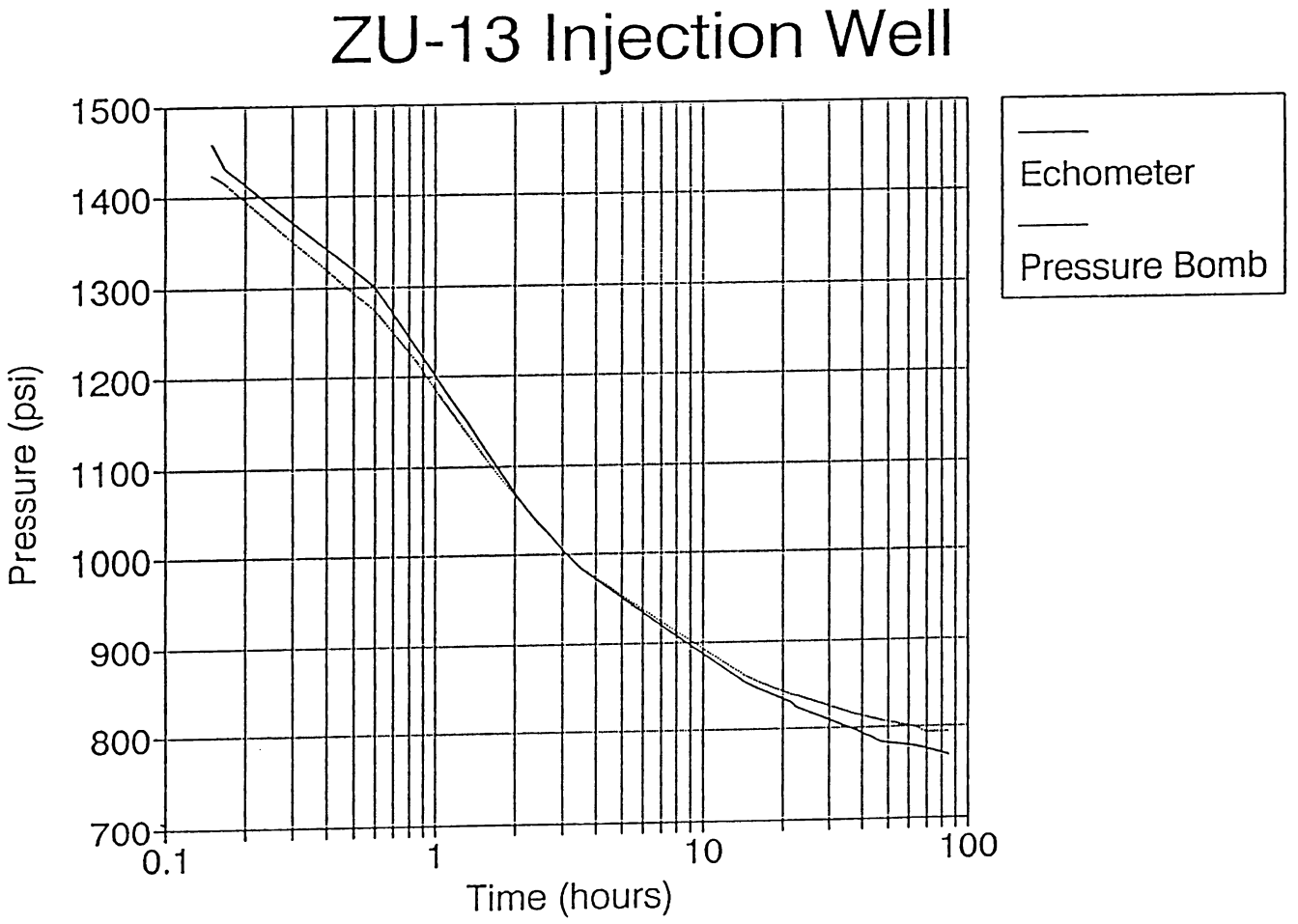

Figure 5.2 Comparison of Bottom-Hole Pressure Calculated from Fluid Level Measurement and Those Obtained from a Sensitive Quartz Crystal Pressure Bomb.

Figure 5.2. The agreement between the pressures is good. To match the "Echometer" pressure with the bomb pressure, a trial and error procedure was used in which the speed of sound in air and the fluid gradient were varied until the lines matched. This resulted in the values given in the previous section, namely 1175 ft/sec for the speed of sound and 0.48 psi/ft for the fluid gradient.

According to speed-of-sound charts provided by the Echometer Company, sound travels through a 0.8 gravity gas at 25 psi and 90° Fahrenheit, at 1175 ft/sec. A fluid gradient of 0.48 psi/ft corresponds to a chloride concentration in brine of approximately 70,000 parts-per-million. (Dowell-Schlumberger, 1989) Original gas gravity of believed to be 0.68. Addition of air and the loss of the more volatile hydrocarbons would tend to increase this value over time. Data found for chloride concentration in the Zenith Field for 1966 indicate that the brine had a concentration of between 50,000 and 80,000 parts-per-million. This agreement between actual and estimated fluid properties adds more confidence to the values of bottom-hole pressure calculated from the "Echometer."

5.2.3 Procedure for Performing Build-up and Fall-off Tests

Build-up and fall-off tests are performed by shutting off a well's production or injection respectively.

Pressure measurements are then made from time zero when flow was terminated. The "Echometer" records the change in fluid level during the test, which is then converted to bottom-hole pressure as described in the previous section.

Figure 5.3 shows the wells that are still completed in the Zenith Field. Build-up tests were performed on ZU-15 and ZU-31. Fall-off tests were performed on Hayes #3, Hayes #5, ZU-5W, ZU-13, ZU-25, and ZU-29. The selection of the wells was constrained to oil wells having low production rates and injection wells so as not to decrease the total field oil production substantially and thus minimize the cost of the test. Also taken into consideration was the location of wells and the known information about the formations open to the wellbore. As Figure 5.3 shows, the wells tested were spread over a large area of the reservoir.

In many cases the formations open to the wellbore were not known precisely because of communication behind the casing or substantial skin factors plugging off a certain zone. Because of this, most of the tests were useful for only a qualitative estimate of reservoir permeability.

Injection profiles were run on ZU-13W, ZU-29W, and ZU-25 to determine the percent of water going to each zone. Because of problems with the wellbores of the other injection wells, the three wells indicated were the only wells in which profiles could be completed. It was found

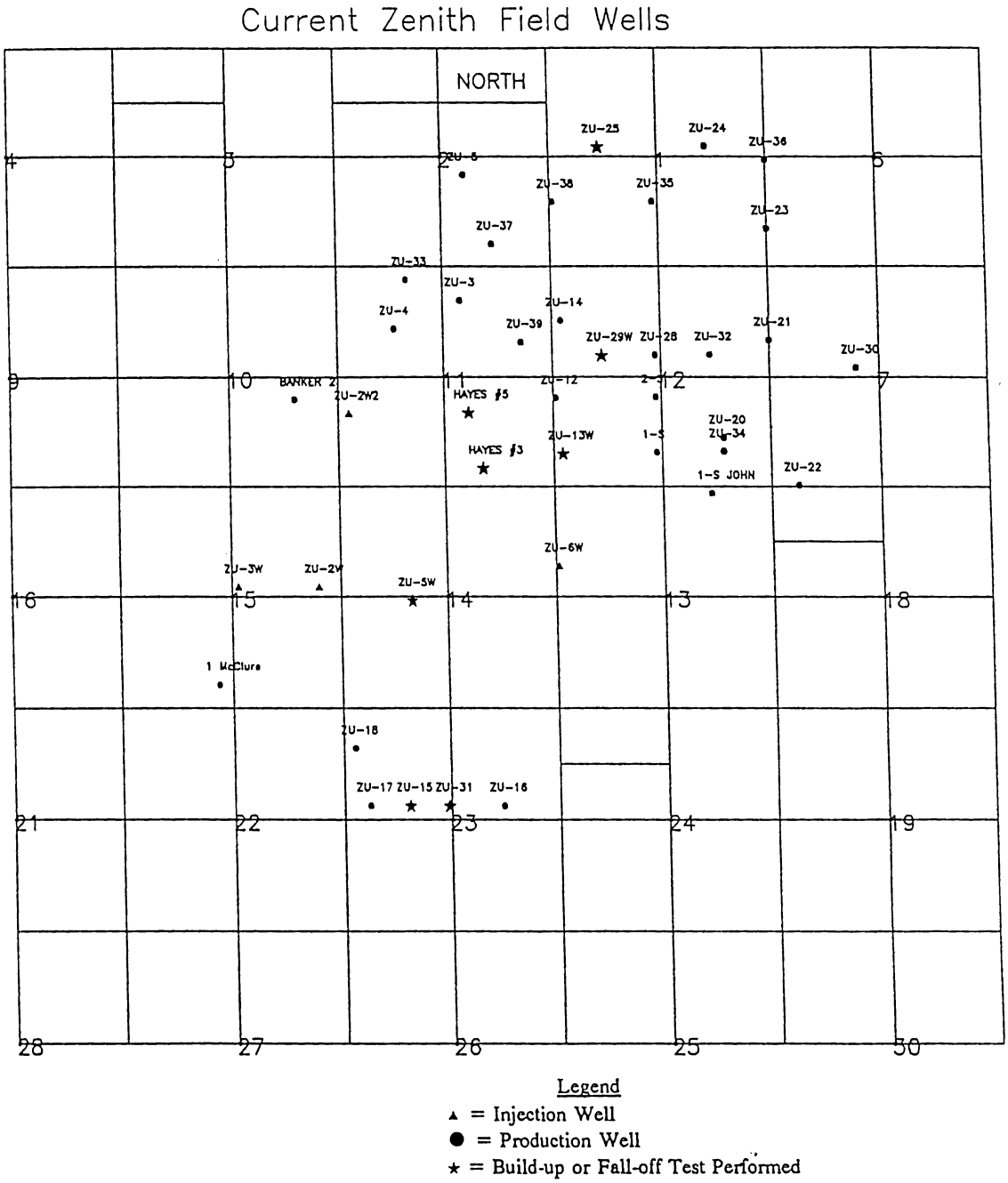

Figure 5.3 Location of Wells on which Build-up or Fall-off Tests were Performed

that 100 percent of the water being injected into ZU-13W and ZU-29W was going into the lower zone of the Lower Misener Sandstone. In ZU-25, fifty percent of the water was going to the upper zone of the Lower Misener Sandstone and the other fifty percent of the water was going into a local porosity streak in the Fernvale.

Before performing a build-up or a fall-off test, the wells to be tested were monitored to obtain an average daily production or injection. In the Zenith Field, monthly barrel tests were performed to get the production well rates, while injection wells were monitored by flow meters to get the daily injection rate for each well.

After performing several well tests in the Zenith Field, a set of procedures was developed that can be used when conducting well tests with an "Echometer." Although it will vary from field to field, it was found in the Zenith Field that a test time of forty-eight hours was sufficient and in many cases a twenty-four hour test provided the needed data. The time required to run a build-up or a fall-off test depends on the permeability of the formation, the formation damage around the wellbore, and the degree of wellbore storage that occurs.

It is important not to cut the test short such that the data collected are dominated by wellbore storage. Wellbore storage is a phenomenon that occurs from shutting the well in at the surface and not at the formation face.

This allows fluid to enter or leave the wellbore during the test, and obscures the true pressure response from the formation. The data can be evaluated in a preliminary manner on site to see if the pressure response is clear of wellbore storage effects. This could be done with a portable personal computer, or more simply, using a sheet of log-log graph paper. A discussion of how to tell if the data are free from wellbore storage effects is presented in the next section.

Data collection during the transient test should be taken about every five minutes during the beginning of the test. After the first thirty minutes to one hour, the interval should be increased to one shot per hour. After eight to ten hours, it is possible to go several hours while not taking data on the well. However, it should be remembered that one can never have too much data from a build-up or fall-off test.

5.2.4 Analysis of Build-up and Fall-off Tests

This section contains a general discussion of the method used to analyze the transient tests. The results on a well-by-well basis will then be presented.

The first step in analyzing the well tests was to make plots of pressure versus time on log-log, semi-log and cartesian coordinate scales in order to analyze the

different regions of pressure response. All plots used in the analysis of the build-up and fall-off tests are located in Appendix III.

Log-Log Plot to Determine Duration of Afterflow

The first plot that was made was a log-log plot of pressure change versus shut-in time. Figure 5.4 shows an example of a log-log plot for ZU-13. This plot is useful in determining when the pressure response is no longer influenced by wellbore storage, or afterflow, effects. Theoretically, during wellbore storage, the curve should increase at approximately unit slope. After wellbore storage has diminished, the curve flattens out to a much smaller slope and the pressure response from the formation being tested is dominant. Wellbore storage is prevalent in the Zenith Field because the wells inject or produce with no surface pressure. This increases the amount of afterflow because fluid continues to enter the formation until the reservoir pressure is approximately equal to the pressure exerted by the fluid column.

As Figure 5.4 shows, afterflow dominates the pressure response for the first ten hours of the test. The other tests were similar, with wellbore storage lasting from thirty minutes to several hours, depending on the characteristics of the formation. Most of the curves did not have a slope of one during wellbore storage. This could be attributed to skin around the wellbore, the

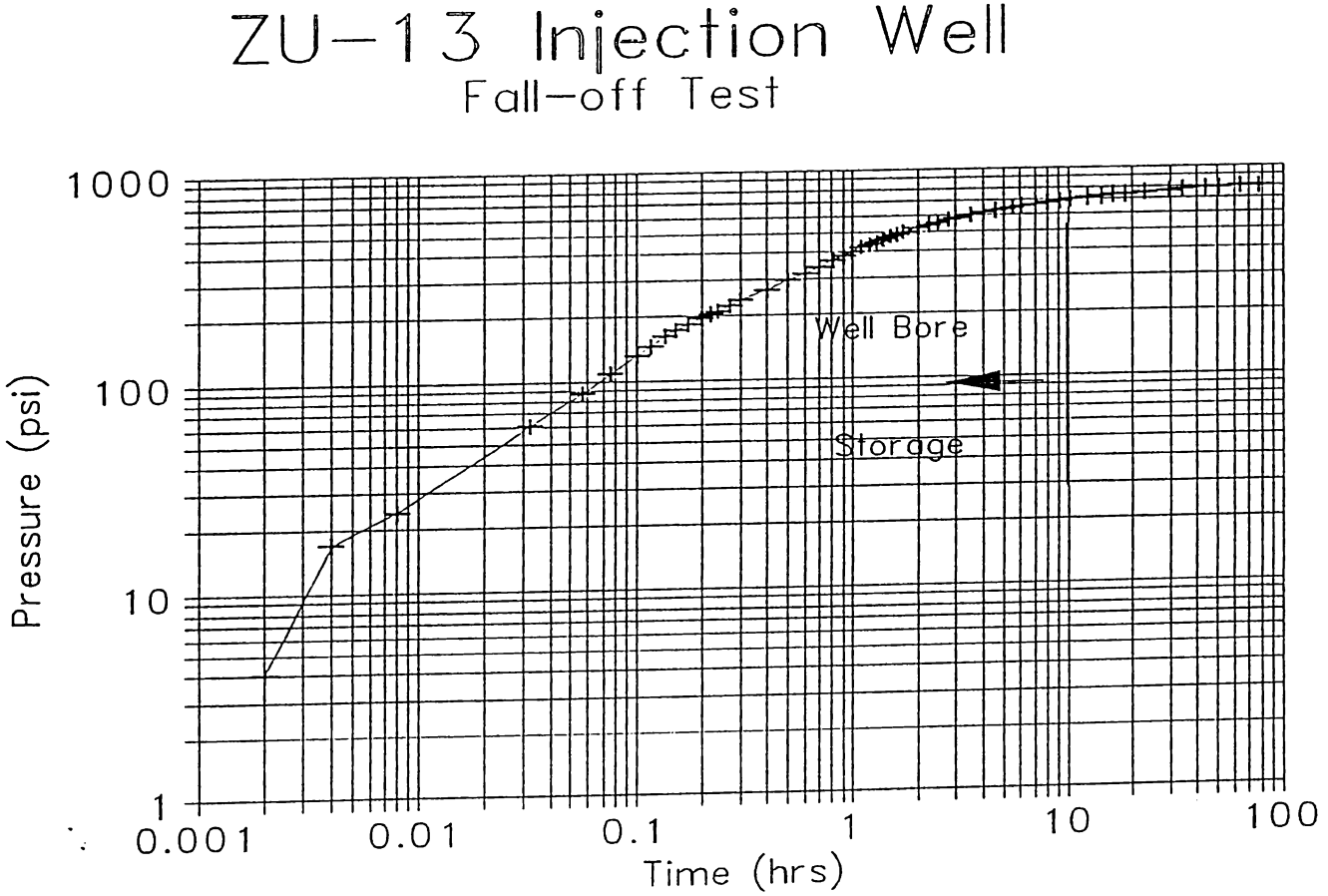

Figure 5.4 Log-Log Plot of Pressure Change Vesus Shut-in Time for ZU-13, showing the Duration of Wellbore Storage

presence of fractures, or from multiple layers being tested simultaneously. (Earlougher, 1977)

Horner and Semi-log Plots

The plot that is analyzed to calculate formation characteristics is a Horner plot. A Horner plot is a graph of bottom-hole pressure versus the log of a dimensionless time called Horner time. Horner time is defined as follows:

$$Horner\ Time = \frac{T_p + \Delta T}{\Delta T} \qquad (5.1$$

Where: T_p = Producing time before the well is shut in. (hours).

ΔT = Time after well is shut in (hours).

If the length of time the well is shut in is negligible compared to the producing time, a Horner plot and a semi-log plot of bottom-hole pressure versus shut in time will yield the same straight line. This latter type of analysis is called MDH analysis. (After Miller, Dyes, and Hutchinson) In the case of the Zenith Field, a producing time of 6480 hours, or nine months, was used. This clearly makes the time the wells were shut in negligible so both types of plots were used interchangeably. When examining the Horner plots remember that as shut-in time increases, Horner time decreases, so shut-in time increases from right to left.

For the analysis of build-up and fall-off tests, the pressure response from the late transient period is examined. On a semi-log plot of bottom-hole pressure versus shut-in time, this period should appear as a straight line. The slope of this line is used to calculate the permeability-thickness product and the skin factor with the following equations.

$$K*h = \frac{162.6*q*B*\mu}{m} \qquad (5.2$$

$$S = 1.151\left[\frac{P_{ws}(1hr) - P_i}{m} - \log\left(\frac{k}{\phi*\mu*c_t*r_w^2}\right) + 3.23\right] \qquad (5.3$$

Where: K = Formation Permeability, md.
h = Formation Thickness, ft.
q = Flow Rate before Shut-in, STB/day.
B_o = Formation Volume Factor, rb/STB.
μ = Fluid Viscosity, cp.
m = Slope of Semi-log Straight Line.
S = Skin Factor.
P_{ws}(1 hr) = Value of Pressure on Semi-log Straight Line at Δt = 1 hour, psi.
P_i = Initial Flowing Pressure, psi.
ϕ = Formation Porosity, fraction.
c_t = Formation Total Compressibility, 1/psi.
r_w = Wellbore Radius, ft

Figure 5.5 is a semi-log plot for ZU-13. As seen, it is difficult to determine the straight line portion of the data.

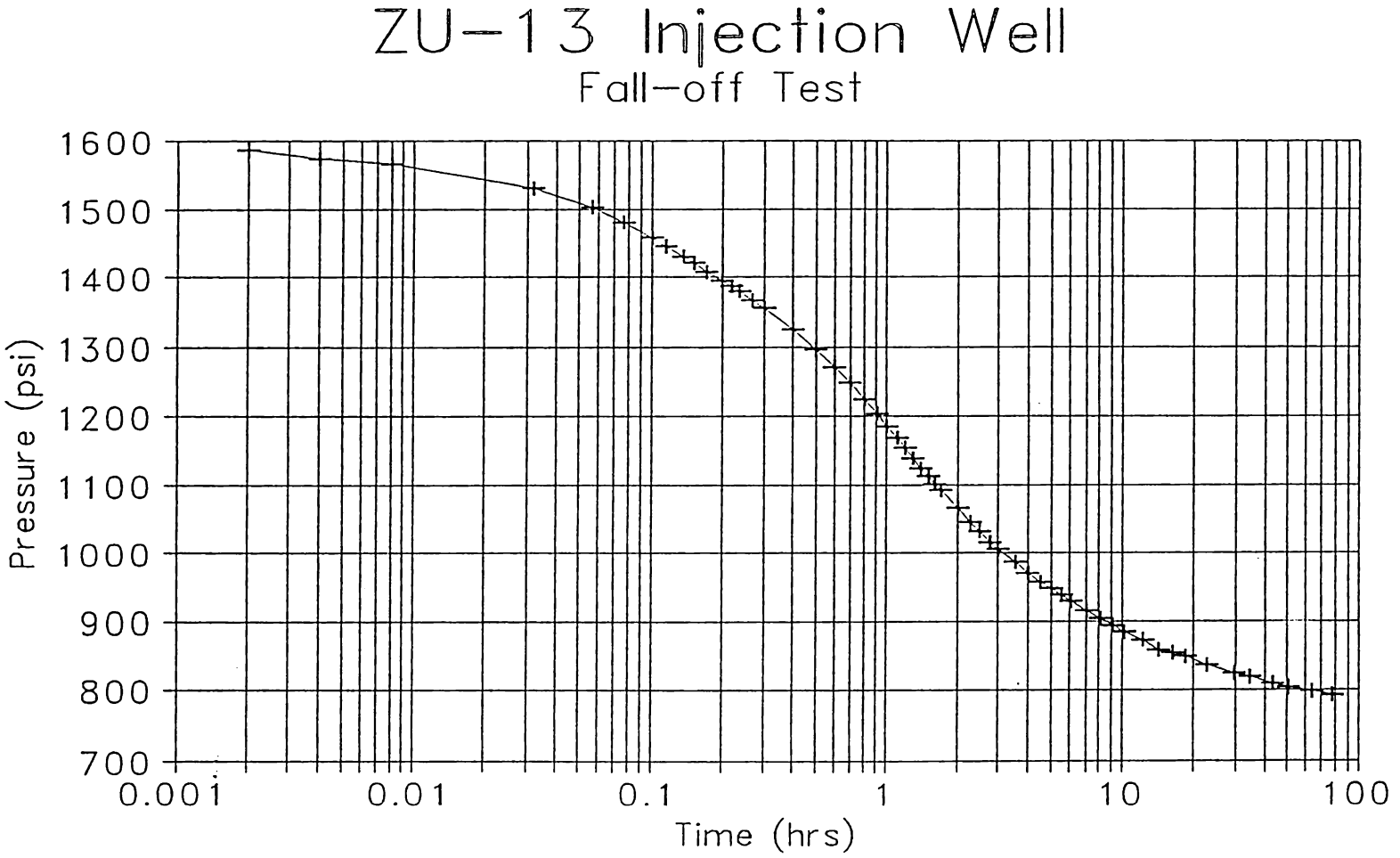

Figure 5.5 Semi-Log Plot of Bottom-Hole Pressure Vesus Shut-in Time for ZU-13

Cartesian Plot to Determine Pseudo-Steady State Behavior

Another plot that will help in making the decision of where to draw the straight line through the data on a semi-log plot is a Cartesian plot of bottom-hole pressure versus shut-in time. This plot is used to determine if transient behavior has ended and pseudo-steady state behavior has begun. Pseudo-steady state data will plot on this graph as a straight line. Figure 5.6 shows a blown up portion of a Cartesian graph for ZU-13. The time when pseudo-steady state is assumed to begin is indicated on the graph. Even though any two points will make a straight line, the time that is labeled was assumed to be the start of pseudo-steady state because the curve was approximately linear over the last several data points. This plot is not always necessary if the straight-line portion of the semi-log plot is easily picked out as is the case for most of the tests in the Zenith Field.

After analyzing all three plots for ZU-13, it is seen that wellbore storage ceases after approximately ten hours and pseudo-steady state is assumed to start at approximately sixty hours. Therefore, the portion of the transient test to be analyzed is between ten and sixty hours. Figure 5.7 is a semi-log plot for ZU-13 with the appropriate section enlarged for easier analysis. A straight line is drawn through the data between the indicated times. The semi-log straight lines for each test

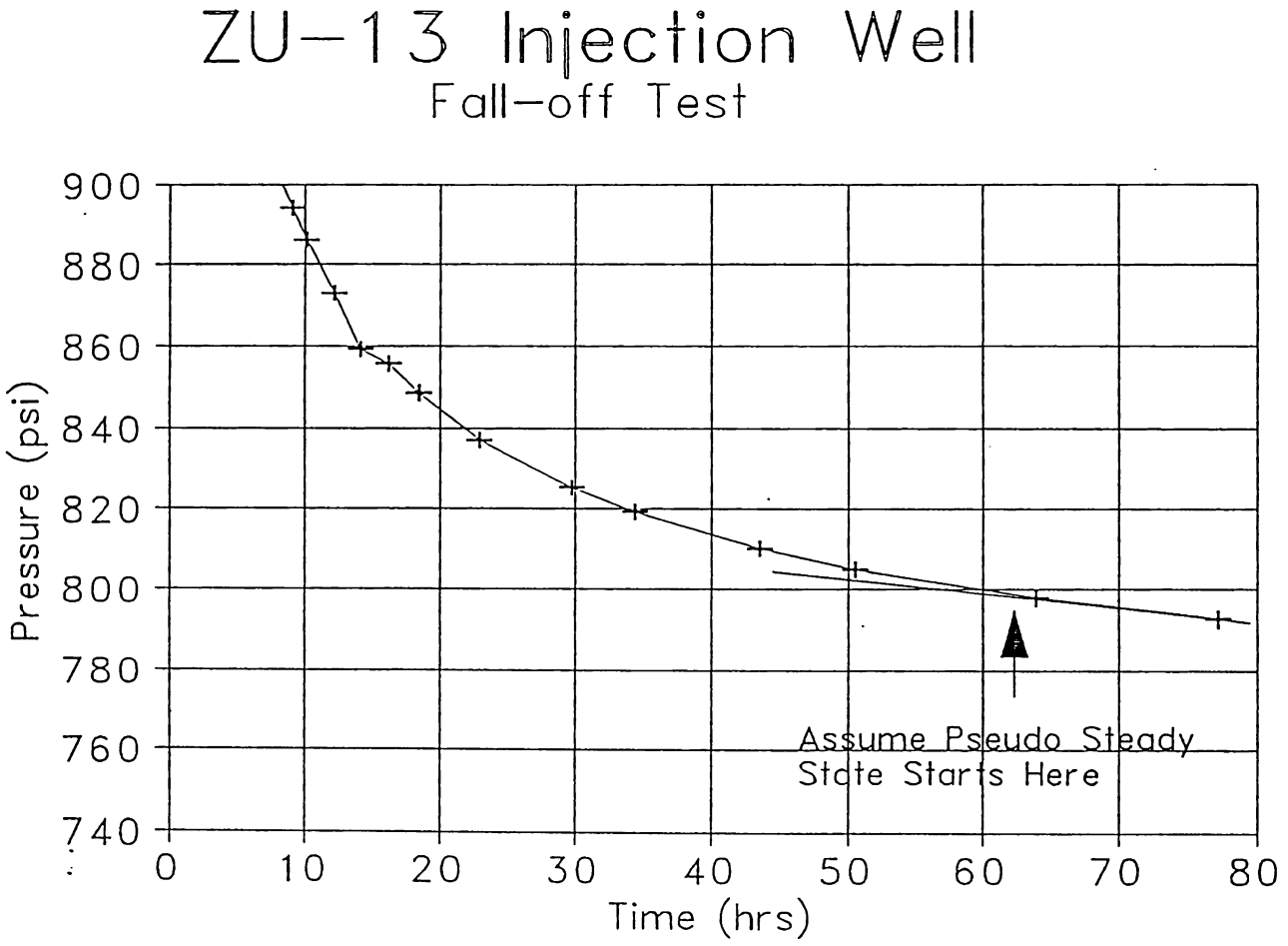

Figure 5.6 Cartesian Plot of Bottom-Hole Pressure Vesus Shut-in Time for ZU-13, Showing Start of Pseudo-Steady-State Behavior

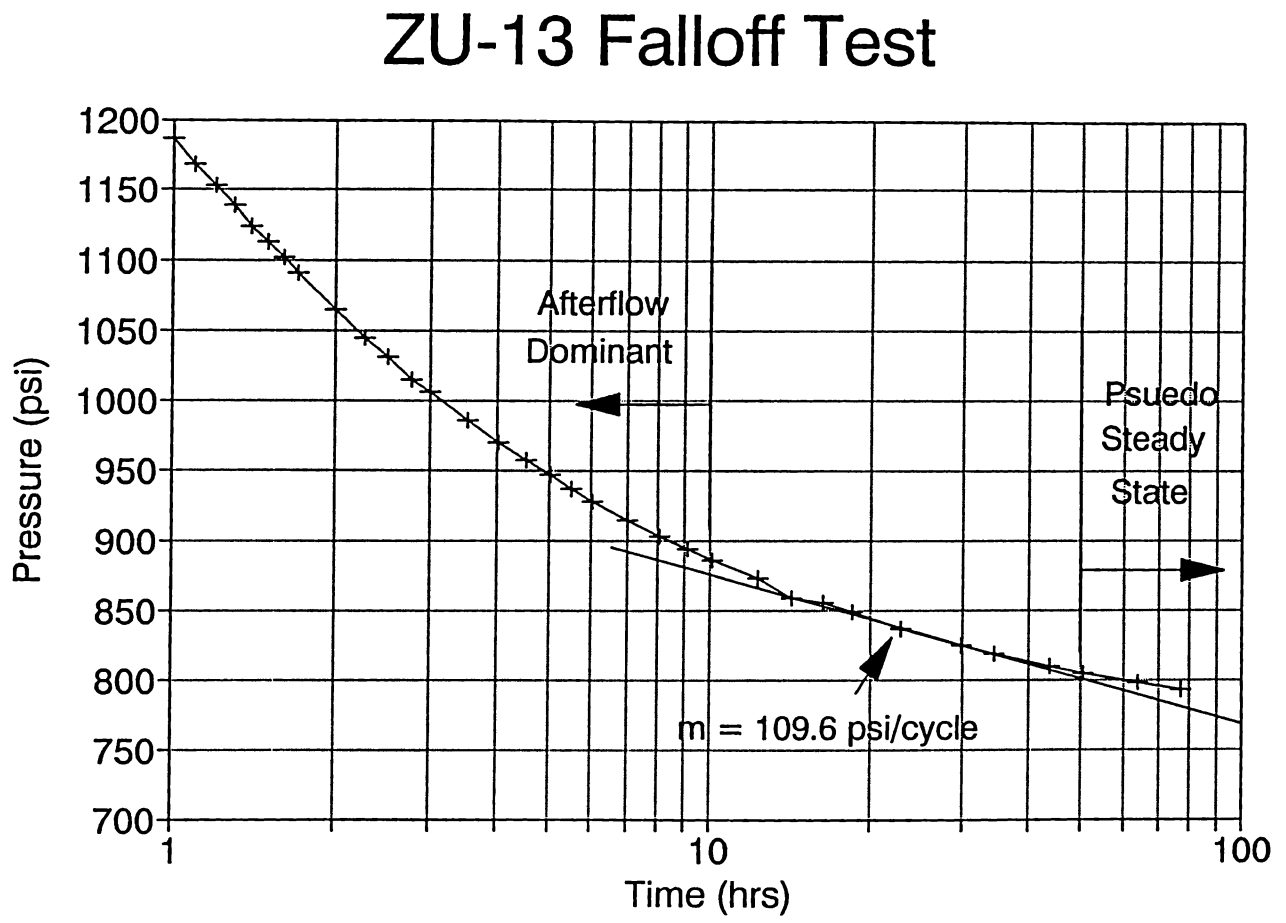

Figure 5.7 Semi-log Plot of Bottom-Hole Pressure versus Shut-in Time for ZU-13 with Analyzed Portion Enlarged

are indicated on the respective Horner or semi-log plots in Appendix III.

Type Curve Matching

In some cases, there may not be enough pressure data to identify a straight line on a semi-log plot. In this case, type-curve matching must be used. Type-curve matching was performed on ZU-15 because not enough data were taken for a straight line to be drawn on a semi-log plot. Type-curve matching was also performed on ZU-13, ZU-25, and ZU-29 as a check of the previous analyses.

Type-curve matching involves comparing the pressure data obtained from a build-up or fall-off test with a set of dimensionless curves that theoretically describe pressure behavior. The type curve used to analyze the pressure tests is found in Figure 5.8 (Ramey, 1970) In these type curves dimensionless pressure is plotted versus dimensionless time for several different values of dimensionless storage coefficient and skin factor.

The procedure in type-curve matching is to plot pressure change versus shut in time on a log-log scale that is the same physical size as the type curve. A plot for ZU-13 is given in Figure 5.9 as an example. The rest of the plots are located in Appendix III. Next, the wellbore storage coefficient should be calculated in order to determine which set of type curves to use. The wellbore storage coefficient is calculated as follows:

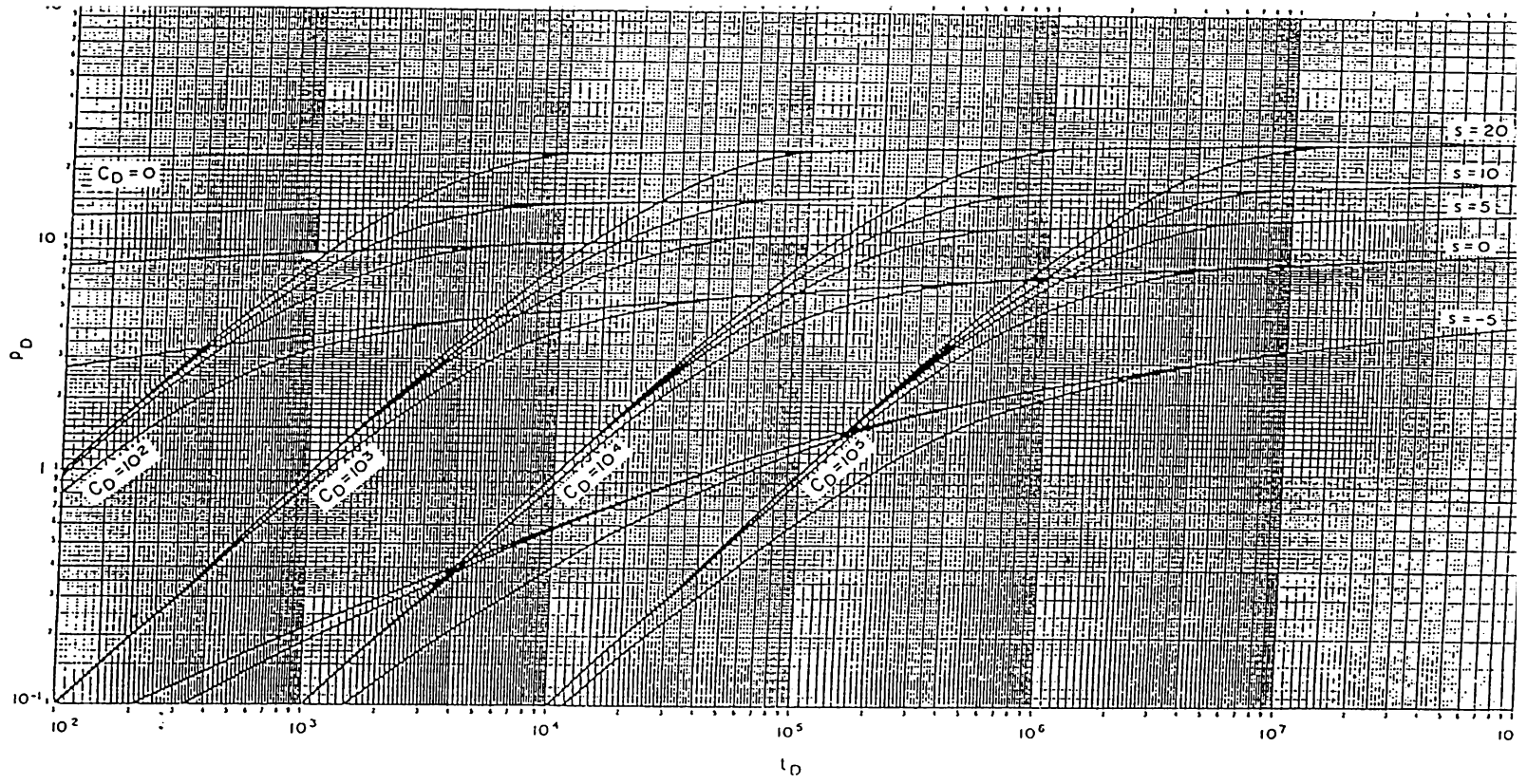

Figure 5.8 Ramey's Type Curves Used for Analyzing Build-Up and Fall-Off Tests (Earlougher, 1977)

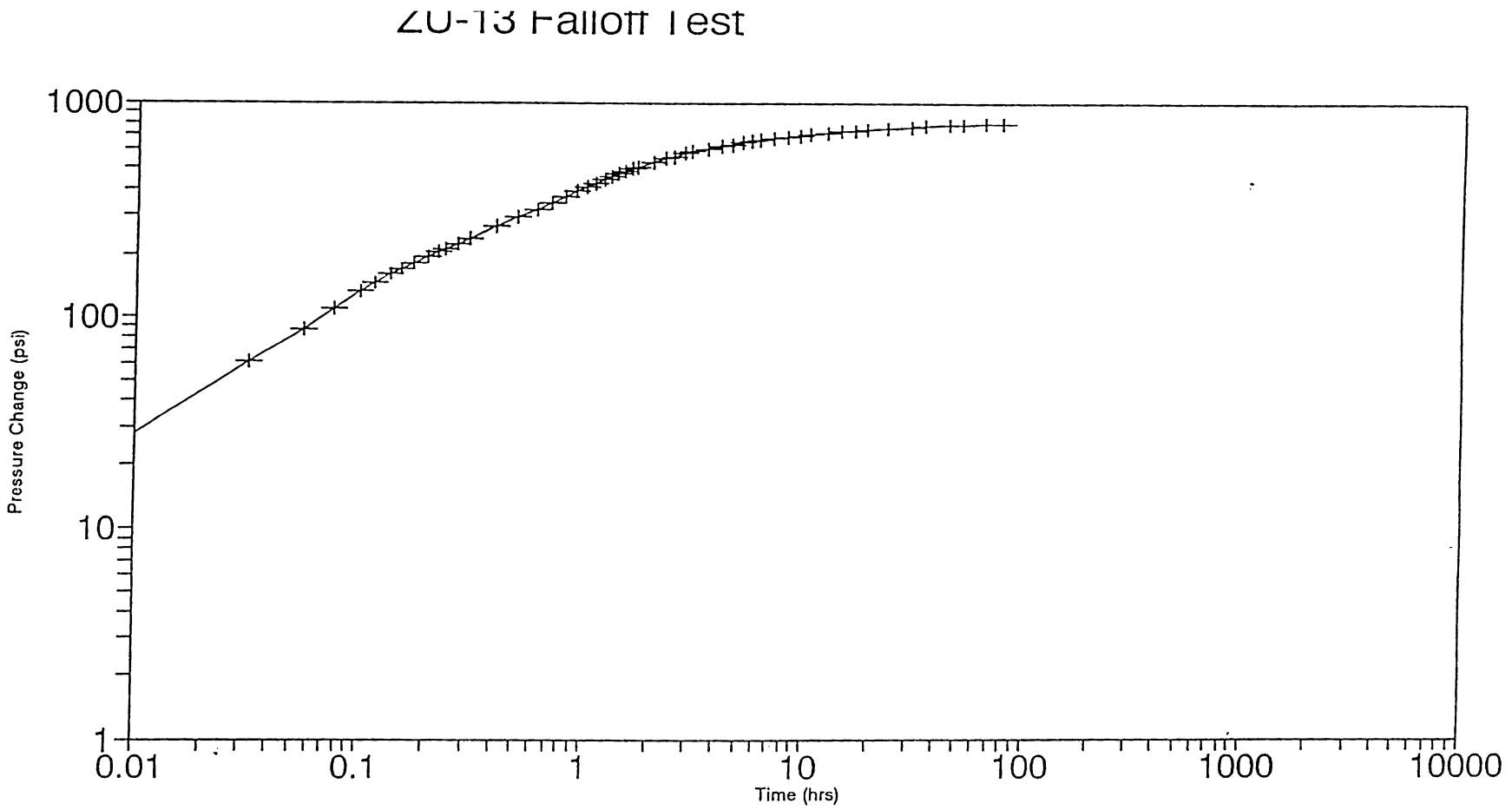

Figure 5.9 Plot of Pressure Change Versus Shut-In Time on Same Size Graph as Figure 5.8. Used for Type Curve Matching of Fall-Off Test Conducted on ZU-13

$$C_s = \frac{q*B}{24}\left(\frac{t}{P_i - P_{wf}}\right)_{unit\ slope} \qquad (5.4$$

If no unit slope line is present then:

$$C_s = \frac{144*A_{wb}}{5.615*\rho} \qquad (5.5$$

and:

$$C_{sd} = \frac{.894*C_s}{\phi*C_t*h*r_w^2} \qquad (5.6$$

where: C_s = Wellbore Storage Coefficient.
C_{sd} = Dimensionless Storage Coefficient.
ρ = Fluid Density, lb/ft^3

$\left(\frac{t}{P_i - P_{wf}}\right)_{unit\ slope}$ = Ratio of the coordinates of any point on the unit slope line.

Using the set of curves that is closest to the dimensionless storage coefficient calculated from Equation 5.6, move the plot of pressure change versus shut-in time vertically and horizontally over the set of type curves. The curve the data matches closest provides an estimate of the skin factor for the well. The next step is to pick an arbitrary point and read the (x,y) coordinate from each graph. With this match point, the following equations are used to calculate reservoir permeability and compressibility:

$$K*h = 141.2*q*B*\mu*\left(\frac{P_d}{\Delta P}\right)_m \qquad (5.7$$

and:

$$\phi*C_t = \frac{0.00264*K}{\mu*r_w^2}\left(\frac{\Delta t}{t_d}\right)_m \qquad (5.8$$

where: $\left(\frac{P_d}{\Delta P}\right)_m$ = Ratio of Dimensionless Pressure to Pressure Change at the Match Point.

$\left(\frac{\Delta t}{t_d}\right)_m$ = Ratio of Shut in Time to Dimensionless Time at the Match Point.

5.2.5 Results and Discussion of Build-up and Fall-off Tests

Table 5.1 presents the results for the build-up and fall-off tests conducted in the Zenith Field. Included in the table are estimates of permeability-thickness product, permeability, the zones that were assumed open in order to calculate that permeability, skin factor, total compressibility, and the method of analysis that was used to calculate the property. "NA" means that property is not calculated from the specified type of analysis.

Several permeabilities are listed for some of the wells because it was not certain which formations were open to the wellbore. In these cases, the test result gives more of a qualitative estimate for the permeability. The formation taking water was known precisely in wells ZU-13,

Table 5.1 Results of Build-up and Fall-off Tests Conducted in the Zenith Field

Well Name	Perm (md)	Zones Assumed	Skin Factor	C_t (1/psi)	Method of Analysis
Hayes #3	970	MSS	18	NA	Horner
	390	Vio 1			
	280	MSS&Vio			
K*h =	5830 md-ft				
Hayes #5	400	MSS	13	NA	Horner
	219	Vio 1			
	161	MSS&Vio			
K*h =	4360 md-ft				
ZU-5W	534	MLS	19	NA	Horner
	412	MLS&MSS			
	206	All Zones			
K*h =	9075 md-ft				
ZU-13	151	MSS2	-0.2	NA	MDH
	83	MSS2	-2.5	5.4e-06	Type Curve
K*h =	1662 md-ft				
ZU-15	60	MSS	20	49e-06	Type Curve
K*h =	1026 md-ft				
ZU-25	27	MSS1	-4.2	NA	Horner
	28		-5	12e-06	Type Curve
K*h =	270 md-ft				
ZU-29	75	MSS2	-2.4	NA	Horner
	82	MSS2	0	49e-06	Type Curve
K*h =	1725 md-ft				
ZU-31	65	MSS	30	NA	Horner
	30	MSS&Vio1			
K*h =	1172 md-ft				

ZU-25, and ZU-29. Therefore the permeability given represents the permeability at residual oil for that formation around that wellbore.

The skin factors for five of the eight wells are relatively large. The values calculated for Hayes #3,

Hayes #5, and ZU-5W could be in error because of the difficulty in measuring the flowing pressure just before shut in. These are all injection wells and, unlike production wells, a measurement before shut in was not able to be taken. Therefore, the first fluid level measurement after shut in was used as the initial pressure. Also, the fact that the permeability was not known precisely could lead to errors in calculating the skin factor. This is not as important as the initial pressure because the permeability is included in a logarithmic term so its effect is diminished.

The total compressibilities reported in Table 5.1 vary by a significant amount. There are several possible reasons for this. First, two wells reported are injection wells and one is a production well. This could cause a difference because the area around each wellbore contains different relative amounts of oil and water. Second, the value of porosity used in Equation 5.8 could be in error causing the calculated total compressibility to be in error. Third, permeability enhancement (negative skin) around a wellbore could cause the actual effective wellbore radius to be larger than the radius of 0.21 ft (5") that was used in the calculation. Finally, type-curve matching is not an exact technique. Errors made during the curve matching process could lead to errors in the calculated parameters.

5.3 Interference Tests Performed on the Zenith Field

5.3.1 Procedure for the Design and Completion of Interference Tests

An interference test is a multi-well pressure transient test designed to evaluate the reservoir permeability between wells. The procedure when performing an interference test is to change the production or injection rate in one well and measure the pressure response in surrounding wells.

The design of the test in the Zenith Field had to take into consideration several factors. First, the pressure bombs were rented for seventy-two hours. Therefore, the wells had to be spaced close enough to be able to detect a sufficient pressure response in this time period. It was estimated that a 5 psi change in pressure would be adequate to analyze. Also, five quartz crystal pressure bombs were rented. One was to be placed in the center well of the test pattern in order to perform a fall-off test and check the validity of the tests conducted with the "Echometer," as discussed earlier. This left four bombs to conduct the interference test, three of which were required to estimate directional permeability in the test area. Also required was a knowledge of the zone into which water was being injected in the center well. This required being able to run an injection profile on the well.

The first step in designing the interference test was to calculate the time it would take a pressure perturbation to be transmitted a certain distance. This was done using the line-source solution of the diffusivity equation which gives pressure, $p_{r,t}$, as a function of position and time. (Dake, 1978)

$$P_{r,t} = P_i - 70.6 * \frac{q*\mu*B}{K*h} ei\left(\frac{948*\phi*C_t*\mu*r^2}{K*t}\right) \quad (5.9$$

where: $P_{r,t}$ = Pressure at Distance, r, and Time, t.
P_i = Initial Pressure, psi.
$e_i(x)$ = Exponential Integral
r = Distance from Active Well, ft.
t = Time After Rate Change, hr.

From fall-off and build-up tests, it was found that the permeability of the Misener Sandstone was in the range of 100 to 300 millidarcies. Using Equation 5.9 and assuming a ten feet thick zone, a maximum radius at which a 5 psi pressure change would be seen in seventy-two hours was 3500 ft, or about three-quarters of a mile.

The restriction on distance between observation well and active well calculated above put a limit on the number of patterns that could be used. It was also preferred that temporarily abandoned wells be used where possible so that active production wells would not have to be shut in. With this in mind, it was decided that ZU-13 would be used as

the active injection well, and ZU-39, ZU-29, ZU-12, and Stewart 1-S would be used as observation wells. Figure 5.10 shows the relative positions of the wells. The largest distance from ZU-13 is to ZU-39 at about 3,000 feet.

The initial plan was to shut in ZU-12 and ZU-29 one week before the test was to be run. This would give the field time to stabilize before the test was to be conducted. An injection profile was run on ZU-13 to ensure that injection was only going into the lower zone of the Misener Sandstone. Injection was then to be shut off in ZU-13, while conducting a fall-off test with the "Echometer." The pressure bombs were to be taken out of the holes seventy-two hours later for analysis.

On the day of the test, it was found that ZU-12 had a check valve in the bottom of the tubing. This prevented the running of a pressure bomb in that well because fluid would not be able to move freely in and out of the tubing. It was decided to monitor ZU-12 with the "Echometer" and to place the pressure bomb in the temporarily abandoned well ZU-14 instead.

5.3.2 Analysis of Interference Tests

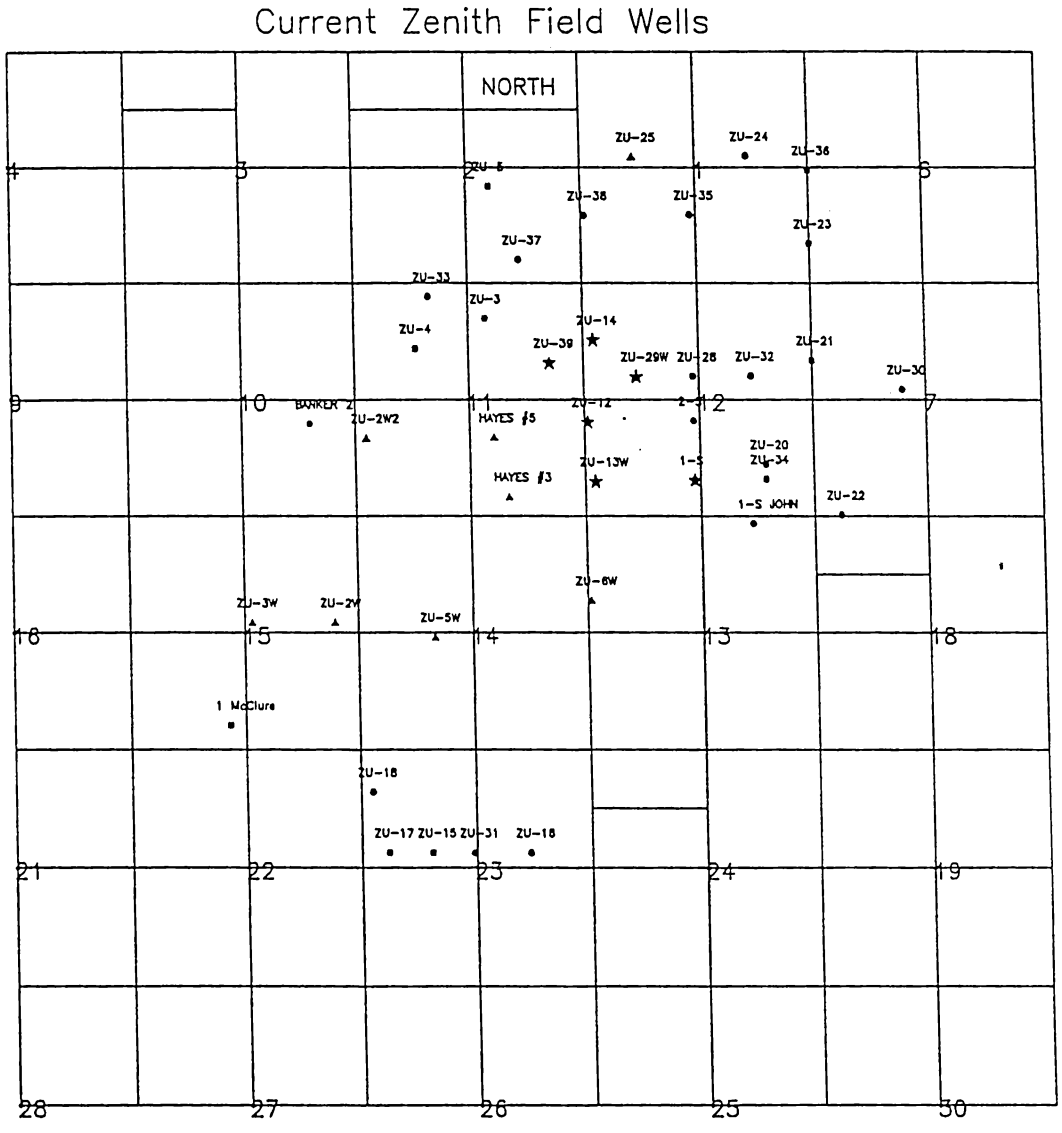

Figure 5.10 Location of Wells on which Interference Tests were Performed

The analysis of interference tests was accomplished by type curve matching. The type curve used is shown in Figure 5.11. A typical pressure response at an observation well is shown in Figure 5.12. A time lag exists between the time the active well is shut in and the time a pressure response is seen at the observation well.

The method of analyzing interference tests is to plot pressure change at the observation well versus shut in time of the active well on a log-log plot that is the same physical size as the type curve. (see Appendix III) The pressure change is defined as the difference between the established trend and the actual pressures at the observation well. (see Figure 5.12) The next step is to shift the plot over the type curve horizontally and vertically, until the two curves match up. A match point is selected as before, and the permeability and compressibility are calculated as follows:

$$K = \frac{141.2 * q * B * \mu}{h} \left(\frac{P_d}{\Delta P} \right)_m \qquad (5.10$$

and:

$$\phi * C_t = \frac{0.0002637 * K}{\mu * r^2} \left(\frac{t}{t_d / r_d^2} \right)_m \qquad (5.11$$

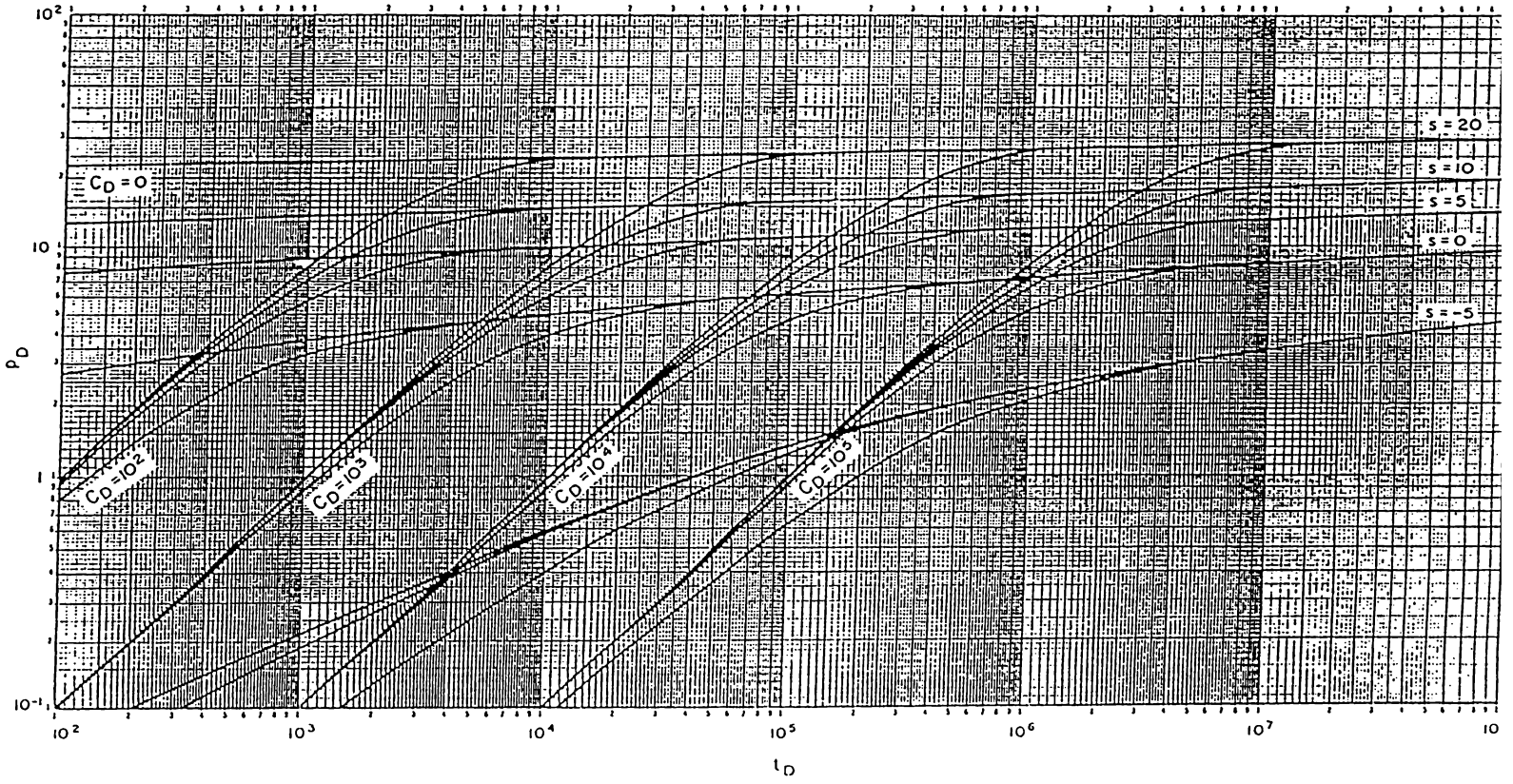

Figure 5.11 Dimensionless Pressure for a Single Well in an Infinite System, No Skin No Wellbore Storage. Used in the Analysis of Interference Tests. (Earlougher, 1977)

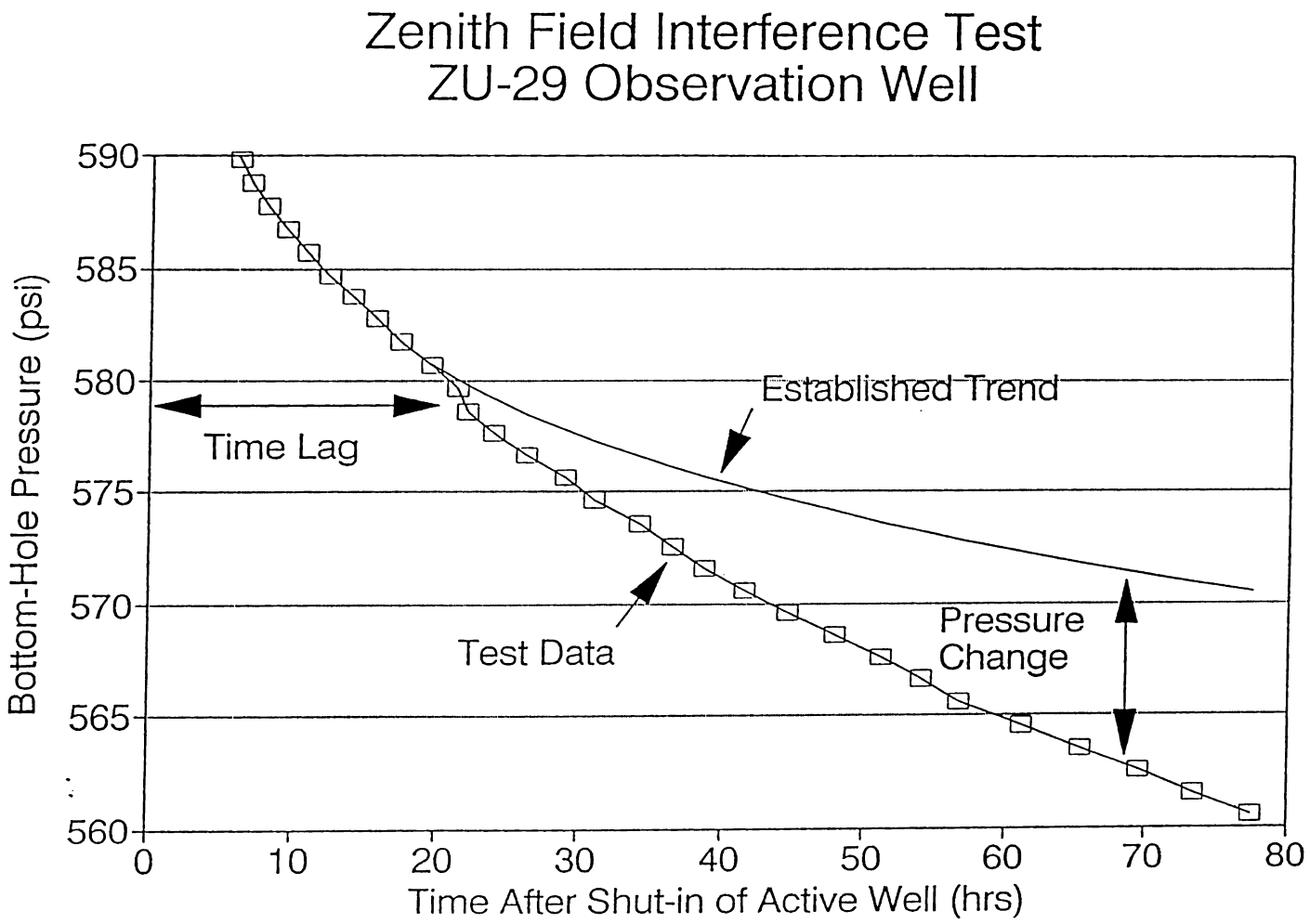

Figure 5.12 Typical Pressure Response at an Observation Well in an Interference Test

where: r = Distance Between Active Well and Observation Well, ft.

5.3.3 Results and Discussion of Interference Tests Conducted in the Zenith Field

Table 5.2 Results from Interference Tests Conducted on the Zenith Field

Well	Perm (md)	C_t (1/psi)	Check w/ Eq. 5.9
ZU-29	294	20e-06	Actual = 3 psi @ 35 hr Theor. = 3 psi @ 35 hr
ZU-12 min	56.5	14e-06	Actual = 25 psi @ 50 hr Theor. = 28 psi @ 50 hr
ZU-12 max	92	22e-06	Actual = 17 psi @ 50 hr Theor. = 16 psi @ 50 hr
Stew. 1-S	1300	36e-06	Actual =2.5 psi @ 40 hr Theor. =2.1 psi @ 40 hr

Table 5.2 presents the results from the interference test conducted on the Zenith Field. The table includes permeabilities and compressibilities calculated from the analysis of the tests. It also includes a comparison of the actual pressure drop at a certain time with the pressure drop calculated from Equation 5.9 at the same time. This was done as a check of the analysis of the interference test.

Calculated total compressibilities again vary significantly. The same reasons as those given in Section

5.2.5 apply here to explain the variation in the compressibilities calculated from build-up and fall-off tests.

As the table shows, the maximum permeability is in a direction east of ZU-13 toward Stewart 1-S. This large permeability is probably indicative of the conglomerate that lies in localized areas at the base of the Misener Sandstone section. Core reports do indicate that permeabilities in the lower section of the Misener Sandstone can be on the order of 700 to 800 millidarcies. (see Appendix I)

A minimum and a maximum value are reported for ZU-12. As Figure 5.13 shows, an established trend could not be obtained from the data available. Therefore, a minimum estimate and a maximum estimate are given. The minimum estimate extrapolates the established trend as equal to the first data point presented in the figure. The maximum estimate connects the first two data points as the established trend.

Pressure response was not seen in ZU-14 and ZU-39 in the seventy-two hours of the test. This indicates that the permeability in the north to northwest direction is less than 300 millidarcies which was used in the initial design of the test. This is also substantiated by the results from ZU-12. The lower permeability to the north of ZU-13 is believed to be caused by directional variations in the

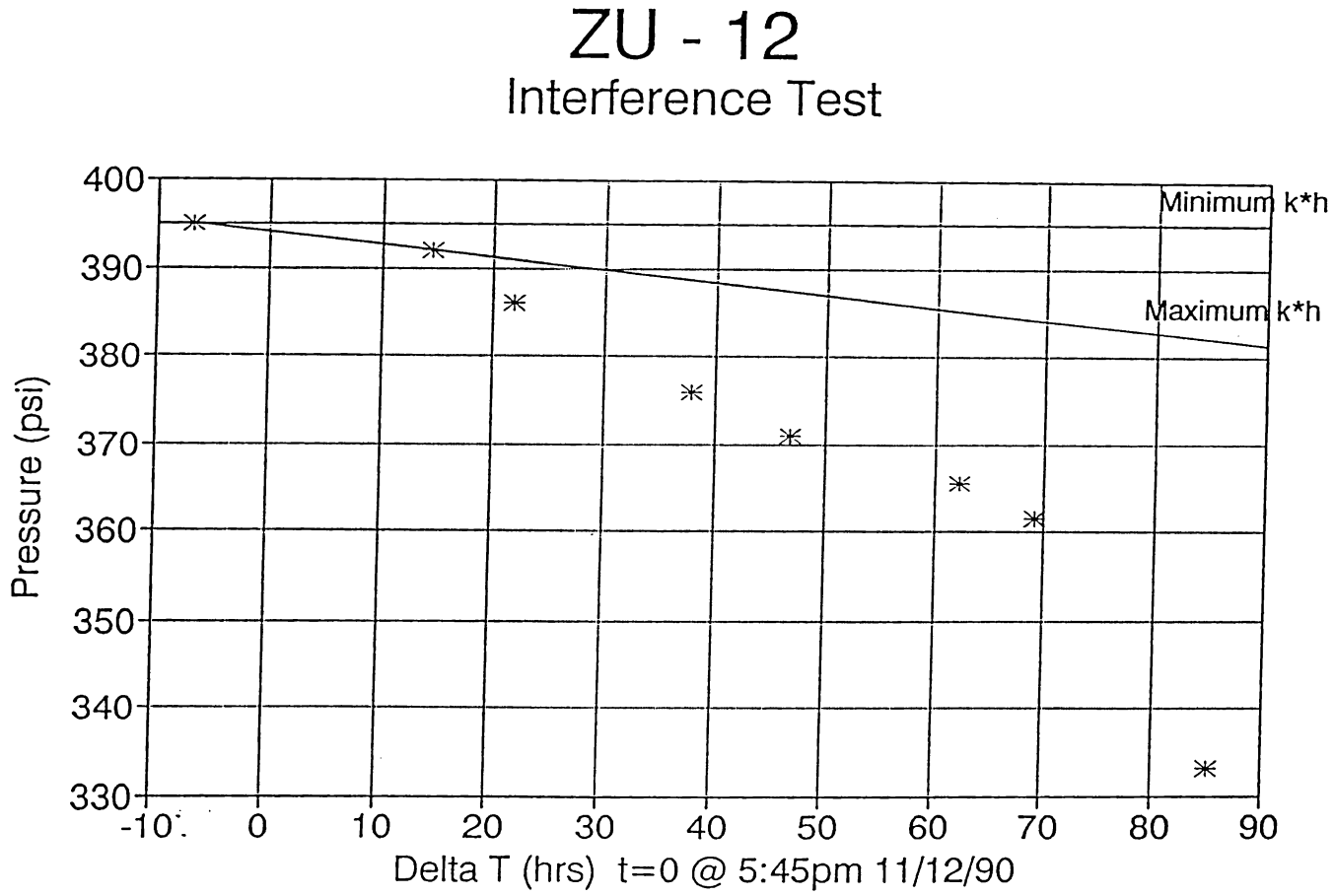

Figure 5.13 Plot of Bottom-Hole Pressure Versus Time After Shut-in of Active Well for ZU - 12, Showing Maximum and Minimum Established Trend

permeability around ZU-13. The porosity log for ZU-14 in Figure 3.3 shows that the porosity around ZU-14 is substantially lower in the lower zone of the Misener Sandstone than in the upper zone. This indicates that the permeability of the lower zone decreases north from ZU-13 toward ZU-12 and ZU-14.

5.4 Summary Conclusions of Transient Tests Conducted in the Zenith Field

1. Build-up, fall-off, and in some instances, interference tests can be conducted with an "Echometer."
2. A procedure for conducting build-up and fall-off tests with an "Echometer" was defined.
3. Build-up, fall-off, and interference tests conducted in the Zenith Field indicate that the permeability of the lower layer of the Misener Sandstone lies in the range of 100 to 300 millidarcies, with the conglomerate at the base of the sandstone having a permeability of more than one darcy. The permeability of the upper layer is on the order of 50 millidarcies.

4. Since many of the wells had multiple formations open to the wellbore, an accurate value for the

permeability could not be obtained for a single zone in these wells. The results do indicate that the permeability on a field-wide basis is generally at or above 100 millidarcies.

5. An average compressibility for the Zenith Field was calculated to be 32 X 10^{-6} 1/psi from build-up, fall-off, and interference tests.

6. Skin factors on some of the wells were quite large, indicating workovers may be needed.

Chapter 6. Selection of Mathematical Simulator

This chapter discusses the process used in determining the simulator to be used to model the Zenith Field. The two simulators that were studied are presented with a discussion of the advantages and disadvantages of each.

6.1 BOAST II

BOAST II was initially selected as the simulator to model the Zenith Field. It is a three dimensional, three phase, black oil simulator available at no cost from the Department of Energy (DOE). BOAST II was chosen because it was felt that if its use could be demonstrated on the Zenith Field, it could be applied to other reservoirs by independent oil companies in Kansas.

BOAST II models the three dimensional flow of oil, gas, and water through porous media. It has several advantages. First, it is free thus small oil companies with simulation experience could obtain a copy. Second, it models most types of simple reservoirs, and third, it comes in a PC version for small fields which makes it even more applicable to smaller companies that do not have main frame or work station access.

Some disadvantages do exist in using BOAST II. It is relatively difficult to use. Large amounts of time were

expended in debugging input files. It also cannot be used on complex reservoirs, especially reservoirs that are fractured.

Analysis of reservoir data indicated that the Viola Limestone was fractured. Data that support this conclusion are listed as follows:

1. Four core reports were available from the Zenith Field. These were discussed in Chapter 3. There were several indications of vertical fractures in the core reports that were available. (Appendix I)

2. Many of the wells that were drilled into the Viola reported initial potentials of between 10,000 and 30,000 STB/day. Matrix permeability reported in cores was of the order of ten millidarcies, which could not support the initial potentials that were reported.

3. Poor waterflood response was recorded in the field, which is sometimes indicative of fractures.

As mentioned in a previous chapter, a literature search indicated that a simple three-dimensional, three-phase black-oil simulator would give erroneous results if used to model a naturally fractured reservoir. Because the Viola was believed to be fractured, BOAST II could not be used to model the Zenith Field. A simulator with dual-porosity capability needed to be used.

6.2 VIP Simulator

After examining several simulators, it was found that Western Altas' VIP simulator had dual-porosity capability. This simulator had been used in a previous project. Arrangements were made for the updated version of VIP to be sent to the University of Kansas.

The version of VIP that was used is a three-dimensional, three-phase black oil simulator with dual-porosity and dual-permeability capability. Dual-porosity means that a small portion of the reservoir contributes significantly to fluid flow, but has insignificant storage capability, in other words, a fractured reservoir.

A dual-porosity simulator consists of grid blocks that are divided into smaller matrix blocks which are surrounded by fractures. Dual-porosity indicates that fluid flow occurs in the fractures only and the matrix rock acts as a source or a sink to the fractures. Dual-porosity/dual-permeability indicates that fluid flow occurs in both the matrix and the fractures.

Dual-porosity/dual-permeability simulators are much more computationally intensive than dual-porosity simulators. (Dean and Lo, 1988) Many reservoirs can be sufficiently modeled with dual-porosity only, thus saving computer time. However, reservoirs in which some formations are fractured others are not, require the dual-

porosity/dual-permeability option. (VIP Manual, 1990) The Zenith Field is such a reservoir since the Misener formation is not thought to be fractured while the Viola formation is believed to be fractured.

The VIP simulator is very easy to use. Input data are entered in a straight forward manner, with column heading and comment statements used to make the data entries easy to follow. Example initialization and recurrent input data files are located in Appendix VI. VIP makes a list of input data errors or inconsistencies in a log file which makes debugging simple. This was a major advantage as compared to BOAST II which gave no such listing.

Output is in large data files. Fortran computer programs were written to extract the data from the output files and reformat them into files that were easy to read. The programs that were used are located in Appendix IV, and are listed below along with their function:

1. MAP.FOR - This program reads the data from the map file written by VIP and outputs grids of datum pressure, gas saturation, oil saturation, and water saturation for each layer. It also calculates a pore volume weighted datum pressure and writes it out to a separate file.

2. PLOT.FOR - This program extracts data written to a plot file by VIP. It can extract whole field data, or if the field is broken down into regions, it can extract individual region data.

3. WELL.FOR - This program extracts well data written to the plot file by VIP. It lists the well number along with producing rates and gridblock and bottom-hole pressure for that well.

As a check of the simulator, the material balance calculated by the simulator was compared to the volumetric analysis presented previously. The results are shown in Table 6.1. The agreement between the two methods is generally very good. Discrepancy in the Misener Sandstone is due to adjustment of some grid-block porosities during the history matching process.

Table 6.1 Comparison of Original Oil in Place of the Zenith Field

	OOIP (MMSTB)	
Formation	Volumetric Analysis*	Simulator Output
Misener Limestone	25.06	24.99
Misener Sandstone	34.11	38.05
Maquoketa Dolomite	5.82	5.96
Viola Limestone Pay 1	40.05	42.36
Total	105.04	113.93

* From (Schoeling, 1990)

Chapter 7. Data Used in the Simulation of the Zenith Field

Data available for the simulation of the Zenith Field were developed in a comprehensive study of the field conducted in 1989 through 1990 (TORP-KGS, 1991). This chapter presents a summary of relevant input data and field performance data that were found through that search. The method of estimation of properties that were not available from known data is also discussed. This chapter will first describe the data that was input into the simulator, including fluid and rock properties, aquifer data, fault data, and oil production data. This is followed by a discussion of the data that was used in the history matching process, namely field pressure, water cuts, and gas-oil ratio.

7.1 Input Data Used in the Simulation

7.1.1 Fluid Properties

Limited fluid property data were available for the Zenith Field. The data that were available were in the form of PVT tests conducted on the oil in the early stages of production in the Zenith Field. These test results are shown in Appendix I. They consist of plots of gas in solution versus pressure, and oil formation volume factor

versus pressure, along with some data regarding oil density, initial bubble point, formation temperature, oil compressibility, and chemical composition of the oil. The following is a discussion of the oil, gas, and water properties of the Zenith Field.

The stock tank oil in the Zenith Field had a gravity of 42 degrees API. The bubble point was estimated to be about 1100 psi with an initial solution gas-oil ratio (R_s) of 345 SCF/STB. This gas-oil ratio was obtained from the plot of GOR versus time given by the 1942 engineering committee. The value of R_s that corresponds to 1100 psi in the PVT analysis is 363 SCF/STB. There is clearly a discrepancy. This was investigated in the history matching procedure and will be discussed in the next chapter. The initial temperature of the reservoir was 118° Fahrenheit. Data for gas in solution and oil formation volume factor required by VIP were input directly from the plots shown in Appendix I. Oil viscosity was unknown, so a correlation from Beggs and Robinson was used. (Bradley, 1987) Table 7.1 shows the oil properties as a function of pressure that were used in the simulation.

Very little gas property data were available so gas properties were estimated through correlations. The initial specific gravity of the gas was reported to be 0.68 (air = 1.0) in the 1984 Questa Engineering Study. Gas

Table 7.1 Oil PVT Properties used in the Simulation of the Zenith Field

Press (psi)	R_s (SCF/STB)	B_o (res. bbl./STB)	μ_o (cp)
2000	540	1.286	0.713
1700	478	1.266	0.767
1500	440	1.254	0.807
1300	402	1.241	0.850
1200	382	1.234	0.875
1100	363	1.228	0.900
1000	344	1.221	0.928
700	285	1.198	1.029
500	242	1.182	1.124
200	162	1.144	1.373
100	116	1.125	1.581

compressibility was obtained from the Standing and Katz chart of gas compressibility as a function of pseudo reduced pressure and pseudo reduced temperatures (Bradley, 1987). Gas viscosity was obtained from a correlation by Carr *et al.* which estimates gas viscosity based on gas gravity, with a correction to reservoir pressure and temperature. (Bradley, 1987) Table 7.2 presents the gas properties as a function of pressure.

Water viscosity was reported as 0.7 cp in the 1965 Yates engineering study. Water specific gravity was assigned a value of 1.04 which, based on a chloride concentration of 30,000 ppm for the reservoir brine, was obtained from a field data handbook. (Dowell-Schlumberger, 1988) Water formation volume factor was assigned a value of 1.05 res. bbl./STB.

Table 7.2 Gas PVT Data Used in the Simulation of the Zenith Field

Pressure (psi)	Compressibility Factor	μ_g (cp)
2000	0.898	
1700	0.905	
1500	0.914	
1300	0.921	
1200	0.925	
1100	0.931	
1000	0.938	
700	0.952	
500	0.968	
200	0.984	
100	0.992	

7.1.2 Rock Properties

Limited data were available describing rock properties of the Zenith Field. Drillers logs were available for nearly every well drilled in the field. These logs specified the tops and the bottoms of each formation. About fifty electric logs were run on wells that were drilled when the waterflood was implemented in the 1960's. Records indicate that many of the wells were cored, but only four core analysis reports were found. A Lotus spreadsheet of available data was constructed (TORP-KGS, 1991) which included, among other things, the tops and bottoms of each formation for every well drilled in the field, and individual porosity estimations where they were available.

Gross Thickness

Gross thickness of each formation was obtained from

driller's logs. Driller's logs are records made during the time of drilling of the tops and bottoms of each formation. By subtracting the bottom depths from the top depths, a value of gross thickness for a given formation was calculated. A grid of gross thickness was obtained with the use of "Surfer," an IBM compatible, geo-statistical mapping program. The input grids for gross thickness are located in Appendix V.

The more data points that are available when estimating grid values, the more confidence one can have in the accuracy of that grid. Because there were over 500 wells drilled in the Zenith Field, there was a large amount of data regarding formation thickness. Therefore, high confidence is placed in the thickness values assigned to the model, with the exception of the upper and lower layers of the Misener Sandstone.

As discussed in a previous chapter, the lower Misener Sandstone layer is less shaly than the upper layer and is a better reservoir rock. This difference can be seen on gamma ray logs as shown by the type curve in Figure 3.3. The upper and lower sandstone layers were then picked off of gamma ray logs. Because there were not as many data points, less confidence is placed in the gross thickness estimations for the upper and lower layers of the Misener Sandstone.

In order to make the sum of the Misener Sandstone

layers more consistent with the total sandstone interval obtained from the drillers logs, a ratio of individual layer thickness to the total interval thickness taken from the electric logs was calculated. This ratio was then multiplied times the total interval thickness obtained from the drillers logs.

Net thickness was calculated for each of the formations. (TORP-KGS, 1991) Net thickness was calculated based on a porosity cut-off obtained from plots of permeability versus porosity for each formation. These plots will be presented in a subsequent section. The porosity that corresponded to a permeability of 1 millidarcy was used as the cut-off. The porosity cut-offs for each formation are listed as follows:

Misener Limestone = 11%
Misener Sandstone = 5%
Maquoketa Dolomite = 8%
Viola Limestone = 8%

The Viola Limestone Pay 1 was the only formation for which net thickness was included in the model. No significant difference was detected between the gross thickness and the net thickness of the Misener Sandstone. The net thicknesses for the Misener Limestone and the Maquoketa Dolomite were not added to the model because it was judged that the reduction in oil volume from the addition of net pay would have had a minimal effect on the simulation results.

Porosity

Porosity was calculated from neutron porosity and density porosity logs with a correction for shale included. (TORP-KGS, 1991) As mentioned previously, approximately fifty wells over the entire field had electric logs. Therefore less than fifty data points were available to be gridded by "Surfer" for each formation. The porosity input grids are shown in Appendix V. Because so few porosity data points were available, the confidence in the porosity grid is not as high as the confidence in the gross thickness grid. For this reason, porosity was changed slightly during the simulation in an attempt improve the history match.

Permeability

The absolute permeabilities of each formation were estimated by making plots of log permeability versus porosity using the available core data. These plots are shown in Figures 7.1 through 7.3. The plot for the Misener Sandstone in Figure 7.2 has the two sandstone beds separated. As the figure shows, the lower sandstone bed has a substantially higher permeability than the upper sandstone bed. Once a value of porosity was calculated for a certain grid point, the crossplot was used to obtain an initial estimate of permeability for that point. The initial permeability input grids are located in Appendix V.

Only four core analysis reports were located for the

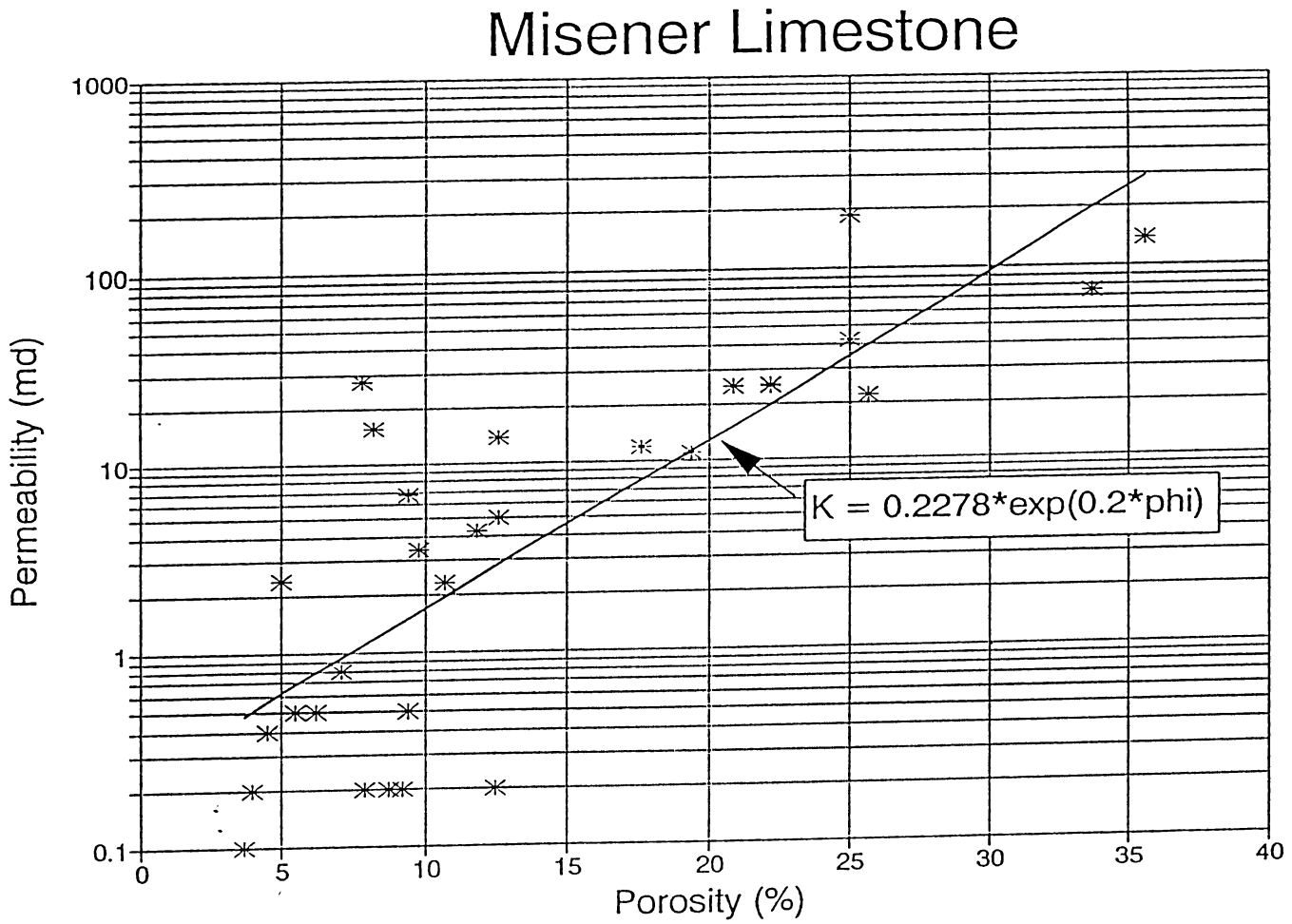

Figure 7.1 Permeability Versus Porosity Crossplot for Misener Limestone

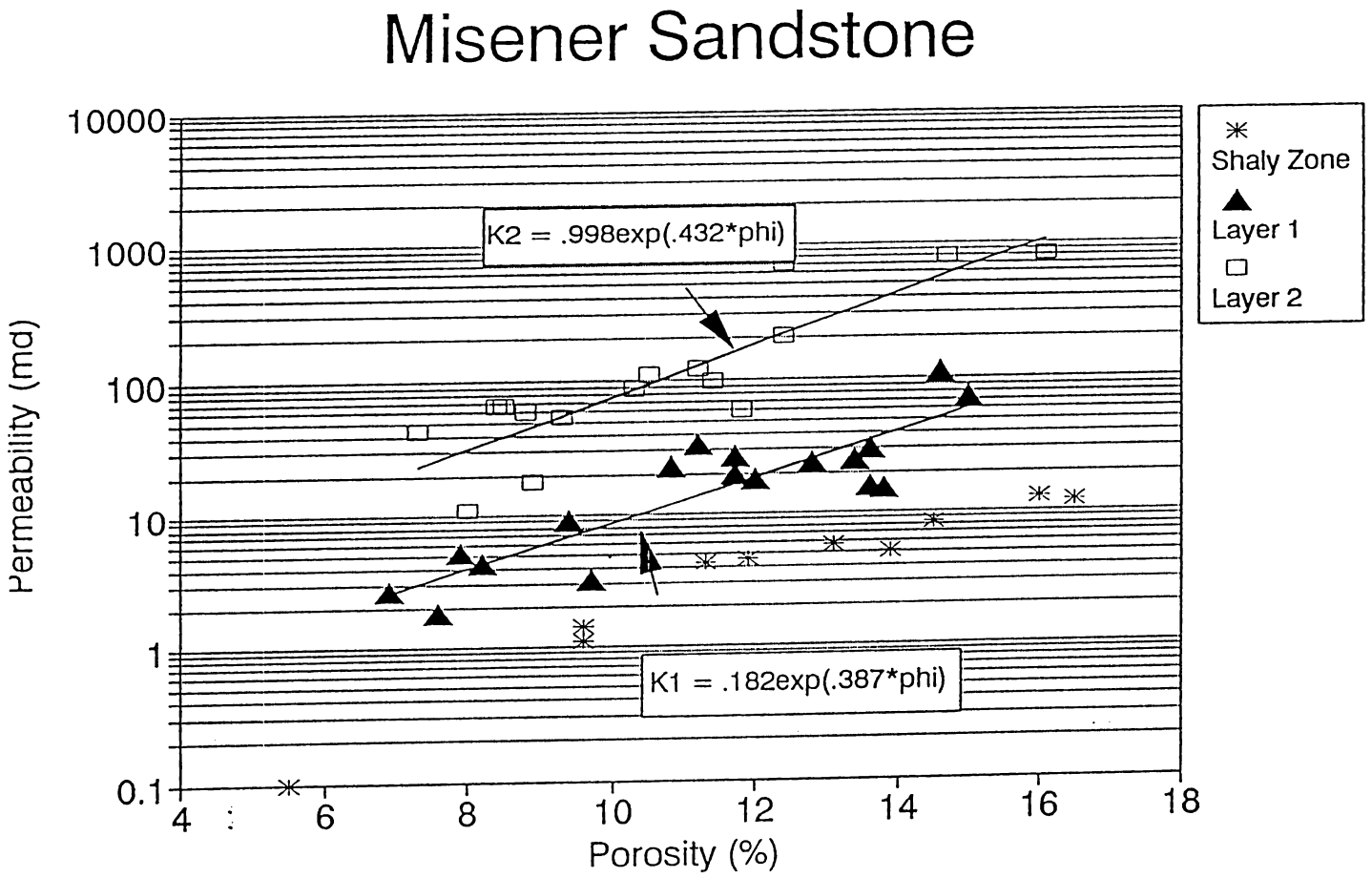

Figure 7.2 Permeability Versus Porosity Crossplot for Misener Sandstone

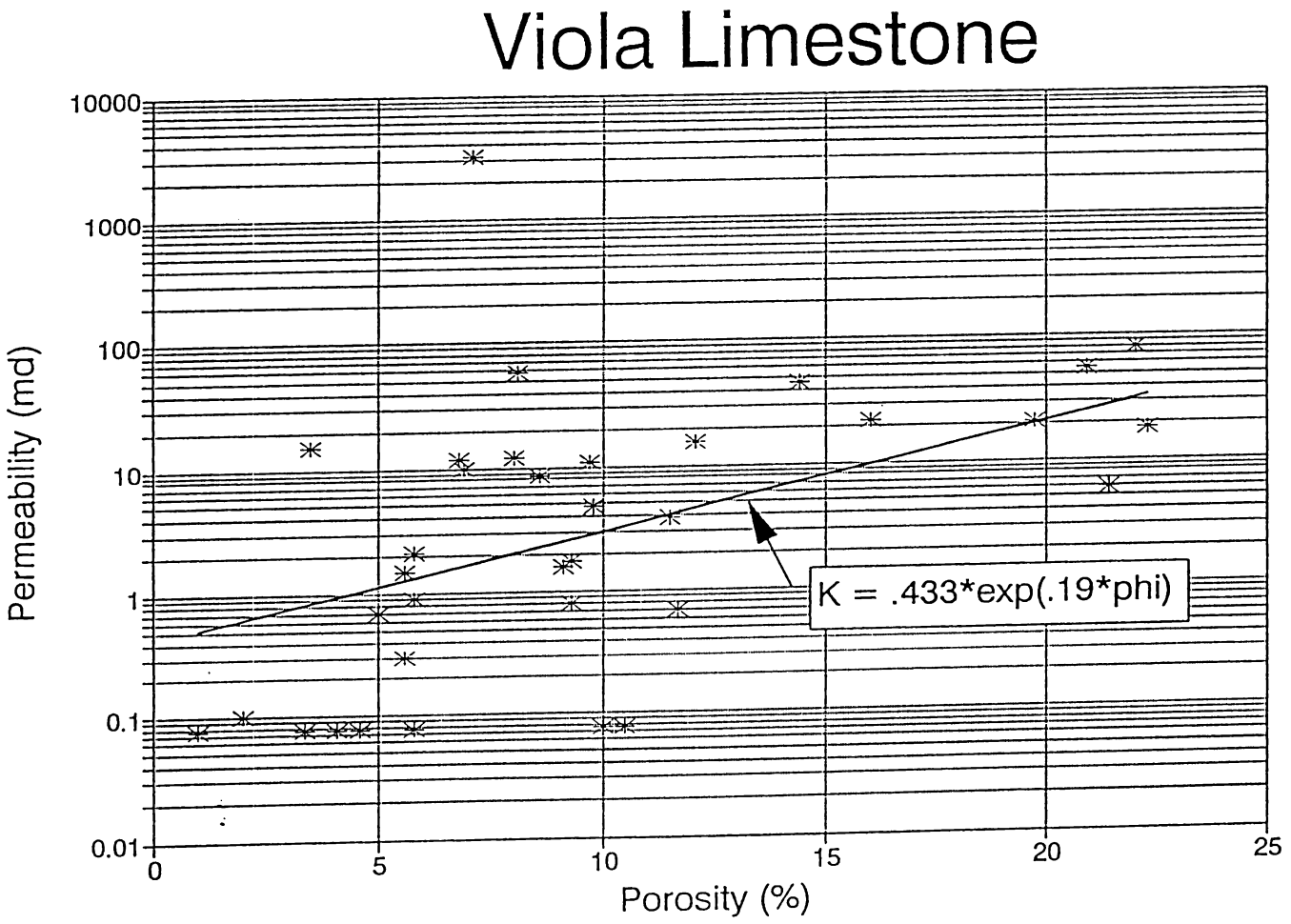

Figure 7.3 Permeability Versus Porosity Crossplot for Viola Limestone

entire Zenith Field. This, along with the uncertainty in the porosity estimation, leads to the conclusion that the values obtained for absolute permeability are very questionable.

Even with the uncertainty, it was felt that the permeability estimates for the Misener Limestone, the Maquoketa Dolomite, and the Viola Limestone could be input into the simulator, while the fracture characteristics of these formations could be adjusted to obtain a history match. The permeability estimates for the Misener Sandstone were input initially. However, the matrix permeability of the sandstone was one of the parameters varied in trying to history match the reservoir.

Relative Permeability

The only relative permeability data available from the core reports were average endpoint effective permeabilities for the Misener Sandstone. These data indicated a relative permeability to water at residual oil of approximately 15 percent and a relative permeability to oil at connate water of approximately 70 percent. Not much confidence was placed in these values since they came from only one core in the field. They were used only as verification of the end points calculated from correlations that were used to estimate the relative permeability curves. (Honarpour et. al., 1982) These correlations predict the relative permeability of water, oil, and gas, as a function of

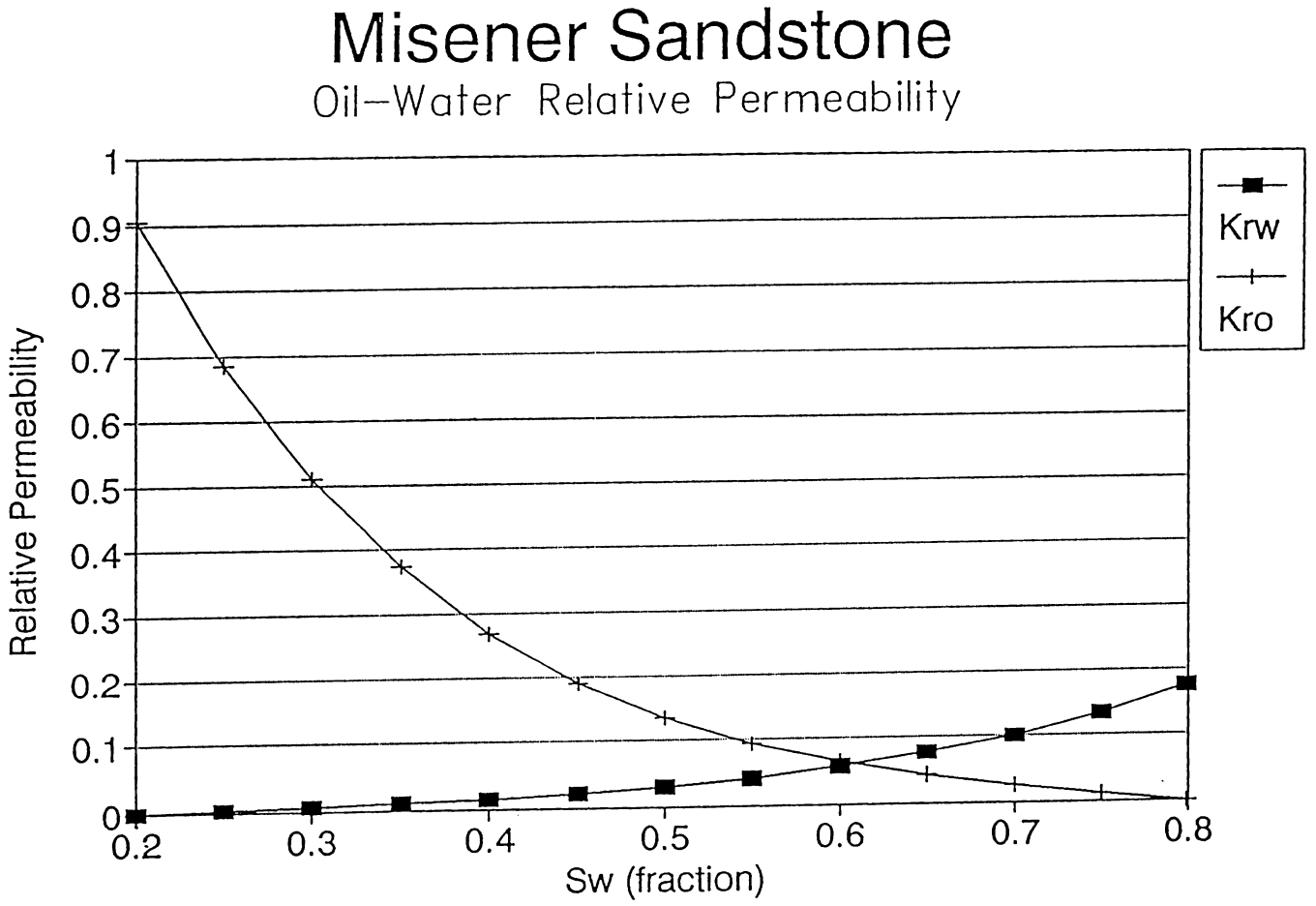

Figure 7.4 Initial Relative Permeability Input for the Misener Sandstone

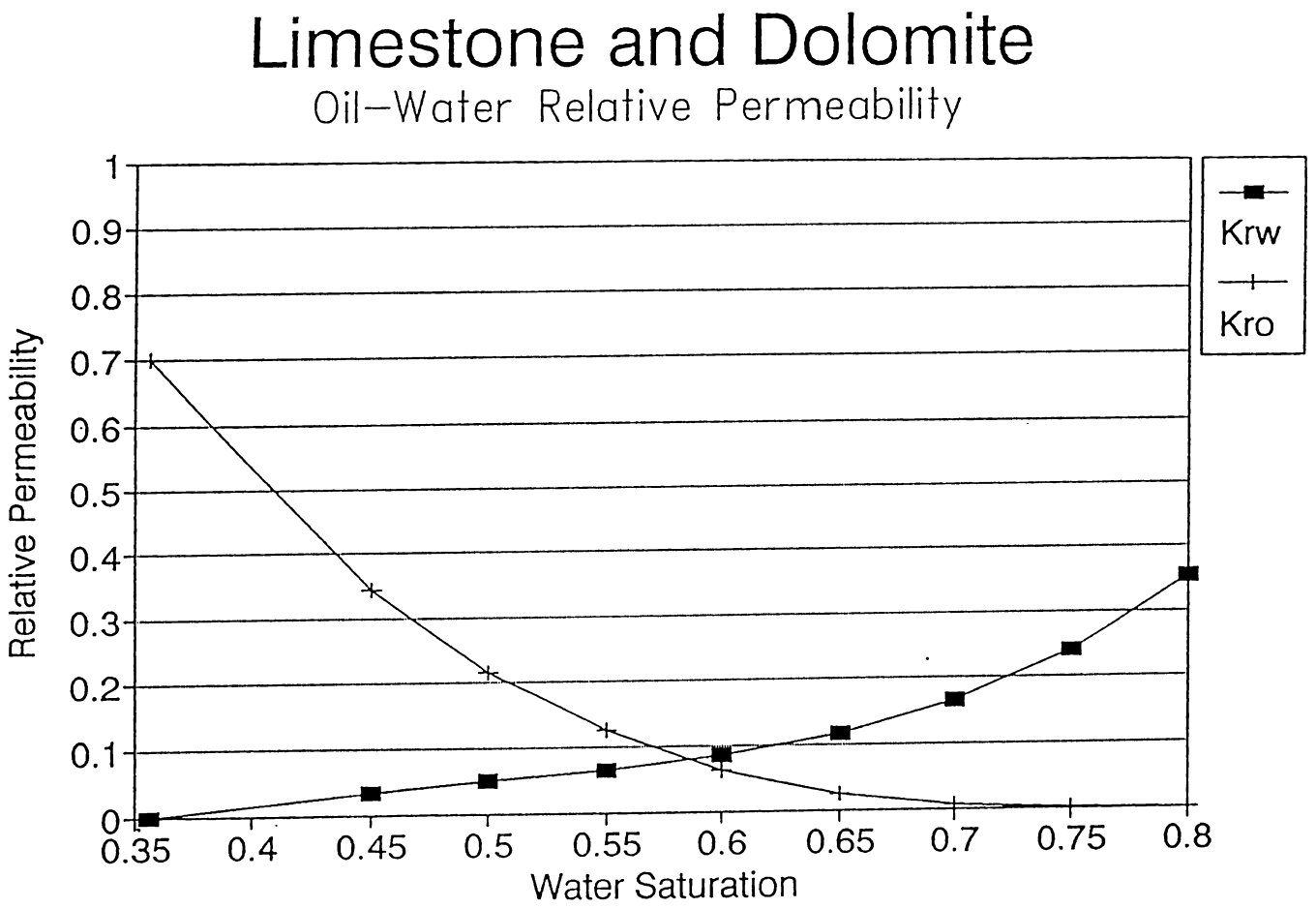

Figure 7.5 Initial Water-Oil Relative Permeability Input for the Carbonate Formations

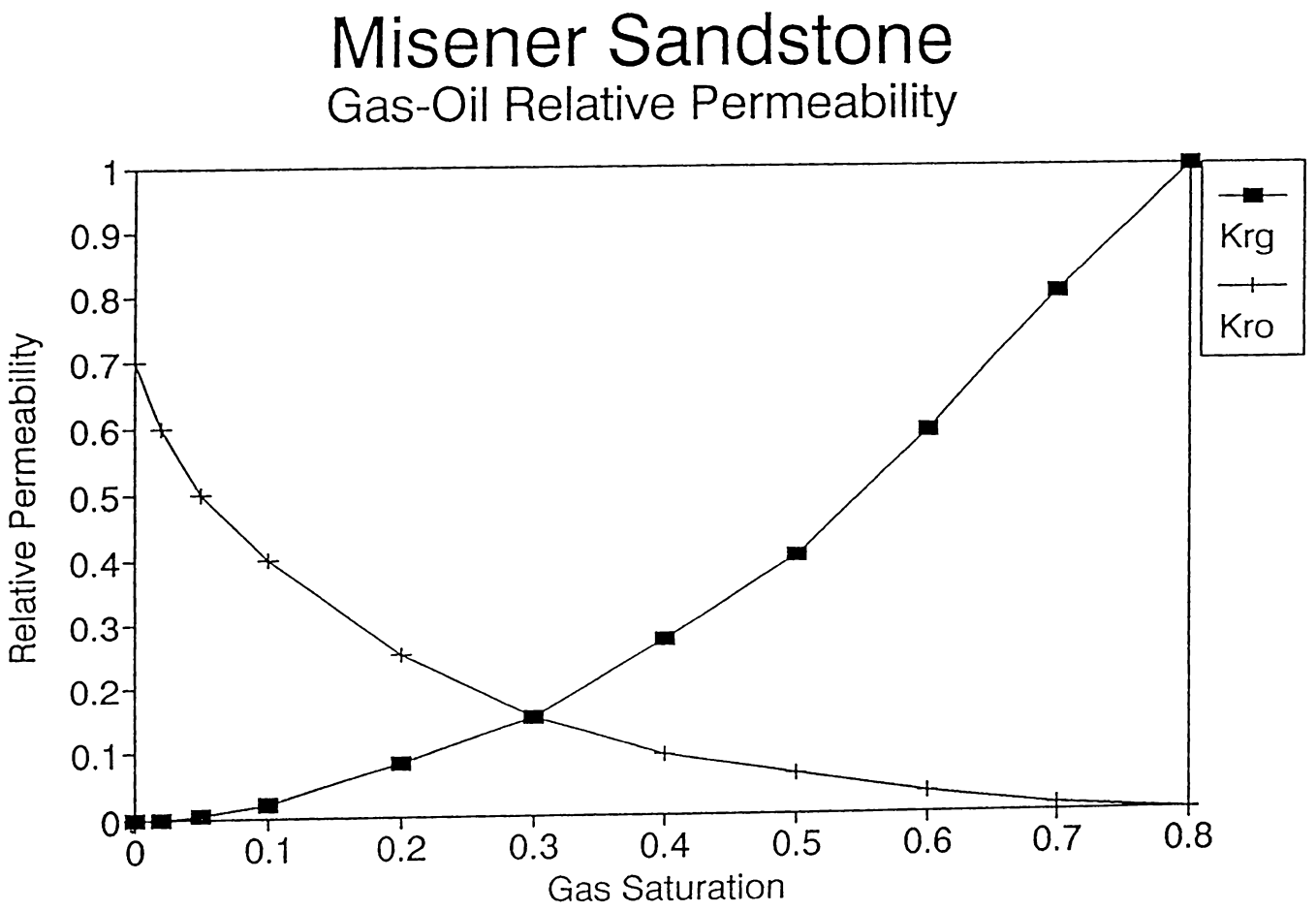

Figure 7.6 Initial Gas-Oil Relative Permeability Input for the Misener Sandstone

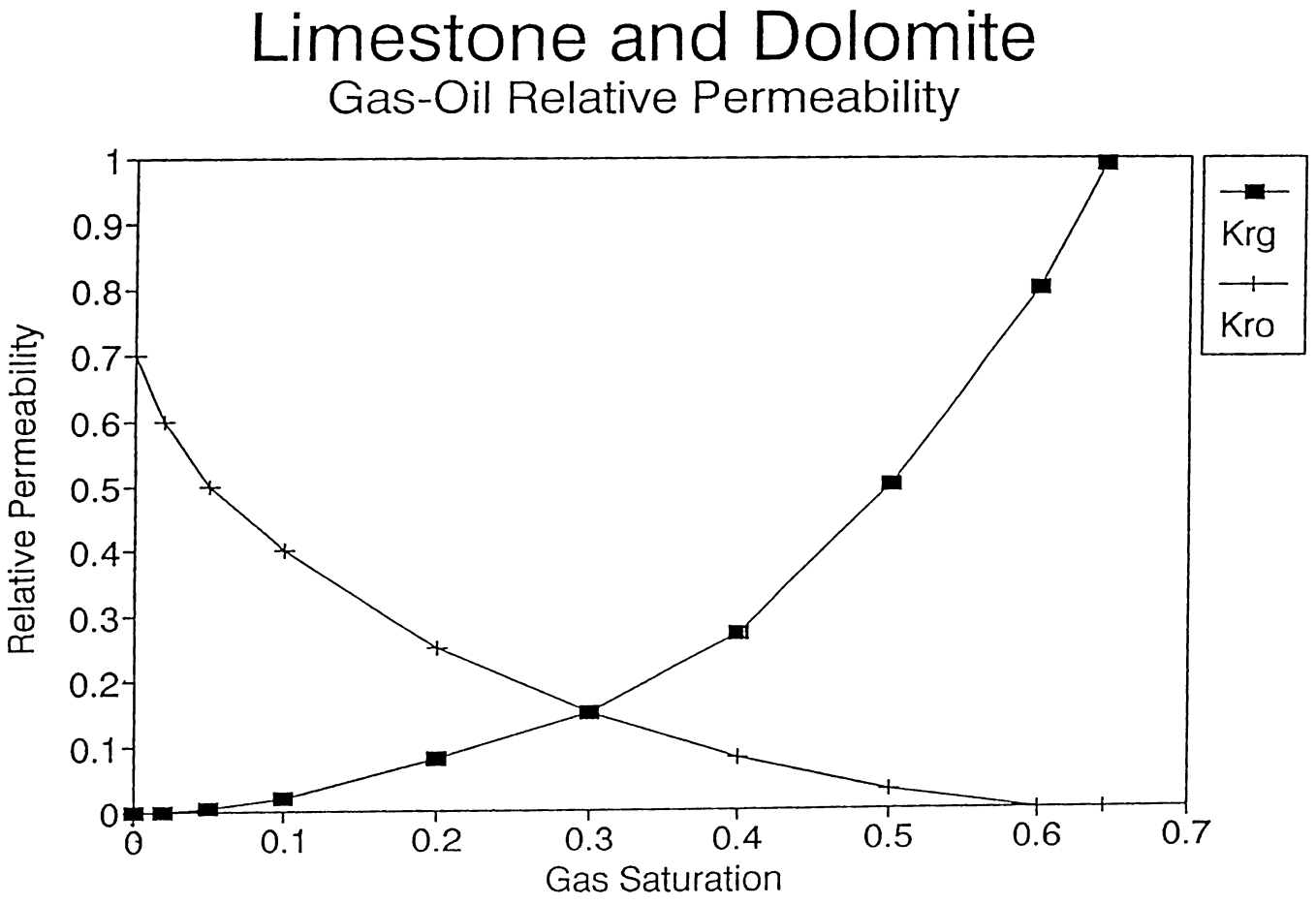

Figure 7.7 Initial Gas-Oil Relative Permeability Input for the Carbonate Formations

several variables, including saturation, fluids in the system, lithology, wettability, residual saturations, and in some cases porosity. Figures 7.4 through 7.7 show the water-oil and gas-oil relative permeability curves for limestone and sandstone lithologies. These curves were used as a starting point, and were changed during the course of the simulation in order to history match actual behavior.

Fractures

Fractures are believed to exist in the Viola Limestone, and possibly in the Maquoketa Dolomite, the "Fernvale," and the Misener Limestone. Evidence that the Viola is fractured comes from references to vertical fractures in four core reports, as discussed previously, and the very high initial potentials reported in the early stages of the field's development. The other carbonate formations are believed to be fractured because of results from simulation studies which will be discussed later.

Very little is known about the characteristics of the fractures in the Viola Limestone. No field tests were conducted in which the Viola was examined exclusively. Fracture spacing, porosity, and permeability, which the model needs as input, are all unknown. An attempt was made to use the radial model available with the VIP simulator to simulate a single well in the Zenith Field. This was done to obtain an estimate for the values of fracture spacing

and fracture permeability that would yield the indicated initial potentials reported in the field. The simulation performed was on a representative well in the northwest quarter of section 13. The initial potentials in this quarter section were reported to be between 10,000 and 30,000 STB/day and are the highest in the field. According to the model, a fracture spacing of fifty feet and a fracture permeability of 2000 md would yield an initial production rate of 22,000 STB/day in this quarter section at an initial reservoir pressure of 1100 psi and a bottom hole pressure of 600 psi. The bottom-hole pressure of 600 psi was selected after analyzing the initial potential test data that were available.

A method to estimate fracture spacing and permeability was found in a paper written by Sener (1987). In the paper, he estimates fracture characteristics using initial production potential data, reservoir thickness, and qualitative geological information, most of which are available for the Zenith Field. A general discussion of the calculation process is given below.

The basic calculation procedure is to use the areal variation of initial production potential as a relative indicator of fracture spacing and permeability. The smallest fracture spacing is given to the area of the field with the largest initial potentials. For the Zenith Field, initial production potential was averaged on a quarter

section basis. The area of highest initial potential is in the northwest quarter of section 13. Therefore, the 50 foot fracture spacing and the 2,000 millidarcy fracture permeability calculated from the radial simulation were assigned to this quarter section. Fracture spacing and fracture permeability for the rest of the field are calculated through a transformation of initial potentials, reservoir thickness, and dimensionless fracture width. The resulting grid of fracture spacing is presented in Table 7.3. As the table shows, the maximum fracture spacing was calculated to be larger than the grid block size in some grid blocks. This indicates that the Viola is not fractured in those areas. Fracture permeability only varied between 1,800 and 2,000 millidarcies, so a constant value of 2,000 millidarcies was used.

Table 7.3 Fracture Spacing Input into Model

2778	1558	2134	1350	3294	4395	1108	665	75
2888	197	81	69	69	2370	1360	498	76
529	308	76	53	223	1172	1049	1711	204
5138	288	219	111	198	162	124	1617	1350
6489	695	593	72	56	50	74	58	147
1070	1204	546	121	126	104	84	111	182
909	1029	789	123	134	105	110	115	187
720	786	1058	173	122	117	147	153	185
587	579	944	141	190	153	169	196	212

7.1.3 Aquifer Data

Little is known about the extent or the strength of the aquifer. The water-oil contact in the reservoir is at -2019 ft sub sea. Water-cut maps were prepared by an engineering committee in 1942. These are shown in Appendix II. From the June 1940 and January 1941 maps, which were made before many wells were deepened into the Viola, it appears that the water that is entering the Misener Sandstone is coming in through the northwest quarter of section 24 and then spreading through the rest of the sandstone. Figure 7.8 shows that this is the area where the southern lobe of the Maquoketa Dolomite is in communication with the Misener Sandstone. This will be discussed further in a subsequent section.

Aquifers are modeled by the Carter-Tracy method. Aquifer data is input into VIP in the form of several parameters describing aquifer strength and extent. These parameters are Binf, Tc, and a table of dimensionless time versus dimensionless pressure. They are defined as follows:

$$B_{inf}=\frac{2*\pi*\phi*C_t*h*r_e^2*s}{5.6146}$$

and

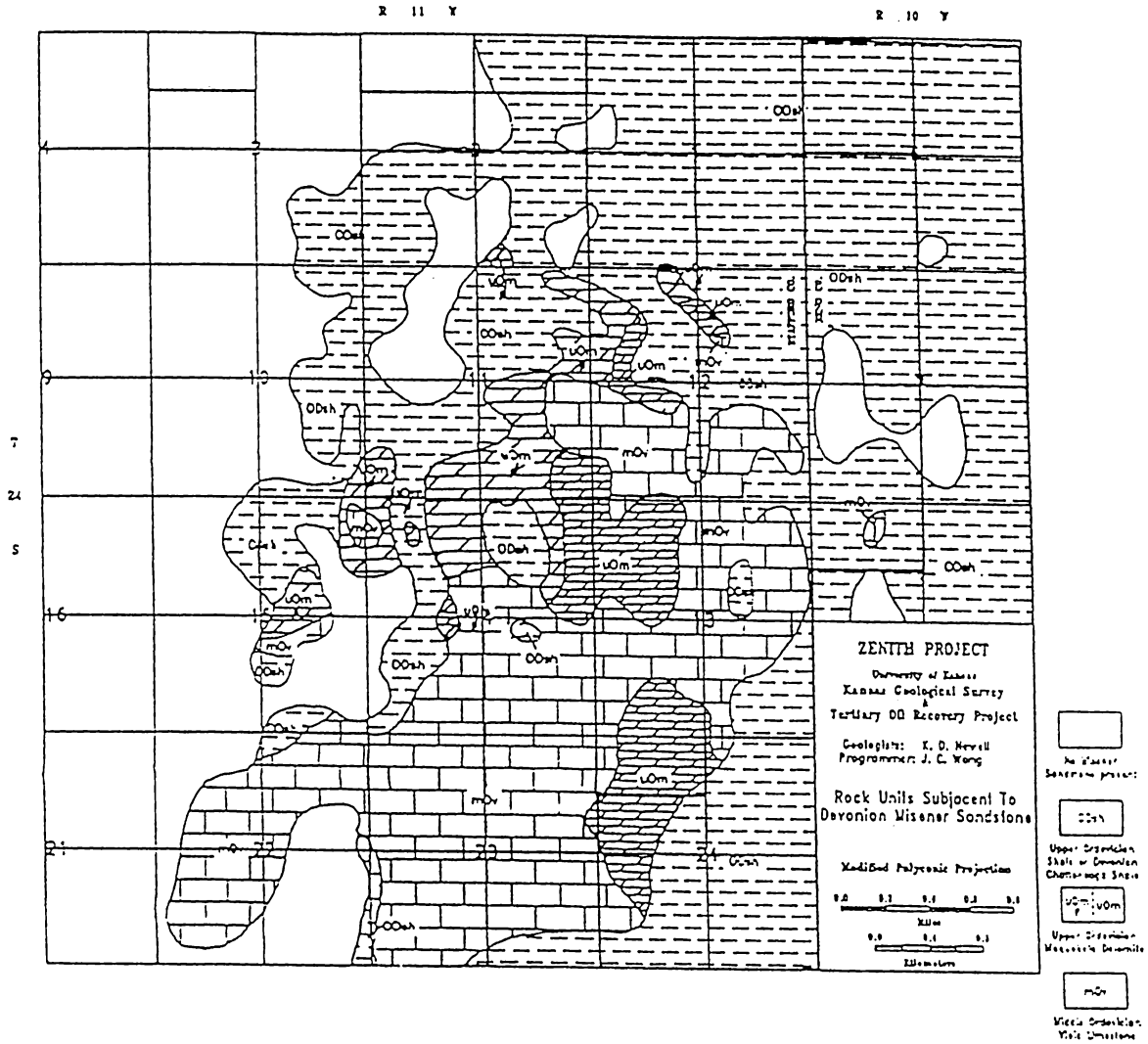

Figure 7.8 Rock Units Subjacent to the Misener Sandstone (TORP-KGS, 1991)

$$T_c = \frac{0.006328 * K}{c_t * \phi * \mu * d^2}$$

where: B_{inf} = Parameter B1 as defined by Carter and Tracy, rb/psi.
ϕ = Average Porosity of the Aquifer, frac.
c_t = Total Compressibility of the Fluid and rock in the Aquifer, 1/psi.
h = Net Thickness of the Aquifer.
S = Fraction of a Circle that the Boundary Between the Reservoir and the Aquifer Completes.
r_e = d = Radius to the Boundary Between Reservoir and the Aquifer, ft.
t_c = Value used to Convert Time to Dimensionless Time, 1/day.
k = Average Permeability of the Aquifer, md.
μ = Viscosity of the Fluid in the Aquifer, cp

The values of BINF and Tc were initially set to 4390 and 8E-04 respectively which correspond to an aquifer permeability of 30 md, a net thickness of 30 ft, and a porosity of 10 percent. The values of dimensionless time versus dimensionless distance are a function of the aquifer extent and are found in the Petroleum Engineering Handbook. (Bradley, 1987) The values listed in the input data file are for a dimensionless radius (aquifer radius divided by field radius) of 2.5. Due to the lack of knowledge of the aquifer, these values were adjusted over a large range during the history match.

7.1.4 Fault Data

A fault is known to exist on the eastern edge of the reservoir. Figure 7.9 shows a structure map of the top of the Viola. The fault can be seen by the dense grouping of the contour lines in the east and southeast portion of the field. The transmissibility across the fault was not known, so this was another parameter to be adjusted in the history match.

7.1.5 Well Data

The only data available on individual wells were the depths to the tops and bottoms of formations obtained from driller's logs. No oil or gas production was available for individual wells during primary production. Pressure data were limited to about a dozen initial potential tests. These tests did not include all of the pressure data and therefore could not be analyzed to calculate a permeability. It is known that large acid treatments were performed on the wells in order to increase their allowable. However, because of the large grid size, it is impossible to incorporate this type of information since production data for individual wells is not known.

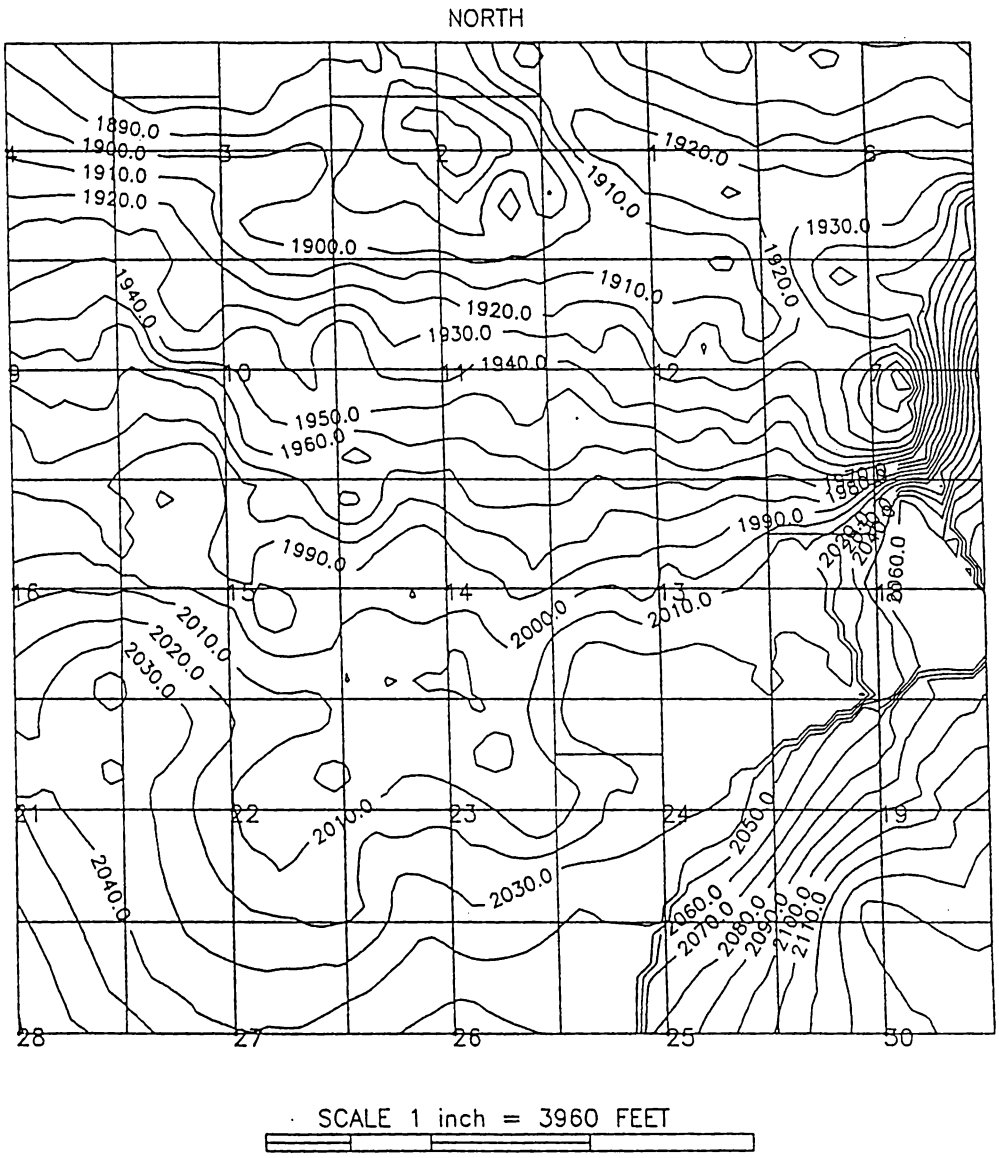

Figure 7.9 Sub-Sea Structure Map of Viola/Maquoketa Top

7.1.6 Production Data

Oil production rates were required to be input so that the field could be history matched with pressures, water cuts, and gas-oil ratios. The available production data were monthly oil sales by lease. Where necessary, lease production data were combined to obtain monthly oil production by quarter section since the model calculation was done with grid sizes of a quarter section.

Because of the large number of wells and the very large amount of work required to input the production rates each month, the data were averaged over yearly intervals. These data were then divided by 30.5 to get an average daily production rate and then by the number of wells in the quarter section to obtain average production rates for individual wells for a specific year. Figure 7.10 shows the actual cumulative oil production reported by the 1942 engineering study versus the cumulative oil production calculated by the model. The agreement between the two curves is very good.

7.2 Data Available for History Matching

The plan to simulate the Zenith Field was to input production rates, and then try to match predicted pressures, water volumes and gas-oil ratios with actual

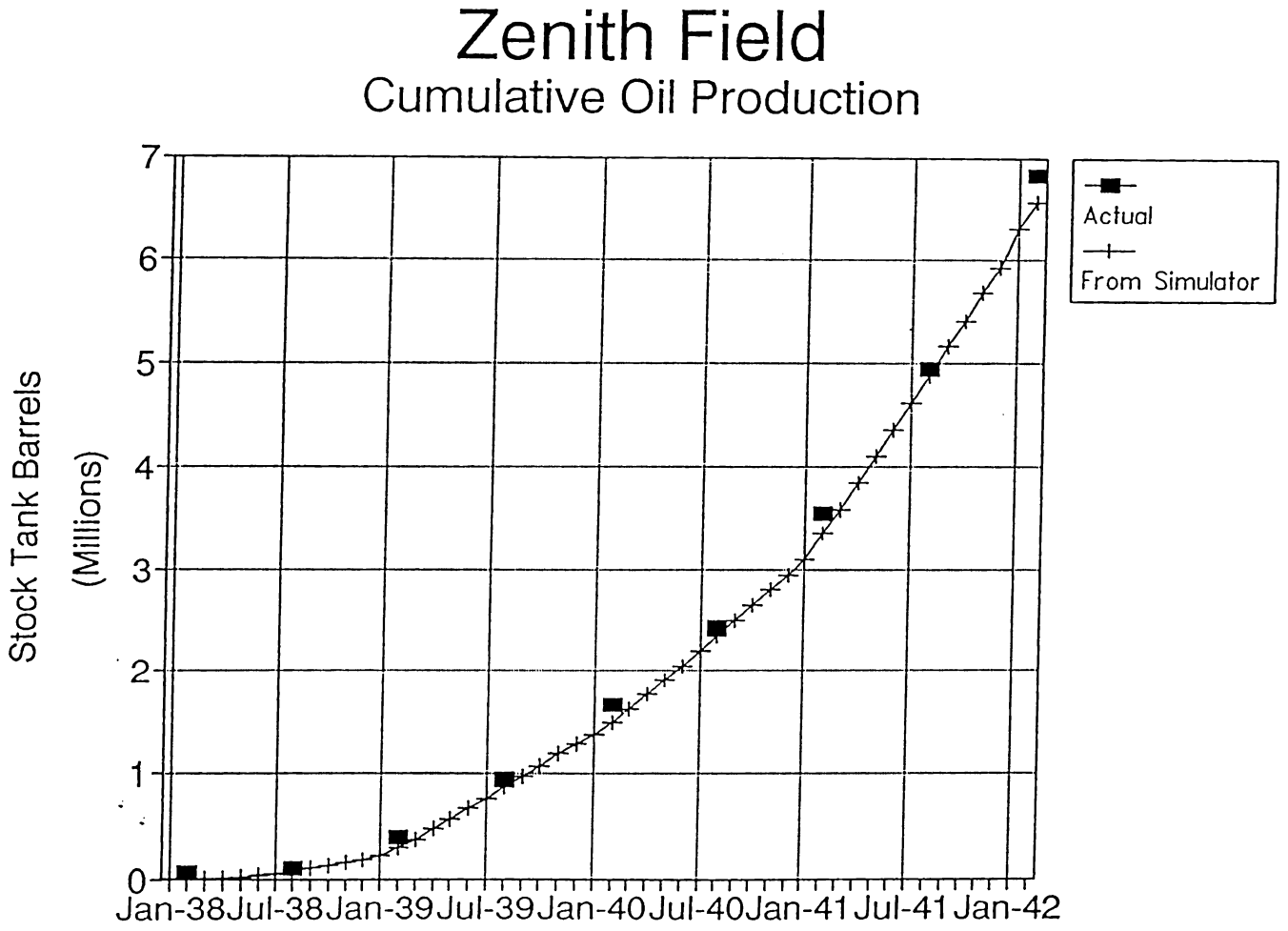

Figure 7.10 Cumulative Oil Production Versus Time in the Zenith Field, 1938 - 1942

field performance. To do this data describing the actual field performance were needed. The data were found through the data search conducted by the Tertiary Oil Recovery Project and the Kansas Geological Survey of the University of Kansas. (TORP-KGS, 1991) The data found consisted of field pressure maps, water cut maps, and plots of field oil, gas and water production versus time.

7.2.1 Isobaric Maps

Pressure maps were constructed for the Zenith Field at approximately six-month intervals by an engineering committee in 1942. These pressures are reported at a sub-sea datum of -1900 feet and are shown in Appendix II. A map was also constructed for a unitization hearing in 1944 and is the last pressure map available during primary production.

It is not known by what method the pressures were measured to make these maps. It is assumed that they indicate the final pressure after a twenty-four hour build-up test as this was a standard procedure used during the time period in question. Because of this uncertainty, the pressures reported can only be used as approximate values. Therefore, in the history match of the pressures, a calculated pressure within ten percent of the reported total drawdown to that point was assumed to be acceptable.

Fortran computer programs were written to extract data from the output file created by VIP and to reformat it into a useable form. The Fortran program created to output a pressure grid was MAP.FOR (Appendix IV). This program calculates a pore-volume weighted pressure for each (x,y) location in the grid. At given time steps, this pressure was subtracted from the actual reported pressure and a pressure difference grid was created. The program also calculates an absolute average pressure difference, which gives an indication of how close the predicted pressures are on a field wide basis. More discussion about the use of the pressure maps in history matching will be given in a later chapter.

7.2.2 Water Cut Maps

Maps that show the water cut of oil producing wells were also prepared by the engineering committee in 1942. These maps are in approximately six month intervals and are located in Appendix II. The last map available is from July 1942. These maps show that water encroachment primarily came from the south until 1942, after which the Viola was discovered and water started being produced over most of the field.

Since the grid size for the simulation was 160 acres, the water cut for each quarter section was taken as an

estimated average over the entire quarter section in order to match the predicted water cuts with the reported water cuts.

7.2.3 Production History Plots

Also available from the 1942 engineering committee report were plots of cumulative oil production versus time, cumulative water production versus time, and gas-oil ratio versus time. These plots are shown in Figures 7.10 through 7.12.

The cumulative oil production plot was mentioned previously, and the simulator provided a good match of oil production. The cumulative water production plot, along with the water cut maps, were intended to be used to obtain a realistic match of water production.

Little gas production data were available. A plot of gas-oil ratio versus time was one of the data sources originally intended to be used in history matching the field. A map of GOR over the field for 1942 and 1944 was also available. However, the reported gas-oil ratio for wells in a given quarter section varied by a large amount, in some instances by several thousand standard cubic feet per stock tank barrel. This individual well variation could not be predicted since the grid size in the simulation was so large. Because of this, it was felt that

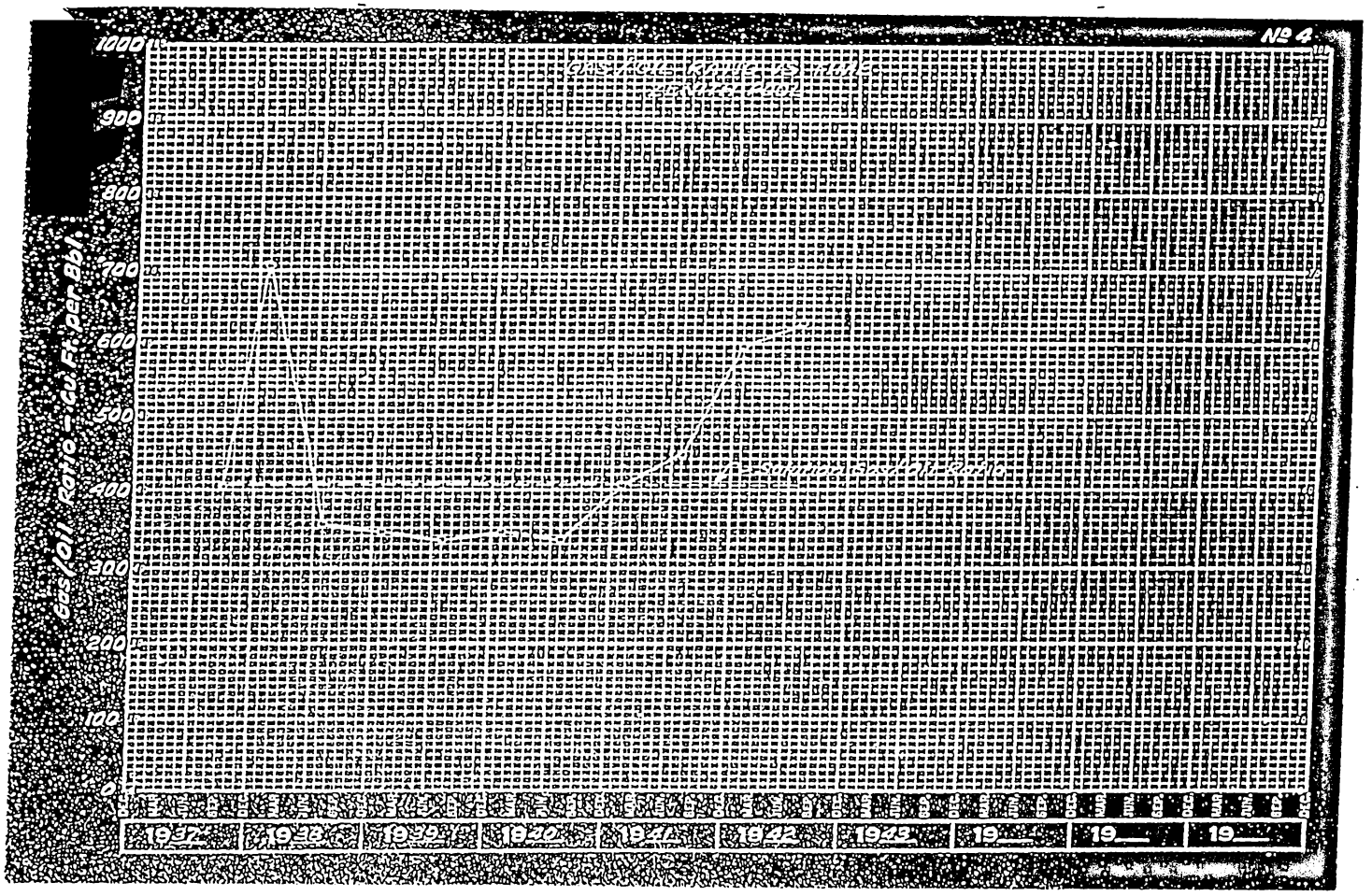

Figure 7.11 Zenith Field Producing Gas-Oil Ratio, 1938 - 1942

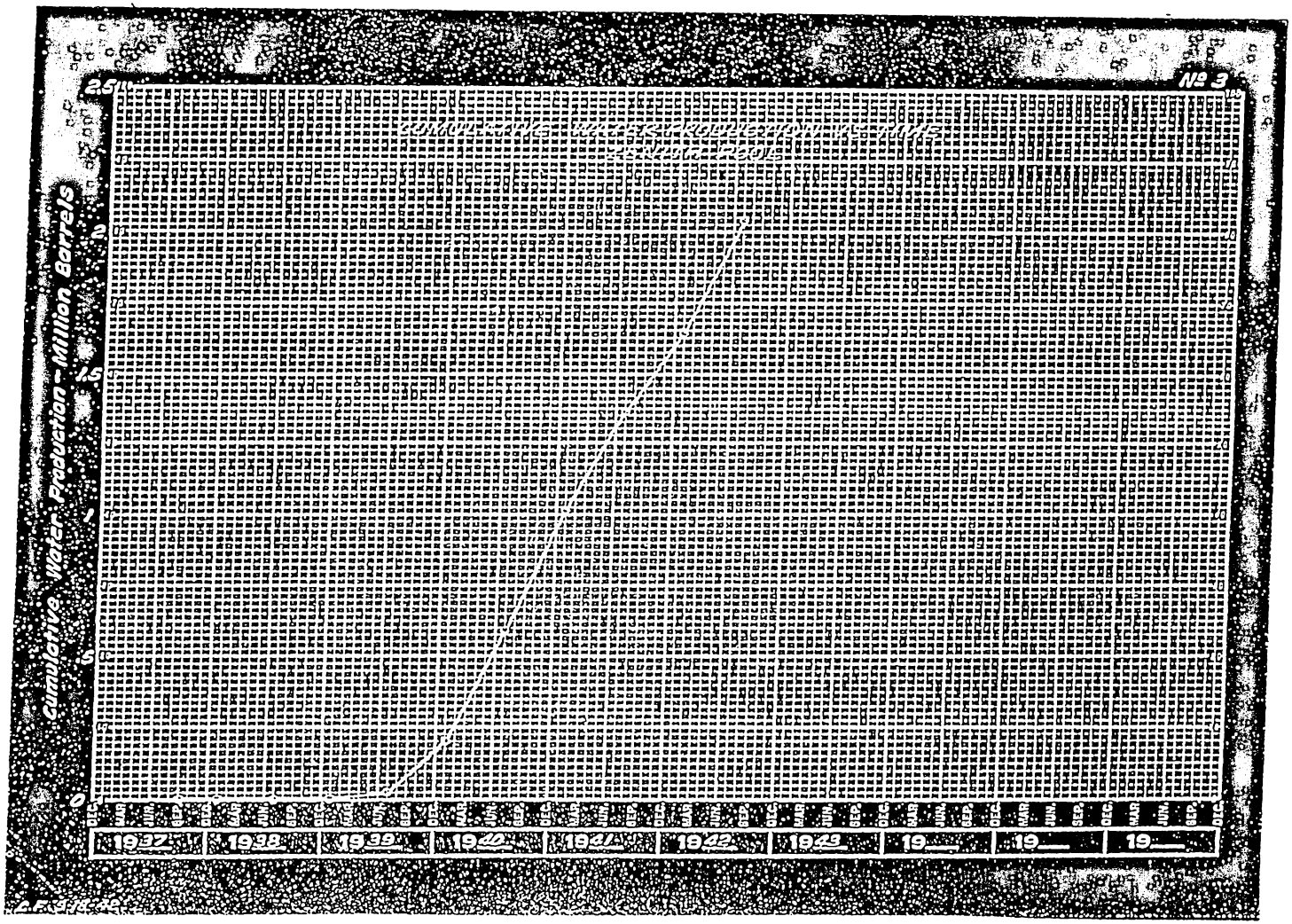

Figure 7.12 Cumulative Water Production in the Zenith Field, 1938 - 1942

a match of total field GOR would be sufficient for the history match of gas production.

Chapter 8. History Match of Primary Production in the Zenith Field

8.1 Introduction

The Zenith Field is a complex reservoir with a large amount of oil that could potentially be recovered. It was the purpose of this project to create a simulation of primary production in the Zenith Field. This model was to be used in another project to simulate secondary recovery. It was intended to use these models to estimate where recoverable oil may be located in the Zenith Field.

In this chapter the procedure that was used in simulating the Zenith Field is described. The results from the first two years history match are next presented followed by a discussion of the steps that were taken in order to obtain those results. The reliability of the history match and problems encountered when history matching the Zenith Field are included where appropriate. A discussion of the simulation of the remainder of primary production is presented finally.

8.2 Simulation Procedure

8.2.1 Initial Procedure

There are five different producing formations in the Zenith Field. Production was commingled and thus production could not be assigned to individual formations. However, the Misener Limestone and the Misener Sandstone were produced for two years before the Viola Limestone was discovered. It was felt that this information could be used to history match the different formations independently.

An initial simulation procedure was developed:

1. Use a grid block size of ten acres to match primary production in the Zenith Field. This would allow one well to be placed in each grid block.

2. History match production in the Misener Limestone for the first two years of production in the Zenith Field.

3. Add the Misener Sandstone and match the first two years of Sandstone production.

4. Add the Maquoketa Dolomite and the Viola Limestone and match primary production beyond the first two years.

With the above procedure, it was believed that a reliable match would be obtained because each of the formations would be modeled independently.

It was initially believed that the Misener Limestone and the Misener Sandstone could be modeled independently

because they were thought to have a small amount of commingled production. However, this proved not to be true and it was not possible to assign production to each formation in the center of the field where the zones overlap. Also, the pressure data available were in the form of pressure maps over the entire field. No individual formation pressure data were available. Trying to match limestone and sandstone pressures independently with this type of data was not feasible.

The initial grid size of ten acres was found to be too small to effectively match production. First, oil, gas, and water production for individual wells were not known. The production data available were in the form of monthly oil sales by lease. A typical lease size was half of a quarter section, and in some cases a full quarter section. The production allocated to an individual well would be the average production per well for each lease. With each well in a lease having the same production characteristics, it was felt that modeling the field on such a small grid size was not necessary.

Another problem with the small grid size was that very little was known about the producing mechanisms in the field. With the computer available during this study, a ten acre grid size would have resulted in very large computation time. Much of the information that was discovered through the simulation was obtained through a

trial-and-error history matching procedure. This involved running many different simulations. It was felt that if a ten acre grid size was used, the larger scale producing mechanisms of the field would have been more difficult to discover because of the decreased number of simulations that could be performed.

8.2.2 Final Simulation Procedure

Taking into account the problems with the initial simulation procedure, an alternate method was developed to model the Zenith Field. This method is similar to the one stated before. It utilizes the two years of Misener production before the Viola was discovered. There are two differences with this procedure. First, the Misener Limestone and the Misener Sandstone were to be modeled simultaneously for the period before the wells were deepened into the Viola. Second, the grid size was increased to 160 acres. The reasons for these changes were stated in the previous section. The rest of the procedure is as stated in the previous section.

8.3 History Match of Initial Two Years of Production from the Misener Limestone and Misener Sandstone

8.3.1 Result

Figure 8.1 shows a map of the actual pressures reported for the field in January of 1940. This map is taken from the January 1940 pressure map in Appendix II. Values of pressure for each quarter section were estimated and plotted on a nine-by-nine grid with "Surfer." Figure 8.2 is the final history match pressure map output by the Fortran computer program MAP.FOR. A comparison of the figures shows that the contours are of the same general shape and magnitude.

Table 8.1 shows the final history match pressure values at grid nodes for 181 days, 577 days, and 791 days, which correspond to May 1938, June 1939, and January 1940 respectively. Included in this table is a pressure difference for 791 days. The pressure difference is calculated by subtracting the actual field pressures, read from the January, 1940 iso-baric map, from the simulated pressures. The average absolute pressure difference is 8.13 psi at 791 days as indicated in the table. This value will be used to compare other simulations with the final match. The pressure difference map includes some zero values in places where there was no Misener Limestone or Sandstone present and also in areas where actual pressure

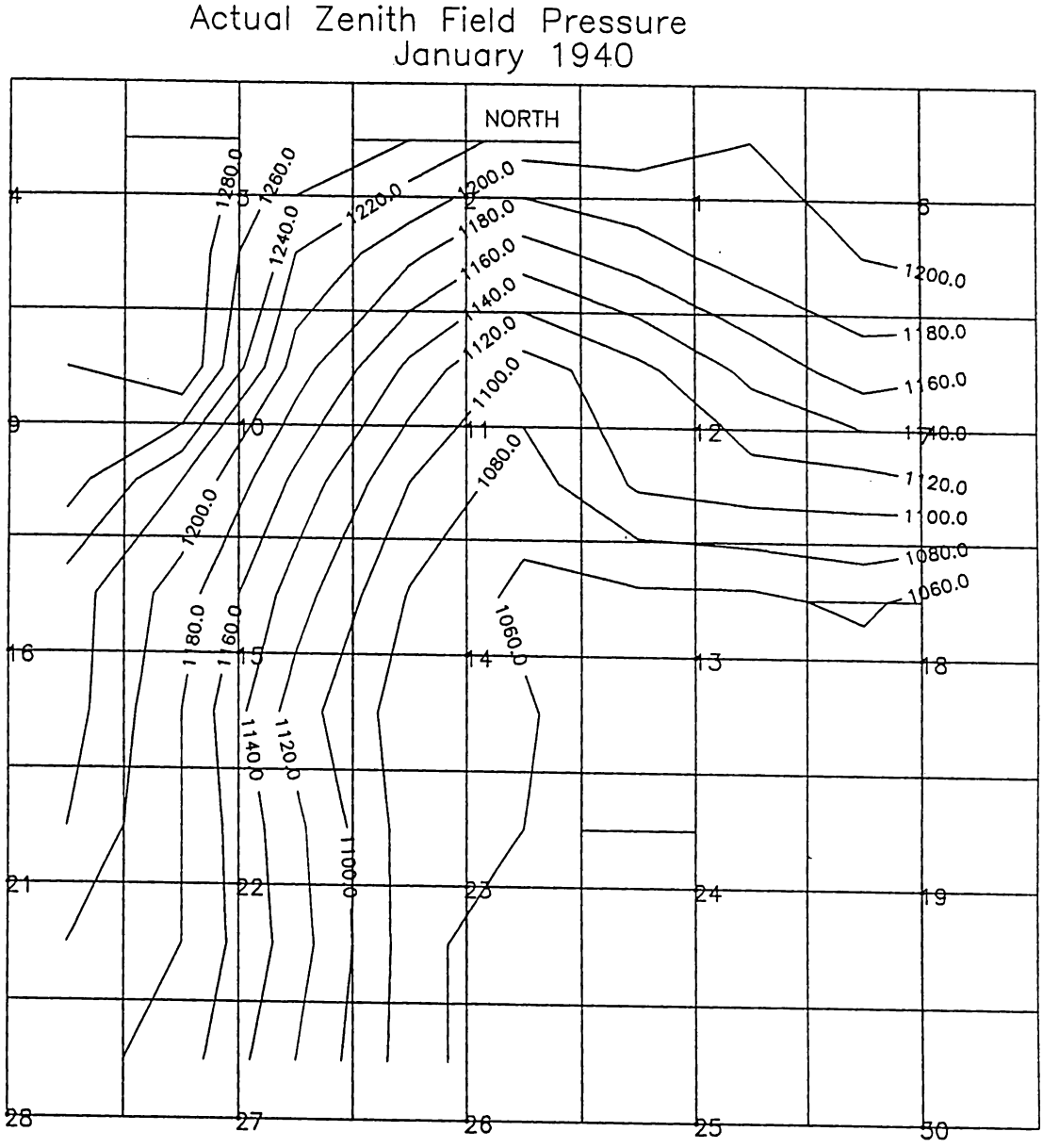

Figure 8.1 Actual Reported Pressures for the Zenith Field, January 1940

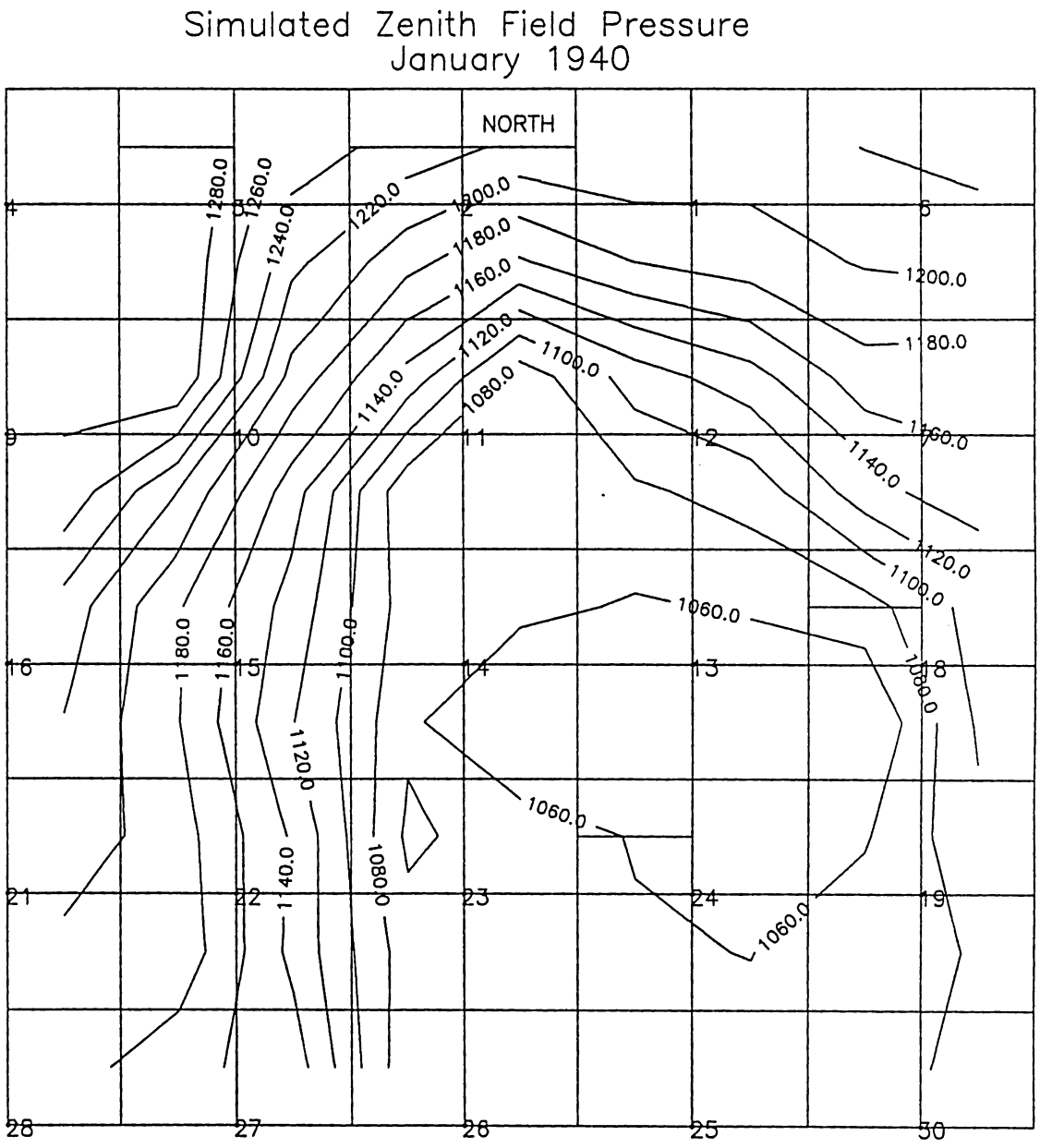

Figure 8.2 Final History Match of Pressures for the Zenith Field, January 1940

Table 8.1 Pressure Grid for Final History Match of First Two Years of Primary Production in the Zenith Field

TIME STEP = 0.0 TIME = 0.00 days
DATUM PRESSURE WEIGHTED BY TOTAL PORE VOLUME

0.00	0.00	1300.00	1300.00	1300.00	1300.00	1300.00	1300.00	1300.00
1300.00	0.00	1300.00	1300.00	1300.00	1300.00	1300.00	1300.00	1300.00
1300.00	0.00	1300.00	1300.00	1300.00	1300.00	1300.00	1300.00	1300.00
1300.00	1300.00	1300.00	1300.00	1300.00	1300.00	1300.00	1300.00	1300.00
1300.00	1300.00	1300.00	1300.00	1300.00	1300.00	1300.00	1299.99	1286.06
1299.99	1299.99	1300.00	1300.00	1300.00	1299.76	1299.99	1299.99	1286.07
1300.64	1299.83	1300.00	1300.00	1300.00	1299.79	1290.65	1286.08	1286.28
1287.60	1298.70	1299.99	1296.47	1298.89	1290.08	1285.98	1286.18	1286.36
1285.37	1285.93	1296.49	1285.99	1285.97	1285.94	1286.12	1286.24	1286.21

TIME STEP = 9.0 TIME = 181.00 days
DATUM PRESSURE WEIGHTED BY TOTAL PORE VOLUME

0.00	0.00	1299.98	1299.96	1299.83	1299.91	1299.89	1299.91	1299.93
1299.99	0.00	1299.94	1299.87	1299.24	1299.76	1299.82	1299.86	1299.87
1299.98	0.00	1299.74	1299.56	1297.55	1299.31	1299.51	1299.72	1299.69
1299.95	1299.76	1299.14	1298.26	1296.10	1298.73	1299.10	1299.22	1299.56
1299.38	1298.79	1297.69	1295.23	1294.53	1295.73	1296.68	1297.32	1285.36
1299.00	1297.68	1295.11	1291.33	1287.80	1293.58	1296.25	1296.94	1285.27
1299.25	1297.32	1293.11	1282.58	1294.75	1295.27	1287.76	1283.93	1285.19
1286.05	1296.63	1294.14	1286.46	1292.68	1285.00	1283.94	1284.64	1285.07
1283.69	1283.01	1292.13	1277.62	1279.57	1280.52	1284.37	1284.85	1285.05

TIME STEP = 25.0 TIME = 577.00 days
DATUM PRESSURE WEIGHTED BY TOTAL PORE VOLUME

0.00	0.00	1288.08	1280.22	1279.21	1284.66	1282.36	1284.65	1285.66
1297.04	0.00	1278.08	1256.23	1244.57	1272.87	1277.41	1279.83	1279.49
1296.64	0.00	1263.27	1211.61	1172.91	1241.88	1256.32	1269.64	1264.42
1293.33	1273.19	1237.79	1170.95	1170.88	1218.34	1237.08	1243.13	1256.94
1278.32	1256.76	1226.09	1171.83	1165.90	1161.79	1165.42	1176.09	1214.38
1272.31	1250.78	1210.82	1164.04	1135.93	1128.97	1130.78	1146.32	1210.02
1269.51	1255.74	1219.95	1154.15	1166.29	1160.34	1153.37	1165.99	1200.40
1254.44	1258.90	1220.03	1169.13	1172.01	1162.92	1167.85	1181.47	1190.32
1250.67	1236.27	1227.96	1164.51	1161.60	1161.53	1175.79	1186.31	1193.11

TIME STEP = 32.0 TIME = 791.00 days
DATUM PRESSURE WEIGHTED BY TOTAL PORE VOLUME

0.00	0.00	1250.22	1232.51	1214.87	1218.37	1209.67	1220.37	1227.82
1286.36	0.00	1225.36	1187.21	1157.74	1180.13	1190.25	1201.67	1206.53
1285.10	0.00	1193.31	1133.56	1067.59	1109.13	1131.85	1171.47	1167.38
1275.16	1220.09	1149.09	1065.40	1070.43	1076.56	1087.49	1131.34	1155.36
1231.91	1182.48	1131.71	1070.47	1065.46	1057.77	1063.93	1071.34	1108.68
1219.04	1181.12	1120.90	1064.42	1035.39	1025.75	1025.85	1039.10	1103.17
1212.14	1189.41	1137.30	1055.71	1071.71	1058.64	1047.10	1058.14	1094.44
1194.62	1194.66	1134.29	1069.36	1073.32	1062.39	1059.49	1072.03	1081.40
1189.54	1166.23	1150.56	1064.89	1061.60	1060.24	1066.93	1076.45	1082.41

PRESSURE DIFFERENCE AT 791 DAYS

0.0	0.0	-9.8	-7.5	-15.1	-1.6	-0.3	20.4	0.0
6.4	0.0	5.4	2.2	7.7	10.1	0.3	11.7	0.0
5.1	0.0	3.3	-1.4	-22.4	-4.9	-13.1	1.5	0.0
15.2	10.1	-5.9	-34.6	0.4	-26.4	-22.5	21.3	0.0
1.9	-7.5	1.7	-7.5	10.5	2.8	8.9	6.3	0.0
-11.0	1.1	10.9	-3.6	-27.6	-14.3	-14.1	-0.9	0.0
-7.9	9.4	12.3	-14.3	11.7	18.6	0.0	0.0	0.0
-5.4	14.7	9.3	-0.6	33.3	22.4	0.0	0.0	0.0
-0.5	-3.8	30.6	4.9	21.6	20.2	0.0	0.0	0.0

AVERAGE ABSOLUTE DIFFERENCE = 8.132894

values were not reported, such as the east and southeast portion of the field.

Table 8.2 lists values of actual and simulated water cuts for each quarter section that was producing water in January 1940.

Table 8.2 Water Cuts and Cumulative Water From Field Data and from Simulation for January 1940.

Sec. #	Water Cut (%) Simulated	Actual
SE 13	3.8	1
SW 13	21.8	20
SE 14	0.3	2
SW 14	4.4	4
NE 23	19.8	25
NW 23	6.2	10
NW 24	73.1	70
Total Water Production =	195,000 STB	200,000 STB

The actual values are an estimated average over each quarter section from the water cut maps presented in Appendix II. Also included is a comparison of cumulative water production at that point in time.

Field data indicate that the gas production was coming from solution gas at the end of the first two years of production. Gas-oil ratio was matched for the first two years with a value of 345 SCF/STB calculated by the simulator.

8.3.2 Steps Taken to Obtain History Match

This section will describe the steps taken and the parameters that were adjusted in order to obtain the history match indicated above. Where needed, a comparison to the final history match will be made by showing the pressure grids along with the value of the average absolute pressure difference.

Initial Input Data

Base data that were input into the simulator for the initial simulation were as follows:

1. A grid size of 160 acres was used for the simulation. This corresponded to a 9 X 9 matrix for the area being studied. Three layers were defined for the simulation. The layers were the Misener Limestone, and the two zones in the Misener Sandstone.

2. The Misener Limestone was given a fracture porosity of 0.005, a fracture permeability of 800 millidarcies, and a fracture spacing of 264 feet. The Misener Sandstone was assumed to not be fractured, so the fracture permeability and porosity were set to zero.

3. Matrix permeability and porosity were input as described in the previous chapter.

4. Rock and fluid properties were obtained as described in the previous chapter.

5. An aquifer was placed on the south side of the field, connected to grid blocks in row nine. The initial parameters for the aquifer, as described in the previous chapter, were:

$$B_{inf} = 4390$$
$$T_c = 8 \times 10^{-4}$$

6. One well was placed in each quarter section, with all of the quarter section's production coming from that well.

Addition of all Producing Wells to the Model

After initial simulations, it was found that the model was not producing enough oil as compared to the actual reported field production. The reason for this was due to summing production from all wells in a quarter section and then assigning that production to one well in the center of the grid block. The well in the center of the grid block needed a large pressure drawdown to produce the amount of oil that was required. Once the calculated bottom hole pressure had met a limit that was set in the input file, the oil production rate for that well was automatically reduced by the simulator. To correct this, the number of wells actually producing from the field were input into the model and the resulting oil production is as shown in Figure 7.10.

Adjustment of Bubble Point

Oil PVT data obtained from the 1942 engineering committee report indicate that the initial bubble point of the oil was 1100 psi with a gas-in-solution of 363 SCF/STB. The plot of field gas-oil ratio (GOR) versus time shown in Figure 7.12 indicates a value for solution gas of approximately 345 SCF/STB. This corresponds to a bubble point of 1000 psi from the PVT data available.

Simulations indicate that if a bubble point of 1100 psi is used, free gas is produced during the first two years of production. Gas relative permeability curves were adjusted, but the field GOR data could not be matched using a bubble point of 1100 psi. The bubble point was changed to 1000 psi, and a history match of GOR data was obtained.

Addition of Maquoketa and Viola

Initially, only the first two years of production in the Misener Limestone and the Misener Sandstone were considered. After initial simulation, it was found that the simulated pressures were far too low compared to those pressures actually reported. This indicated that too much fluid was being taken out of those formations. It was postulated that the Maquoketa Dolomite and possibly the Viola Limestone were contributing to the production during these first two years. These formations were added to obtain the history match reported previously. Table 8.3 shows a pressure grid resulting from no Maquoketa and Viola included in the model. Table 8.4 shows a pressure grid with Maquoketa added, but no Viola. As the tables show the average absolute pressure differences are 113.67 psi and 89.09 psi respectively compared to 8.13 psi obtained from the history match. Simulated pressures were far too low when the Maquoketa and/or the Viola were not added, indicating that too much fluid was being withdrawn from the Misener formations. The addition of the Maquoketa and

Viola provided more reservoir volume through vertical communication and an increase in simulated pressure resulted.

Since permeability of the matrix rock in the Fernvale is believed to be less than one millidarcy, this simulation indicates that the Fernvale is fractured since the Viola Limestone is believed to contribute to production.

The Maquoketa is present only in a portion of the Zenith Field. Therefore, some grid blocks had zero Maquoketa thickness. In those areas of no Maquoketa, there was a barrier to flow from the Viola to the Misener Sandstone. In order to allow communication between these two layers, 15 feet of a "pseudo" Fernvale were added to the grid blocks in the Maquoketa Dolomite's layer that did not contain any Maquoketa pay. This can be seen in the input file located in Appendix VI. The "pseudo" Fernvale was given a porosity of one percent and a permeability of 0.5 millidarcies. It did not contribute to the reservoir volume, but through fractures, it allowed communication between the Viola and the Misener Sandstone.

To control fluid movement from the Maquoketa and the Viola into the Misener Sandstone, the vertical permeability of the matrix and the fractures was adjusted. Vertical permeability was allowed only in areas where there was no shale above the Maquoketa or Fernvale. This area can be seen in the map of rock units subjacent to the Misener

Table 8.3 Pressure Grid for First Two Yeras of Production
with no Maquoketa Dolomite or Viola Limestone

TIME STEP = 0.0 TIME = 0.00 days
DATUM PRESSURE WEIGHTED BY TOTAL PORE VOLUME

0.00	0.00	1300.00	1300.00	1300.00	1300.00	1300.00	1300.00	1300.00
1300.00	0.00	1300.00	1300.00	1300.00	1300.00	1300.00	1300.00	1300.00
1300.00	0.00	1300.00	1300.00	1300.00	1300.00	1300.00	1300.00	1300.00
1300.00	1300.00	1300.00	1300.00	1300.00	1300.00	1300.00	1300.00	1300.00
1300.00	1300.00	1300.00	1300.00	1300.00	1300.00	1300.00	1299.99	1286.06
1299.99	1299.99	1300.00	1300.00	1300.00	1299.76	1299.99	1299.99	1286.07
1300.64	1299.83	1300.00	1300.00	1300.00	1299.79	1290.65	1286.08	1286.28
1287.60	1298.70	1299.99	1296.47	1298.89	1290.08	1285.98	1286.18	1286.36
1285.37	1285.93	1296.49	1285.99	1285.97	1285.94	1286.12	1286.24	1286.21

TIME STEP = 9.0 TIME = 181.00 days
DATUM PRESSURE WEIGHTED BY TOTAL PORE VOLUME

0.00	0.00	1299.94	1299.87	1299.54	1299.69	1299.50	1299.57	1299.60
1299.97	0.00	1299.80	1299.52	1298.05	1299.05	1299.21	1299.31	1299.27
1299.95	0.00	1299.05	1298.88	1293.76	1296.71	1297.63	1298.63	1298.25
1299.85	1299.13	1296.87	1293.04	1283.87	1293.78	1295.42	1295.98	1297.50
1298.65	1296.45	1291.99	1282.37	1270.06	1278.62	1282.58	1285.53	1281.56
1297.73	1293.34	1282.59	1256.55	1264.91	1277.06	1283.46	1285.14	1281.02
1297.78	1294.20	1284.09	1261.36	1270.85	1278.03	1276.29	1273.62	1280.33
1284.44	1294.18	1285.93	1269.30	1274.08	1267.05	1275.30	1278.88	1279.23
1281.91	1279.28	1285.49	1261.78	1262.42	1263.65	1277.18	1279.39	1280.08

TIME STEP = 29.0 TIME = 577.00 days
DATUM PRESSURE WEIGHTED BY TOTAL PORE VOLUME

0.00	0.00	1259.27	1234.41	1231.56	1246.33	1232.81	1239.88	1241.25
1289.96	0.00	1227.05	1167.28	1142.25	1208.72	1218.64	1224.12	1218.78
1288.62	0.00	1182.11	1088.33	992.88	1112.72	1152.40	1192.11	1163.00
1277.63	1213.10	1111.62	982.73	965.94	1063.86	1100.22	1120.90	1142.72
1223.37	1154.88	1074.84	975.79	929.16	921.30	897.77	952.77	1043.58
1204.00	1144.49	1048.66	944.76	907.72	892.88	897.74	935.28	1032.68
1192.58	1156.68	1074.83	950.07	914.14	917.84	928.34	942.60	1020.23
1171.58	1164.67	1060.40	956.92	941.69	920.44	949.67	981.99	993.71
1163.91	1123.55	1084.72	949.59	931.80	923.25	964.73	988.44	999.71

TIME STEP = 42.0 TIME = 791.00 days
DATUM PRESSURE WEIGHTED BY TOTAL PORE VOLUME

0.00	0.00	1180.50	1153.44	1127.93	1132.72	1116.76	1132.23	1140.36
1262.71	0.00	1136.82	1088.88	1050.78	1081.32	1092.84	1104.94	1104.08
1259.91	0.00	1080.29	1059.47	941.20	1001.05	1025.26	1062.02	1032.93
1238.40	1129.63	1016.74	942.35	901.83	954.11	972.12	988.57	1011.48
1124.06	1042.33	981.35	930.31	803.96	783.02	773.89	814.63	872.83
1101.01	1044.92	968.66	853.40	783.19	756.28	752.09	803.74	863.38
1087.53	1053.74	980.78	860.95	816.76	798.64	789.22	797.09	861.01
1066.23	1060.68	968.91	875.55	846.67	814.35	810.15	839.43	841.14
1058.85	1022.43	996.45	862.96	835.61	820.26	825.37	843.93	849.09

PRESSURE DIFFERENCE AT 791 DAYS

0.0	0.0	-79.5	-86.6	-102.1	-87.3	-93.2	-67.8	0.0
-17.3	0.0	-83.2	-96.1	-99.2	-88.7	-97.2	-85.1	0.0
-20.1	0.0	-109.7	-75.5	-148.8	-112.9	-119.7	-108.0	0.0
-21.6	-80.4	-138.3	-157.7	-168.2	-148.9	-137.9	-121.4	0.0
-105.9	-147.7	-148.7	-147.7	-251.0	-272.0	-281.1	-250.4	0.0
-129.0	-135.1	-141.3	-214.6	-279.8	-283.7	-287.9	-236.3	0.0
-132.5	-126.3	-144.2	-209.1	-243.2	-241.4	0.0	0.0	0.0
-133.8	-119.3	-156.1	-194.5	-193.3	-225.7	0.0	0.0	0.0
-131.1	-147.6	-123.6	-197.0	-204.4	-219.7	0.0	0.0	0.0

AVERAGE ABSOLUTE DIFFERENCE = 113.6670

Table 8.4 Pressure Grid for First Two Years of Primary Production with no Viola Limestone Included

TIME STEP = 0.0 TIME = 0.00 days
DATUM PRESSURE WEIGHTED BY TOTAL PORE VOLUME

0.00	0.00	1300.00	1300.00	1300.00	1300.00	1300.00	1300.00	1300.00
1300.00	0.00	1300.00	1300.00	1300.00	1300.00	1300.00	1300.00	1300.00
1300.00	0.00	1300.00	1300.00	1300.00	1300.00	1300.00	1300.00	1300.00
1300.00	1300.00	1300.00	1300.00	1300.00	1300.00	1300.00	1300.00	1300.00
1300.00	1300.00	1300.00	1300.00	1300.00	1300.00	1300.00	1299.99	1286.06
1299.99	1299.99	1300.00	1300.00	1300.00	1299.76	1299.99	1299.99	1286.07
1300.64	1299.83	1300.00	1300.00	1300.00	1299.79	1290.65	1286.08	1286.28
1287.60	1298.70	1299.99	1296.47	1298.89	1290.08	1285.98	1286.18	1286.36
1285.37	1285.93	1296.49	1285.99	1285.97	1285.94	1286.12	1286.24	1286.21

TIME STEP = 9.0 TIME = 181.00 days
DATUM PRESSURE WEIGHTED BY TOTAL PORE VOLUME

0.00	0.00	1299.94	1299.85	1299.25	1299.60	1299.53	1299.63	1299.67
1299.97	0.00	1299.80	1299.45	1296.54	1298.98	1299.27	1299.41	1299.42
1299.96	0.00	1299.24	1298.22	1289.14	1297.10	1298.00	1298.89	1298.66
1299.88	1299.32	1297.54	1293.67	1284.92	1295.17	1296.45	1297.08	1298.13
1299.11	1297.67	1294.41	1283.77	1283.15	1286.42	1287.18	1289.38	1283.25
1298.53	1296.07	1290.49	1279.32	1277.08	1285.29	1289.01	1289.90	1282.90
1298.69	1296.11	1289.57	1273.67	1282.70	1286.08	1281.24	1277.92	1282.40
1285.42	1295.67	1290.65	1278.90	1283.94	1275.76	1278.46	1280.80	1281.53
1282.97	1281.45	1289.26	1270.54	1271.56	1272.18	1279.50	1281.13	1281.82

TIME STEP = 24.0 TIME = 577.00 days
DATUM PRESSURE WEIGHTED BY TOTAL PORE VOLUME

0.00	0.00	1257.63	1232.76	1232.83	1249.41	1240.13	1247.39	1249.91
1290.63	0.00	1225.98	1166.06	1139.33	1215.59	1227.07	1233.47	1230.75
1289.38	0.00	1184.40	1070.34	980.67	1131.30	1168.53	1205.63	1183.84
1279.07	1216.54	1117.79	981.63	969.02	1084.22	1122.08	1143.13	1165.86
1240.53	1172.80	1086.90	967.00	961.81	963.32	963.39	991.44	1086.44
1223.60	1166.02	1067.78	961.99	940.00	932.80	942.20	964.96	1076.21
1214.36	1179.66	1095.95	966.61	956.39	956.98	965.27	985.10	1058.53
1194.72	1188.28	1085.34	974.54	966.15	953.92	986.22	1014.21	1032.13
1187.73	1148.32	1108.69	970.82	957.40	953.85	999.52	1021.73	1035.13

TIME STEP = 41.0 TIME = 791.00 days
DATUM PRESSURE WEIGHTED BY TOTAL PORE VOLUME

0.00	0.00	1178.68	1150.72	1130.95	1138.30	1124.44	1141.20	1151.52
1264.61	0.00	1134.70	1083.94	1046.61	1086.97	1100.21	1114.45	1117.50
1261.87	0.00	1079.36	1030.58	926.52	1005.72	1031.81	1074.46	1055.02
1240.80	1131.25	1015.73	930.69	915.12	973.88	986.05	1022.90	1039.65
1145.10	1055.44	983.11	909.58	902.14	902.24	907.13	926.37	943.36
1122.92	1064.80	978.76	902.28	871.34	862.96	866.94	900.91	936.53
1111.28	1078.66	1008.34	912.31	902.83	897.55	885.55	890.85	932.19
1091.32	1086.59	1006.26	928.68	919.16	900.80	892.38	907.34	915.03
1085.15	1053.23	1033.49	920.90	907.60	901.14	898.82	909.54	914.28

PRESSURE DIFFERENCE AT 791 DAYS

0.0	0.0	-81.3	-89.3	-99.0	-81.7	-85.6	-58.8	0.0
-15.4	0.0	-85.3	-101.1	-103.4	-83.0	-89.8	-75.5	0.0
-18.1	0.0	-110.6	-104.4	-163.5	-108.3	-113.2	-95.5	0.0
-19.2	-78.8	-139.3	-169.3	-154.9	-129.1	-123.9	-87.1	0.0
-84.9	-134.6	-146.9	-168.4	-152.9	-152.8	-147.9	-138.6	0.0
-107.1	-115.2	-131.2	-165.7	-191.7	-177.0	-173.1	-139.1	0.0
-108.7	-101.3	-116.7	-157.7	-157.2	-142.5	0.0	0.0	0.0
-108.7	-93.4	-118.7	-141.3	-120.8	-139.2	0.0	0.0	0.0
-104.8	-116.8	-86.5	-139.1	-132.4	-138.9	0.0	0.0	0.0

AVERAGE ABSOLUTE DIFFERENCE = 89.08847

Sandstone presented in Figure 7.8. The match was obtained with vertical permeabilities in the matrix varying from .5 to 5 millidarcies and from 10 to 500 millidarcies in the fractures. Changing only the vertical permeability worked to modify the pressures to a certain extent. However, once a certain vertical permeability value was reached, it no longer had a significant influence on the pressure.

Aquifer Strength and Placement

An aquifer exists to the south of the field. As mentioned in Chapter 7, little is known about the aquifer. Simulations do indicate that the aquifer played a role in pressure maintenance during primary production. Table 8.5 shows a pressure grid with no water aquifer included. The average absolute pressure difference is 42.72 as compared to 8.13 from the final history match. The difference in the average absolute pressure differences indicates that the aquifer had a substantial effect on pressure maintenance during the first two years of primary production.

Since it was discovered that the aquifer plays an important role in the field's production, an assumption about aquifer placement was made, and the aquifer strength was used as a matching parameter. A value for B_{inf} of 6,000 was used to obtain the reported history match. Figure 7.8 is a map of rock units subjacent to the Misener Sandstone.

The figure indicates that the Misener Sandstone and the Maquoketa Dolomite are in direct communication in NW Sec. 24. This is also the area in which water is being produced during the first two years of production as indicated by the water-cut maps in Appendix II. Therefore, it was decided to place the aquifer on the south edge of the Viola Limestone and have the water migrate through the Maquoketa Dolomite and into the Misener Sandstone in section twenty four.

The vertical permeability helped to control water movement into the Misener Sandstone, but only to a certain extent. Once the aquifer strength had reached its limit, changing the vertical permeability had little effect of water cuts or pressures. Therefore, a balance between aquifer strength and vertical permeability had to be achieved in order to match water cuts and pressures at the same time.

Lateral Fluid Movement

Once historical pressures and water cuts were matched relatively well by adjusting vertical permeability and aquifer strength, the history match was improved by adjusting the X and Y direction permeabilities of the Misener Sandstone, and the fracture permeability of the Misener Limestone. This had the effect of controlling the direction from which the fluid movement was occurring and thus controlling the pressure distribution in the

Table 8.5 Pressure Grid for First Two Years of Primary Production with no Water Aquifer

TIME STEP = 0.0 TIME = 0.00 days
DATUM PRESSURE WEIGHTED BY TOTAL PORE VOLUME

0.00	0.00	1300.00	1300.00	1300.00	1300.00	1300.00	1300.00	1300.00
1300.00	0.00	1300.00	1300.00	1300.00	1300.00	1300.00	1300.00	1300.00
1300.00	0.00	1300.00	1300.00	1300.00	1300.00	1300.00	1300.00	1300.00
1300.00	1300.00	1300.00	1300.00	1300.00	1300.00	1300.00	1300.00	1300.00
1300.00	1300.00	1300.00	1300.00	1300.00	1300.00	1300.00	1299.99	1286.06
1299.99	1299.99	1300.00	1300.00	1300.00	1299.76	1299.99	1299.99	1286.07
1300.64	1299.83	1300.00	1300.00	1300.00	1299.79	1290.65	1286.08	1286.28
1287.60	1298.70	1299.99	1296.47	1298.89	1290.08	1285.98	1286.18	1286.36
1285.37	1285.93	1296.49	1285.99	1285.97	1285.94	1286.12	1286.24	1286.21

TIME STEP = 9.0 TIME = 181.00 days
DATUM PRESSURE WEIGHTED BY TOTAL PORE VOLUME

0.00	0.00	1299.98	1299.95	1299.75	1299.86	1299.84	1299.87	1299.89
1299.99	0.00	1299.92	1299.80	1298.87	1299.64	1299.74	1299.79	1299.80
1299.98	0.00	1299.66	1299.36	1296.43	1298.97	1299.28	1299.59	1299.53
1299.94	1299.68	1298.88	1297.53	1294.48	1298.18	1298.68	1298.87	1299.33
1299.32	1298.59	1297.12	1293.34	1292.63	1294.18	1295.20	1296.05	1284.91
1298.91	1297.38	1294.26	1289.15	1285.82	1292.03	1294.93	1295.69	1284.76
1299.14	1297.08	1292.42	1280.78	1292.25	1293.37	1286.43	1282.68	1284.59
1285.92	1296.44	1293.40	1284.84	1290.71	1283.01	1282.71	1283.75	1284.28
1283.54	1282.67	1291.51	1276.09	1277.81	1278.71	1283.20	1283.96	1284.29

TIME STEP = 25.0 TIME = 577.00 days
DATUM PRESSURE WEIGHTED BY TOTAL PORE VOLUME

0.00	0.00	1282.48	1271.23	1270.31	1278.00	1274.32	1277.57	1278.84
1295.81	0.00	1268.18	1237.69	1222.49	1261.59	1267.68	1270.91	1270.08
1295.25	0.00	1247.69	1176.88	1126.21	1219.48	1238.75	1257.03	1248.49
1290.56	1262.02	1212.98	1124.25	1121.09	1189.56	1213.21	1222.00	1238.55
1270.41	1239.37	1196.33	1120.44	1114.05	1111.79	1115.32	1131.28	1186.29
1262.06	1232.56	1178.34	1111.52	1083.78	1077.23	1081.66	1100.39	1180.48
1257.85	1239.38	1191.68	1105.71	1111.14	1107.45	1106.67	1122.91	1168.32
1241.77	1243.81	1189.62	1121.47	1120.32	1110.12	1124.16	1142.14	1153.99
1237.25	1217.07	1201.20	1117.73	1111.27	1110.27	1133.36	1147.57	1156.57

TIME STEP = 32.0 TIME = 791.00 days
DATUM PRESSURE WEIGHTED BY TOTAL PORE VOLUME

0.00	0.00	1229.99	1205.70	1186.87	1193.37	1183.00	1196.52	1205.58
1280.99	0.00	1195.86	1144.25	1108.35	1145.65	1159.12	1173.16	1178.33
1279.25	0.00	1152.18	1073.97	988.63	1058.35	1087.16	1135.18	1126.80
1265.52	1189.47	1092.02	983.63	981.54	1015.59	1031.41	1080.67	1110.36
1206.50	1137.26	1065.65	976.88	972.55	972.41	976.54	989.86	1043.49
1188.74	1136.22	1052.61	969.36	948.12	939.78	945.35	962.63	1035.96
1178.92	1147.84	1076.65	968.41	971.13	964.12	962.07	974.78	1024.67
1159.45	1155.18	1069.18	979.19	976.57	964.23	974.51	992.00	1005.05
1153.04	1119.85	1092.35	975.17	966.35	963.46	982.41	996.34	1004.71

PRESSURE DIFFERENCE AT 791 DAYS

0.0	0.0	-30.0	-34.3	-43.1	-26.6	-27.0	-3.5	0.0
1.0	0.0	-24.1	-40.8	-41.7	-24.4	-30.9	-16.8	0.0
-0.8	0.0	-37.8	-61.0	-101.4	-55.7	-57.8	-34.8	0.0
5.5	-20.5	-63.0	-116.4	-88.5	-87.4	-78.6	-29.3	0.0
-23.5	-52.7	-64.3	-101.1	-82.4	-82.6	-78.5	-75.1	0.0
-41.3	-43.8	-57.4	-98.6	-114.9	-100.2	-94.7	-77.4	0.0
-41.1	-32.2	-48.3	-101.6	-88.9	-75.9	0.0	0.0	0.0
-40.6	-24.8	-55.8	-90.8	-63.4	-75.8	0.0	0.0	0.0
-37.0	-50.1	-27.6	-84.8	-73.7	-76.5	0.0	0.0	0.0

AVERAGE ABSOLUTE DIFFERENCE = 42.71680

reservoir.

Initially, the values of permeability from the plots of permeability versus porosity were input into the simulator. These permeabilities were able to be used for the Misener Limestone, the Maquoketa Dolomite, and the Viola Limestone in the history match by adjusting only the fracture characteristics for these formations. However, because of uncertainty in the permeabilities obtained from the plots of permeability versus porosity and the difficulty of history matching starting with a different permeability for each grid block, a uniform permeability of 50 millidarcies was set for the upper layer of the Misener Sandstone and 300 millidarcies was set for the lower layer of the Misener Sandstone. To obtain the final history match, these permeabilities were varied over a range of 10 to 200 millidarcies for the upper sandstone layer and from 60 to 1200 millidarcies for the lower sandstone layer. These values are believed to be within the expected values of permeability in the Misener Sandstone.

By increasing or decreasing the permeability of a certain grid block, the water production rate could be increased or decreased. Oil production was set as an input parameter, but water production varied with the permeability of the rock. Adjustment of permeability helped to control water cuts and also pressures because the total fluid withdrawal from a grid block could be

controlled to a certain extent.

Misener Limestone Fractures

The pressure distribution on the west side of the field was controlled by adjusting fracture permeability of the Misener Limestone and leaving matrix permeabilities as they were obtained from the permeability-porosity crossplots. It is not actually known if the Misener Limestone is fractured. To obtain a match, fracture permeabilities on the order of 10 to 50 millidarcies were used with a fracture spacing of 1320 feet. This magnitude of effective permeability does not indicate fractured rock. However, according to the permeability-porosity crossplots, typical matrix permeability is on the order of 1 to 10 millidarcies. The difference between simulated permeabilities and permeabilities reported from cores could be attributed to slight permeability enhancement of the Misener Limestone through limited natural fractures or to the lack of core data available on the Misener Limestone. This model uses the assumption of the former, while in reality the latter may be more plausible.

Pore Volume Adjustments

Some adjustments to pore volume of the formations were made to match pressures. Pore volume was changed mainly through porosity. As mentioned previously, formation thickness was known with relatively high confidence. Therefore it was not changed significantly during the

simulation. Porosities were much more questionable because of the lack of original porosity data. It was therefore believed that changing the porosity by three or four porosity percent in certain areas of the field was justified.

With the oil rate set, increasing or decreasing the original amount of oil in place in a grid block would increase or decrease the pressure after a set amount of oil was withdrawn. This turned out to have minimal effect on the pressures over the range that the porosity was varied.

A problem was encountered in that calculated pressures were too low in the northern grid blocks. Two more grid rows to the north were added to increase the oil volume and increase the pressure. "Surfer" was used to set the parameters of the new 9 X 11 grids for each formation. Table 8.6 shows the pressure grid for the case when the additional grid blocks were not added and indicates an average absolute pressure difference of 8.96 psi. Comparing this with the history matched grid in Table 8.1, the average absolute pressure difference does not change substantially. However, the pressures of the grid blocks on the northern edge of the field are matched better when the extra grid blocks are included.

Relative Permeability Adjustment

In an attempt to match water cuts and cumulative water production, water-oil relative permeability was changed for

the Misener Sandstone. Figure 8.3 shows the relative permeability curves that were used initially and those that were used to obtain the indicated match. The large increase needed to match water production could be attributed to absolute permeabilities in the Misener Sandstone being too small. Also, the high permeability conglomerate that lies locally at the base of the Misener Sandstone interval could be an easy path for water migration and might have allowed more water production than initially believed.

Fault Transmissibility

As mentioned previously, a fault lies on the eastern edge of the Zenith Field. The fault displacement ranges from a few feet in the center of section twenty-four to over 100 feet on the far eastern edge of the field. VIP has an option to allow communication across a fault from one layer to another. The value of this transmissibility was used as a matching parameter. Table 8.7 shows a pressure grid with no communication across the fault. An average absolute pressure difference of 8.20 indicates that the communication across the fault had minimal effect.

8.3.3 Discussion of History Match

The results presented in 8.3.1 appear to represent the first two years of production in the Zenith Field

Table 8.6 Pressure Grid for First Two Years of Primary Production with no Extra Grid Blocks on North Edge of Field

TIME STEP = 0.0 TIME = 0.00 days
DATUM PRESSURE WEIGHTED BY TOTAL PORE VOLUME

0.00	0.00	1300.00	1300.00	1300.00	1300.00	1300.00	1300.00	1300.00
1300.00	0.00	1300.00	1300.00	1300.00	1300.00	1300.00	1300.00	1300.00
1300.00	0.00	1300.00	1300.00	1300.00	1300.00	1300.00	1300.00	1300.00
1300.00	1300.00	1300.00	1300.00	1300.00	1300.00	1300.00	1300.00	1300.00
1300.00	1300.00	1300.00	1300.00	1300.00	1300.00	1300.00	1299.99	1286.06
1299.99	1299.99	1300.00	1300.00	1300.00	1299.76	1299.99	1299.99	1286.07
1300.64	1299.83	1300.00	1300.00	1300.00	1299.79	1290.65	1286.08	1286.28
1287.60	1298.70	1299.99	1296.47	1298.89	1290.08	1285.98	1286.18	1286.36
1285.37	1285.93	1296.49	1285.99	1285.97	1285.94	1286.12	1286.24	1286.21

TIME STEP = 9.0 TIME = 181.00 days
DATUM PRESSURE WEIGHTED BY TOTAL PORE VOLUME

0.00	0.00	1299.98	1299.96	1299.82	1299.90	1299.88	1299.91	1299.92
1299.99	0.00	1299.94	1299.86	1299.18	1299.74	1299.81	1299.85	1299.86
1299.98	0.00	1299.73	1299.54	1297.37	1299.27	1299.49	1299.71	1299.68
1299.95	1299.75	1299.12	1298.19	1295.91	1298.68	1299.05	1299.19	1299.53
1299.38	1298.78	1297.65	1295.08	1294.39	1295.60	1296.52	1297.19	1285.34
1299.00	1297.66	1295.07	1291.22	1287.68	1293.50	1296.16	1296.84	1285.25
1299.24	1297.31	1293.08	1282.50	1294.66	1295.19	1287.69	1283.87	1285.17
1286.05	1296.63	1294.11	1286.40	1292.60	1284.93	1283.89	1284.60	1285.04
1283.68	1283.00	1292.11	1277.56	1279.51	1280.46	1284.33	1284.82	1285.02

TIME STEP = 25.0 TIME = 577.00 days
DATUM PRESSURE WEIGHTED BY TOTAL PORE VOLUME

0.00	0.00	1287.44	1279.09	1278.09	1283.92	1281.53	1283.94	1285.00
1296.94	0.00	1276.89	1253.61	1241.28	1271.56	1276.37	1278.91	1278.56
1296.52	0.00	1261.55	1206.08	1165.29	1239.25	1254.33	1268.30	1262.78
1293.09	1272.10	1235.07	1164.39	1163.60	1214.84	1234.29	1240.78	1254.99
1277.81	1255.32	1223.08	1165.26	1159.33	1155.58	1158.92	1170.44	1212.12
1271.60	1249.25	1207.58	1158.07	1129.84	1123.01	1125.02	1141.00	1207.58
1268.71	1254.46	1217.31	1149.11	1160.45	1154.77	1148.47	1161.70	1197.60
1253.56	1257.78	1217.31	1164.35	1166.70	1157.53	1163.63	1177.91	1187.10
1249.73	1234.74	1225.60	1159.86	1156.49	1156.35	1171.87	1182.90	1190.00

TIME STEP = 32.0 TIME = 791.00 days
DATUM PRESSURE WEIGHTED BY TOTAL PORE VOLUME

0.00	0.00	1247.41	1228.69	1211.05	1215.07	1206.22	1217.33	1225.03
1285.79	0.00	1221.25	1181.04	1150.70	1175.59	1186.21	1198.01	1202.97
1284.47	0.00	1187.89	1124.80	1055.66	1102.54	1126.07	1166.82	1162.25
1274.06	1216.28	1141.84	1054.18	1058.86	1068.76	1080.30	1124.89	1149.69
1229.41	1177.42	1123.98	1059.40	1054.41	1046.95	1052.98	1061.14	1101.49
1215.97	1176.29	1113.28	1053.88	1024.67	1015.10	1015.29	1028.81	1095.72
1208.75	1185.03	1130.66	1045.92	1061.30	1048.31	1037.16	1048.70	1086.66
1191.03	1190.56	1127.35	1059.67	1063.21	1052.20	1050.05	1063.18	1072.93
1185.81	1161.39	1144.41	1055.33	1051.61	1050.16	1057.73	1067.72	1073.94

PRESSURE DIFFERENCE AT 791 DAYS

0.0	0.0	-12.6	-11.3	-18.9	-4.9	-3.8	17.3	0.0
5.8	0.0	1.2	-4.0	0.7	5.6	-3.8	8.0	0.0
4.5	0.0	-2.1	-10.2	-34.3	-11.5	-18.9	-3.2	0.0
14.1	6.3	-13.2	-45.8	-11.1	-34.2	-29.7	14.9	0.0
-0.6	-12.6	-6.0	-18.6	-0.6	-8.1	-2.0	-3.9	0.0
-14.0	-3.7	3.3	-14.1	-38.3	-24.9	-24.7	-11.2	0.0
-11.3	5.0	5.7	-24.1	1.3	8.3	0.0	0.0	0.0
-9.0	10.6	2.4	-10.3	23.2	12.2	0.0	0.0	0.0
-4.2	-8.6	24.4	-4.7	11.6	10.2	0.0	0.0	0.0

AVERAGE ABSOLUTE DIFFERENCE = 8.955857

relatively well. However, these results should not be regarded as the absolute answer. Because the Zenith Field is so complex, there is likely to be more than one possible way to simulate the field.

As discussed above, there were a large number of parameters that were unknown in the Zenith Field. Ideally, several of these parameters should be known so as to reduce the number that are actually adjusted during history matching. In this simulation, there were a large number of parameters that were unknown and able to be adjusted. Information that is typically available for a field, such as cores, electric logs and field tests, was scarce in the Zenith Field. This information could have given a better idea of relative permeability curves, porosity distributions and permeability distributions and would have reduced the number of completely unknown parameters substantially. This alone would have dramatically increased the confidence in the results obtained from the model.

Another cause for uncertainty in the history match is in the comparison of the pressures predicted with the model to the actual reported pressures. First, the manner in which the pressures were obtained for the iso-baric maps constructed by the engineering committee in 1942 was not known. Also, the grid block pressures calculated by the fortran computer program MAP.FOR only included the Misener

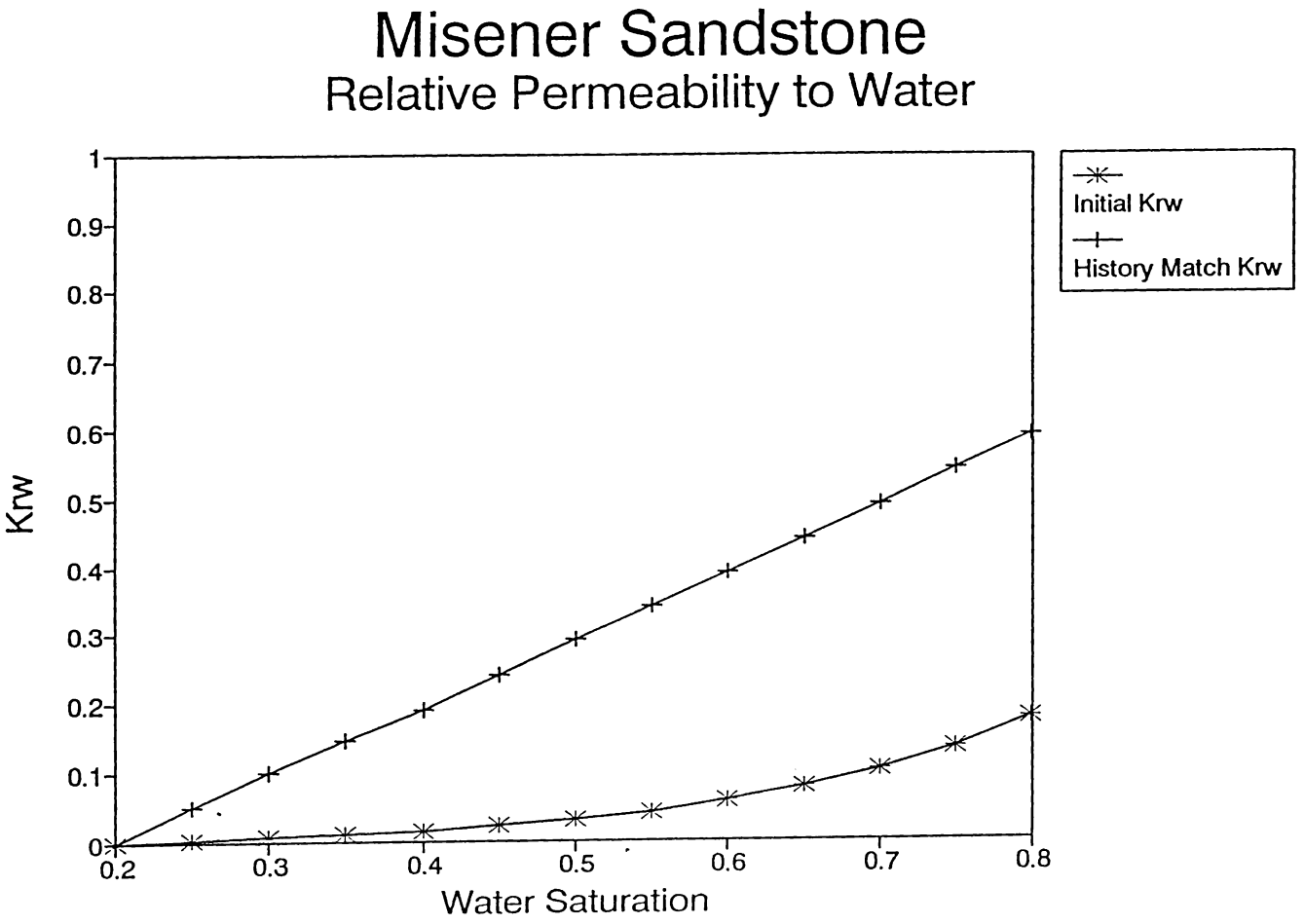

Figure 8.3 Misener Sandstone Relative Permeability to Water. Comparison of Values Initially Input with Those Resulting in the History Match.

Table 8.7 Pressure Grid for First Two Years of Primary Production with no Communication Across Fault

TIME STEP = 0.0 TIME = 0.00 days
DATUM PRESSURE WEIGHTED BY TOTAL PORE VOLUME

0.00	0.00	1300.00	1300.00	1300.00	1300.00	1300.00	1300.00	1300.00
1300.00	0.00	1300.00	1300.00	1300.00	1300.00	1300.00	1300.00	1300.00
1300.00	0.00	1300.00	1300.00	1300.00	1300.00	1300.00	1300.00	1300.00
1300.00	1300.00	1300.00	1300.00	1300.00	1300.00	1300.00	1300.00	1300.00
1300.00	1300.00	1300.00	1300.00	1300.00	1300.00	1300.00	1299.99	1286.06
1299.99	1299.99	1300.00	1300.00	1300.00	1299.76	1299.99	1299.99	1286.07
1300.64	1299.83	1300.00	1300.00	1300.00	1299.79	1290.65	1286.08	1286.28
1287.60	1298.70	1299.99	1296.47	1298.89	1290.08	1285.98	1286.18	1286.36
1285.37	1285.93	1296.49	1285.99	1285.97	1285.94	1286.12	1286.24	1286.21

TIME STEP = 9.0 TIME = 181.00 days
DATUM PRESSURE WEIGHTED BY TOTAL PORE VOLUME

0.00	0.00	1299.98	1299.96	1299.83	1299.91	1299.89	1299.91	1299.93
1299.99	0.00	1299.94	1299.87	1299.23	1299.76	1299.82	1299.86	1299.87
1299.98	0.00	1299.74	1299.56	1297.54	1299.30	1299.51	1299.72	1299.69
1299.95	1299.76	1299.14	1298.25	1296.10	1298.73	1299.09	1299.22	1299.56
1299.38	1298.79	1297.69	1295.21	1294.52	1295.72	1296.68	1297.31	1285.37
1299.00	1297.67	1295.10	1291.31	1287.78	1293.58	1296.26	1296.94	1285.28
1299.25	1297.31	1293.11	1282.56	1294.73	1295.26	1287.81	1283.96	1285.23
1286.05	1296.63	1294.13	1286.44	1292.65	1284.98	1284.08	1284.78	1285.14
1283.69	1283.00	1292.12	1277.60	1279.55	1280.50	1284.56	1285.00	1285.16

TIME STEP = 25.0 TIME = 577.00 days
DATUM PRESSURE WEIGHTED BY TOTAL PORE VOLUME

0.00	0.00	1288.05	1280.18	1279.18	1284.64	1282.34	1284.63	1285.65
1297.03	0.00	1278.03	1256.14	1244.49	1272.83	1277.39	1279.81	1279.47
1296.63	0.00	1263.19	1211.44	1172.75	1241.83	1256.28	1269.61	1264.41
1293.31	1273.12	1237.64	1170.67	1170.67	1218.28	1237.04	1243.12	1256.93
1278.26	1256.64	1225.87	1171.44	1165.63	1161.66	1165.54	1176.17	1214.20
1272.23	1250.63	1210.53	1163.54	1135.56	1128.75	1130.77	1146.31	1209.83
1269.42	1255.60	1219.68	1153.65	1165.67	1160.10	1153.91	1165.98	1200.86
1254.33	1258.78	1219.74	1168.65	1171.49	1162.50	1169.33	1183.95	1191.27
1250.56	1236.10	1227.71	1164.04	1161.10	1161.09	1178.57	1189.01	1195.08

TIME STEP = 32.0 TIME = 791.00 days
DATUM PRESSURE WEIGHTED BY TOTAL PORE VOLUME

0.00	0.00	1250.13	1232.38	1214.79	1218.31	1209.61	1220.32	1227.78
1286.33	0.00	1225.22	1187.02	1157.59	1180.05	1190.18	1201.61	1206.49
1285.07	0.00	1193.09	1133.29	1067.32	1109.02	1131.76	1171.41	1167.35
1275.10	1219.91	1148.75	1064.98	1070.12	1076.43	1087.39	1131.29	1155.33
1231.70	1182.14	1131.27	1069.93	1065.07	1057.57	1064.04	1071.41	1108.51
1218.80	1180.77	1120.40	1063.76	1034.89	1025.43	1025.73	1039.00	1102.91
1211.86	1189.07	1136.82	1055.01	1070.90	1058.29	1047.36	1057.70	1095.21
1194.33	1194.34	1133.78	1068.68	1072.61	1061.82	1060.05	1074.60	1082.52
1189.24	1165.86	1150.10	1064.22	1060.91	1059.63	1068.67	1079.25	1085.12

PRESSURE DIFFERENCE AT 791 DAYS

0.0	0.0	-9.9	-7.6	-15.2	-1.7	-0.4	20.3	0.0
6.3	0.0	5.2	2.0	7.6	10.0	0.2	11.6	0.0
5.1	0.0	3.1	-1.7	-22.7	-5.0	-13.2	1.4	0.0
15.1	9.9	-6.3	-35.0	0.1	-26.6	-22.6	21.3	0.0
1.7	-7.9	1.3	-8.1	10.1	2.6	9.0	6.4	0.0
-11.2	0.8	10.4	-4.2	-28.1	-14.6	-14.3	-1.0	0.0
-8.1	9.1	11.8	-15.0	10.9	18.3	0.0	0.0	0.0
-5.7	14.3	8.8	-1.3	32.6	21.8	0.0	0.0	0.0
-0.8	-4.1	30.1	4.2	20.9	19.6	0.0	0.0	0.0

AVERAGE ABSOLUTE DIFFERENCE = 8.201472

Limestone and the Misener Sandstone pressures in the weighting. It was established that there was some communication with the Maquoketa Dolomite and the Viola Limestone and thus these formations may have had an effect, although unknown, on the predicted pressures. If the Maquoketa and the Viola were included in the weighting, it was found that the predicted pressure decreased significantly. Because of these uncertainties, even less confidence can be placed on the history match.

Even with the lack of data and the questions regarding the validity of the data, a history match was obtained that is a possible representation of how the field actually produced. There may be different ways that the field could be modeled, and this one or any one of them could be the right way. This model does not include any unrealistic assumptions that cannot be supported by available data. For this reason, it is felt that the match that is presented is the best that could be done utilizing the data that are presently available.

8.4 Simulation of Primary Production, 1940 - 1942.

8.4.1 Attempted History Matching

Field data were only available up to 1942 from the engineering committee's report. Therefore, an attempt to

simulate the period from 1940 to 1942 was made. New wells were drilled into the Viola, and existing wells were deepened as indicated by driller's logs. It was hoped that the remaining period of primary production could be matched by changing the characteristics of only the Viola Limestone. After some simulation runs, it was felt that not enough was known about the reservoir, specifically the Viola Limestone and individual well production, to obtain a history match of the remainder of primary production in the short time available.

Gas - Oil Ratio

The first problem that was encountered involved production of gas. There was a large discrepancy between actual field gas-oil ratio and predicted gas-oil ratio for the period from 1940 to 1942.

Initially it was believed that the relative permeability to gas could be decreased to reduce the gas production. Several runs were made decreasing the gas relative permeability. It was found that gas production could not be matched without increasing the critical gas saturation to thirty percent in the matrix and the fractures. This was felt to be out of the range of likely critical gas saturations. Therefore, it was felt that there was an additional reason for the discrepancy in gas-oil ratios.

It was believed that the actual GOR versus time curve

reported for the field could be in error. According to the proration rules, wells did not have to monitor gas production until they reached a GOR of 1,000 SCF/STB. This could have lead to some errors in the reported gas-oil ratio curve.

Water Production

A history match of water production was attempted by adjusting oil-water relative permeability curves of the Viola Limestone and the fractures, and also through slight changes in the aquifer strength. Cumulative water production was matched relatively well at the end of 1941. Due to limited time, and since the calculated cumulative water production appeared to be of the same order of magnitude as the actual production, there was not much effort made in matching individual water cuts for each quarter section.

8.4.2 Discussion of Simulation of Primary Production from 1940 through 1942

Since the field gas-oil ratio could not be matched for 1940 through 1942, it was felt that attempts to simulate primary production further would be useless. The results obtained would be so uncertain that no valid conclusions could be drawn from additional simulations.

The difficulty in matching primary production after 1939 was attributed to the lack of data available on the

Zenith Field. Individual well production data along with the super-computer version of VIP, more core reports over a larger area of the field, and more transient tests conducted in the field would have helped in the simulation of the Zenith Field.

It is known that grid size plays an important role in numerical modeling. Individual well production data and the super-computer version of VIP would have allowed a smaller grid size to be used in the simulation. The large grid size required from the lack of production data and the computer that was available during this simulation could be a possible reason for the inability to obtain a history match of primary production after 1939.

A large amount of time was expended during the TORP-KGS study of the Zenith Field trying to locate additional core reports. It was found that many of the wells in the field had been cored. However, only the four core reports presented in Appendix I were found. Additional core reports for other wells in the Zenith Field may have allowed a better estimation of relative permeability of the formations, as well as better initial estimates of porosity and permeability. They could have also given an indication of fracture characteristics in the Viola Limestone.

Individual formation permeability was one of the parameters that was largely unknown. Estimation of permeability from plots of permeability versus porosity

results in a large amount of uncertainty. Additional well tests on individual formations would have given a better indication of actual field permeability, and would have greatly aided in the simulation of the Zenith Field.

It is believed that if the above mentioned data and resources had been available, a history match could have been achieved for all of the period of primary production in the Zenith Field. These data are believed to be the minimum amount required when simulating complex reservoirs such as the Zenith Field.

Chapter 9 Conclusions and Recommendations

9.1 Conclusions

1. The Misener Sandstone was found to consist of three distinct layers: a lower permeability upper layer, a middle shaly layer, and a high permeability lower layer. These layers are generally distinguishable on a gamma ray log, and were able to be mapped for the simulation.

2. The Viola Limestone, and possibly the Maquoketa Dolomite, are believed to be naturally fractured. Indications of fractures in core reports and very high initial production potentials reported for the Viola Limestone lead to this conclusion.

3. Build-up, fall-off, and in some instances interference tests can be performed with an "Echometer." On-site evaluation of the data was used to minimize the amount of time a well was shut in.

4. Transient tests indicate that the permeability of the lower Misener Sandstone layer lies in the range of 100 to 300 millidarcies. The conglomerate that lies

locally at the base of the sandstone interval is believed to have a permeability in excess of one darcy. The permeability of the upper sandstone interval is on the order of 50 millidarcies.

5. Skin factors on some of the wells were large, indicating workovers may be needed.

6. Original oil in place calculated from the VIP simulator (113 MMSTB) and from a volumetric analysis (105 MMSTB) agreed well with discrepancy attributed to adjustment of porosity during the history matching process.

7. Field pressure, gas-oil ratio, water cuts, and cumulative water production were matched for the first two years of primary production.

8. The history match of gas production was obtained with a bubble point of 1000 psi instead of the 1100 psi reported in the PVT analysis. This was justified by comparison of the field gas-oil ratio values with the PVT test analysis.

9. It was found that the Maquoketa Dolomite and the Viola Limestone contributed to oil production during the first two years of primary production even though these formations had not been discovered at the time.

10. The water aquifer located on the southern edge of the field was found to provide a moderate amount of pressure maintenance during the first two years of primary production.

11. A history match of primary production from 1940 through 1944 was not obtained due to the lack of data and time. Additional data that would have aided in the simulation of the Zenith Field are additional core analyses, more field testing, and individual well production data.

12. Gas-oil ratio could not be matched with actual field data without having a critical gas saturation of 30 percent in both the matrix and the fractures. This was felt to be out of the range of likely critical gas saturations, especially in the fractures. This indicates that an unknown process is controlling gas production. Because of the discrepancy in gas-oil ratio, no attempt to match field pressures was made.

9.2 Recommendations

1. An "Echometer" should be used to perform build-up and fall-off tests on all wells in the field to determine the skin effect for each well. Workovers should be completed accordingly.

2. On-site evaluation of transient test data should be performed, especially on producing wells, to minimize the amount of time the well is shut in for a transient test.

3. When attempting to model reservoirs as large and complex as the Zenith Field in the future, more data should be available. Individual well production data, numerous core reports, and numerous transient tests of individual formations are a must.

4. With the available data and computer resources, simulation of secondary recovery in the Zenith Field will be very difficult if not impossible. The super-computer version of VIP may help in the simulation. The use of smaller size grid blocks should be investigated with the super-computer.

References

Beggs, H.D. and Robinson, J.R., "Estimating the Viscosity of Crude Oil Systems", J. Pet. Tech., Sept, 1975, p. 1140 - 1141.

Berendsen, P., Blair, K.P., "Subsurface Structural Maps over the Central North American Rift System (CNARS), Central Kansas, with discussion", Kansas Geological Survey, Subsurface Geology Series 8, 1986.

Bradley, H.B., Petroleum Engineering Handbook, Society of Petroleum Engineers, Richardson, TX, 1987.

Carr, N.L., Kobayashi, R., and Burrows, D.B., "Viscosity of Hydrocarbon Gases Under Pressure", Trans. AIME Vol. 201, 1954, p. 264 -278.

Carter, R.D. and Tracy, G.W., "An Improved Method for Calculating Water Influx," Trans. AIME, Vol 219, 1960, p. 415 - 417.

Dake, L.P., Fundamentals of Reservoir Engineering, Elsevier Scientific Publishing Company, Amsterdam, The Netherlands, 1978.

Dean, R.H., Lo, L.L., "Simulations of Naturally Fractured Reservoirs", SPE Reservoir Engineering, May 1988, p. 638 - 648.

Dowell-Schlumberger, Field Data Handbook.

Earlougher, R.C., Advances in Well Test Analysis, 1977, SPE Monograph.

Engineering Committee Established by the Kansas Corporation Commission, L.B. Taylor, Chairman, 1942.

Gilman, J.R. and Kazemi, H., "Improvements in Simulation of Naturally Fractured Reservoirs," Society of Petroleum Engineers Journal, August 1983, p. 695 - 707.

Honarpour, M., Koederitz, L.F., Harvey, A.H., "Empirical Equations for Estimating Two-Phase Relative Permeability in Consolidated Rock", J. Pet. Tech., December 1982, p. 2905 -2908.

Imbt, W.C., "Zenith Pool, Stafford County, Kansas -- an Example of Stratigraphic Trap Accumulation," Stratigraphic Type Oil Fields, A.I. Levorsen, ed., American Association of Petroleum Geologists, Tulsa, OK, 1941, p. 139-165.

McCoy, J.N., Podio, A.L., Huddleston, K.L, Drake, B., "Acoustic Static Bottom-Hole Pressure", SPE 13810, Presented at the SPE 1985 Production Operations Symposium held in Oklahoma City, OK, March 12 - 15, 1985.

McCoy, J.N., "Acoustic Velocity of Natural Gas", available from Echometer Company, Wichita Falls, TX.

Questa Engineering Corporation, "Engineering Study, Zenith Pool, Stafford and Reno Counties, Kansas", August 1984. Update Presented May, 1986.

Ramey, H.J., Jr., "Short-Time Well Test Data Interpretation in the Presence of Skin Effect and Wellbore Storage", J. Pet. Tech., January 1970, p. 97 - 104.

Schoeling, L.G., Newell, K.D., and Wong, J.C., "PC and Mainframe Computer-Graphics Techniques Applied to Volumetric Evaluation of a Mature Oil Field", Society of Petroleum Engineers, Computer Applications, November - December 1990, p. 8 - 14.

Sener, I., "Methodology Used in Estimating the Raman Reservoir Fracture System Data for Simulation", Proceedings of the 62nd Society of Petroleum Engineers Annual Technical Conference and Exhibition in Dallas, TX, 1987, p. 483 - 491.

Standing, M.B. and Katz, D.L., "Density of Natural Gases", Trans. AIME Vol. 146, 1942, p. 140 - 144.

Tertiary Oil Recovery Project-Kansas Geological Survey, "Zenith Field - A Field Demonstration Project for Improved Efficiency for Oil and Gas Recovery in Kansas", Submitted to the Kansas Corporation Commission, 1991.

Warren, J.E. and Root, P.J., "The Behavior of Naturally Fractured Reservoirs", Society of Petroleum Engineers Journal, September 1963, p. 245 - 255.

Western Atlas' Integrated Technologies, Reference Manual for VIP Executive Simulator Version 2.1, April, 1990.

Yates, G.L. and Assoc., "Waterflood Feasibility Study, Zenith Oil Pool", December, 1965.

APPENDIX I

Core Reports and PVT Tests Available for the Zenith Field

This appendix summarizes the four core reports found for wells in the Zenith Field and presents the PVT analysis found in the 1942 engineering committee's report.

Braden-Zenith, Inc.
Zenith Waterflood Unit ZU-3
1100' SNL 600' EWL NE/4 Sec. 11-24S-11W
Analysis by Core Laboratories, Inc.

Sample #	Depth ft	Perm md	Porosity %	Description and Remarks
-------	Misener Limestone			
1	3709.0 - 10.5	15.5	8.2	Lm, chert, pp/vug
2	10.5 - 12.0	2.4	5	Lm, v/cherty
3	12.0 - 13.5	0.2	4	Lm, pp/vug, vert/frac
4	13.5 - 15.0	0.8	7.1	Lm, vuggy, sdy
-------	Misener Sandstone			
5	15.0 - 15.5	27.6	7.8	Sd, sl/shy
	3715.5 - 30.0			Shale
-------	Maquoketa Dolomite			
6	3730.0 - 31.8	175.4	9.5	Dolo, pp/vug, vert/frac
7	31.8 - 32.8	2.8	8.9	Dolo, pp/vug, vert/frac
8	32.8 - 34.1	4.1	11.1	Dolo, vuggy, vert/frac
9	34.1 - 35.4	6	9.2	Dolo, vuggy
10	35.4 - 36.5	0.1	2.6	Lm
11	36.5 - 37.3	0.3	1.1	Lm
12	37.3 - 38.0	0.8	1.9	Lm, pp/vuggy
	3738.0 - 59.0			Drilled or Lost Core
-------	Viola			
13	3759.0 - 60.8	3.8	11.5	Dolo, chert, vuggy
14	60.8 - 62.3	3247	7.1	Dolo, cherty, vert/frac
15	62.3 - 64.0	1.6	9.1	Dolo, cherty
16	64.0 - 65.9	0.9	5.8	Dolo, cherty, sl/vuggy
17	65.9 - 67.7	8.5	8.6	Dolo, cherty, sl/vuggy
18	67.7 - 69.0	11.8	6.8	Dolo, lmy, cherty, vert/frac
19	69.0 - 70.8	0.3	2.7	Lm
20	70.8 - 72.0	<0.1	3.8	Lm
21	72.0 - 73.2	46.5	6.1	Lm, vert/frac
22	73.2 - 74.9	0.4	6.5	Dolo, sl/shy, cherty
23	74.9 - 76.0	<0.1	6	Dolo, cherty, sl/vuggy
24	76.0 - 77.7	2.7	11.1	Dolo, cherty, sl/vuggy
25	77.7 - 78.9	1.7	12.1	Dolo, cherty, sl/vuggy
26	78.9 - 80.3	8.2	12.1	Dolo, cherty, vert/frac
27	80.3 - 81.9	13.4	7.1	Lm, dolo, cherty
28	81.9 - 83.3	59.3	6.6	Lm, dolo, cherty, vert/frac
29	83.3 - 84.9	0.6	8.6	Lm, dolo, cherty, sl/vuggy
30	84.9 - 86.3	13.5	11.5	Dolo, cherty, sl/vuggy

National Cooperative Ref. Assoc.
Core Hole No. 2
SW/4 NW/4 Sec. 13-24S-11W
Analysis by Core Laboratories, Inc.

Sample #	Depth ft	Perm md	Porosity %	Description and Remarks
	3762.0 - 65.7			Sh
-------	Misener Sandstone Layer 1			
1	3765.7 - 66.8	<0.1	4.9	Sd, shy
2	66.8 - 68.7	4.3	8.2	Sd, sl/shy
3	68.7 - 70.0	9.2	9.4	Sd
4	70.0 - 71.0	6.2	7.9	Sd, shy
5	71.0 - 72.0	4.7	11.9	Sd, shy
6	72.0 - 73.0	4.6	11.3	Sd, shy
-------	Misener Shale			
7	73.0 - 74.0	1.3	10.6	Sd, v/shy
8	74.0 - 75.0	2.6	7.4	Sd, v/shy
9	75.0 - 75.9	0.3	7.3	Sd, shy, cong
-------	Misener Sandstone Layer 2			
10	75.9 - 77.1	66	9.3	Sd, sl/shy
11	77.1 - 78.9	207	12.4	Sd
12	78.9 - 79.7	114	10.3	Sd, gil
13	79.7 - 80.8	48	7.3	Sd, sl/shy
14	80.8 - 81.7	67	8.4	Sd, sl/shy
15	81.7 - 83.0	68	8.5	Sd, sl/shy
-------	Viola			
16	83.0 - 84.6	92	8	Lm, sdy, vgy, vert/frac
17	84.6 - 86.0	22	6.7	Lm, sdy, vgy, vert/frac
18	86.0 - 87.5	0.1	8.3	Lm, vgy
19	87.5 - 89.2	3.7	11.6	Lm, vgy
20	3789.2 - 90.5	0.2	9.1	Lm, vgy

National Cooperative Ref. Assoc
Core Hole No. 3
NW NW NE Sec. 12-24S-11W
Analysis by Core Laboratories, Inc.

Sample #	Depth ft	Perm md	Porosity %	Description and Remarks
-------	Misener Sandstone Layer 1			
1	3687.5 - 88.0	17	13.6	Sd
2	88.0 - 89.3	7	13.1	Sd
3	89.3 - 90.3	34	13.6	Sd
4	90.3 - 91.5	19	12	Sd, shy
5	91.5 - 93.0	24	10.8	Sd, sl/shy
6	93.0 - 94.5	28	11.7	Sd, sl/shy
-------	Misener Shale			
7	94.5 - 95.5	1.5	9.6	Sd, shy
8	95.5 - 96.7	0.5	5.9	Sd, sl/shy
9	96.7 - 97.5	3.2	9.7	Sd, cherty
-------	Misener Sandstone Layer 2			
10	3697.5 - 98.8	68	11.8	Sd, shy
-------	Viola			
11	3724.0 - 25.8	10	6.9	Lm, cherty
12	25.8 - 27.5	0.1	2	Lm, cherty
13	27.5 - 28.9	<.1	3.4	Lm, cherty, sl/vgy
14	28.9 - 30.7	15	3.5	Lm, v/cherty, sl/vgy
15	30.7 - 32.0	4.8	9.8	Lm, cherty, vgy, vert/frac
16	32.0 - 32.9	57	8.1	Lm, v/cherty, vert/frac
17	32.9 - 34.5	55	20.9	Dol, cherty, vert/frac
18	34.5 - 35.7	18	22.3	Dol, vgy
19	35.7 - 37.0	5	21.4	Dol, vgy
20	37.0 - 38.0	80	22	Dol, cherty, vert/frac
21	38.0 - 39.7	12	8	Dol, cherty
22	39.7 - 40.9	0.3	5.6	Dol, lmy, cherty
23	3740.9 - 42.0	0.7	5	Lm, cherty

Hartnett Core Test No. 1
Center N/2 N/2 NW Sec. 13-24S-11W
Analysis by Earlougher Engineering

Sample #	Depth ft	Perm md	Porosity %	Description and Remarks
-------	Misener Sandstone Layer 1			
1	3756.5	0.1	5.5	Sd, sl/cherty
2	3757.4	1.1	9.6	Sd, sl/cherty
3	3757.6	12	16.5	Sd, sl/cherty
4	3758.5	8.3	14.5	Sd, shy
5	3759.6	13	16	Sd, shy
6	3760.5	5.1	13.9	Sd
7	3761.5	33	11.2	Sd
8	3762.5	1.4	9.6	Sd
9	3763.2	72	15	Sd, sl/shy
10	3763.5	109	14.6	Sd, sl/shy
11	3764.8	24	12.8	Sd, sl/shy
12	3765.8	15	13.8	Sd, sl/shy
13	3766.6	25	13.4	Sd, sl/shy
14	3767.5	20	11.7	Sd, shy
-------	Misener Shale			
15	3767.7	0.1	8	Sd, shy
16	3768.4	2.6	12.1	Sd, shy
17	3769.6	1.9	9.2	Sd, shy
-------	Misener Sandstone Layer 2			
18	3770.5	793	14.7	Sd
19	3771.6	820	16.1	Sd
20	3771.8	60	8.8	Sd
21	3772.6	111	10.5	Sd, cse
22	3773.5	98	11.4	Sd, cse
23	3774.5	713	12.4	Sd, cse
24	3774.8	1.8	7.6	Sd, cse
25	3775.5	120	11.2	Sd, cse
26	3776.5	18	8.9	Sd, cse
27	3777.5	11	8	Sd, cse
28	3778.5	2.7	6.9	Sd, cse
29	3779	0.5	5.3	Sd, v/cse
30	3779.4	0.5	6.3	Sd, v/cse
31	3780.3	2.5	7.8	Sd, v/cse
-------	Viola			
32	3785.2	0	3.7	Dolo, vert/frac
33	3794	0.4	5.9	Dolo, vert/frac

C O P Y

BOTTOM HOLE SAMPLE DATA

Lease: B. McComb — Well No: 1

Location: SE NE SW 14 24 S-11 W — Division: Central

Field: Zenith — State: Kansas

Elevation: 1817'

Bottom Hole sample taken: March 24, 1938

Total Depth: 3821' Tubing, 3" Depth: 3618'
Sampling Depth: 3610'
Shut in pressure at 3610' = 1213 Lbs./Sq.In.
Fluid Gradient: 0.356 Lbs./Sq.In./Ft.
Shut in pressure, corrected to sampling depth = 1213 Lbs./Sq.In.
Bottom Hole temperature at 3610' = 118°F.
Pressure required to open sampler valve = 1100 #/sq.in.
Pressure dropped back to 1000 Lbs/Sq.In. at 75°F.
Sample transferred to container #5 at 1750 Lbs/sq.in.
Casing pressure, shut in 0 hours, 200 Lbs/sq.in.
Tubing pressure, shut in 0 hours, 178 Lbs/Sq.in.
Fluid level below surface when sampled, 430 Ft.
Sample contains no water
Well shut in 3 hours when sampled
Rate of production before sampling, 3 Bbls/Hr.

GAS-OIL RATIO DATA

Date taken: — Length of Test:

Tubing Pressure: — Casing Pressure:

Oil produced, accurately measured:

Gas produced, accurately measured:

Trap pressure during test:

Trap temperature during test:

Gravity of oil from trap during test:

Choke size:

Calculated Gas-Oil ratio:

C O P Y

STANOLIND OIL AND GAS COMPANY
PRODUCING DEPARTMENT LABORATORY
DIFFERENTIAL AND FLASH VAPORIZATION TEST ON SUB-SURFACE OIL SAMPLE

Date 4-3-38 Sample No. 46 Sample Bomb No. 5

Field Zenith Lease B. McComb Well No. 1

Date Well was Sampled 3-24-38 Date Test was Run 4-1-38

Bubble Point of Oil at 118 °F. 1104 Lbs./Sq.In. Abs.

Compressibility of Sub-surface Oil at 118 °F, 10.4 x 10^{-6} Cu.Ft./Cu.Ft./Lb./Sq.In.

Shrinkage from Bottom Hole Pressure 1227 Lbs./Sq.In. Abs., and 118 °F to 1 atm. and 118 °F. referred to Residual Oil at 60°F. 19.7 %.

Calculated Shrinkage from 1227 Lbs./Sq.In.Abs., and 118 °F. to 1 atm. and 60°F. referred to residual oil at 60°F. 22.5 %.

Gas/Oil ratio at 118 °F. referred to Residual oil at 60°F. 364.3 Cu.Ft./Bbl.

Gravity of Residual Oil 41.5 ° A.P.I.

TESTS COMPLETED ON SAMPLE

Differential Vaporization at Formation Temperature _____

Differential Vaporization at 70°F. _____

Fractionation Analysis _____

Miscellaneous Tests _____

Remarks:

These determinations were made with the new Variable Volume Cell apparatus.

STANOLIND OIL AND GAS COMPANY

ENGINEERING DEPARTMENT LABORATORY REPORT

GAS, GASOLINE, OIL ANALYSIS

Date April 4, 1938 Date sample received 3-29-38 Lab. No. BH-46

Identification of Sample Bottom Hole Sample

Information desired: Fractional Distillation

Company drilling well Stanolind Oil & Gas Company State Kansas

County Stafford Field Zenith Lease B. McComb

Well No. 1 Quarter SE NE SW 14 Sec. or Sur. T. 24S R. 11W

Name of sand From To Depth of Well 3821

Method of collecting sample Stanolind Bottom Hole Sampler

Collected by Floyd Farris Date collected 3-24-38

ANALYSIS SUMMARY

Compound	Mol. Fract	% Volume	Miscellaneous Tests on Residue Oil
Nitrogen			Specific Gravity " .8408 at 60°F.
Oxygen			Net B.T.U. (Calorimetric Test)
Hydrogen Sulphide			Sulphur (A.S.T.M. Method)
Carbon dioxide			G. P. M. (Calculated)
Methane	.1540	6.01	A.P.I. Gravity = 36.3° at 60°F.
Ethane	.0493	2.45	Molecular Weight = 197
Propane	.1010	5.29	
Iso butane	.0350	2.22	Conditions at sampling depth:
Normal butane	.0452	2.77	Depth = 3810'
Iso pentane	.0189	1.54	Pressure = 1213#
Normal pentane	.0214	1.50	Temperature = 118°F.
Hexane and isomers	.0634	5.03	
Heptane and isomers and heavier	.5118	75.39	
Octane and isomers			
Nonane and isomers			
Decane and isomers			
	1.0000	100.00	

Remarks In addition to the above described constituents we found for each 100 cc. of this sample in the liquid, 270 cc. of an inert uncondensable gas believed to be nitrogen, this gas being measured at 760 mm. pressure and 60°F. This gas would not condense at -298°F. The Orant analysis showed no hydrogen sulphide, carbon dioxide or oxygen.

Reservoir Pressure 1765#
GAS IN SOLUTION
GAS LIBERATED
ZENITH KANSAS
B. McComb No. 1 3-24-38
Differential Vaporization
Solubility and Liberation
Curves
Gas and Residual Oil at 60°F.
Test Temperature 118°F.
Tested 4-1-38
Gas cu.ft./bbl. Referred to Residual Oil
400
300
200
100
0
500
1000
1500
Pressure, Lbs./Sq. In. Abs.

Relative Volume of Oil Referred to Residual Oil
1.00
1.05
1.10
1.15
1.20
1.25
Reservoir Pressure 1265 #
0
500
1000
1500
Pressure Lbs./Sq.In. Abs.
ZENITH KANSAS
R. McComb No. 1 3124-38
Sample No 46
Differential Vaporization
Residual Oil at 0 Atm.
and 60 °F.
Test temperature 118 °F.
Tested 4/1/38

APPENDIX II

Semi-Annual Iso-Baric
and Water Cut Maps

This appendix contains the pressure maps and the water-cut maps that were used as actual field data in the history matching process.

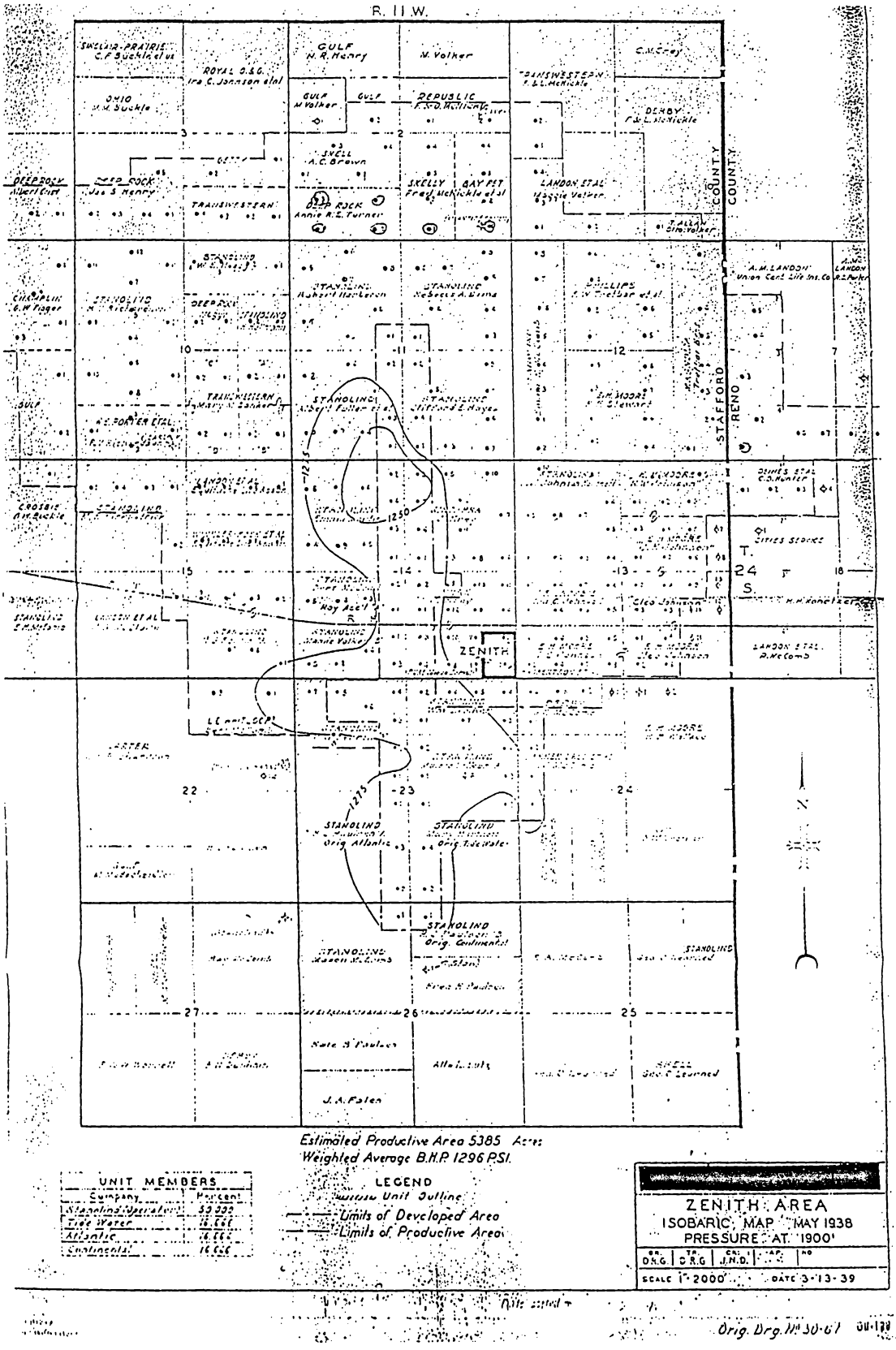
R. 11 W.
COUNTY
STAFFORD
RENO
ZENITH
T. 24 S.
Estimated Productive Area 5385 Acres
Weighted Average B.H.P. 1296 PSI.
UNIT MEMBERS
Company
Percent
Stanolind Operator
53.333
Free Water
16.666
Atlantic
16.666
Continental
16.666
LEGEND
Unit Outline
Limits of Developed Area
Limits of Productive Area
ZENITH AREA
ISOBARIC MAP MAY 1938
PRESSURE AT 1900'
SCALE 1" = 2000'
DATE 3-13-39
Orig. Drg. No. 30-61

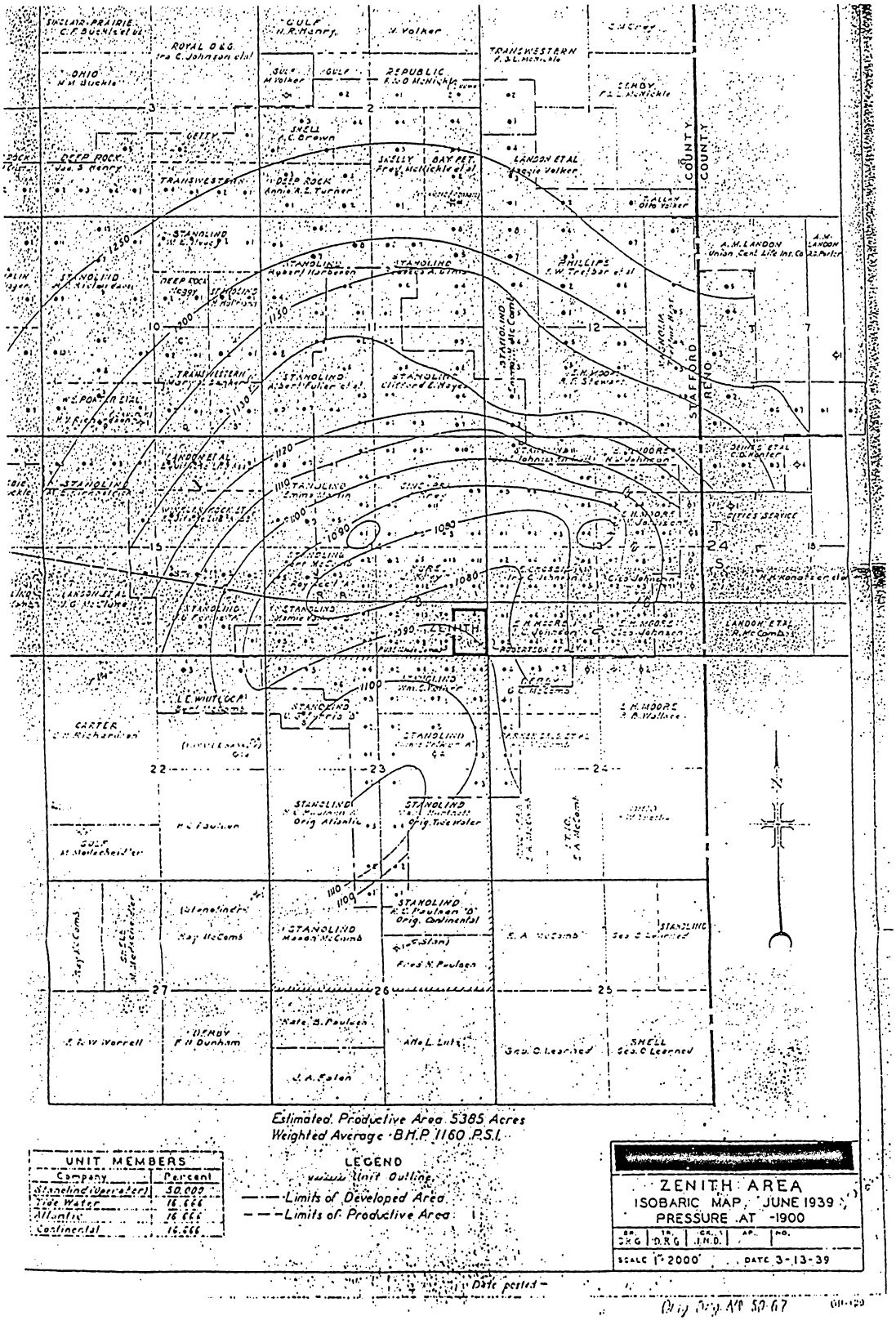
Estimated Productive Area 5385 Acres
Weighted Average B.H.P. 1160 P.S.I.
UNIT MEMBERS
Company | Percent
Stanolind (Operator) | 50.000
Tide Water | 16.666
Atlantic | 16.666
Continental | 16.666
LEGEND
Unit Outline
Limits of Developed Area
Limits of Productive Area
ZENITH AREA
ISOBARIC MAP, JUNE 1939
PRESSURE AT -1900
SCALE 1" = 2000'
DATE 3-13-39
Date posted
ZENITH
COUNTY
STAFFORD
RENO

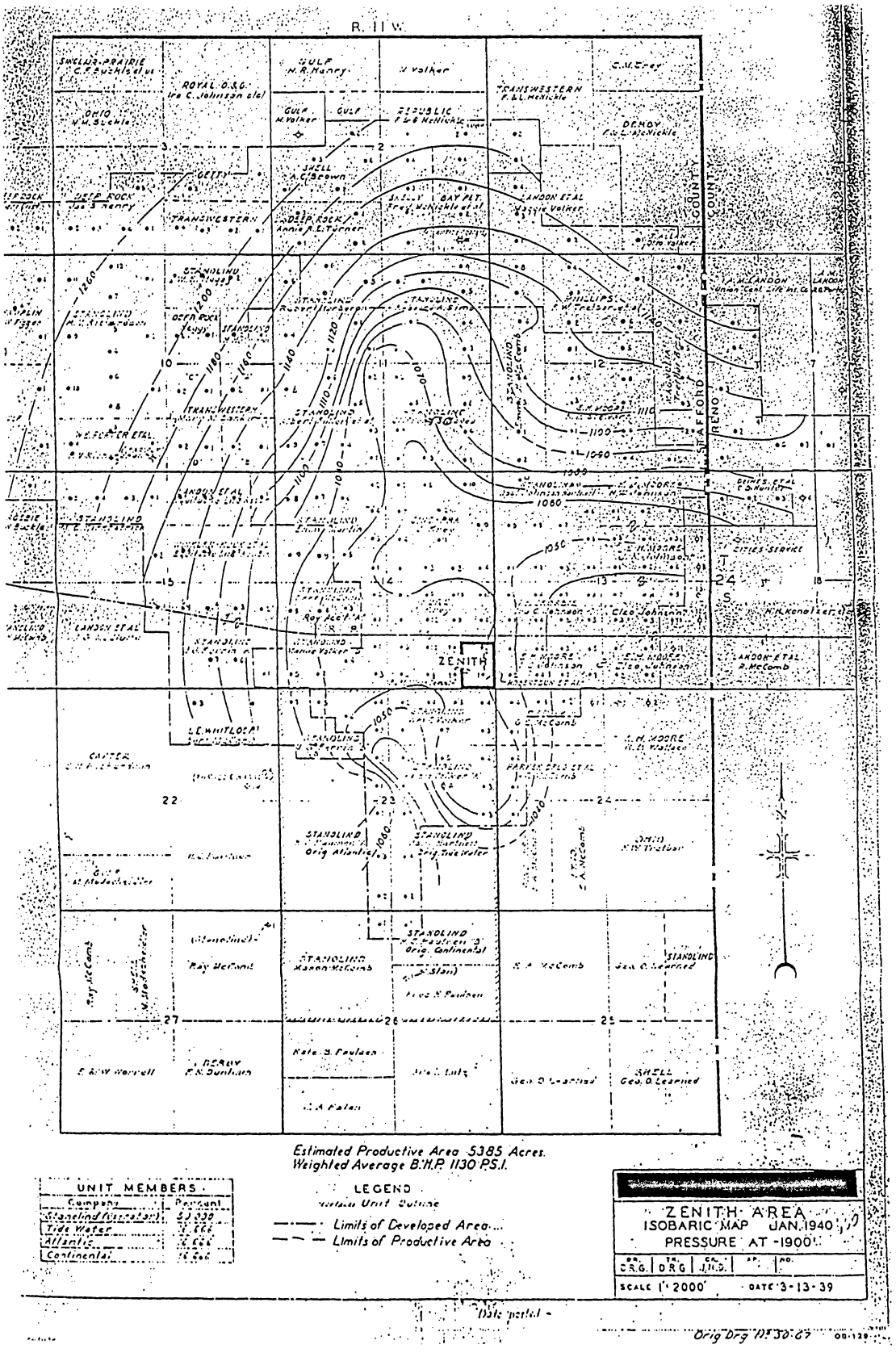
R. 11 W.
ZENITH
Estimated Productive Area 5385 Acres.
Weighted Average B.H.P. 1130 P.S.I.
UNIT MEMBERS
Company
Percent
Stanolind (Operator)
Tide Water
Atlantic
Continental
LEGEND
Limits of Developed Area
Limits of Productive Area
ZENITH AREA
ISOBARIC MAP JAN. 1940
PRESSURE AT -1900'
DR. D.R.G.
TR. D.R.G.
CK. J.H.D.
AP.
NO.
SCALE 1" 2000'
DATE 3-13-39
Orig Drg 11-30-67

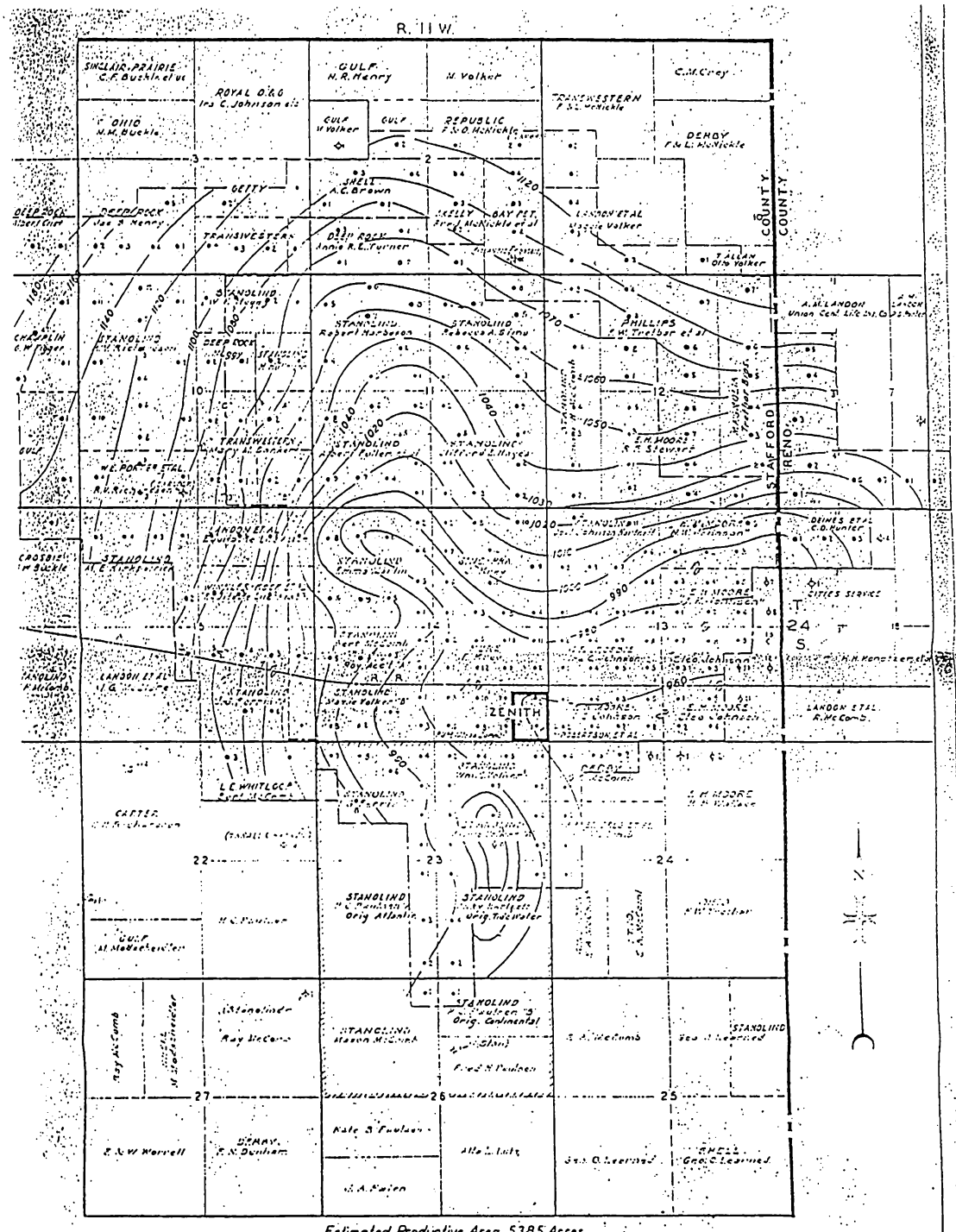
R. 11 W.
ZENITH
STAFFORD COUNTY
RENO COUNTY
T. 24 S.
Estimated Productive Area 5385 Acres
Weighted Average B.H.P. -1045 P.S.I.
UNIT MEMBERS
Company | Percent
Stanolind (Operator) | 50.000
Tide Water | 16.666
Atlantic | 8.666
Continental | 16.666
LEGEND
Unit Outline
Limits of Developed Area
Limits of Productive Area
ZENITH AREA
ISOBARIC MAP JUNE 1940
PRESSURE AT -1900
DR. D.R.G. TR. CH. J.H.D. AP. HC.
SCALE 1" 2000' DATE 3-13-39
Orig. Drg. No. 50-67

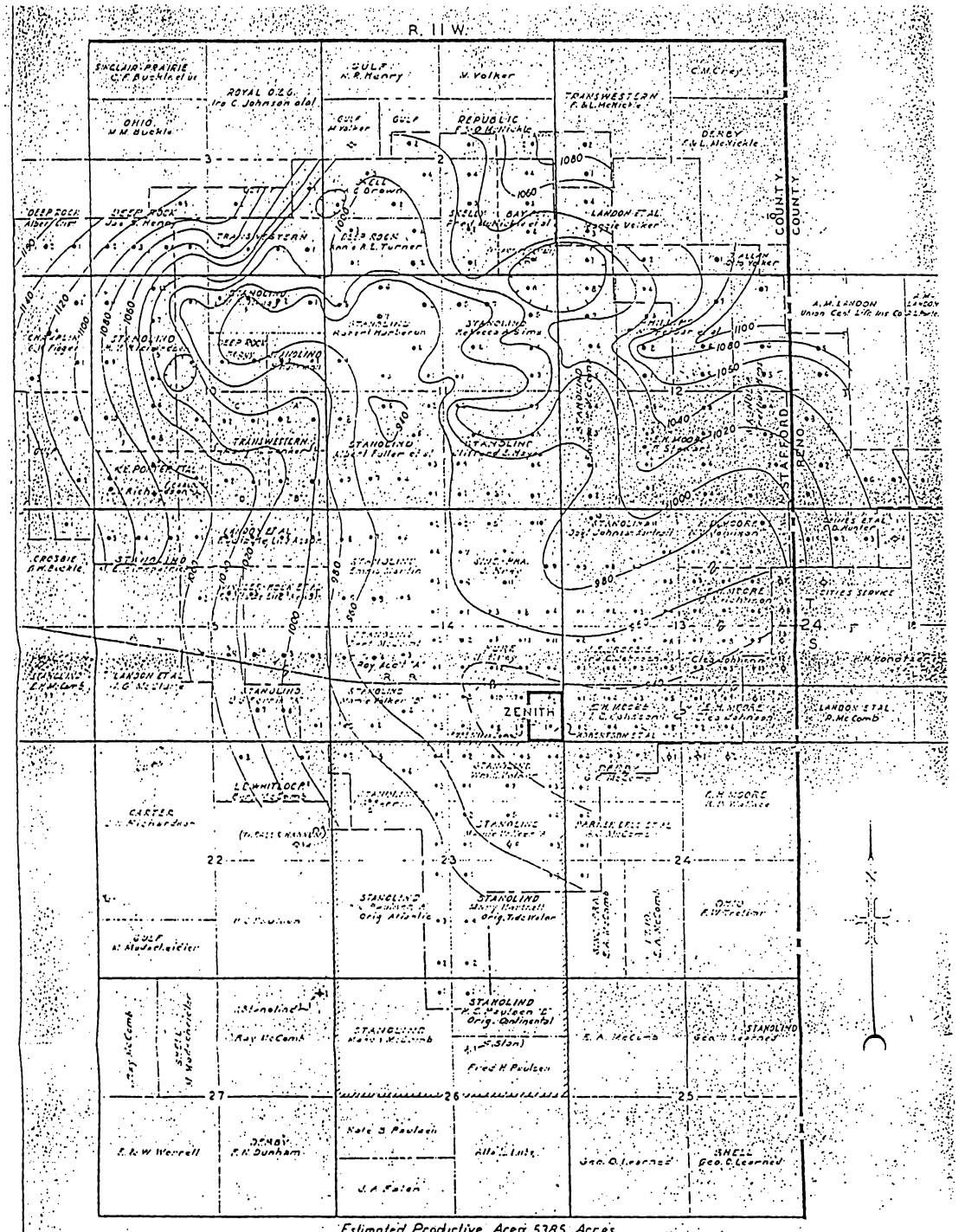
R. 11 W.
COUNTY
STAFFORD
RENO
ZENITH
Estimated Productive Area 5385 Acres
Weighted Average B.H.P. 1001 P.S.I.
UNIT MEMBERS
Company | Percent
Stanolind (Operator) | 30.000
Tide Water | 14.666
Atlantic | 14.666
Continental | 16.666
LEGEND
Outline Unit Outline
Limits of Developed Area
Limits of Productive Area
ZENITH AREA
ISOBARIC MAP DEC. 1940
PRESSURE AT 1900'
DR. O.R.G. | TR. O.R.G. | CK. J.H.D. | AP. | NO
SCALE 1" = 2000' | DATE 3-13-39
Orig Drg. No. 30-67

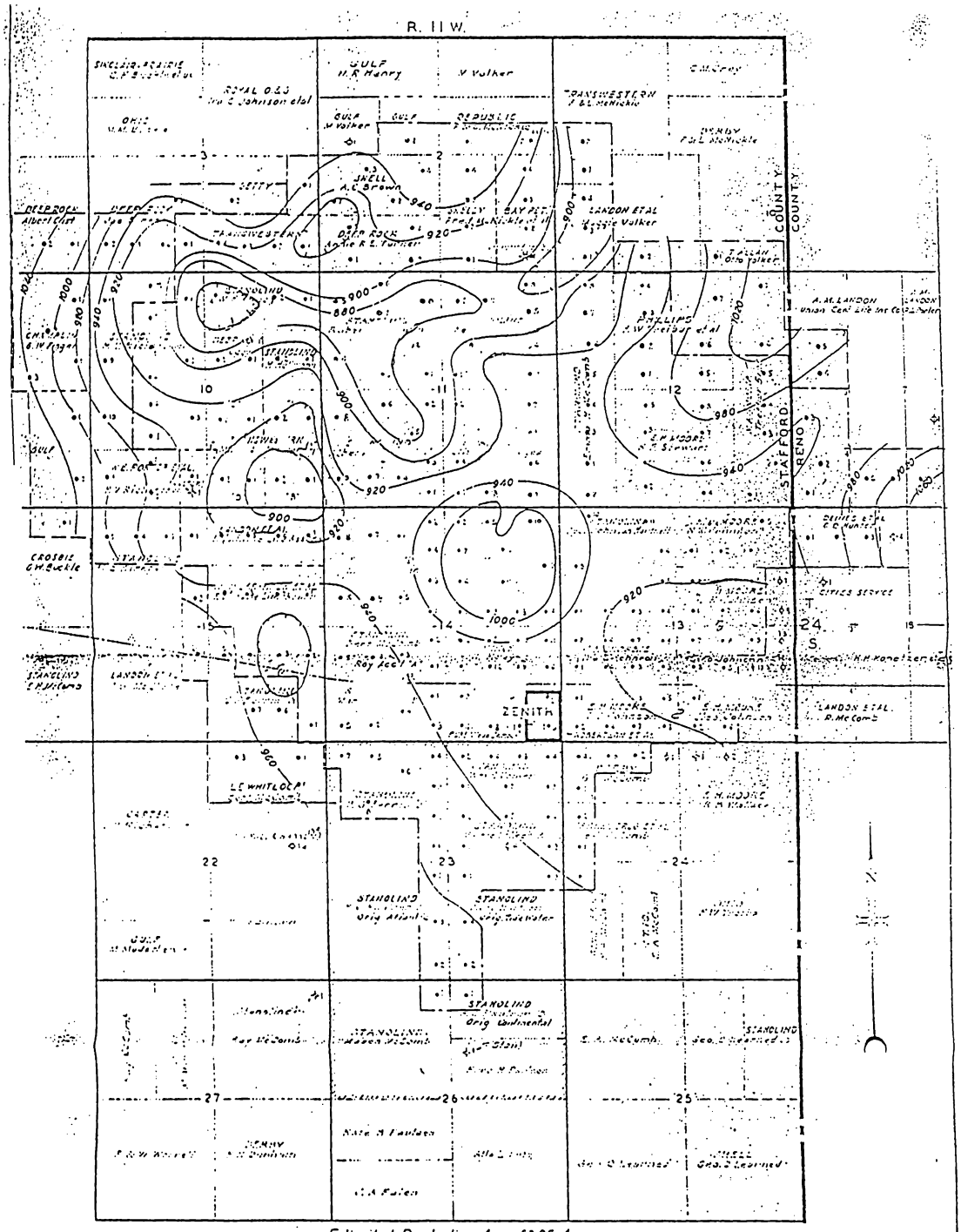
R. 11 W.
COUNTY
COUNTY
STAFFORD
RENO
ZENITH
T. 24 S.
22
23
24
25
26
27
Estimated Productive Area 5385 Acres
Weighted Average B.H.P. 937 P.S.I.
UNIT MEMBERS
Company
Percent
LEGEND
Limits of Developed Area
Limits of Productive Area
ZENITH AREA
ISOBARIC MAP JUNE 1941 -
PRESSURE AT 1900'
SCALE 1" = 2000'
DATE 3-13-39
Orig. Drg. No 50-67

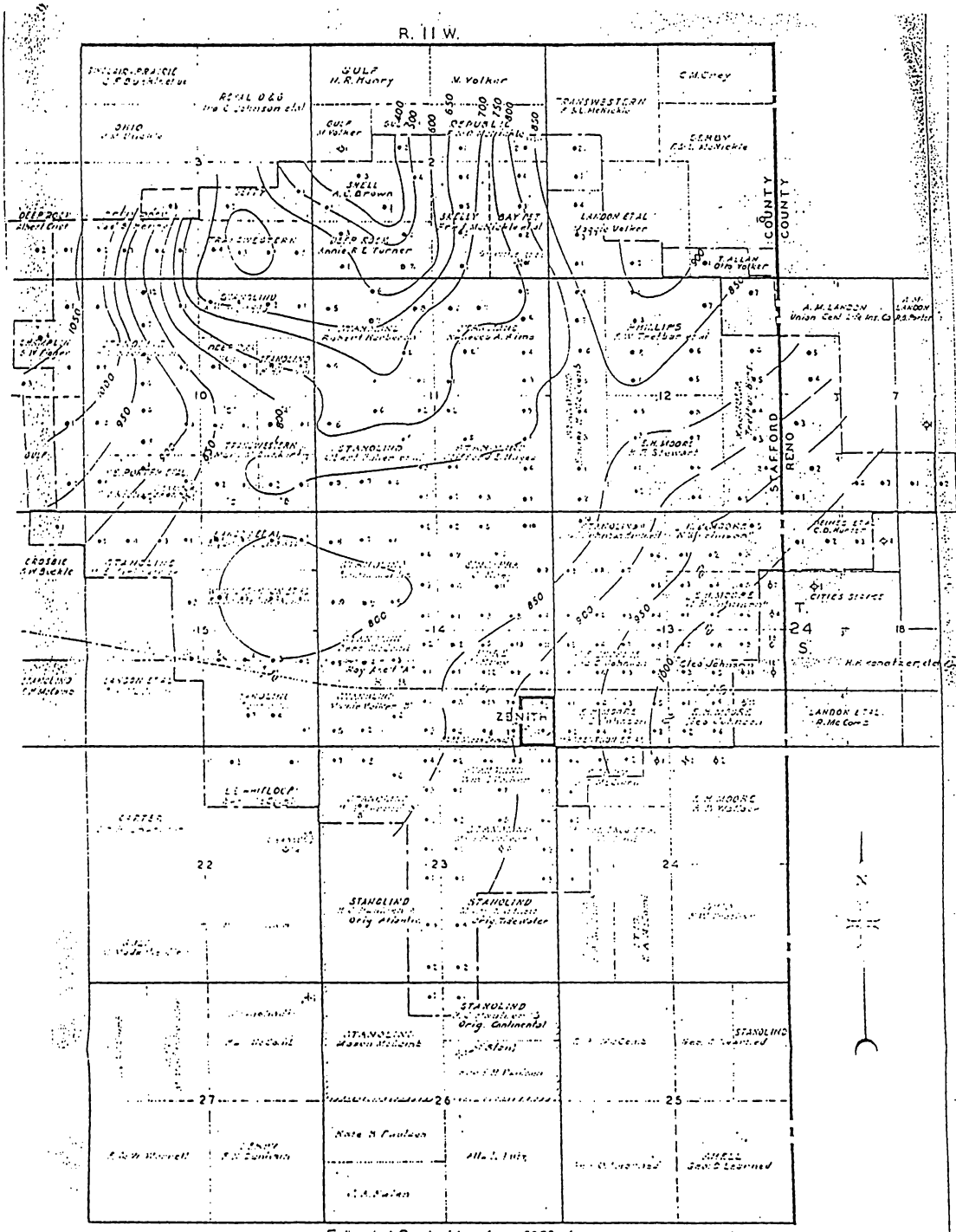
R. 11 W.
STAFFORD COUNTY
RENO COUNTY
ZENITH
T. 24 S.
Estimated Productive Area 5385 Acres
Weighted Average B.H.P. 832 P.S.I.
UNIT MEMBERS
LEGEND
Limits of Developed Area
Limits of Productive Area
ZENITH AREA
ISOBARIC MAP JAN. 1942
PRESSURE AT 1900'
SCALE 1" = 2000'
DATE 3-13-39
Orig. Drg. No. 30-67

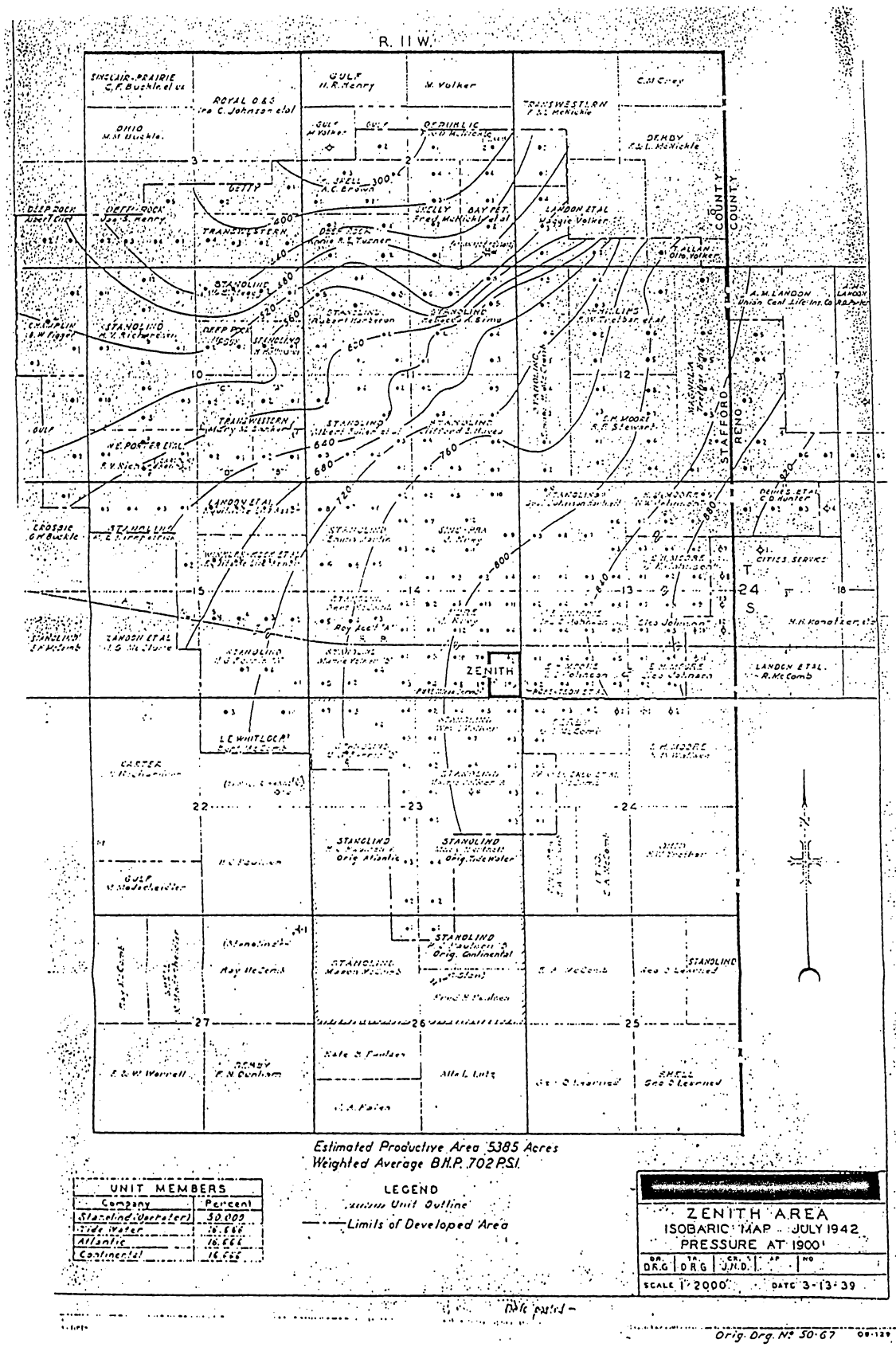
R. 11 W.
COUNTY
STAFFORD
RENO
COUNTY
T. 24 S.
ZENITH
Estimated Productive Area 5385 Acres
Weighted Average B.H.P. 702 P.S.I.
UNIT MEMBERS
Company | Percent
Stanolind (Operator) | 50.000
Tide Water | 16.666
Atlantic | 16.666
Continental | 16.666
LEGEND
Unit Outline
Limits of Developed Area
ZENITH AREA
ISOBARIC MAP - JULY 1942
PRESSURE AT 1900'
DR. D.R.G. | TR. D.R.G. | CK. J.N.D. | AP. | NO.
SCALE 1" = 2000'
DATE 3-13-39
Orig. Drg. No. 50-67

Zenith Field Pressure
July 1944

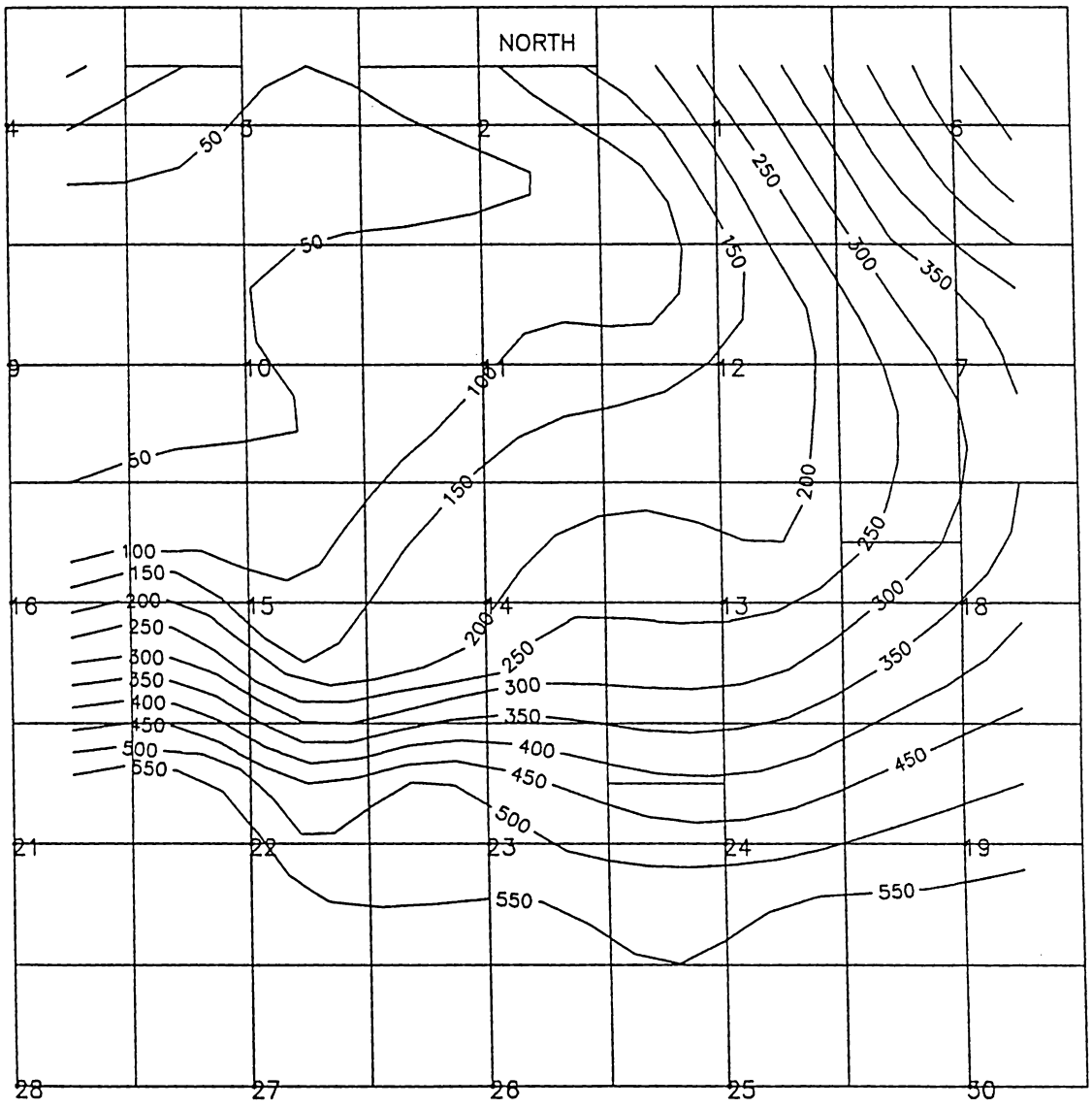

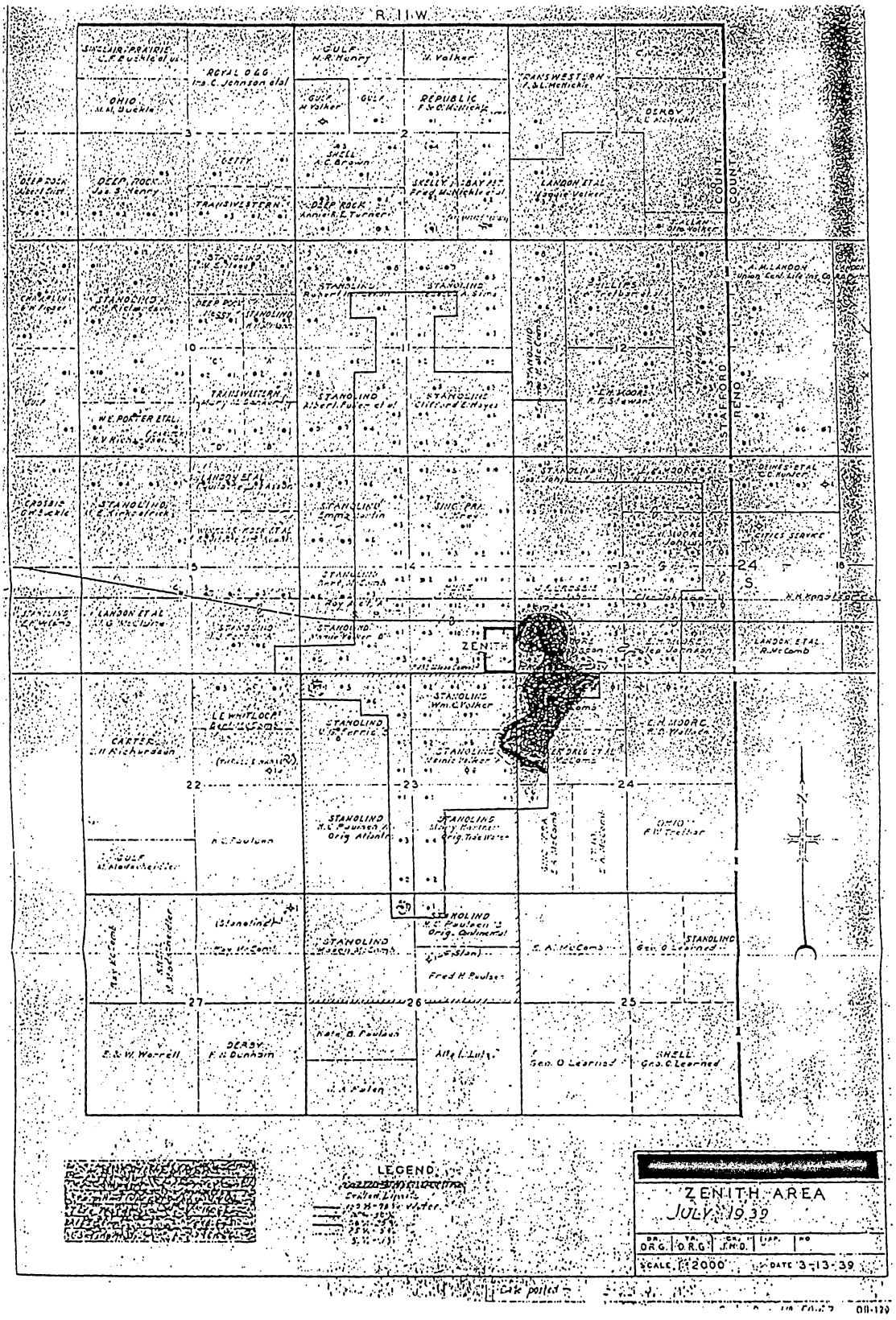
R. 11 W.
ZENITH
STAFFORD COUNTY
RENO
LEGEND
ZENITH AREA
JULY, 1939
SCALE 1" = 2000'
DATE 3-13-39

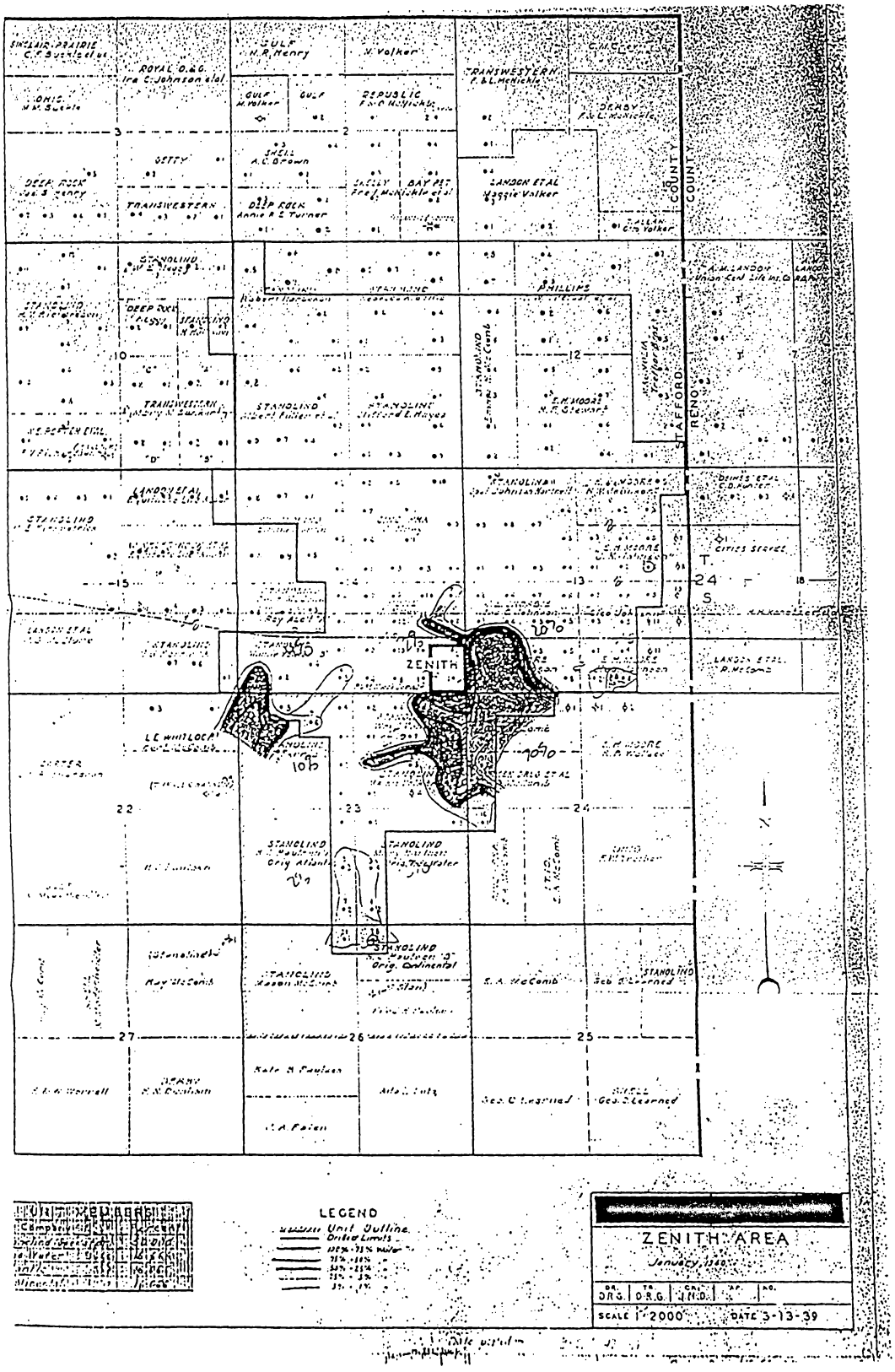
ZENITH
LEGEND
Unit Outline
Drilled Limits
ZENITH AREA
January 1940
SCALE 1" = 2000'
DATE 3-13-39

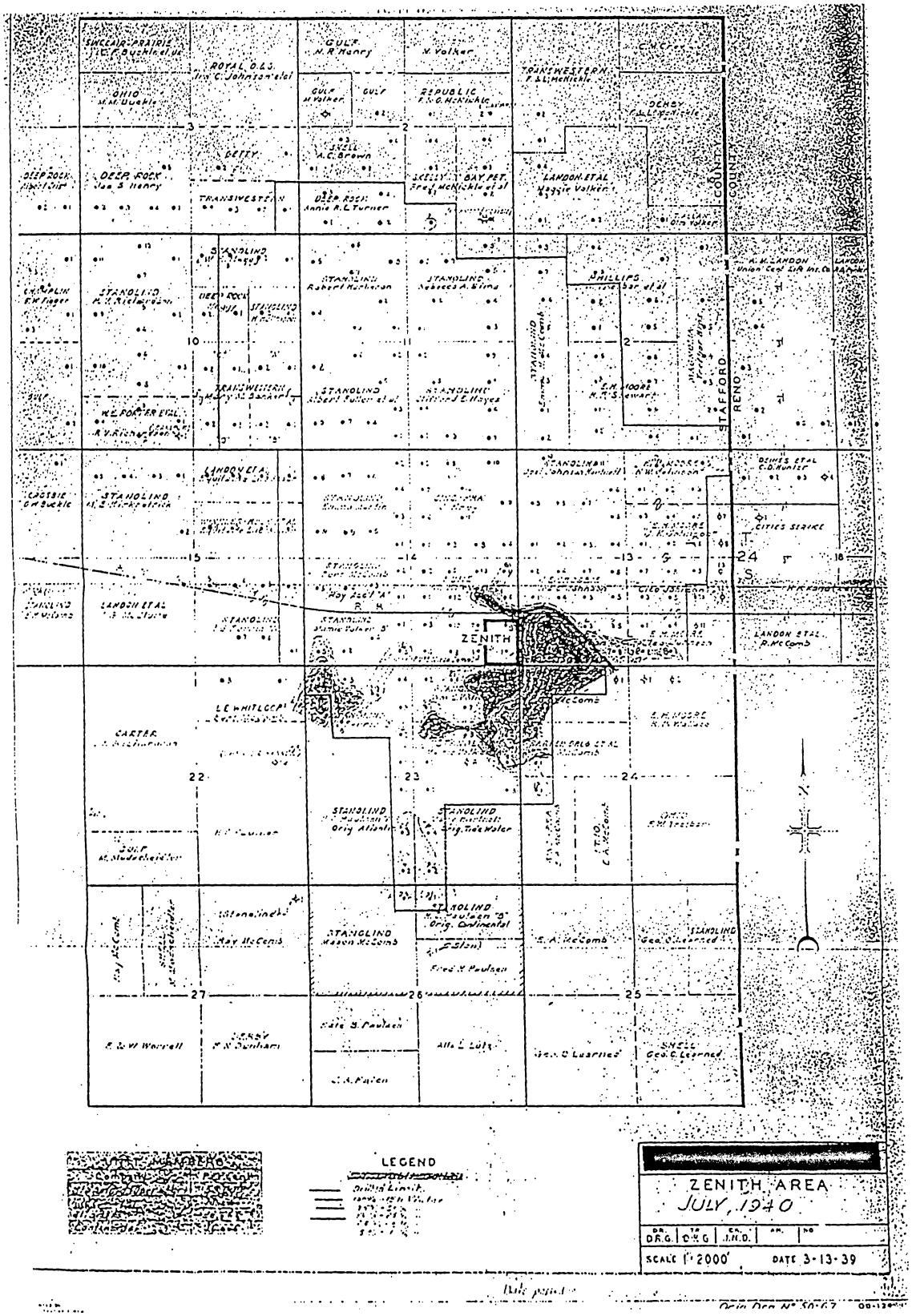
ZENITH
COUNTY
RENO
STAFFORD
LEGEND
ZENITH AREA
JULY, 1940
SCALE 1" = 2000'
DATE 3-13-39

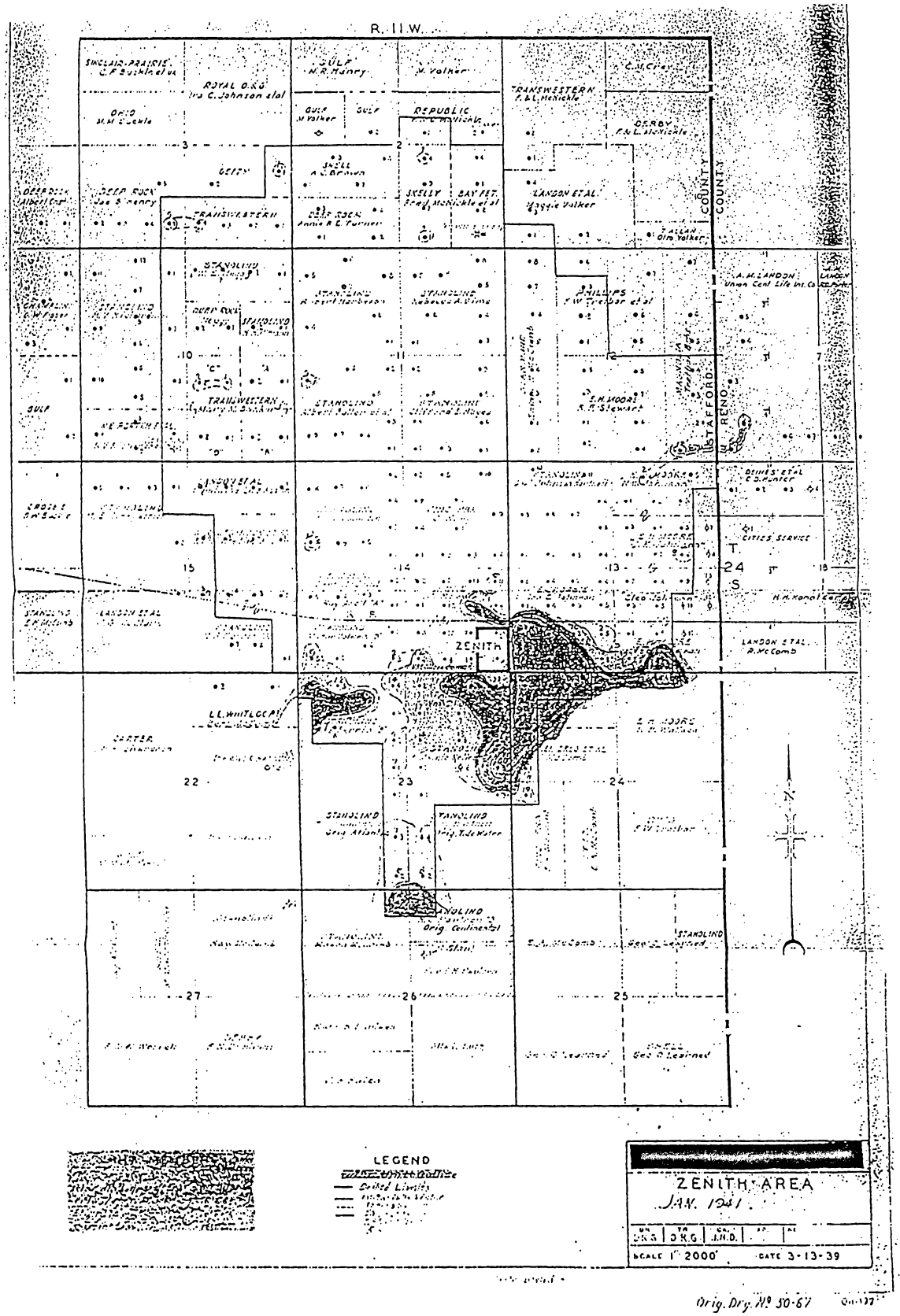
R. 11 W.
COUNTY
STAFFORD
RENO
T. 24 S.
ZENITH
LEGEND
ZENITH AREA
JAN. 1941
SCALE 1" 2000'
DATE 3-13-39
Orig. Drg. No 50-67

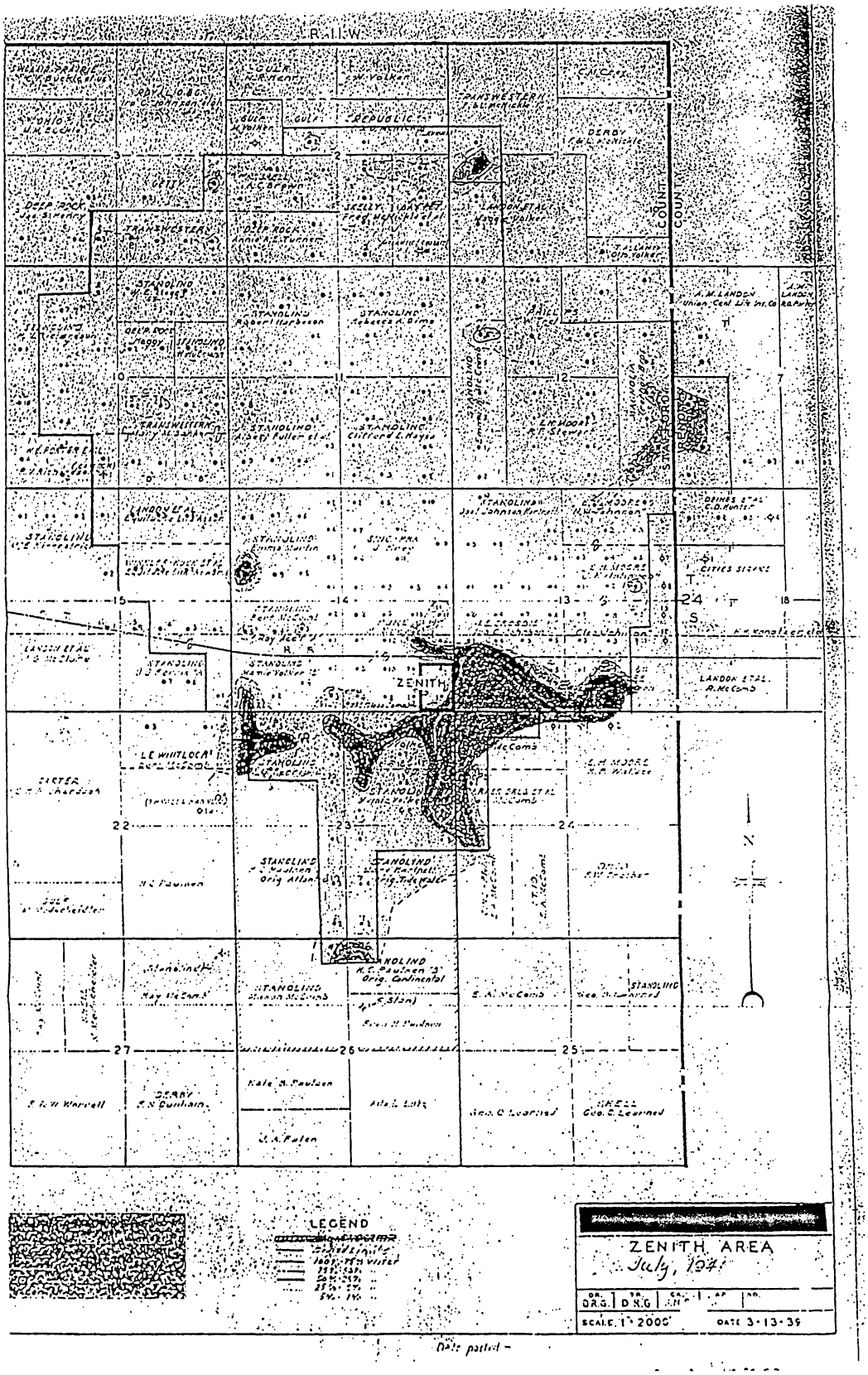
R. 11 W.
ZENITH
LEGEND
ZENITH AREA
July, 1941
SCALE 1" 2000'
DATE 3-13-39
Date posted -

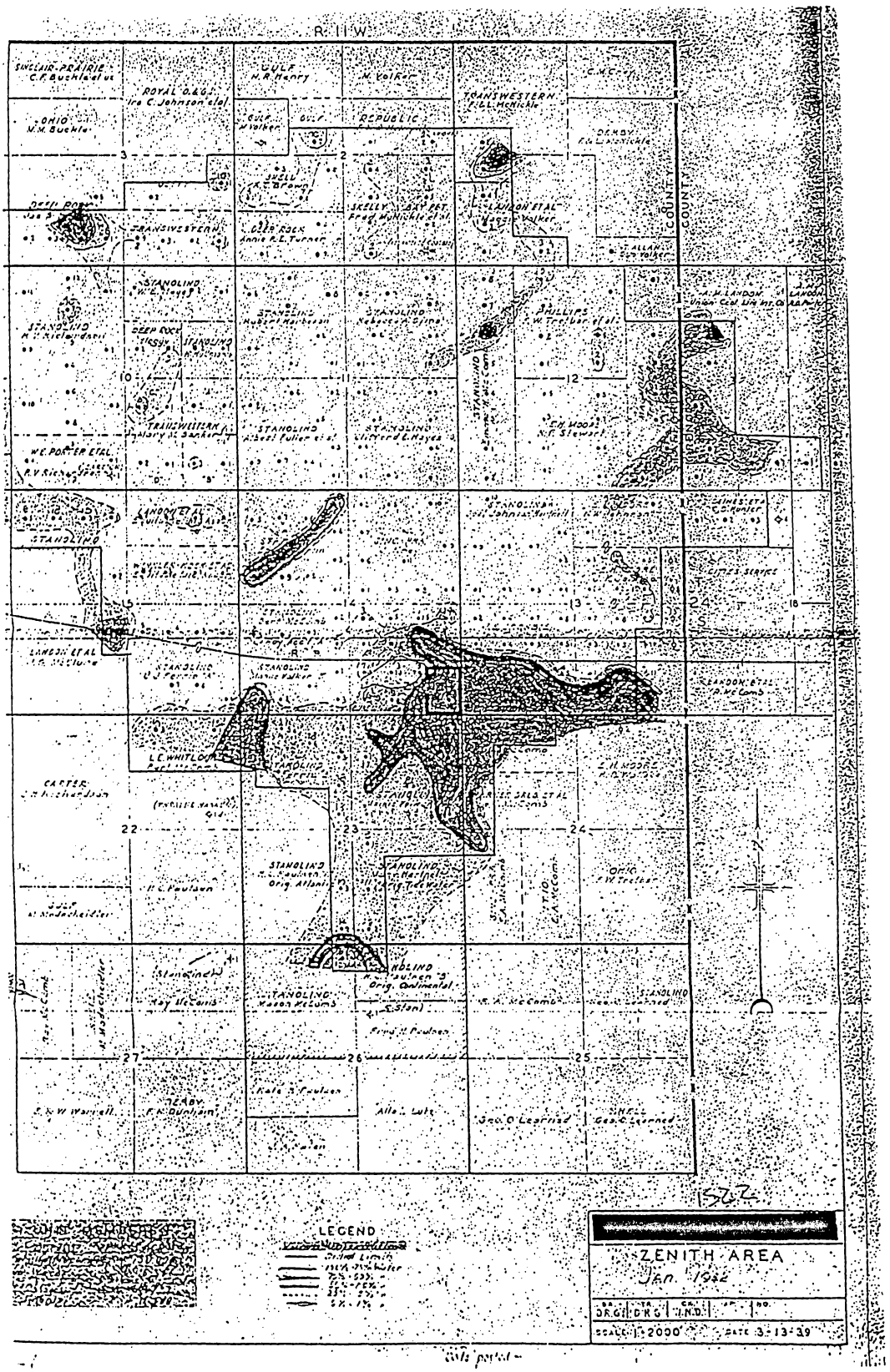
R 11 W
LEGEND
ZENITH AREA
Jan. 1942
SCALE 1:2000
DATE 3-13-39

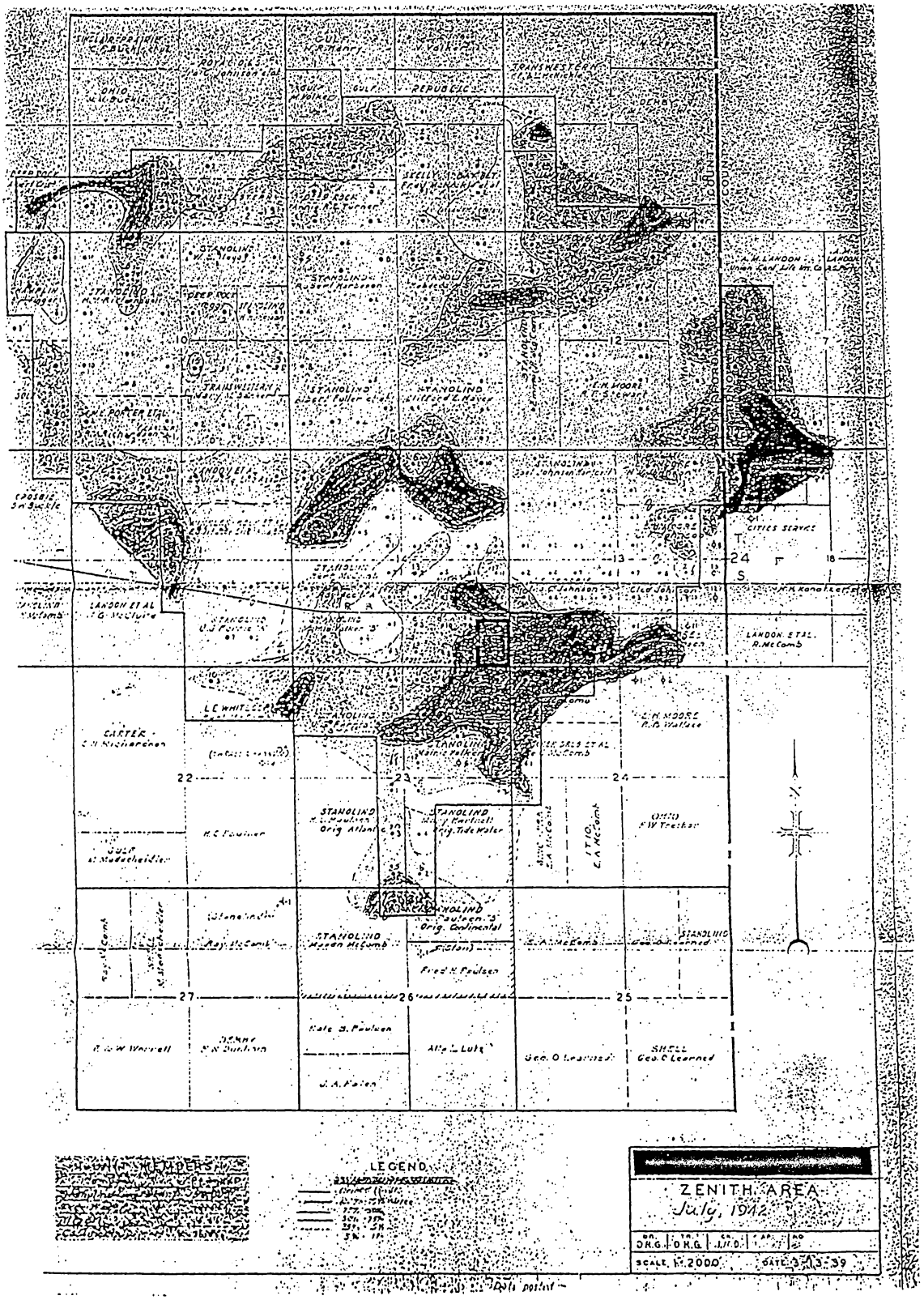
ZENITH AREA
July, 1942
SCALE 1" = 2000'
DATE 3-13-39
LEGEND
T 24 S
R 18
22
23
24
27
26
25
CITIES SERVICE
STANOLIND
GULF
REPUBLIC
LANDON ET AL
CARTER
DENNY
SHELL

APPENDIX III

Plots used in Analysis of Transient Tests

This appendix contains the plots that were constructed when analyzing transient tests conducted on wells in the Zenith Field. Example calculations are provided to demonstrate type-curve matching procedure.

Hayes #3 Falloff Test

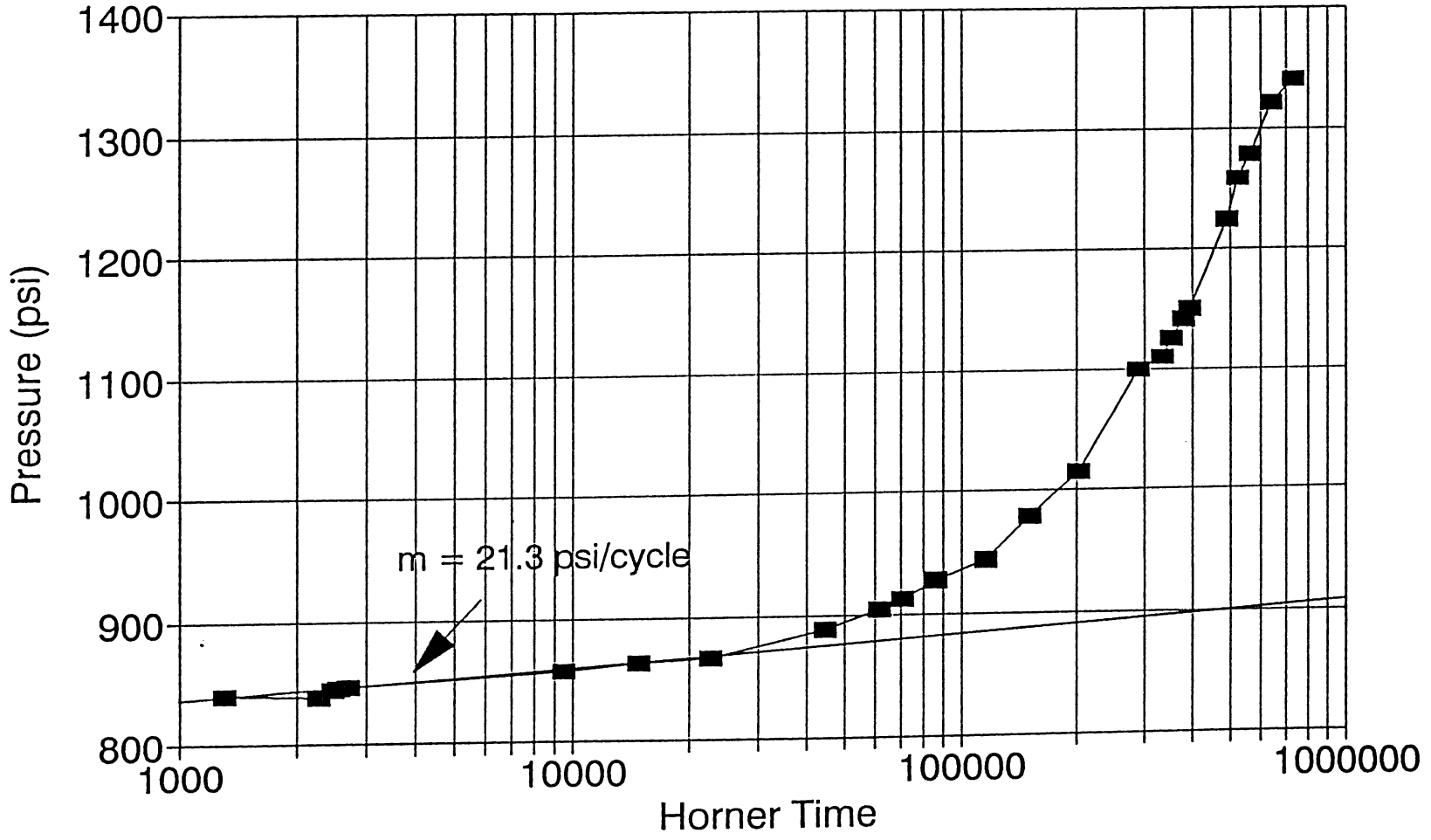

Hayes #3 Fall-off Test

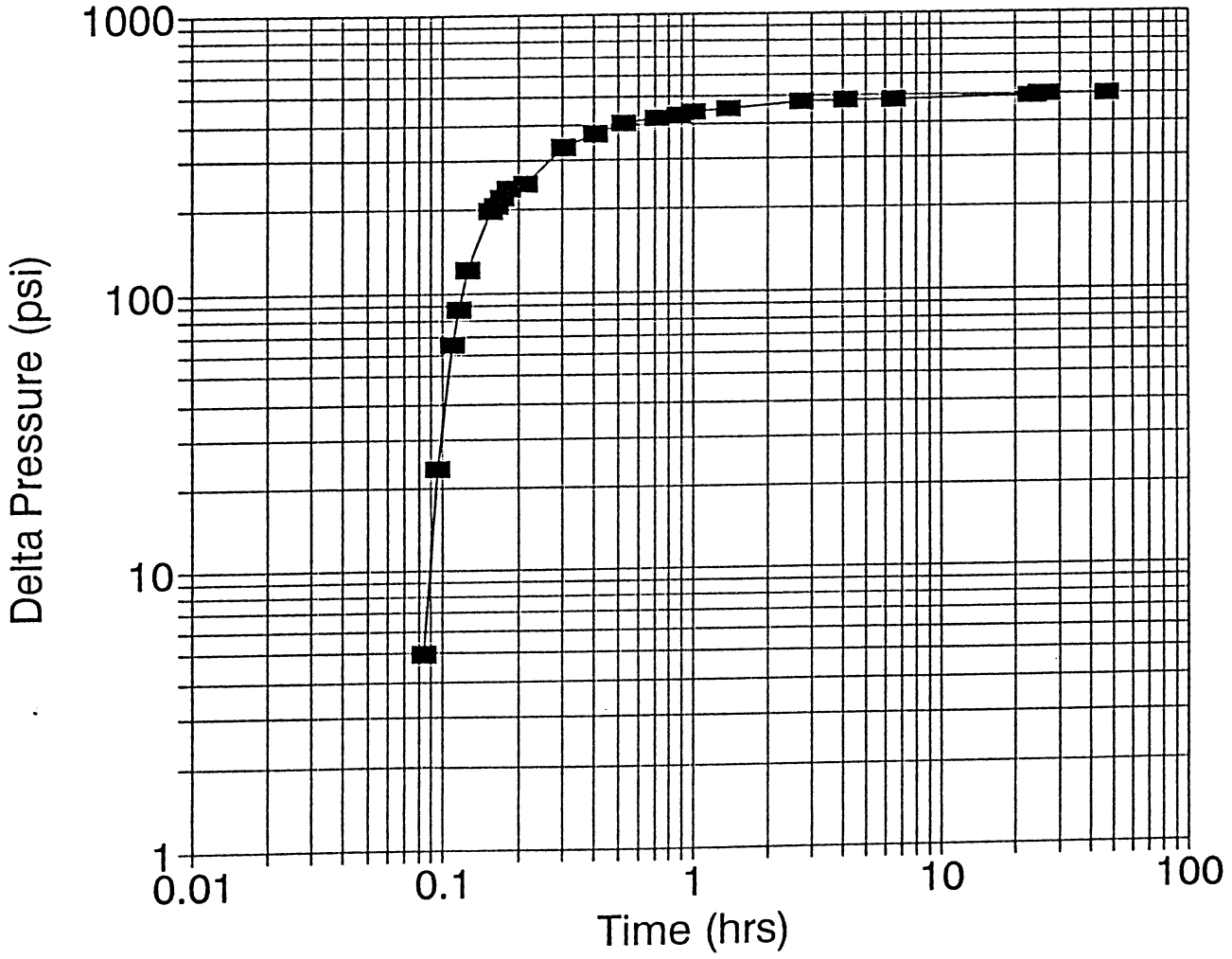

Hayes #5 Falloff Test

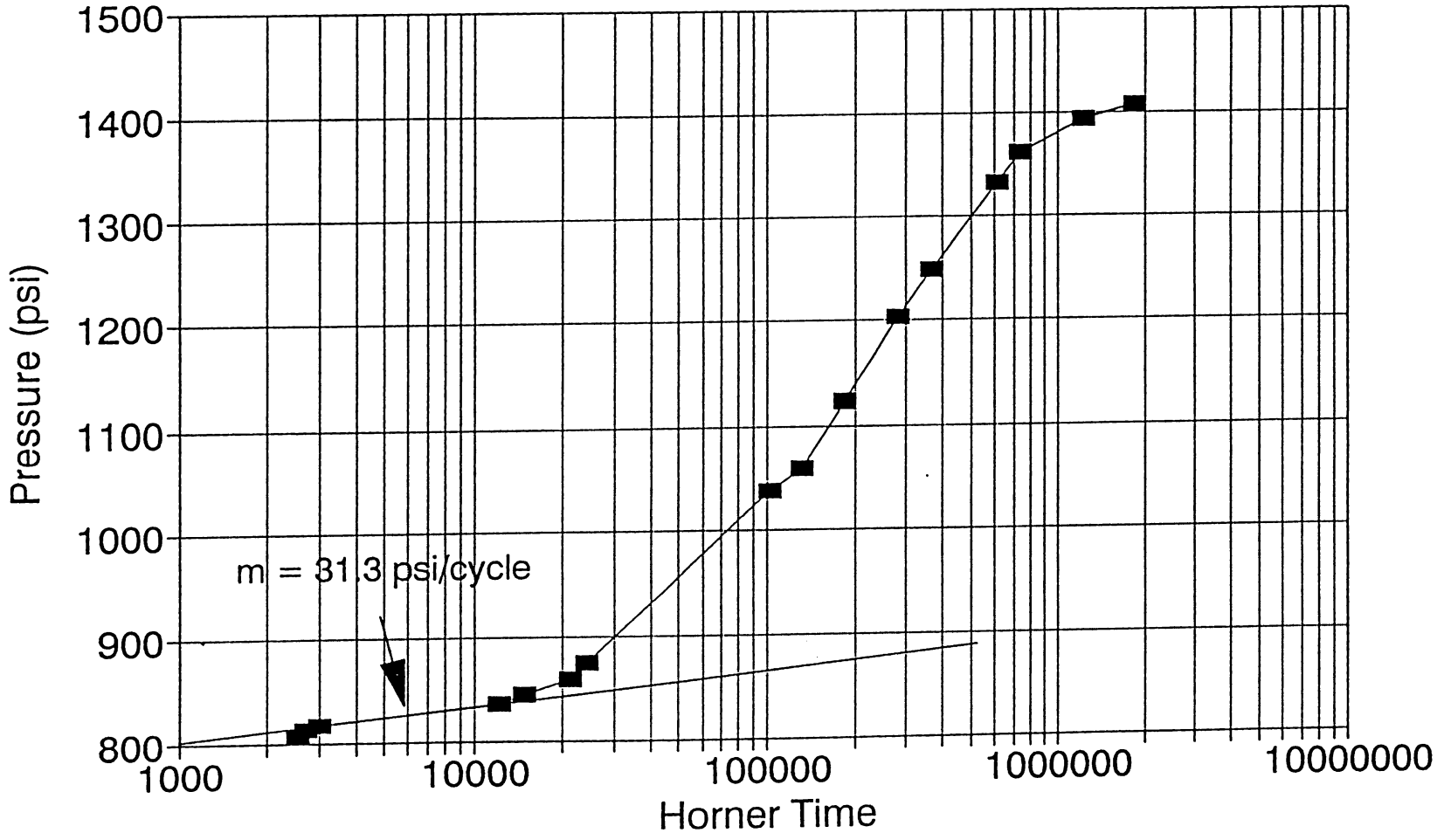

Hayes #5 Fall-off Test

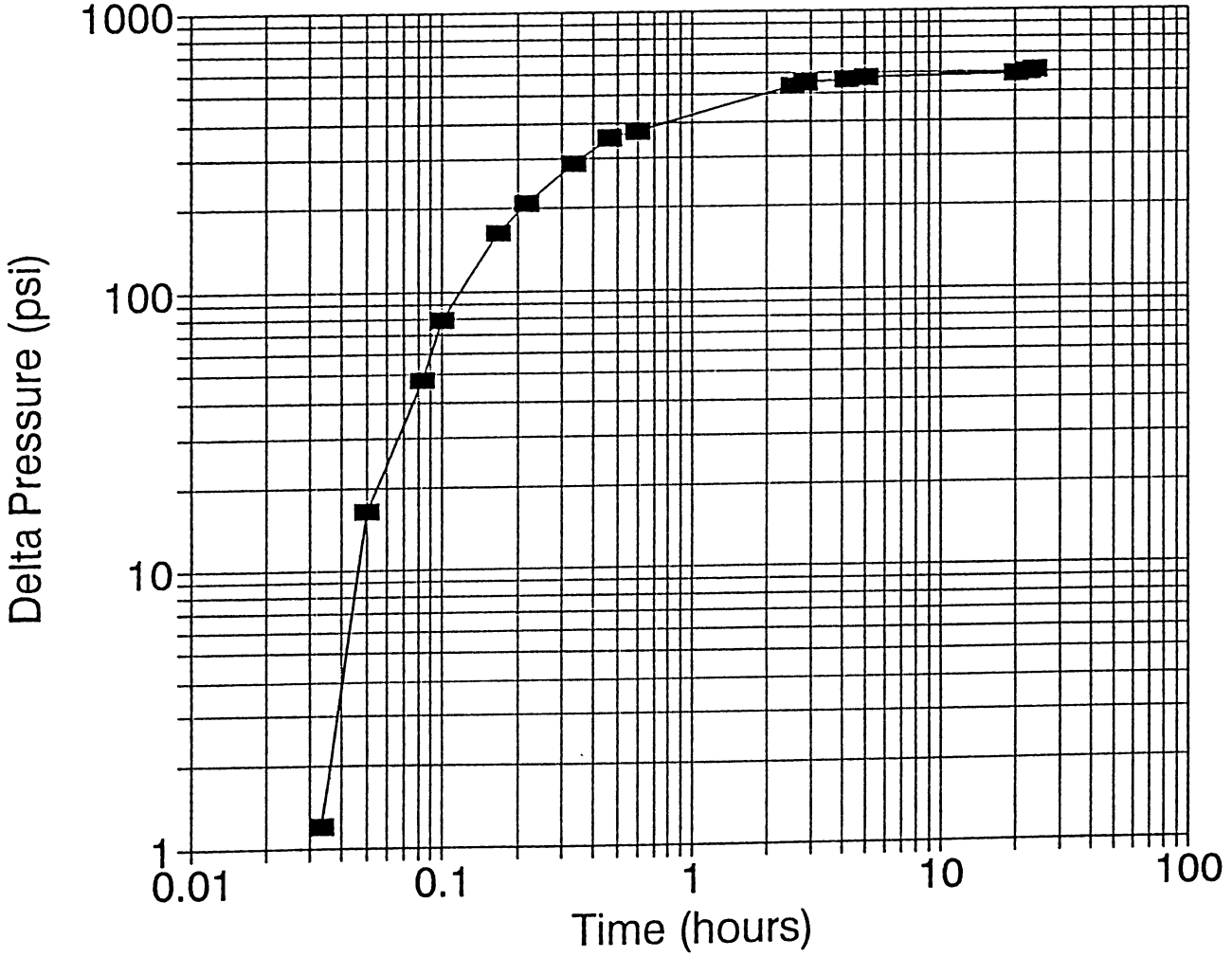

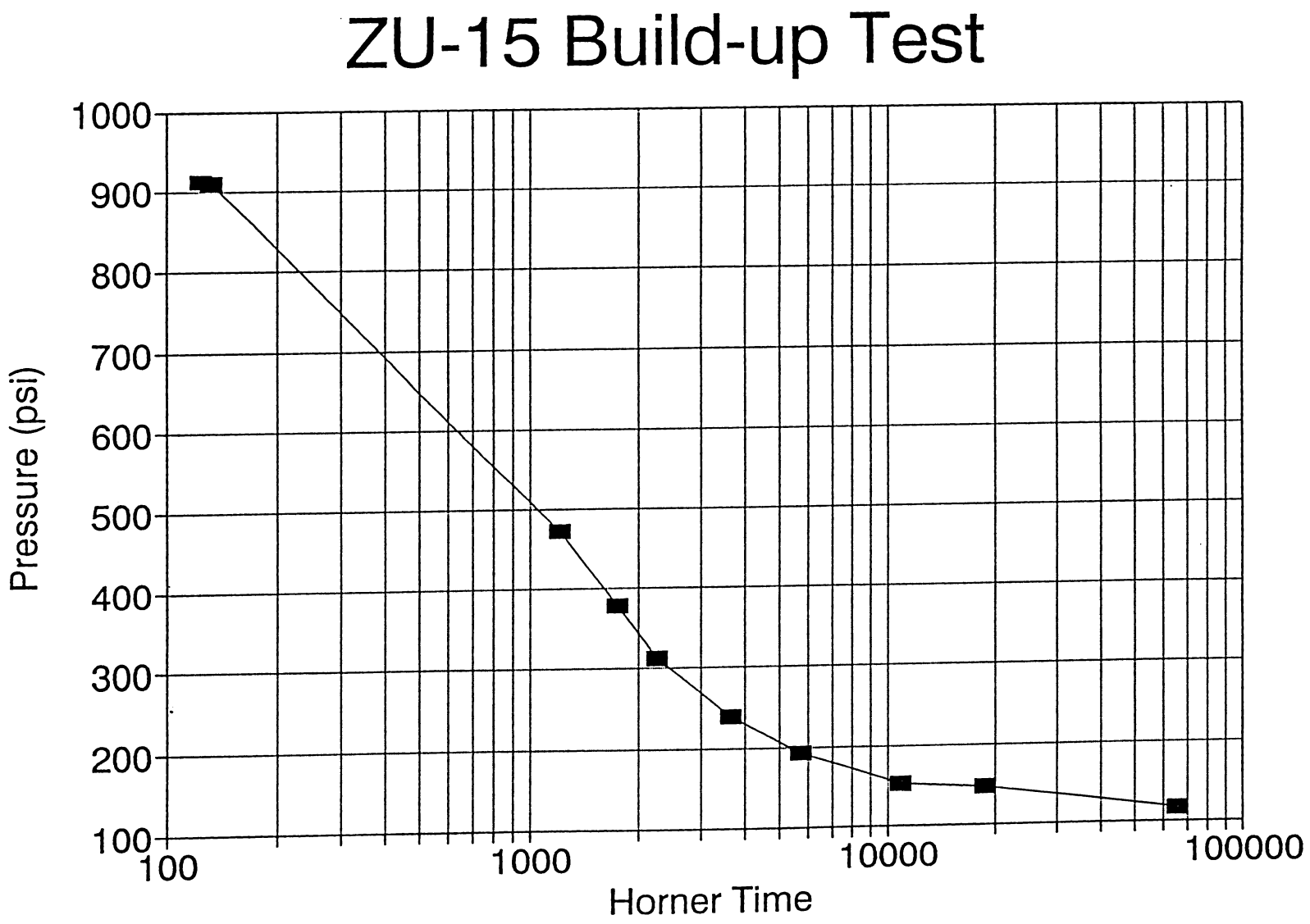
ZU-15 Build-up Test
Pressure (psi)
1000
900
800
700
600
500
400
300
200
100
100
1000
10000
100000
Horner Time

ZU-15 Build-up Test

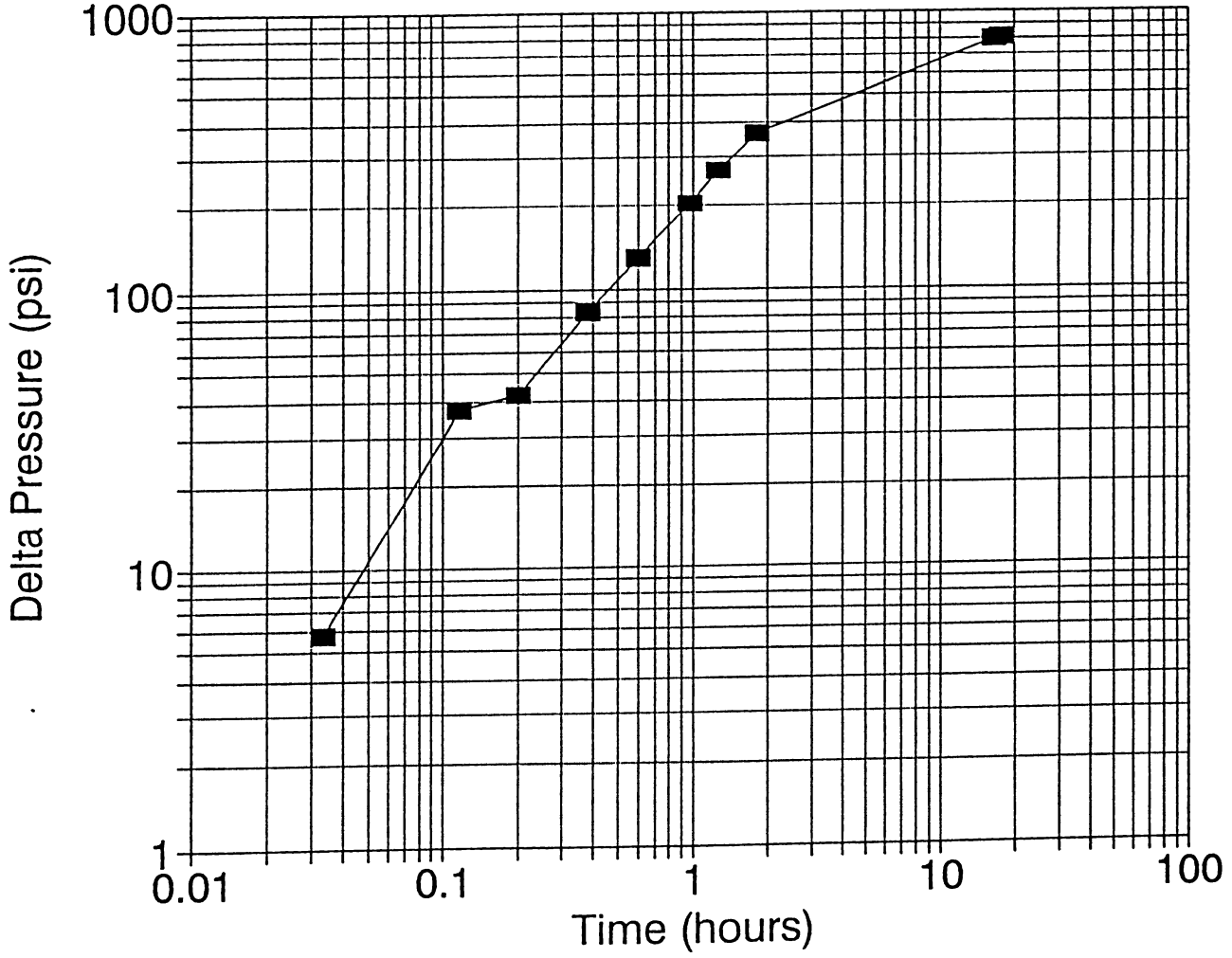

ZU-25 Falloff Test

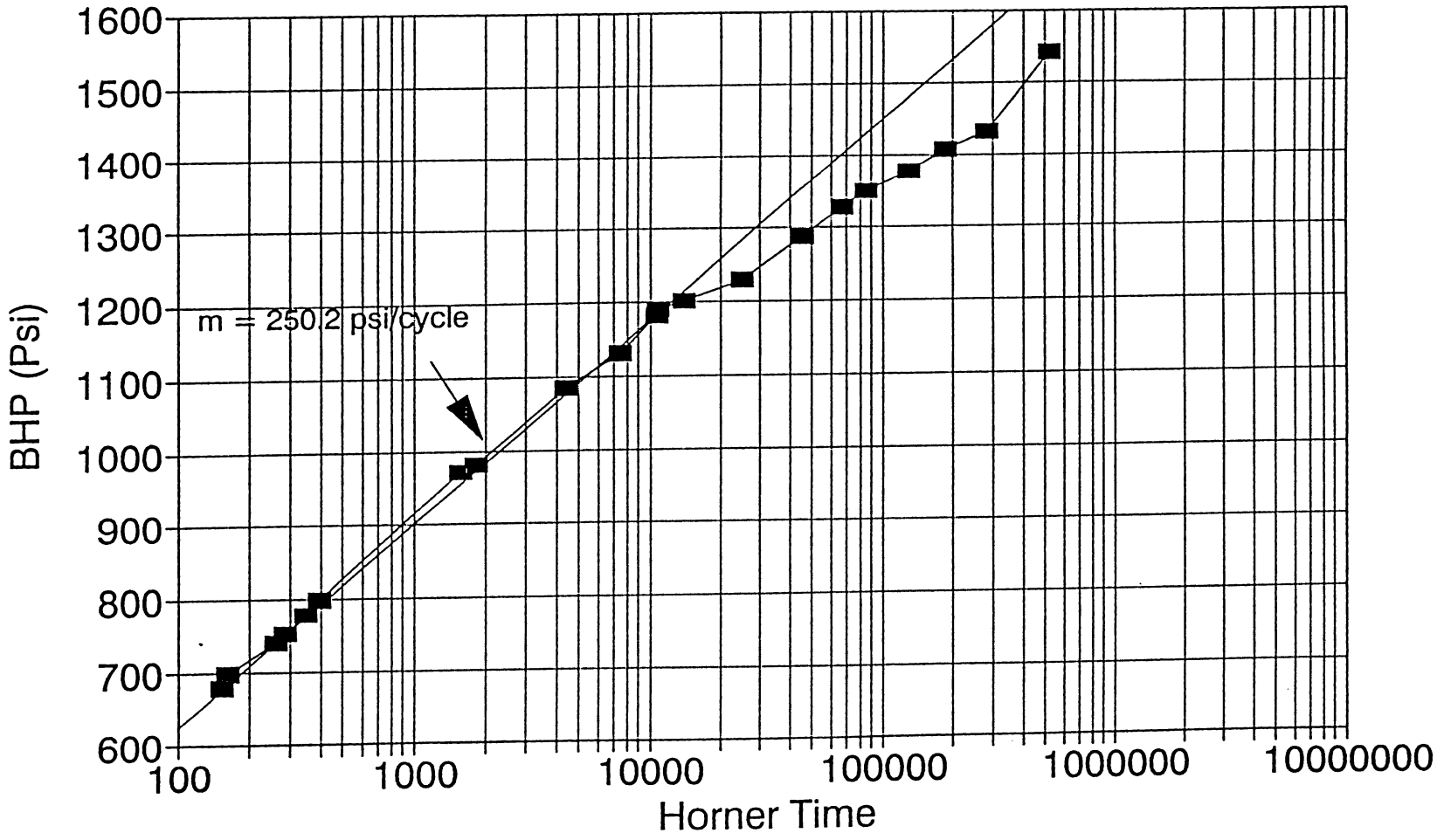

ZU-25 Falloff Test

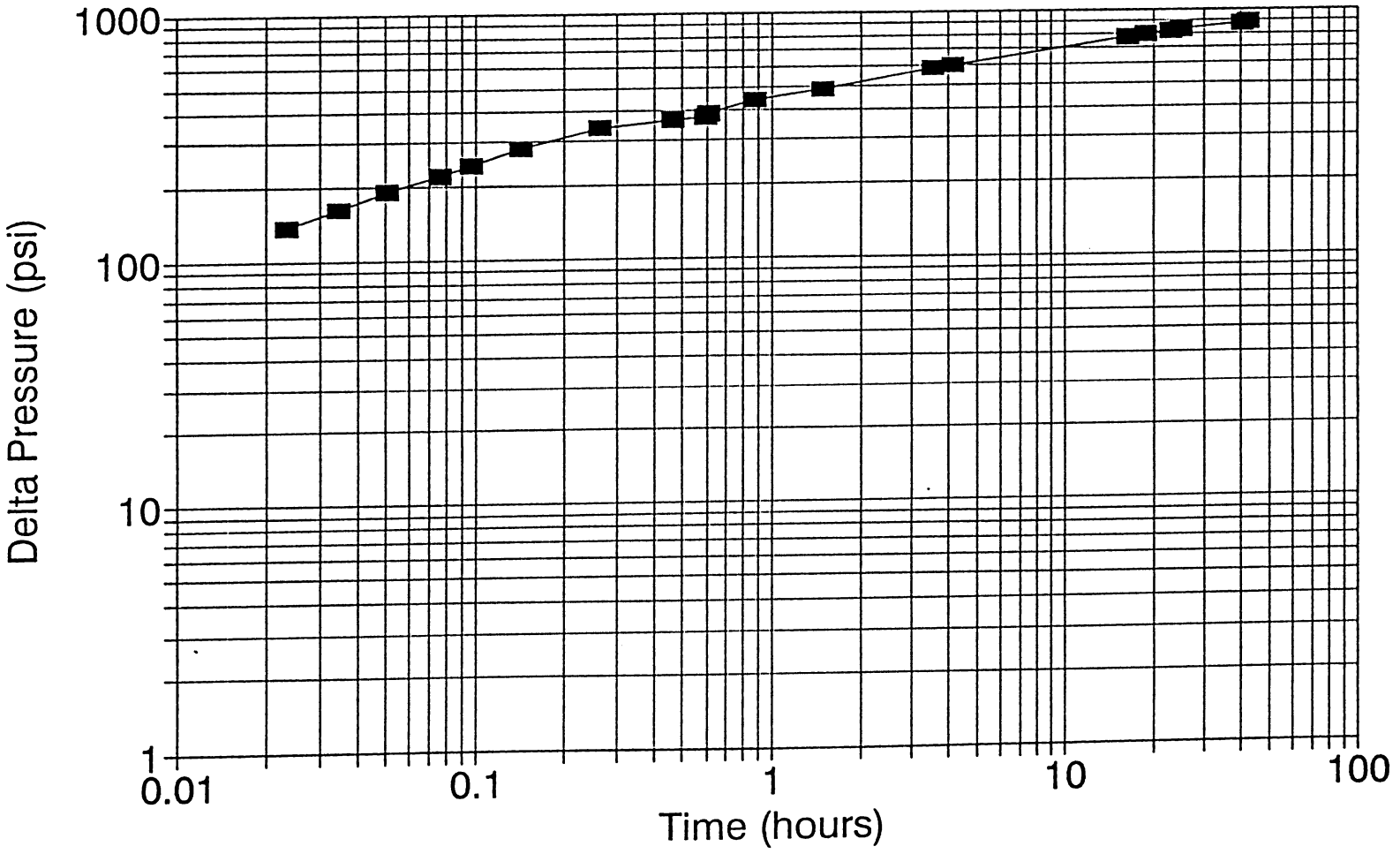

ZU-29 Falloff Test

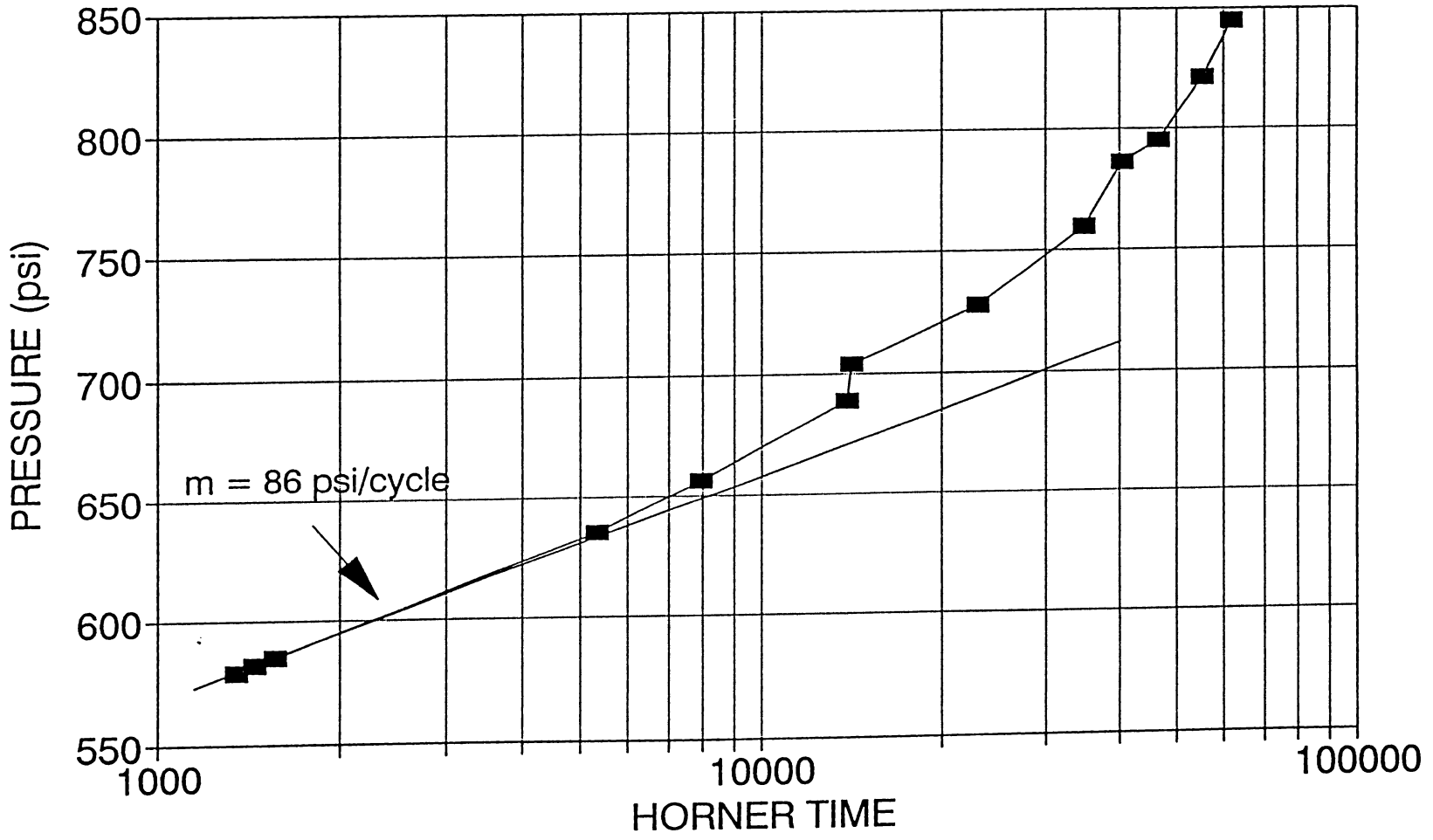

ZU-29 Fall-off Test

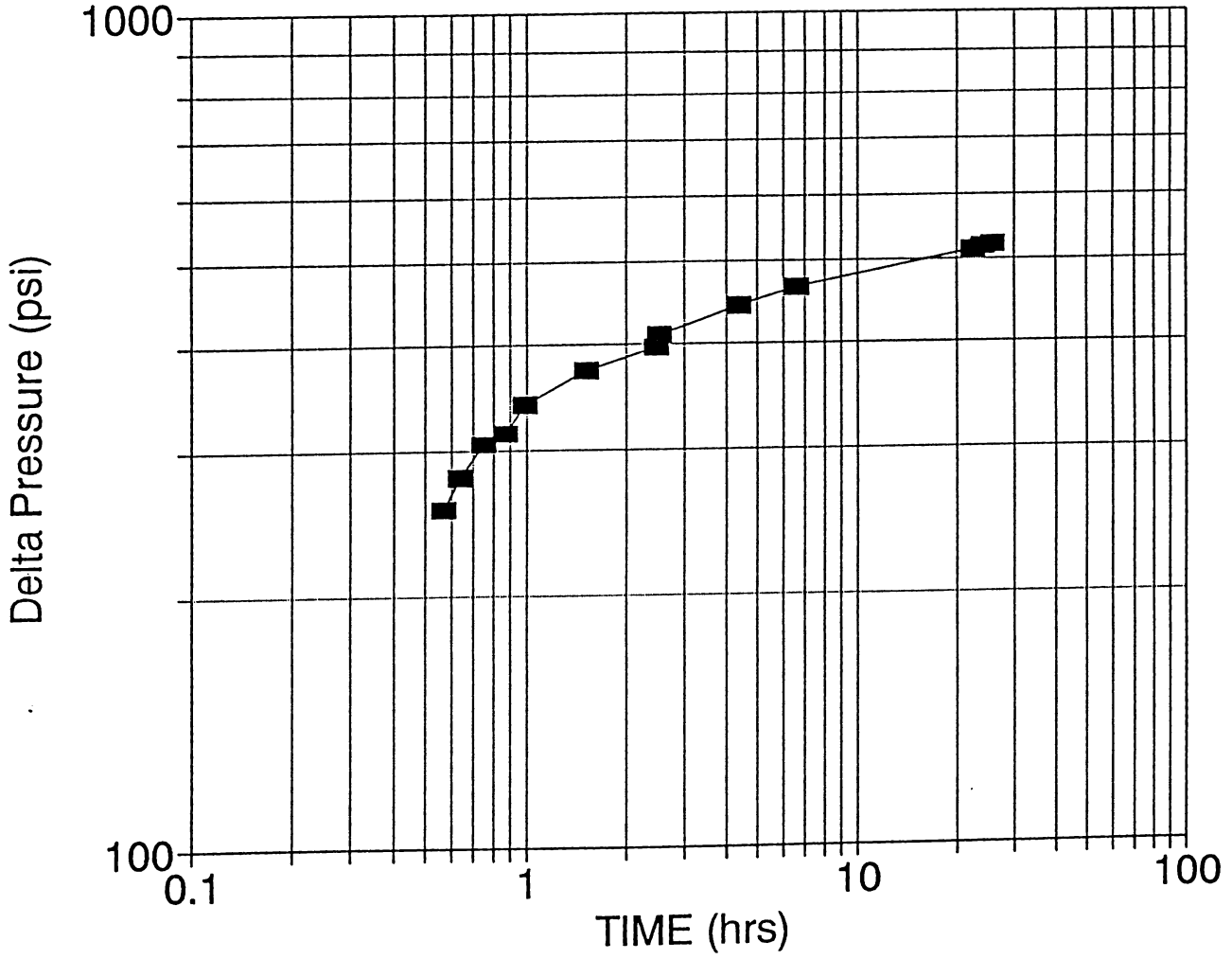

ZU-31 Buildup Test

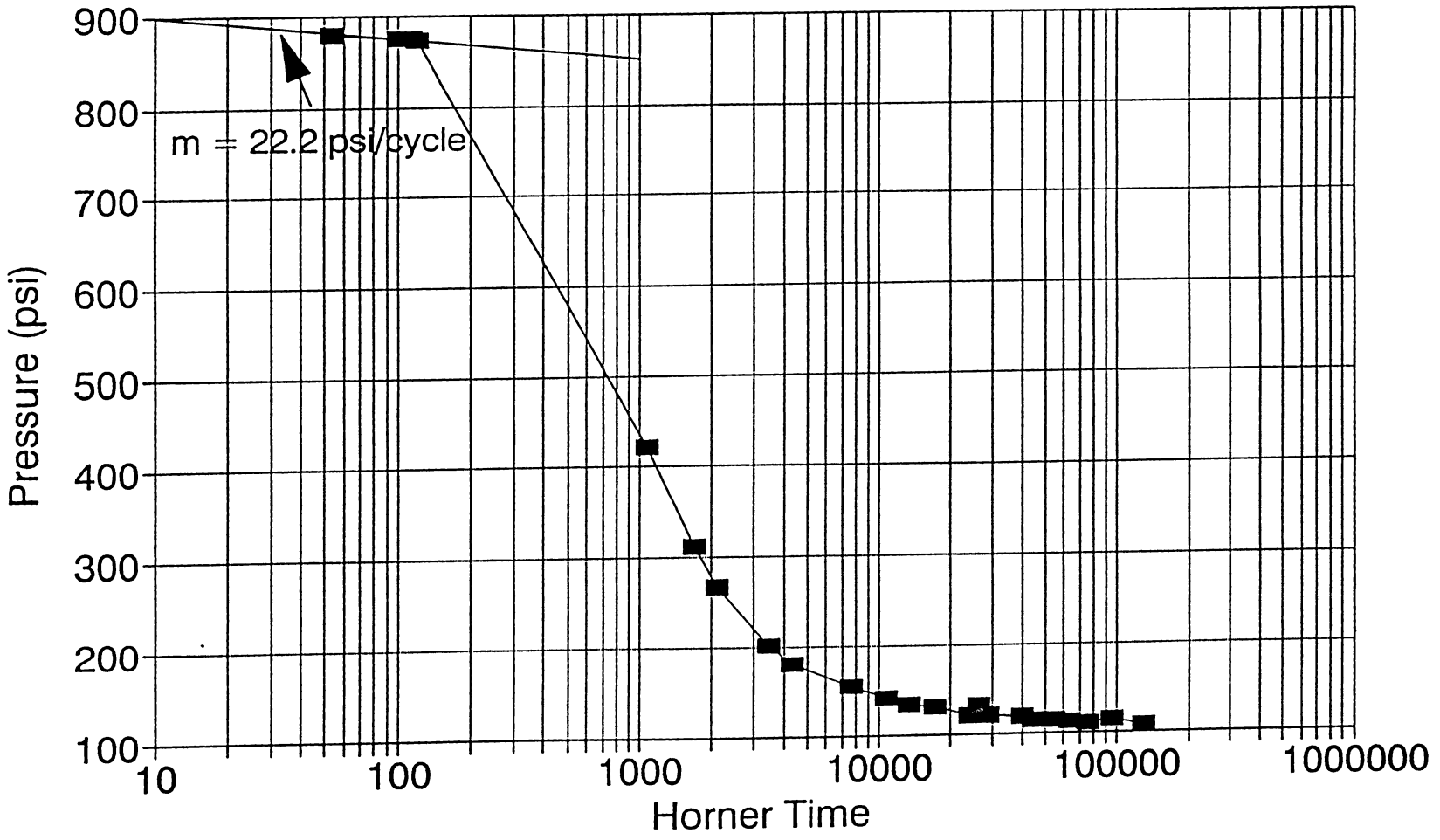

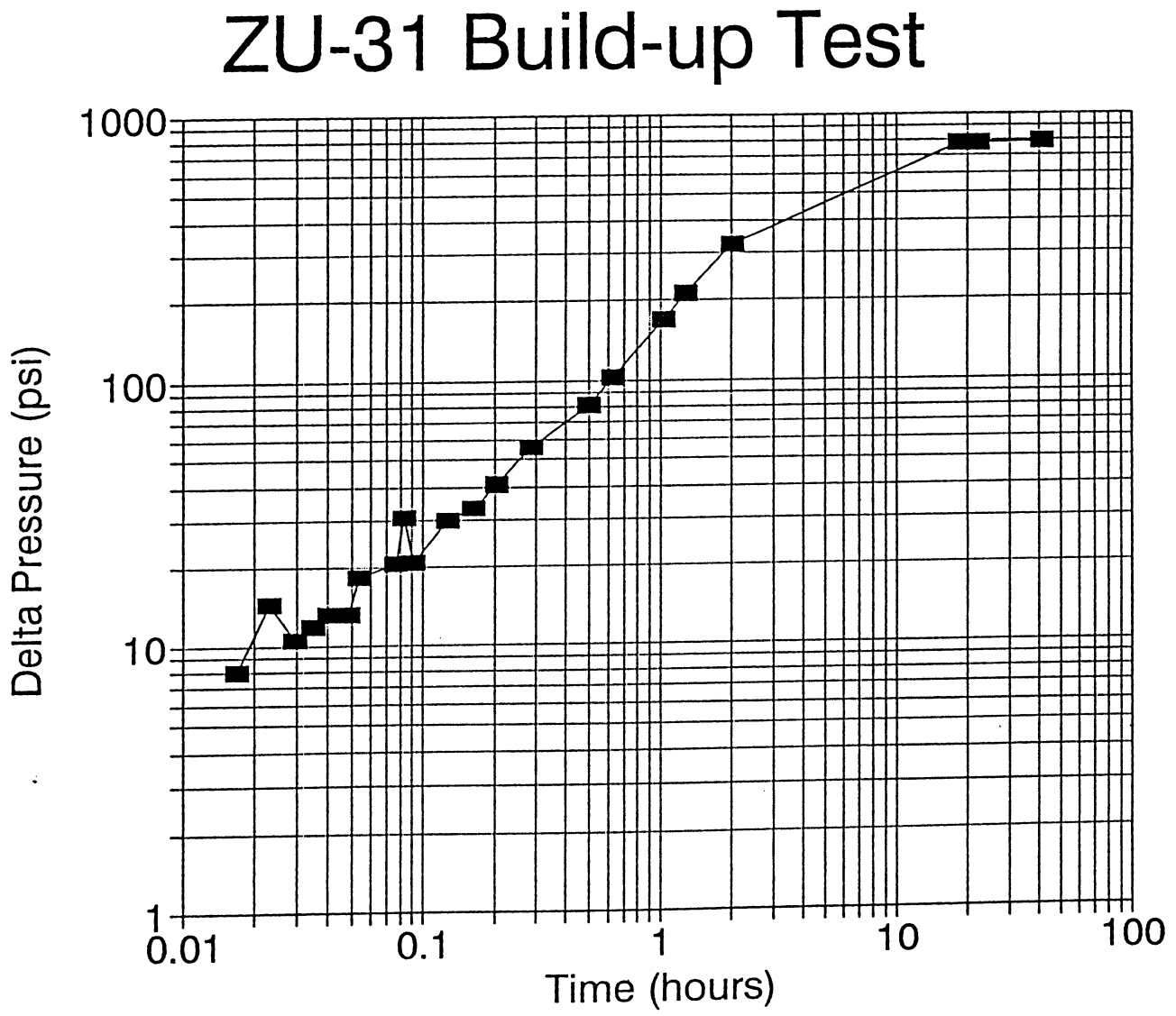
ZU-31 Build-up Test
Delta Pressure (psi)
1000
100
10
1
0.01
0.1
1
10
100
Time (hours)

ZU-5W Falloff Test

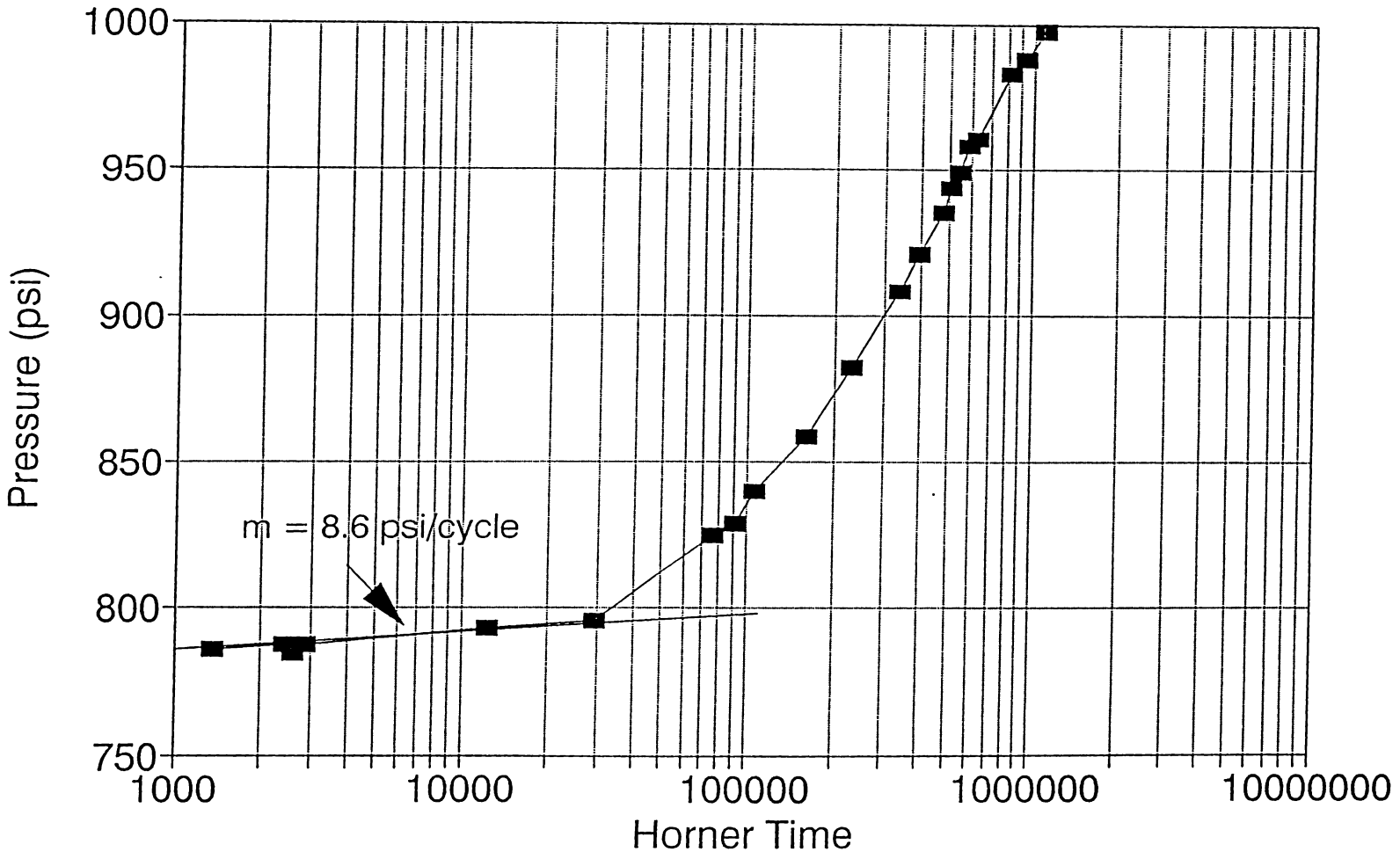

ZU-5W Falloff Test

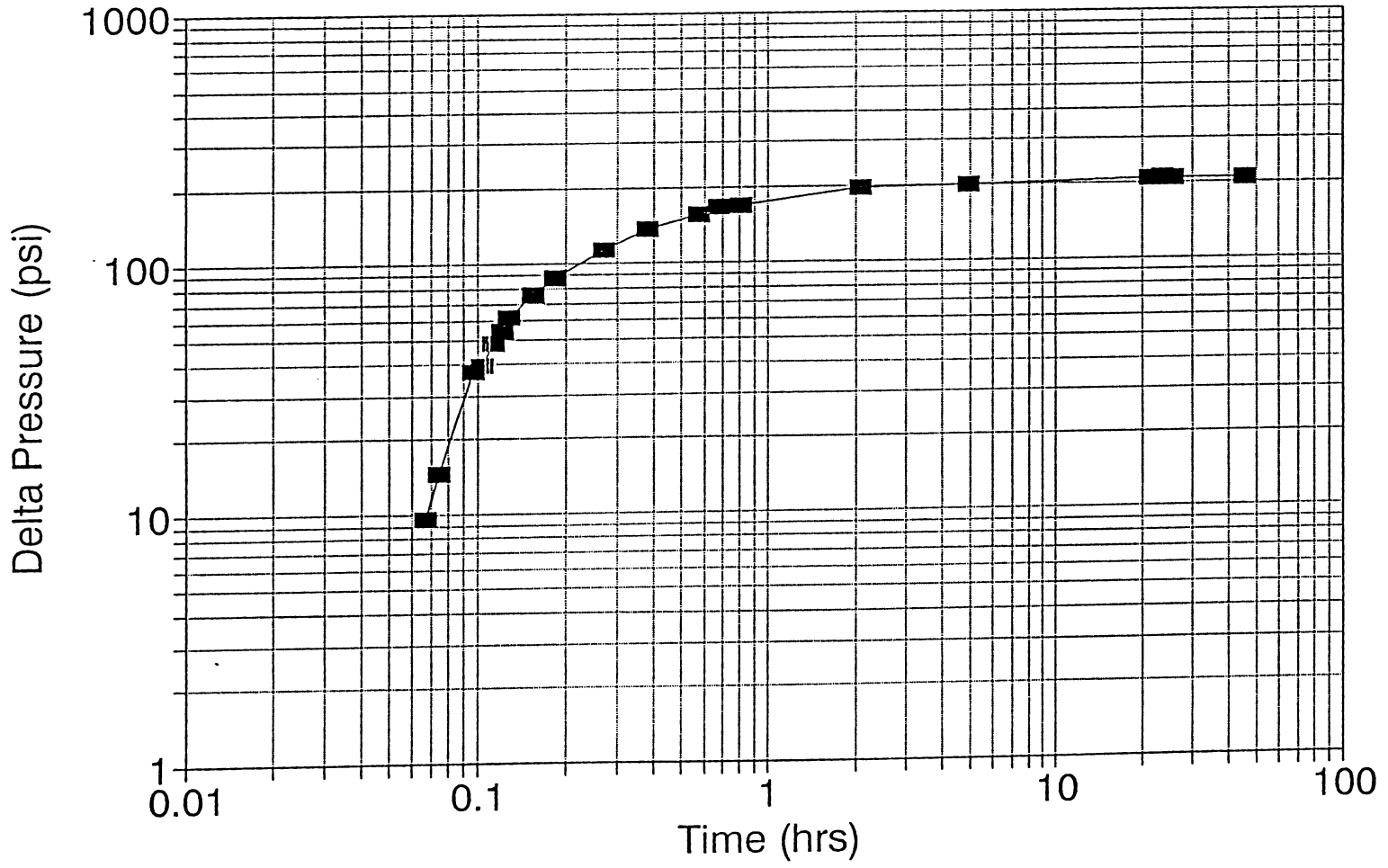

Example Type Curve Analysis
ZU-13 Fall-off Test

Assume the following parameters:

A_{wb} = 0.16 ft^2
ρ = 65 lb/ft^3
ϕ = 10%
c_t = 20 X 10^{-6}
h = 10 ft
r_w = 2.5 in = .21 ft
q = 1600 STB/day
B = 1.0 res. bbl./STB
μ = 0.7 cp

$$C_s = \frac{144*A_{wb}}{5.615*\rho} = 0.063$$

$$C_{sd} = \frac{0.894*C_s}{\phi*c_t*h*r_w^2} = 6.4 \ X \ 10^4$$

Use the 10^5 set of Type Curves.

Skin = -5

The resulting match is shown on the following page.

Match Point

$(P_d)_m$ = 1 $(\Delta P)_m$ = 190 psi

$(t_d)_m$ = 10^6 $(\Delta t)_m$ = 0.76 hours

$$K = \frac{141.2*q*B*\mu}{h}\left(\frac{P_d}{\Delta P}\right)_m = 83 \ md$$

$$c_t = \frac{0.000264*K}{\phi*\mu*r_w^2}\left(\frac{\Delta t}{t_d}\right)_m = 5.4 \ X \ 10^{-6} \ \frac{1}{psi}$$

The assumed and calculated values for c_t show some difference. However, since the calculated value is smaller than the assumed, this would increase the value of C_{sd} further toward 10^5. Therefore, the match is assumed to be as accurate as possible.

Example Type Curve Analysis, ZU-13 Fall-off Test

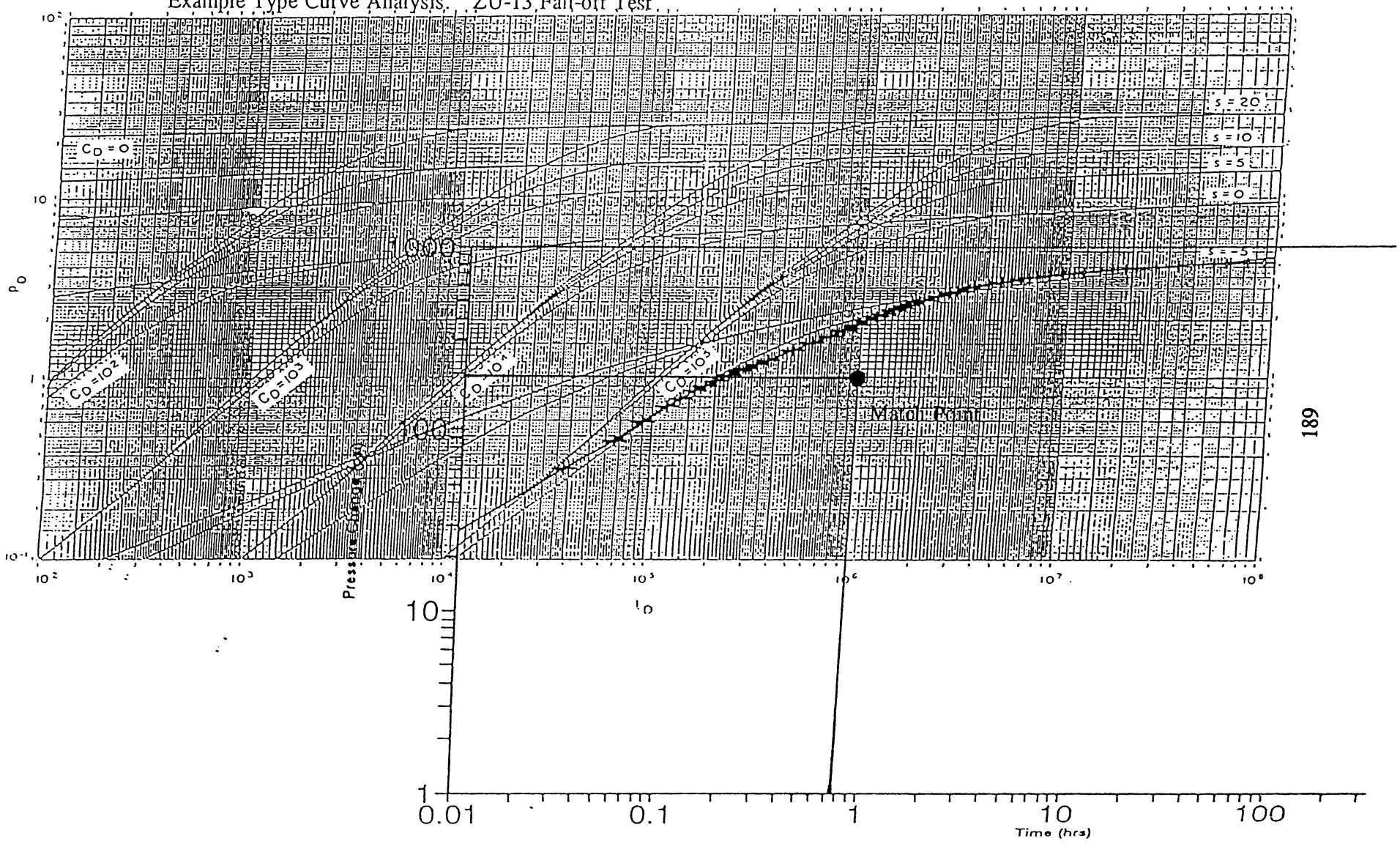

ZU-25 Falloff Test

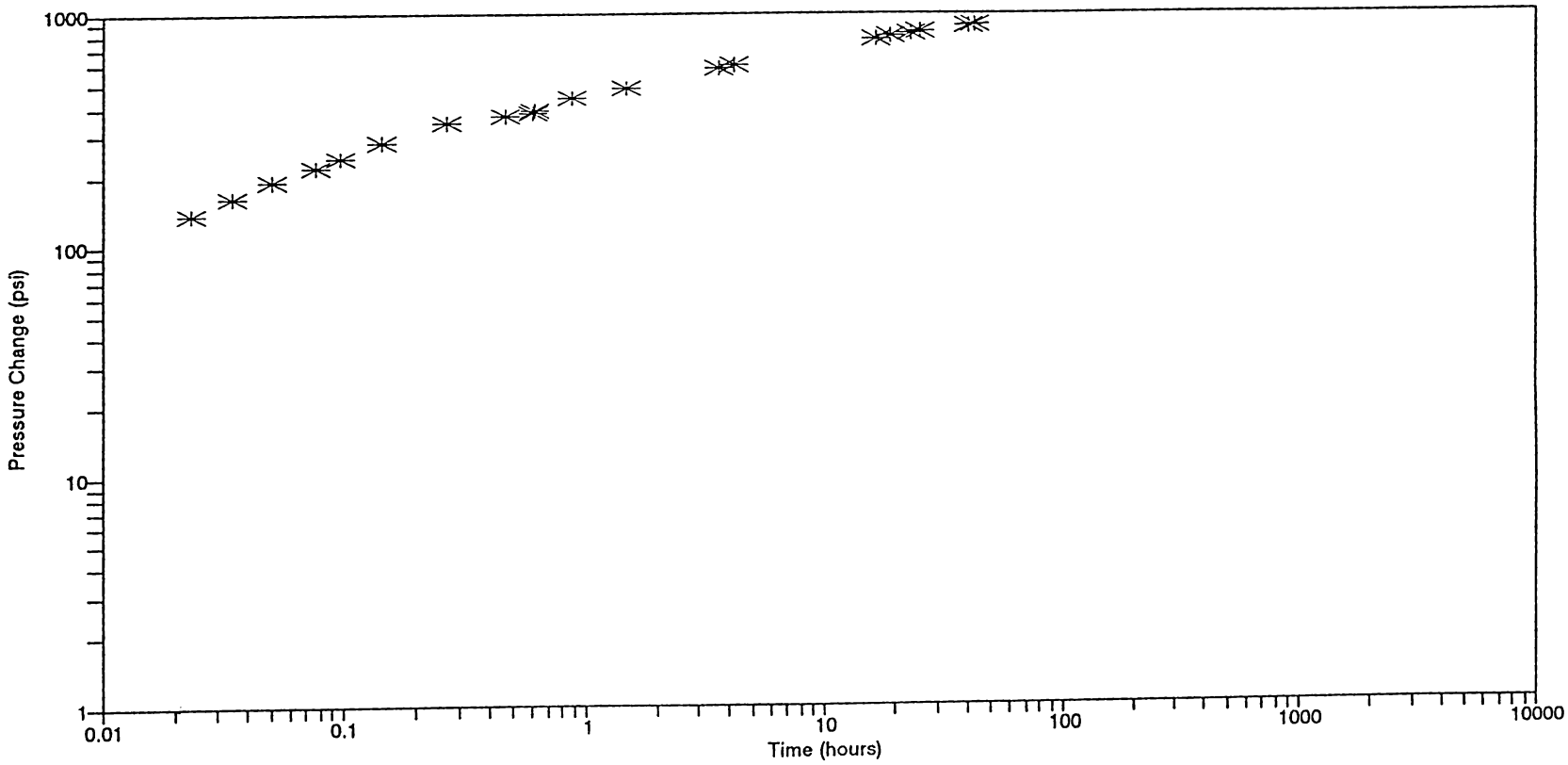

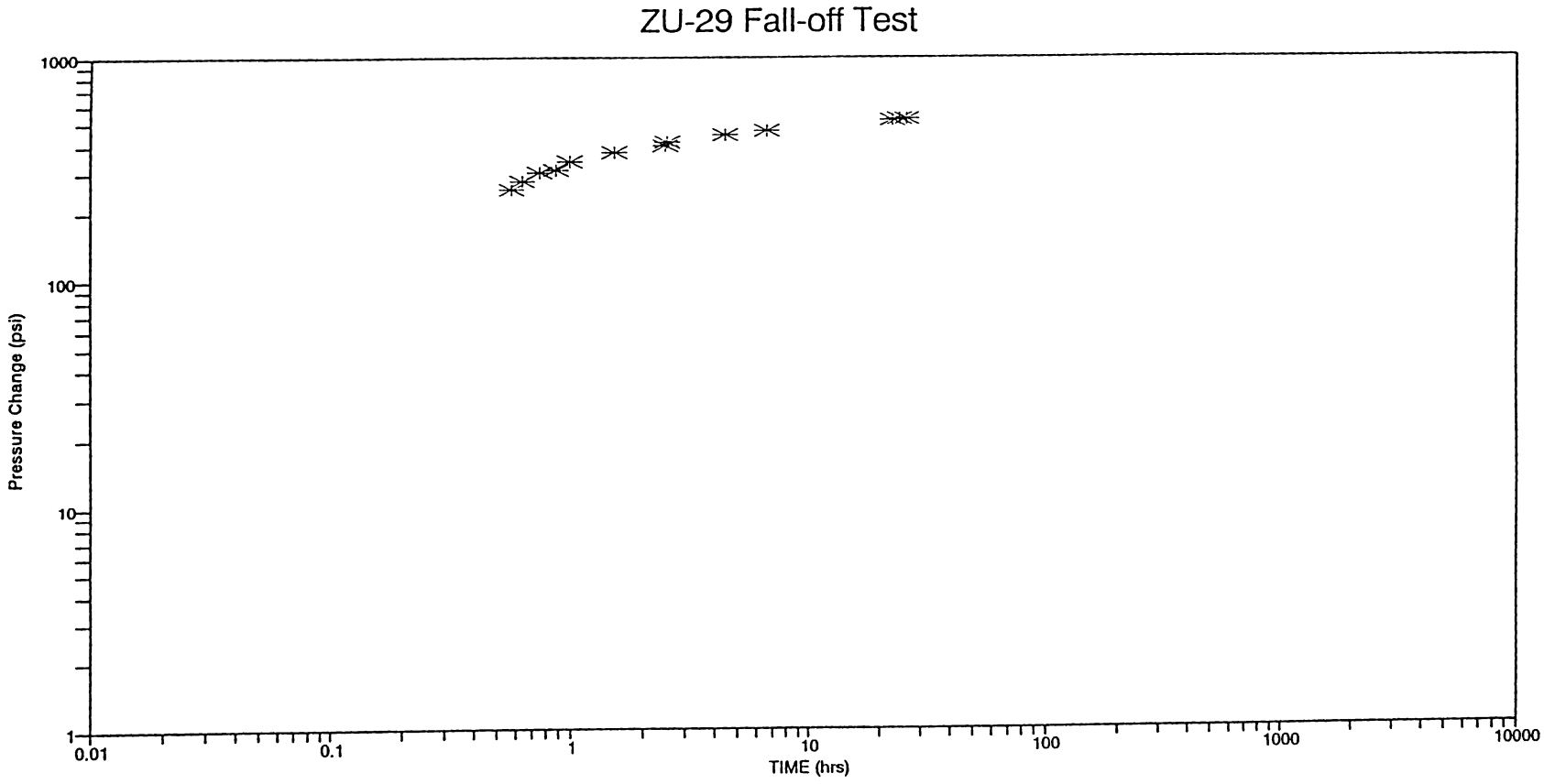
ZU-29 Fall-off Test
1000
100
10
1
Pressure Change (psi)
0.01
0.1
1
10
100
1000
10000
TIME (hrs)

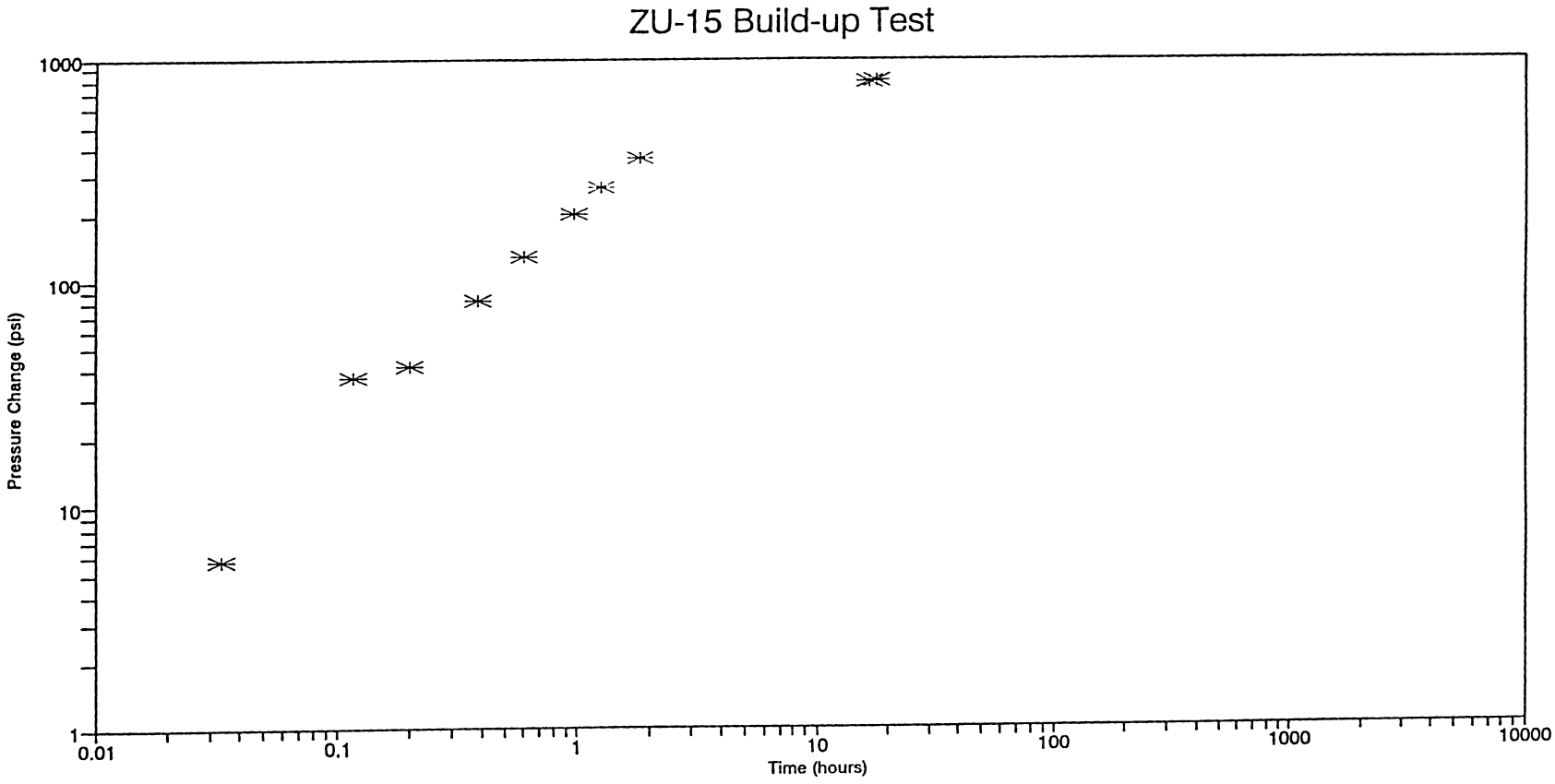
ZU-15 Build-up Test
Pressure Change (psi)
1000
100
10
1
0.01
0.1
1
10
100
1000
10000
Time (hours)

Example Interference Test Analysis
Type Curve Matching
ZU-29 Observation Well

Assume the following parameters:

q = 1600 STB/day
B = 1.0 res. bbl./STB
μ = 0.7 cp
h = 25 ft
r = 2580 ft
ϕ = 10%

Match Point

$(P_d)_m$ = 0.1 ΔP = 2.2 psi

$(t_d/r_d^2)_m$ = 1.0 Δt = 115 hrs

The matched curves are shown on the following page.

Now calculate permeability and total compressibility:

$$K = 141.2 \frac{q*B*\mu}{h}\left(\frac{P_d}{\Delta P}\right)_m = 288\ md$$

$$C_t = 0.0002637 \frac{k}{r^2*\mu*\phi}\left(\frac{\Delta t}{t_d/r_d^2}\right)_m = 19\ X\ 10^{-6}\frac{1}{psi}$$

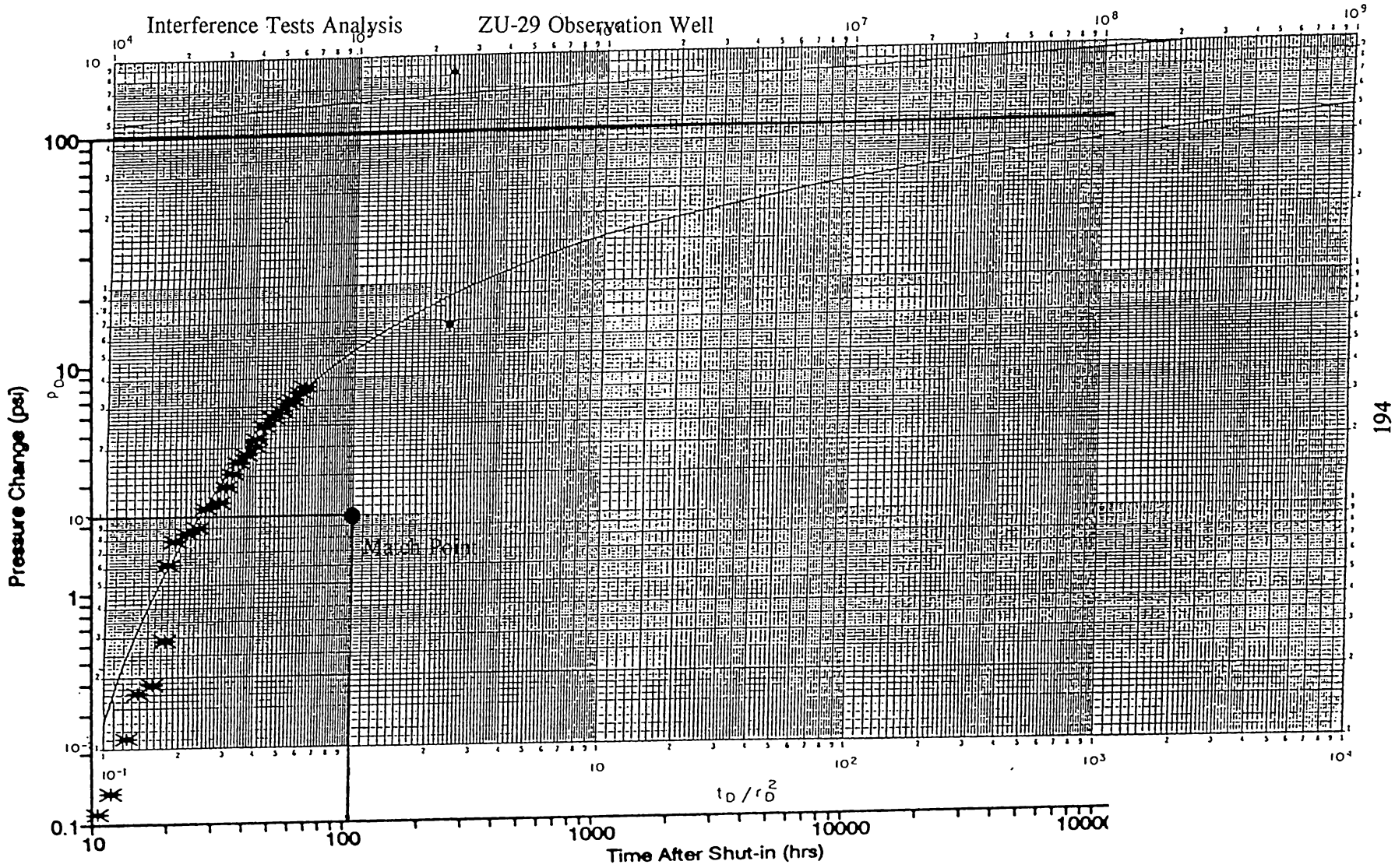
Interference Tests Analysis
ZU-29 Observation Well
Pressure Change (psi)
p_D
Match Point
t_D / r_D^2
Time After Shut-in (hrs)
100
10
1
0.1
10
100
1000
10000

Interference Test
ZU-29 Observation Well

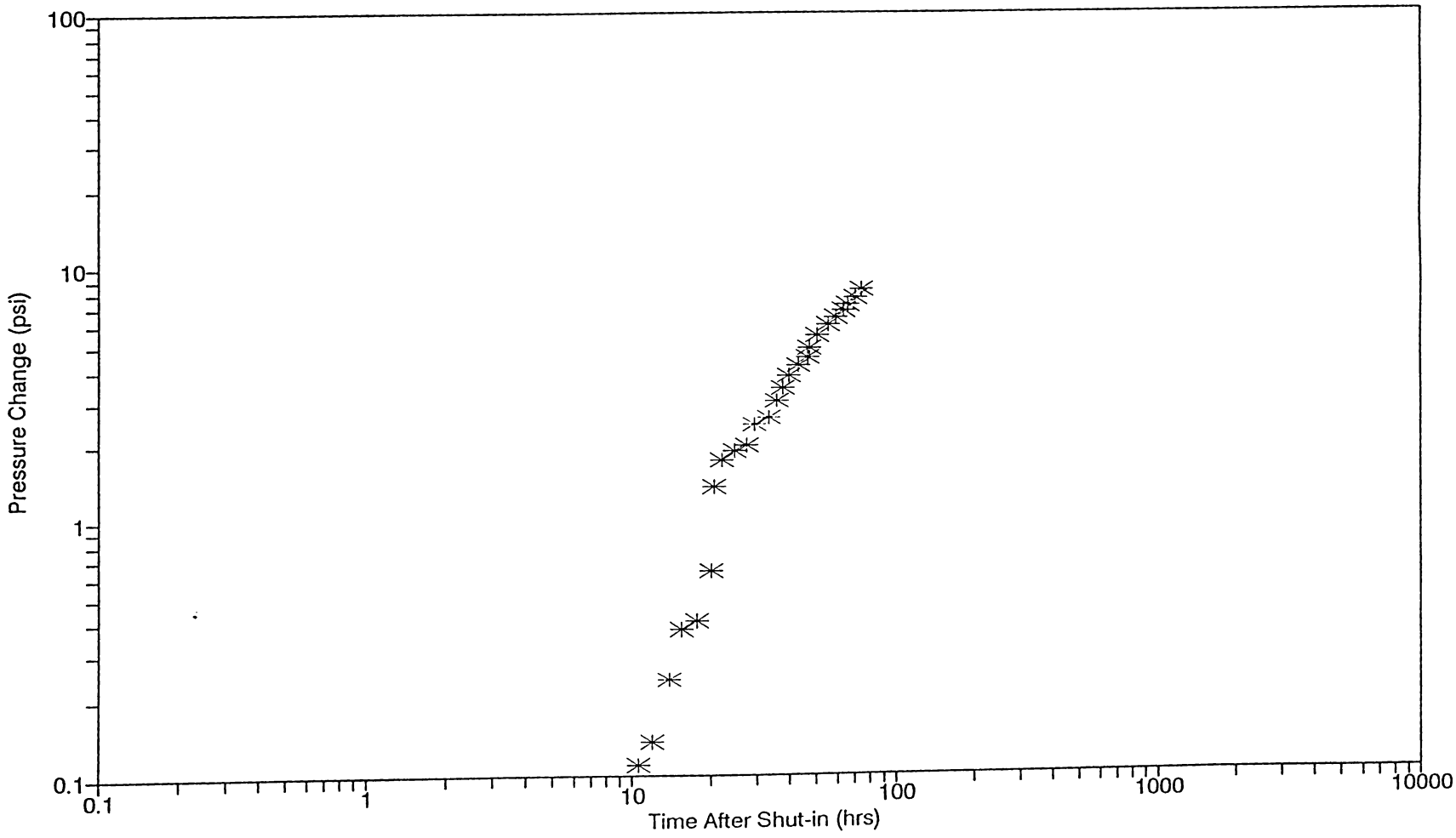

Interference Test
ZU-12 Observation Well

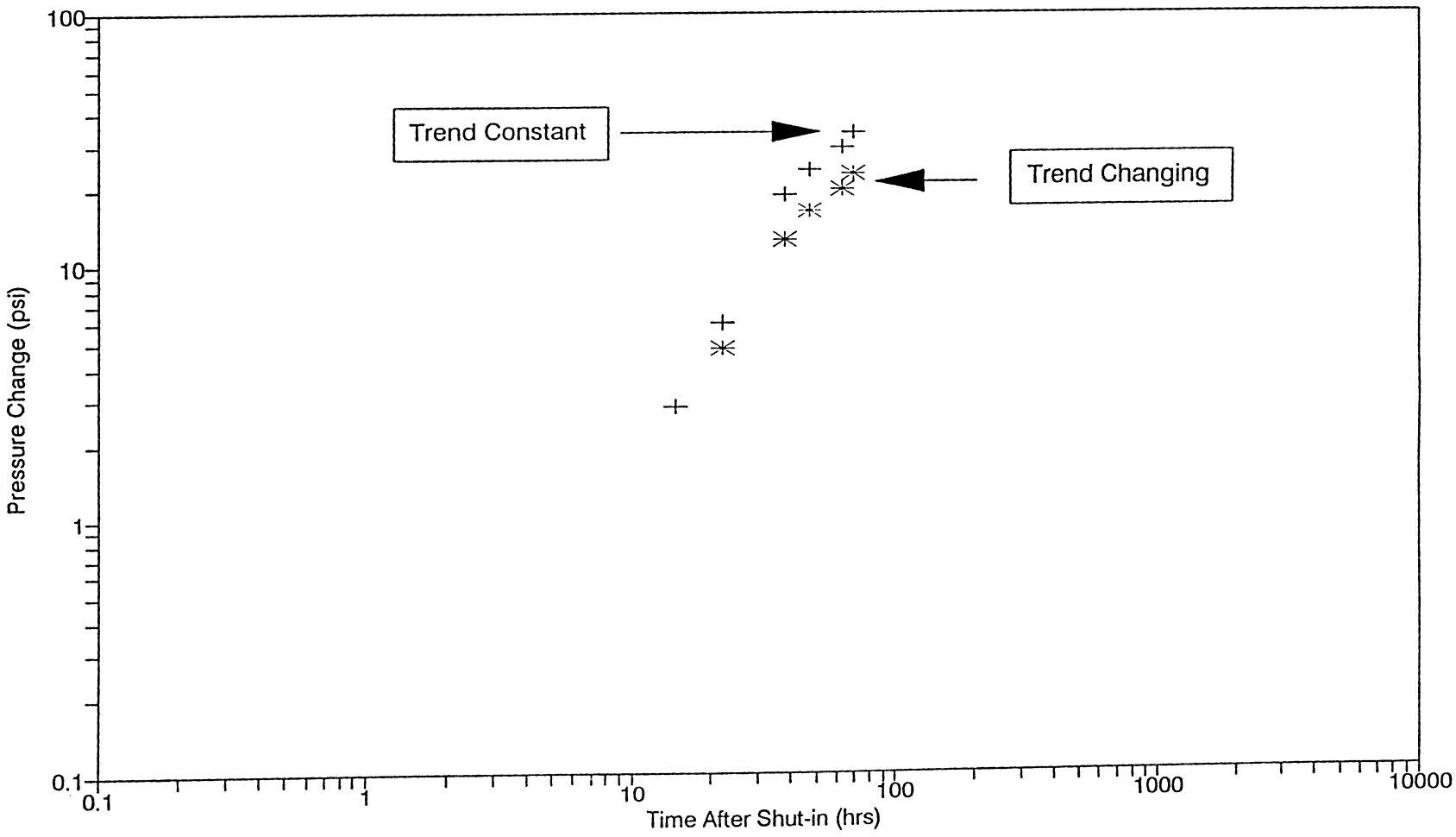

Interference Test
Stewart 1-S Observation Well

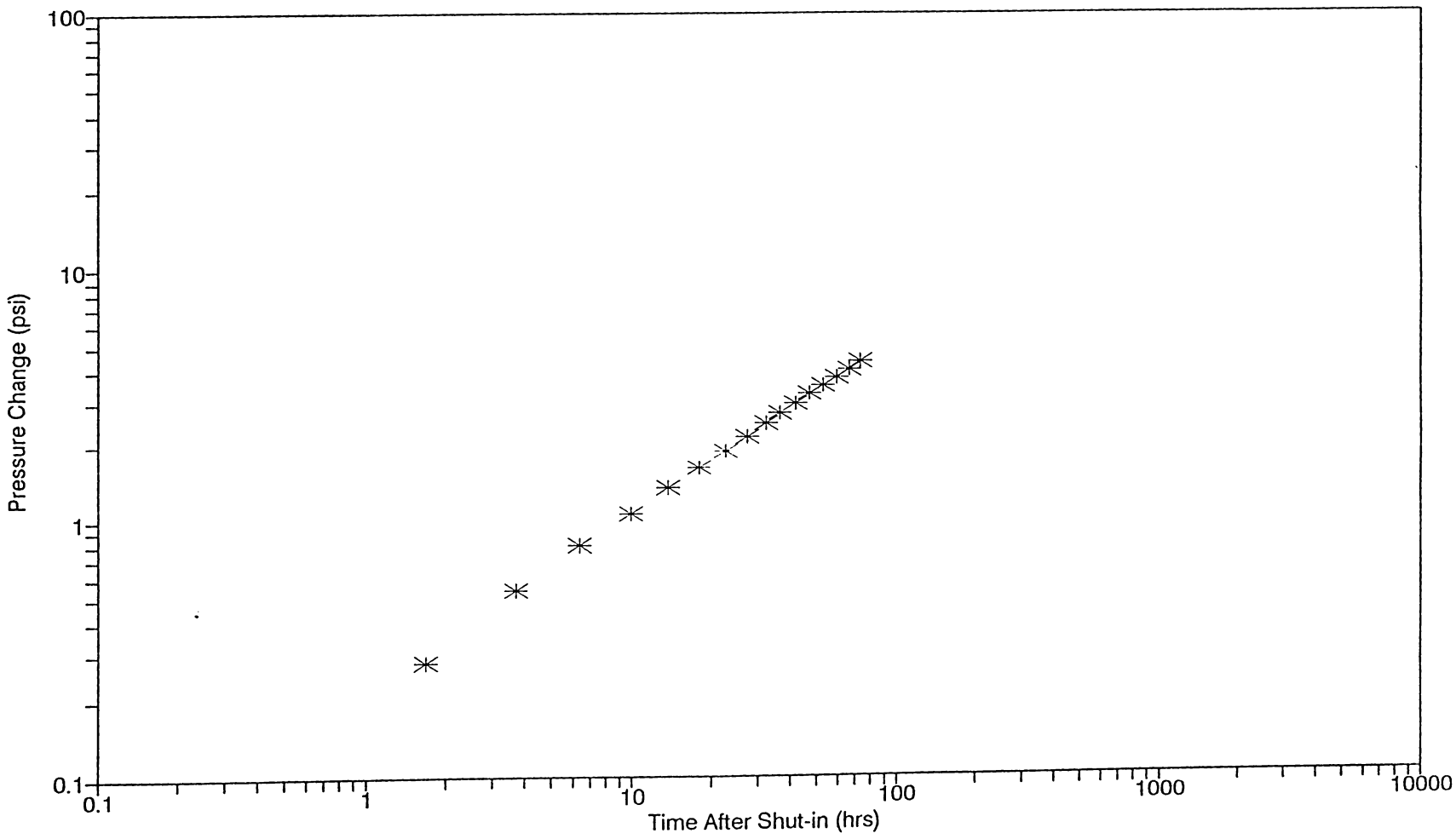

APPENDIX IV

Fortran Computer Programs

This appendix contains the Fortran computer programs that were written to extract important data out of the large data files output by the VIP Simulator and to reformat that data into a useable form. The programs were made as general as possible. However, some modifications may be required to run them with different model specifications.

```
      PROGRAM MAPFORM
C
C THIS PROGRAM READS VALUES FROM THE MAP FILE OUPUT BY
C VIP AND PRINTS THEM TO ANOTHER FILE IN A FORMATTED FORM
C
C THIS PROGRAM PRINTS OUT GRIDS OF WATER, GAS AND OIL
C SATURATION AS WELL AS PRESSURE ALL BY LAYERS IN A FILE
C NAME "MISE.MAP."  IT ALSO PRINTS OUT A PORE VOLUME
C WEIGHTED AVERAGE PRESSURE IN THE FILE "PDAT.MAP."
C
C THIS PROGRAM IS SET UP FOR A 9x9 MATRIX AND SHOULD BE
C MODIFIED THROUGH THE IMAX, JMAX,AND KMAX VARIABLES, AND
C ALSO THROUGH THE REDIMENSIONING OF ARRAYS IF ANOTHER
C MATRIX SIZE IS TO BE USED.  IT IS ALSO SET UP FOR A
C DUAL-PORISITY MODEL.  IF DUAL POROSITY IS NOT USED,
C TAKE THE L = 1,2 OUT OF THE READ STATMENTS.
C
         REAL PRESS(9,11,5,2),SW(9,11,5,2),SG(9,11,5,2)
      REAL SO(9,11,5,2),P791(9,11),DELTAP(9,11)
      REAL PV(9,11,5,2),PDAT(9,11)
      CHARACTER*7 NAME
      OPEN(UNIT = 15,FILE = 'MLMAP.DAT',STATUS = 'OLD')
         OPEN(UNIT = 16,FILE = 'MISE.MAP',STATUS = 'NEW')
      OPEN(UNIT = 17,FILE = 'PDAT.MAP',STATUS = 'NEW')
      OPEN(UNIT = 18,FILE = '791P.DAT',STATUS = 'OLD')
C
      IMAX = 9
      JMAX = 11
      KMAX = 5
1     CONTINUE
      READ(15,2,END=50) NAME
2     FORMAT(A7)
      IF(NAME .EQ. 'RECURR') GOTO 3
      GOTO 1
3     CONTINUE
      READ(15,*)TSTEP,TIME,DUMMY
      WRITE(16,5)TSTEP,TIME
      WRITE(17,5)TSTEP,TIME
5     FORMAT(' ','TIME STEP =',F6.1,2X,'TIME =',F7.2,'
      &   days')
      READ(15,*,END=50) ((((SG(I,J,K,L), I=1,IMAX),
      &  J=1,JMAX), K = 1,KMAX), L = 1,2)
      PRINT*,'SG OK'
      READ(15,*) ((((SW(I,J,K,L), I=1,IMAX), J=1,JMAX),
      &   K = 1,KMAX), L = 1,2)
      PRINT*,'SW OK'
      READ(15,*) ((((SO(I,J,K,L), I=1,IMAX), J=1,JMAX),
      &   K = 1,KMAX), L = 1,2)
      PRINT*,'SO OK'
      READ(15,*,END=50) ((((PV(I,J,K,L), I=1,IMAX),
      &  J=1,JMAX), K = 1,KMAX), L = 1,2)
```

```
      PRINT*,'PV OK'
      READ(15,*,END=50) ((((PRESS(I,J,K,L), I=1,IMAX),
     & J=1,JMAX), K = 1,KMAX), L = 1,2)
      PRINT*,'PRESS OK'
C
C CALCULATE AVERAGE PORE VOLUME DATUM PRESSURE
C
      DO 120 J = 3,JMAX
          DO 130 I = 1,IMAX
       IF(PV(I,J,1,1) .EQ. 0.0 .AND. PV(I,J,2,1) .EQ. 0.0
     & .AND. PV(I,J,3,1) .EQ. 0.0) THEN
         PDAT(I,J) = 0.0
         GOTO 130
       END IF
          PDAT(I,J) = (PV(I,J,1,1)*PRESS(I,J,1,1) +
     & PV(I,J,2,1)*PRESS(I,J,2,1) +
     & PV(I,J,3,1)*PRESS(I,J,3,1))/(PV(I,J,1,1) +
     &  PV(I,J,2,1) + PV(I,J,3,1))
130      CONTINUE
120     CONTINUE
C
C NOW WRITE MAPS IN FORMATTED FORM
C
      WRITE(17,*)'DATUM PRESSURE WEIGHTED BY TOTAL PORE
     & VOLUME'
      DO 10 J = 3,JMAX
        WRITE(17,15) (PDAT(I,J),I = 1,9)
C       WRITE(17,15) (PDAT(I,J),I = 11,20)
15    FORMAT(' ',9(F7.2,1X))
10    CONTINUE
      IF(TIME .EQ. 791.0) THEN
C
C MAKE PRESSURE DIFFERENCE MAP AND ABSOLUTE AVERAGE ERROR
C
      DO 200 J = 3,JMAX
        READ(18,*) (P791(I,J),I=1,9)
200   CONTINUE
      DO  205  I = 7,9
        DO 206 J = 9,11
         P791(I,J) = PDAT(I,J)
206   CONTINUE
205   CONTINUE
         P791(9,7) = PDAT(9,7)
         P791(9,8) = PDAT(9,8)
      DO 210 I = 1,9
       DO 220 J = 3,JMAX
C       PRINT*,P791(I,J),I,J
C       PRINT*,PDAT(I,J),I,J
        DELTAP(I,J) = PDAT(I,J) - P791(I,J)
        PSUM = PSUM + ABS(DELTAP(I,J))
220   CONTINUE
```

```
210   CONTINUE
      DELPAVG = PSUM/81.0
      WRITE(17,*)'PRESSURE DIFFERENCE AT 791 DAYS'
      DO 230 J = 3,JMAX
         WRITE(17,240) (DELTAP(I,J),I=1,9)
230   CONTINUE
240   FORMAT(' ',9(F7.1,1X))
      WRITE(17,*)'AVERAGE ABSOLUTE DIFFERENCE =',DELPAVG
      END IF
C
C PRESSURE
C
      WRITE(16,*)'DATUM PRESSURE'
      DO 100 K = 1,KMAX
      WRITE(16,*)'LAYER',K
      DO 110 J = 1,JMAX
      WRITE(16,15)(PRESS(I,J,K,1), I=1,IMAX)
110   CONTINUE
100   CONTINUE
C
C GAS SATURATION
C
      WRITE(16,*)'SG'
      DO 22 K = 1,KMAX
      WRITE(16,*)'LAYER',K
      DO 20 J = 1,JMAX
           WRITE(16,25) (SG(I,J,K,1),I = 1,9)
C       WRITE(16,25) (SG(I,J,K,1),I = 11,20)
 20   CONTINUE
 22   CONTINUE
C
C WATER SATURATION
      WRITE(16,*)'SW'
      DO 35 K = 1,KMAX
      WRITE(16,*)'LAYER',K
      DO 30 J = 1,JMAX
        WRITE(16,25) (SW(I,J,K,1), I = 1,9)
C       WRITE(16,25) (SW(I,J,K,1), I = 11,20)
 30   CONTINUE
 35   CONTINUE
C
C OIL SATURATION
C
      WRITE(16,*)'SO'
      DO 45 K = 1,KMAX
      WRITE(16,*)'LAYER',K
      DO 40 J = 1,JMAX
        WRITE(16,25) (SO(I,J,K,1),I = 1,9)
C       WRITE(16,25) (SO(I,J,K,1),I = 11,20)
 40   CONTINUE
 45   CONTINUE
```

```
 25   FORMAT(' ',9(F7.4,2X))
C
C READ NEXT ARRAY
C
      GOTO 1
50    STOP
      END
```

```
      PROGRAM PLOTFORM
C
C THIS PROGRAM READS DATA FROM THE PLOT FILE OF VIP AND
C FORMATS THE DATA GIVEN A REGION NUMBER TO LOOK FOR OR
C FOR THE TOTAL FIELD DATA.
C
      INTEGER REGNUM
      CHARACTER*6 CHECK,NAME,PLACE
      CHARACTER*15 FNAME
      PRINT*,'ENTER FILE NAME TO WRITE TO (15 CHAR MAX)'
      READ(*,1)FNAME
1     FORMAT(A)
      OPEN(UNIT=15,FILE='MLPLOT.DAT',STATUS='OLD')
      OPEN(UNIT=16,FILE=FNAME,STATUS='NEW')
C
C GET REGION NUMBER
C
      PRINT*,'ENTER WHAT DATA YOU WANT: FIELD/REGION'
      READ(*,2)PLACE
2     FORMAT(A)
      IF(PLACE .EQ. 'FIELD')GOTO 3
      PRINT*,'INPUT THE REGION NUMBER TO BE SEARCHED FOR'
      READ*,REGNUM
3     CONTINUE
C
C HEADING FOR REGION DATA
C
      IF(PLACE .EQ. 'REGION') THEN
       WRITE(16,*)'REGION NUMBER =',REGNUM
       WRITE(16,65)
65     FORMAT(' ','TIME',4X,'CUM. GAS',4X,'CUM. OIL',4X,
     &     'CUM H2O',3X,'PRESS')
       WRITE(16,70)
70     FORMAT(' ','DAYS',6X,'MSCF',8X,'STB',9X,'STB',
     &    7X,'PSI')
      END IF
C
C HEADING FOR FIELD DATA
C
      IF (PLACE .EQ. 'FIELD') THEN
       WRITE(16,*)'FIELD DATA'
       WRITE(16,75)
75     FORMAT(' ','TIME',6X,'GAS',5X,'OIL',5X,'WATER',
     & 10X,'CUM.' ,6X,'CUM.',8X,'CUM.',5X,'AVG PV')
       WRITE(16,76)
76     FORMAT(' ',10X,'RATE',4X,'RATE',4X,'RATE',11X,
     &  'GAS',7X, 'OIL',9X,'WATER',4X,'PRESS')
       WRITE(16,77)
77     FORMAT(' ','DAYS',5X,'MCFPD',3X,'STBPD',3X,'STBPD',
     &  11X,'MSCF',6X,'STB',10X,'STB',6X,'PSI')
      END IF
```

```
C
C BEGIN LOOP
C
5     CONTINUE
      READ(15,10,END=100)CHECK
10    FORMAT(A)
C     PRINT*,CHECK
      IF(CHECK .EQ. PLACE .AND. PLACE .EQ. 'FIELD')GOTO 15
      IF(CHECK .EQ.PLACE .AND. PLACE .EQ. 'REGION')GOTO 20
      GOTO 5
C
C READ FIELD DATA
C
15    CONTINUE
      READ(15,*)TSTEP,TIME
      READ(15,*)
      READ(15,*)GRATE,ORATE,WRATE,GINJ,WINJ,CUMGAS
      READ(15,*)CUMOIL,CUMH2O,CUMGINJ,CUMWINJ,PVPRESS
      &   ,HCPRESS
      READ(15,*)GRES,ORES,WRES
      IF(ORATE .EQ. 0.0) GOTO 16
      GOR = GRATE*1000./ORATE
16    CONTINUE
      IF(TIME .EQ. 181.0 .OR. TIME .EQ. 577.0 .OR. TIME
      & .EQ. 791.0 .OR. TIME .EQ. 943.0 .OR. TIME .EQ.
      & 1126.0 .OR. TIME .EQ. 1308.0 .OR. TIME .EQ.
      & 1522.0) GOTO 5
      WRITE(16,17)TIME,GRATE,ORATE,WRATE,GOR,CUMGAS,
      & CUMOIL,CUMH2O,PVPRESS
17    FORMAT(' ',F6.1,1X,F6.0,2X,F7.0,1X,F7.0,F6.0,1X,
      & F9.0,1X,F9.0,2X,F9.0,4X,F7.2)
      GOTO 5
C
C READ REGION DATA
C
20    CONTINUE
      READ(15,*)TSTEP,TIME
25    CONTINUE
      READ(15,30)CHECK,NUM
30    FORMAT(A,1X,I4)
C     PRINT*,CHECK,NUM
      IF(NUM .EQ. REGNUM) GOTO 50
      READ(15,*)
      READ(15,*)
      GOTO 25
50    CONTINUE
      READ(15,*)CUMGAS,CUMOIL,CUMH2O,GINJ,WINJ,DATPRESS
      READ(15,*)HCPRESS,PVPRESS,GASRES,OILRES,H2ORES
      WRITE(16,60)TIME,CUMGAS,CUMOIL,CUMH2O,DATPRESS
60    FORMAT(' ',F6.1,1X,F8.2,4X,F9.2,1X,F9.2,3X,F7.2)
      GOTO 5
```

```
100   STOP
      END
```

```
      PROGRAM WELLFORM
C
C THIS PROGRAM READS DATA FROM THE PLOT FILE OF VIP AND
C OUTPUTS DATA FOR INDIVIDUAL WELLS IN A FORMATTED FORM.
C
      INTEGER REGNUM
      CHARACTER*6 CHECK,NAME,PLACE
      CHARACTER*15 FNAME
      PRINT*,'ENTER FILE NAME TO WRITE TO (15 CHAR MAX)'
      READ(*,1)FNAME
1     FORMAT(A)
      OPEN(UNIT=15,FILE='MLPLOT.DAT',STATUS='OLD')
      OPEN(UNIT=16,FILE=FNAME,STATUS='NEW')
C
C BEGIN LOOP
C
5     CONTINUE
      READ(15,10,END=100)CHECK
10    FORMAT(A)
C     PRINT*,CHECK
      IF(CHECK .EQ. 'WELL') GOTO 15
      GOTO 5
C
C READ WELL DATA
C
15    CONTINUE
      READ(15,*)TSTEP,TIME
      WRITE(16,20) TIME
20    FORMAT(' ','TIME =',F7.1,' days')
      WRITE(16,22)
22    FORMAT(' ','WELL',2X,'WELL',3X,'GAS',5X,'OIL',
      &  3X,'WATER', 4X,'CUM.',3X,'WATER',2X,'----
      &  PRESSURES (PSI) ----')
      WRITE(16,23)
23    FORMAT(' ','NAME',3X,'#',4X,'RATE',5X,'RATE',2X,
      &  'RATE',5X,'OIL',6X,'%',8X,'GRID',7X,'BHP')
      DO 30 I = 1,154
      READ(15,25)NAME,NUMBER
25    FORMAT(A6,I5)
      READ(15,*)GRATE,ORATE,WRATE,GINJ,WINJ,CUMGAS
      READ(15,*)CUMOIL,CUMH2O,CUMGINJ,CUMWINJ,PRESS,GBPDAT
      READ(15,*)BHPDAT,ORES,WRES
      IF(WRATE .EQ. 0.0 .AND. ORATE .EQ. 0.0) THEN
       WATER = 0.0
       GOTO 35
      END IF
      WATER = WRATE/(ORATE+WRATE)*100
35    CONTINUE
      WRITE(16,17)NAME,NUMBER,GRATE,ORATE,WRATE,CUMOIL,
      &   WATER,GBPDAT, BHPDAT
30    CONTINUE
```

```
17    FORMAT(' ',A5,1X,I3,1X,F6.1,4X,F5.1,1X,F6.1,1X,F8.1,
     &     2X,F5.1,4X,F7.2,4X,F7.2)
      GOTO 5
100   STOP
      END
```

APPENDIX V

9 X 9 Grids of Rock Properties Initially Input into the VIP Simulator

This appendix contains the 9 X 9 grids of gross thickness, sub-sea depth, porosity, and permeability that were initially input into the VIP Simulator. The grids were calculated with the use of "Surfer," an IBM-compatible, geo-statistical mapping program.

9X9 Grids of Gross Pay Initially Input into VIP Simulator

Misener Limestone Gross Thickness

0.000	0.000	0.000	0.000	0.000	0.000	0.000	0.000	0.000
1.033	0.000	4.782	0.000	1.361	0.000	0.000	0.000	0.000
11.384	0.000	0.601	7.379	7.977	0.000	0.000	0.000	0.000
2.999	1.739	6.249	14.483	7.655	0.000	0.000	0.000	0.000
3.622	3.386	24.014	22.210	0.051	0.000	0.000	0.000	0.000
17.444	7.865	18.593	16.302	0.000	0.000	0.000	0.000	0.000
27.603	32.162	7.863	10.058	0.120	1.828	0.000	0.000	0.000
22.687	17.712	3.257	6.867	1.079	1.927	0.225	0.000	0.000
17.379	8.710	12.611	6.125	1.878	1.860	0.250	0.000	0.000

Misener Sandstone Layer 1 Gross Thickness

0.000	0.000	0.549	0.392	2.142	8.101	7.683	5.726	3.986
0.000	0.000	0.000	0.000	1.709	8.823	9.805	4.919	2.322
0.000	0.337	0.624	0.000	7.152	10.041	6.885	2.408	0.717
0.000	1.603	3.990	2.284	7.975	10.763	6.491	1.239	0.000
0.000	1.028	2.865	5.489	11.708	7.754	4.496	1.550	0.000
0.000	0.000	4.768	16.819	17.331	9.292	3.852	2.102	0.602
0.914	3.445	11.726	18.478	15.505	7.645	3.587	1.212	2.163
3.658	4.867	8.318	9.966	10.516	7.972	3.650	5.455	3.931
3.104	3.818	7.018	6.875	6.785	6.117	5.191	7.675	4.000

Misener Sandstone Layer 2 Gross Thickness

0.000	0.000	0.000	0.000	0.000	0.000	2.195	1.974	2.006
0.000	0.000	0.000	0.000	0.000	1.108	1.850	2.091	2.170
0.000	0.000	0.000	0.000	1.926	10.733	3.788	2.955	2.241
0.000	0.000	0.000	0.000	6.487	11.520	6.086	3.496	2.926
0.000	0.000	0.000	0.000	4.734	8.965	8.001	3.952	2.545
0.000	0.000	0.000	0.000	2.009	3.922	4.369	3.105	2.301
0.000	0.000	0.000	2.581	4.675	3.075	2.816	3.383	2.016
0.000	0.756	1.111	4.355	6.237	4.837	3.667	2.049	2.713
0.000	1.743	2.656	4.307	5.419	5.154	4.584	3.338	2.700

Maquoketa Dolomite Gross Thickness

0.00	0.00	0.00	0.00	0.00	0.00	0.00	0.00	0.00
0.00	0.00	5.42	6.06	7.58	0.00	0.00	0.00	0.00
0.00	0.00	11.90	5.94	6.26	6.21	0.00	0.00	0.00
0.00	0.00	7.10	7.65	1.86	0.00	0.00	0.00	0.00
0.00	0.00	5.26	5.43	3.06	4.87	0.00	0.00	0.00
0.00	1.02	0.00	0.00	0.00	0.00	0.00	0.00	0.00
0.00	0.00	0.00	0.00	0.00	1.38	0.00	0.00	0.00
0.00	0.00	0.00	0.00	0.00	0.00	0.00	0.00	0.00
0.00	0.40	1.87	2.04	0.00	0.00	0.00	0.00	0.00

Viola Limestone Gross Thickness

15.31	14.60	12.68	13.18	12.95	20.81	18.58	20.92	14.27
15.73	14.73	13.97	15.30	15.24	19.42	16.78	17.30	14.41
18.02	16.45	16.34	16.86	16.03	19.28	15.38	15.59	17.56
17.67	19.08	18.43	17.33	17.23	15.04	19.97	23.66	21.13
20.60	21.53	19.43	18.28	18.75	17.35	14.03	15.72	19.35
18.16	19.62	18.40	19.68	20.23	17.87	15.44	18.59	22.15
16.26	17.69	19.46	20.45	20.87	18.21	19.15	21.77	23.39
13.81	14.70	18.02	21.36	19.71	19.55	22.36	24.86	25.39
11.90	11.78	16.69	21.63	23.42	22.98	24.21	26.63	27.00

9X9 Grids of Sub-Sea Depth Initially Input into VIP Simulator

Misener Limestone Sub-Sea Depth

1890.0	1878.4	1882.3	1881.7	1888.8	1907.3	1889.6	1886.8	1897.1
1924.3	1922.7	1895.5	1889.5	1890.8	1893.2	1910.0	1916.9	1925.3
1937.5	1929.8	1926.9	1915.9	1902.9	1902.6	1904.3	1922.7	1953.5
1972.4	1978.1	1940.0	1937.9	1931.6	1928.9	1934.6	1928.1	1947.4
1990.5	1991.1	1960.3	1959.4	1962.5	1965.0	1974.0	2002.7	2058.6
2008.2	2013.0	1971.4	1972.1	1981.6	2005.4	2009.8	2009.2	2060.5
2002.7	1995.3	1988.0	1976.0	1977.2	2006.2	2018.6	2058.3	2096.4
2020.0	2002.5	1998.2	2006.1	2004.8	2016.0	2042.0	2098.3	2117.8
2035.6	2021.6	2010.5	2025.8	2029.7	2031.6	2076.0	2113.3	2133.2

Misener Sandstone Layer 1 Sub-Sea Depth

1880.2	1871.3	1876.4	1873.6	1877.3	1896.8	1883.8	1883.4	1894.2
1909.8	1908.3	1892.7	1877.6	1883.6	1885.8	1903.6	1915.2	1923.8
1929.8	1898.9	1906.0	1901.7	1907.5	1898.5	1897.7	1919.9	1950.9
1956.7	1952.7	1928.8	1949.8	1939.1	1928.3	1931.8	1926.3	1944.9
1975.5	1965.1	1978.9	1982.0	1961.1	1964.9	1974.0	2004.0	2057.8
2017.5	2004.4	1989.9	1988.3	1979.8	2005.1	2009.7	2009.3	2059.7
2025.5	2026.7	1995.8	1986.0	1977.3	2006.0	2018.2	2058.4	2093.3
2040.7	2021.0	2000.7	2013.3	2005.0	2018.0	2041.6	2095.8	2114.6
2053.5	2031.3	2022.1	2028.4	2030.6	2033.5	2074.6	2110.0	2130.6

Misener Sandstone Layer 2 Sub-Sea Depth

1880.2	1871.3	1876.4	1873.6	1879.5	1904.9	1893.1	1890.6	1899.6
1909.8	1908.3	1892.7	1877.6	1885.3	1895.4	1914.8	1921.8	1927.2
1929.8	1898.9	1906.6	1901.7	1915.3	1909.8	1907.0	1922.9	1951.9
1956.7	1954.3	1932.7	1952.1	1947.6	1940.6	1940.4	1927.7	1944.9
1975.5	1966.1	1981.7	1987.5	1973.8	1975.1	1980.7	2006.0	2057.8
2017.5	2004.4	1994.7	2005.1	1997.7	2016.2	2015.3	2012.3	2060.8
2026.4	2030.1	2007.5	2004.5	1993.0	2015.0	2023.3	2060.7	2096.0
2044.4	2025.8	2009.0	2023.3	2015.7	2026.9	2046.3	2101.9	2119.8
2056.6	2035.1	2029.1	2035.3	2037.8	2040.4	2081.0	2119.0	2135.9

Maquoketa Dolomite Sub-Sea Depth

1889.3	1877.0	1880.8	1881.2	1890.5	1916.0	1901.3	1896.5	1904.0
1923.7	1921.3	1899.2	1888.9	1893.7	1904.0	1922.9	1925.6	1931.2
1948.3	1930.1	1927.8	1923.2	1920.4	1924.2	1917.3	1928.8	1956.6
1974.9	1981.4	1950.2	1955.0	1954.1	1952.2	1949.3	1933.0	1950.0
1993.6	1995.6	1987.6	1987.5	1979.8	1984.1	1988.7	2009.9	2062.9
2025.2	2020.2	1994.7	2005.1	1999.8	2020.1	2019.7	2015.4	2064.0
2031.2	2030.8	2007.5	2007.1	1997.7	2020.1	2026.6	2064.1	2101.2
2046.4	2026.6	2010.1	2027.6	2022.9	2031.7	2050.6	2106.5	2125.7
2056.6	2036.9	2031.7	2042.9	2044.2	2045.6	2087.3	2125.5	2142.3

Viola Limestone Sub-Sea Depth

1897.4	1885.5	1890.2	1893.3	1906.5	1931.6	1927.9	1921.6	1918.0
1941.4	1930.3	1916.6	1908.1	1914.0	1918.5	1945.4	1941.5	1944.5
1958.8	1944.5	1950.5	1941.9	1941.6	1944.6	1936.5	1950.9	1976.1
1992.6	2001.0	1968.0	1982.3	1975.1	1975.5	1965.8	1947.3	1974.1
2026.0	2021.7	2010.5	2006.7	2000.3	2006.9	2008.0	2036.2	2090.3
2052.3	2045.0	2017.5	2025.5	2016.9	2035.8	2036.3	2037.2	2087.6
2048.8	2052.8	2032.1	2027.6	2018.3	2038.6	2041.3	2082.4	2121.7
2069.9	2053.7	2036.4	2044.7	2043.3	2049.7	2067.5	2124.2	2144.8
2087.4	2073.5	2057.3	2057.1	2059.6	2062.4	2104.5	2143.1	2160.6

9X9 Grids of Porosity Initially Input into VIP Simulator

Misener Limestone Porosity

0.0542	0.0541	0.0753	0.0970	0.1131	0.0964	0.0992	0.0931	0.0000
0.0467	0.0651	0.0813	0.1192	0.1176	0.0866	0.0871	0.0949	0.0000
0.0788	0.0973	0.1347	0.1528	0.0530	0.0543	0.0624	0.0827	0.0000
0.1057	0.1536	0.2021	0.1456	0.0628	0.0409	0.0411	0.0708	0.0000
0.1416	0.1849	0.1735	0.0874	0.0448	0.0417	0.0385	0.0479	0.0000
0.1748	0.1912	0.1336	0.0604	0.0523	0.0362	0.0560	0.0549	0.0000
0.1948	0.1708	0.1294	0.0498	0.0547	0.0485	0.0656	0.0583	0.0000
0.1679	0.1095	0.0799	0.0555	0.0603	0.0672	0.0697	0.0000	0.0000
0.1749	0.0653	0.0628	0.0617	0.0584	0.0713	0.0714	0.0000	0.0000

Misener Sandstone Layer 1 Porosity

0.1130	0.1132	0.1159	0.1063	0.1230	0.1412	0.1537	0.1591	0.1621
0.1127	0.1137	0.0994	0.0856	0.1060	0.1106	0.1275	0.1527	0.1490
0.1278	0.1222	0.0993	0.0710	0.0747	0.1062	0.1180	0.1407	0.1360
0.1478	0.1345	0.1242	0.0884	0.0991	0.1096	0.1318	0.1209	0.1220
0.1384	0.1432	0.1431	0.1134	0.1001	0.0860	0.0838	0.0974	0.1065
0.1338	0.1274	0.1094	0.1066	0.1121	0.0896	0.0825	0.0898	0.0957
0.1243	0.1198	0.0992	0.0938	0.1169	0.0957	0.0852	0.0885	0.0888
0.1012	0.1203	0.1259	0.1270	0.1212	0.1071	0.1013	0.0973	0.0900
0.1113	0.1130	0.1214	0.1242	0.1206	0.1122	0.0977	0.0946	0.0900

Misener Sandstone Layer 2 Porosity

0.0700	0.0700	0.0838	0.0824	0.1001	0.1069	0.1081	0.1006	0.1004
0.0700	0.0739	0.0747	0.0762	0.0952	0.1194	0.0980	0.0919	0.1032
0.0700	0.0724	0.0674	0.0670	0.0741	0.1175	0.1215	0.1295	0.1152
0.0700	0.0759	0.0665	0.0664	0.0782	0.1183	0.1336	0.1374	0.1225
0.0700	0.0776	0.0703	0.0800	0.0866	0.0965	0.0946	0.1208	0.1207
0.0898	0.0909	0.0844	0.0871	0.0953	0.0940	0.0988	0.1085	0.1117
0.0894	0.0895	0.0888	0.0905	0.1071	0.1007	0.1013	0.1071	0.1116
0.0894	0.0897	0.0907	0.0949	0.1075	0.1054	0.1106	0.1156	0.1089
0.0900	0.0914	0.0934	0.0978	0.1028	0.1037	0.1019	0.1006	0.1000

Maquoketa Dolomite Porosity

0	0	0	0	0	0	0	0	0
0	0	0.033	0.108	0.11	0	0	0	0
0	0	0.115	0.136	0.121	0.048	0	0	0
0	0	0.109	0.095	0.078	0	0	0	0
0	0	0.087	0.065	0.051	0.041	0	0	0
0	0.091	0	0	0	0	0	0	0
0	0	0	0	0	0.026	0	0	0
0	0	0	0	0	0	0	0	0
0	0	0	0	0	0	0	0	0

Viola Limestone Porosity

0.085	0.103	0.094	0.085	0.089	0.081	0.074	0.076	0.075
0.097	0.107	0.100	0.093	0.100	0.106	0.098	0.094	0.074
0.109	0.117	0.099	0.089	0.108	0.136	0.078	0.081	0.059
0.093	0.103	0.088	0.088	0.103	0.120	0.127	0.061	0.051
0.075	0.083	0.090	0.099	0.100	0.102	0.103	0.058	0.048
0.079	0.089	0.101	0.106	0.106	0.096	0.085	0.069	0.057
0.083	0.097	0.124	0.135	0.144	0.117	0.099	0.087	0.073
0.080	0.094	0.122	0.138	0.160	0.151	0.129	0.101	0.106
0.080	0.083	0.101	0.118	0.140	0.143	0.131	0.131	0.130

9X9 Grids of Permeability Initially Input into VIP Simulator

Misener Limestone Permeability

0.68	0.68	1.03	1.60	2.21	1.58	1.67	1.48	0.23
0.58	0.84	1.17	2.50	2.42	1.30	1.31	1.53	0.23
1.11	1.61	3.41	4.91	0.66	0.68	0.80	1.20	0.23
1.90	4.99	13.21	4.25	0.80	0.52	0.52	0.94	0.23
3.92	9.35	7.44	1.32	0.56	0.53	0.49	0.60	0.23
7.63	10.61	3.34	0.77	0.65	0.47	0.70	0.69	0.23
11.41	7.04	3.07	0.62	0.68	0.60	0.85	0.73	0.23
6.64	2.06	1.13	0.69	0.77	0.88	0.92	0.23	0.23
7.65	0.85	0.80	0.79	0.74	0.95	0.96	0.23	0.23

Misener Sandstone Layer 1 Permeability

7.40	7.45	8.22	5.80	10.64	20.60	32.42	39.44	43.98
7.32	7.59	4.52	2.74	5.74	6.78	12.53	31.27	27.34
12.66	10.33	4.50	1.61	1.84	5.78	8.87	20.23	17.05
26.17	16.15	11.11	3.03	4.47	6.54	14.64	9.86	10.26
18.61	22.15	22.07	7.51	4.63	2.78	2.56	4.20	5.84
15.74	12.48	6.49	5.87	7.16	3.16	2.45	3.19	3.95
11.15	9.47	4.48	3.69	8.53	3.95	2.70	3.04	3.07
4.82	9.64	11.82	12.30	9.97	5.97	4.84	4.19	3.21
6.96	7.40	10.04	11.11	9.75	7.19	4.25	3.79	3.21

Misener Sandstone Layer 2 Permeability

8.83	8.83	19.36	17.88	48.95	72.08	77.17	50.36	49.80
8.83	11.02	11.54	12.57	37.04	146.79	43.44	30.70	58.40
8.83	10.12	7.62	7.44	11.15	131.75	165.42	260.79	115.59
8.83	12.35	7.24	7.19	14.08	137.89	329.31	408.80	175.11
8.83	13.61	8.98	15.60	22.71	39.89	35.80	158.96	158.06
27.24	29.00	20.04	23.36	37.25	34.60	45.46	78.95	94.72
26.63	26.78	25.74	28.35	72.90	50.65	52.41	72.90	94.18
26.63	27.09	28.67	36.41	74.58	66.18	88.97	118.25	80.77
27.55	29.84	33.44	42.95	57.08	60.08	54.23	50.36	48.67

Maquoketa Dolomite Permeability

0	0	0	0	0	0	0	0	0
0	0	3.3	10.8	11	0	0	0	0
0	0	11.5	13.6	12.1	4.8	0	0	0
0	0	10.9	9.5	7.8	0	0	0	0
0	0	8.7	6.5	5.1	4.1	0	0	0
0	9.1	0	0	0	0	0	0	0
0	0	0	0	0	2.6	0	0	0
0	0	0	0	0	0	0	0	0
0	0	0	0	0	0	0	0	0

Viola Limestone Permeability

2.3	3.2	2.7	2.3	2.4	2.1	1.8	1.9	1.9
2.9	3.5	3.0	2.6	3.0	3.4	2.9	2.7	1.8
3.6	4.2	3.0	2.4	3.5	6.1	2.0	2.1	1.4
2.6	3.2	2.4	2.4	3.2	4.5	5.1	1.4	1.2
1.9	2.2	2.5	3.0	3.0	3.1	3.2	1.3	1.1
2.0	2.4	3.1	3.4	3.4	2.8	2.3	1.7	1.3
2.2	2.9	4.8	6.0	7.1	4.2	3.0	2.4	1.8
2.1	2.7	4.6	6.3	9.7	8.2	5.3	3.1	3.4
2.1	2.2	3.1	4.3	6.6	7.0	5.5	5.5	5.4

APPENDIX VI

Example Input Files for VIP

This chapter contains copies of the initialization data file and the recurrent data file required for input into the VIP Simulator. The files are those that resulted from the history match of the first two years of primary production.

```
INIT
NOLIST
C
C Initialization Input File for the Final History Match of
C the First Two Years of Primary Production in the Zenith
C Field
C
TITLE1
                        ZENITH FIELD
TITLE2
          MISENER LIMESTONE AND SANDSTONE 1 AND 2
TITLE3
                     PRIMARY SIMULATION
C
C ====== UTILITY DATA =======
C
DATE 15 11 1937
MAP FORM PDAT SG SW SO PV
PLOT  FORM
C INTSAT
C
FAULTS
DUAL
VEWO
VEGO
C
C ====== PRINT CONTROL ======
C
PRINT  EQUIL  NONE
PRINT  COMP   NONE
PRINT  TABLES NONE
PRINT  ARRAYS NONE
PRINT  COEFS  NONE
PRINT  INFLUX NONE
PRINT  INIT   NONE
PRINT  FAULTS  NONE
PRINT  CORNER  NONE
PRINT  SEPARATOR  NONE
PRINT  REGION  NONE
C
C ====== GRID SYSTEM OPTIONS =======
C
NX     NY     NZ      NCOMP
 9      11      5        2
C
C ====== PHYSICAL PROPERTY CONSTANTS =========
DWB         BWI         VW          CW          CR          TRES       TS
PS
1.02        1.045       .7          3.25E-6     1.0349E-5 118          60
14.7
C
C
C ====== EQUILIBRIUM, SATURATION, PVT TABLES =========
TABLES
IEQUIL  PINIT    DEPTH    PCWOC     WOC     PCGOC      GOC
   1    1300.    1900.      0.      2019.     0.      1850.
C
C
BPTAB 1
DEPTH      PSAT
1850       1000
```

```
1900       1000
1975       1000
2000       1000
2010       1000
2050       1000
2100       1000
2200       1000
C
C BLACK OIL PVT DATA
C
BOTAB
API        WTRO
42.        197
C
C PVT TABLE WAS OBTAINED BY FLUID TEST REPORT
C GR WAS OBTAINED FROM QUESTA REPORT(8/8/84) pg 57
C VO AND VG WERE OBTAINED FROM CORRELATIONS
C
PSAT       RS         BO         ZG         GR         VO         VG
 2000     540         1.286      0.89847    0.680     0.713       0.01628
 1700     478         1.266      0.90498    0.680     0.767       0.01568
 1500     440         1.254      0.91385    0.680     0.807       0.01509
 1300     402         1.241      0.92120    0.680     0.850       0.01470
 1200     382         1.234      0.92487    0.680     0.875       0.01451
 1100     363         1.228      0.93132    0.680     0.900       0.01423
 1000     344         1.221      0.93777    0.680     0.928       0.01395
  700     285         1.198      0.95238    0.680     1.029       0.01340
  500     242         1.182      0.96789    0.680     1.124       0.01287
  200     162         1.144      0.98359    0.680     1.373       0.01234
  100     116         1.125      0.99242    0.680     1.581       0.01205
 14.7       0         1.00       1.00000    0.680     2.820       0.01200
PSAT 1000
DP         BOFAC      VOFAC
900        .9910      1.0589
C
C MATRIX SATURATION TABLES
C
C
C
C
C MISENER LIMESTONE, MOQUOKETA AND VIOLA  RELATIVE PERMEABILITY
C
SWT  1
  SW         KRW         KROW         PCWO
 .356        0.0         .70           0.0
 .40         .010        .53           0.0
 .45         .035        .34           0.0
 .50         .050        .21           0.0
 .55         .066        .13           0.0
 .60         .086        .06           0.0
 .65         .117        .03           0.0
 .70         .166        .008          0.0
 .75         .241        .001          0.0
 .80         .354        .00           0.0
 .85         .516       0.0            0.0
 .90         .741       0.0            0.0
1.00        1.00        0.0            0.0
```

```
C
C MISENER SANDSTONE RELATIVE PERMEABILITY
C
SWT  2
   SW        KRW        KROW         PCWO
  .20        0.0        .91           0.0
  .25        .05       .69           0.0
  .30        .10        .51           0.0
  .35        .145       .37           0.0
  .40        .19        .27           0.0
  .45        .24        .19           0.0
  .50        .29        .13           0.0
  .55        .34        .092          0.0
  .60        .39        .063          0.0
  .65        .43        .042          0.0
  .70        .47        .026          0.0
  .75        .53        .012          0.0
  .80        .57        0.0           0.0
  .85        .70        0.0           0.0
  .90        .80        0.0           0.0
 1.00        1.00       0.0           0.0
SGT 1
 SG         KRG        KROG        PCGO
 0.00       0.00       0.70        0.0
 0.02       0.00       0.695
 0.05       0.00       0.687
 0.10       0.00       0.674
 0.20       0.066      0.649
 0.30       0.115      0.623
 0.40       0.252      0.597
 0.50       0.683      0.184
 0.60       0.976      0.00
 0.644      0.990      0.00        0.0
SGT 2
 SG         KRG        KROG       PCGO
 0.00       0.00       0.91       0.0
 0.02       0.00       0.877
 0.05       0.00       0.828
 0.10       0.0        0.747
 0.15       0.0        0.65
 0.20       0.135      0.583
 0.30       0.253      0.420
 0.40       0.403      0.152
 0.50       0.584      0.044
 0.60       0.796      0.009
 0.70       0.90       0.00
 0.80       0.95       0.00       0.0
C
C FRACTURE SATURATION TABLES
C
SWTF 1
 SW         KRW        KROW        PCWO
0.01        0.00       0.99        0.00
0.10        0.10       0.90        0.00
0.20        0.20       0.80        0.00
0.30        0.30       0.70        0.00
0.40        0.40       0.60        0.00
0.50        0.50       0.50        0.00
0.60        0.60       0.40        0.00
0.70        0.70       0.30        0.00
0.80        0.80       0.20        0.00
```

```
0.90       0.90       0.10       0.00
0.99       0.99       0.00       0.00
1.00       1.00       0.00       0.00
C
SWTF 2
 SW         KRW        KROW       PCWO
0.01       0.00       0.99       0.00
0.10       0.10       0.90       0.00
0.20       0.20       0.80       0.00
0.30       0.30       0.70       0.00
0.40       0.40       0.60       0.00
0.50       0.50       0.50       0.00
0.60       0.60       0.40       0.00
0.70       0.70       0.30       0.00
0.80       0.80       0.20       0.00
0.90       0.90       0.10       0.00
0.99       0.99       0.00       0.00
1.00       1.00       0.00       0.00
SGTF  1
 SG         KRG        KROG       PCGO
 0.0        0.0        .99         0.0
 .02        0.0        .98         0.0
 .10        0.0        .90         0.0
 .5         .5         0.0         0.0
.99        .99         0.0         0.0
SGTF  2
 SG         KRG        KROG       PCGO
 0.0        0.0        .99         0.0
 .02        0.0        .98         0.0
 .5         .5        0.0         0.0
.99         .99        0.0         0.0
C
C ===== THICKNESS, POROSITY, PERMEABILITY ARRAY DATA ========
C
ARRAYS
DX CON
2640.
DY CON
2640.
C
C MISENER LIMESTONE GROSS THICKNESS
DZ VALUE
0.001   0.001   0.001   0.001   0.001   0.001   0.001   0.001   0.001
0.001   0.001   0.001   0.001   0.001   0.001   0.001   0.001   0.001
0.001   0.001   0.001   0.001   0.001   0.001   0.001   0.001   0.001
1.033   0.001   5.782   2.0     1.361   0.001   0.001   0.001   0.001
15.38   0.001   1.601   7.0     7.977   0.001   0.001   0.001   0.001
 3.99   2.739   6.249  12.0     7.655   0.001   0.001   0.001   0.001
 3.62   3.386  24.014  22.210   1.051   0.001   0.001   0.001   0.001
17.44   7.865  18.593  16.302   1.001   0.001   0.001   0.001   0.001
27.60  32.162   7.863  10.058   0.120   1.828   0.001   0.001   0.001
22.68  17.712   3.257   6.867   1.079   1.927   0.225   0.001   0.001
17.37   8.710  12.611   6.125   1.878   1.860   0.250   0.001   0.001
C
C MISENER SANDSTONE LAYER 1 GROSS THICKNESS
C
0.000   0.000   3.0     5.82   10.33    11.68   19.33    5.99    3.37
0.000   0.000   3.500   3.44    8.39   10.87   10.87    2.35    2.66
0.000   0.000   4.000   4.0     2.810   9.651   8.480   1.622   2.969
0.000   0.000   4.500   3.200   2.210  10.758  13.564   3.596   1.579
0.000   0.000   2.500   4.000   5.596  10.023   7.793   3.0     1.450
```

```
0.000   0.000   2.340   4.673   6.483   6.799   6.545   2.381   1.001
0.000   0.000   2.050   3.074  13.962   9.678   5.019   0.800   2.153
0.000   0.000   0.500   4.460  22.217  17.652   6.593   2.304   1.709
0.000   2.740   7.210   9.0     8.464   8.323   5.220   1.987   1.526
0.000   2.080   0.680  10.659   9.481   9.201   6.314   4.042   0.001
0.000   0.730   1.995   7.746   8.173   8.418   4.489   2.606   3.165
C
C MISENER SANDSTONE LAYER 2 GROSS THICKNESS
C
0.0     0.0     0.0     0.0     0.0     0.0     1.0     0.0     0.0
0.000   0.000   0.000   0.000   0.000   0.0     2.0     0.5     1.0
0.000   0.000   0.000   0.000   0.000   0.079   3.115   0.752   2.247
0.000   0.000   0.000   0.000   0.000   1.509   3.486   1.554   1.532
0.000   0.000   0.000   1.000   2.571  19.964   6.567   1.448   4.643
0.000   0.000   0.000   1.095   7.704  10.544   8.360   1.215   2.647
0.000   0.000   0.000   0.287   5.101   9.705  10.549   2.225   6.267
0.000   0.000   0.000   4.000   3.257   5.393   4.5     2.927   6.030
0.000   0.000   0.000   5.0     4.940   5.102   3.297   5.904   1.332
0.000   0.000   0.000   5.317   6.202   6.472   7.180   1.290   0.001
0.000   0.000   0.898   4.831   6.118   7.298   4.375   1.283   1.880
C
C MOQUOKETA DOLOMITE GROSS THICKNESS/THE 15.0 ARE "PSEUDO FERNVALE"
C THESE WILL HAVE 1% POROSITY AND .5 md PERM.
C
 15.0    15.0    15.0    15.0    15.0    15.0    15.0    15.0    15.0
 15.0    15.0    15.0    15.0    15.0    15.0    15.0    15.0    15.0
 15.0    15.0    15.0    15.0    15.0    15.0    15.0    15.0    15.0
 15.0    15.0     5.42    6.06    7.58   15.0    15.0    15.0    15.0
 15.0    15.0    11.90   12.0     6.26    6.21   15.0    15.0    15.0
 15.0    15.0     7.10   10.0     1.86   15.0    15.0    15.0    15.0
 15.0    15.0     5.26    5.43    3.06    4.87   15.0    15.0    15.0
 15.0     1.02   15.0    15.0    15.0    15.0    15.0    15.0    15.0
 15.0    15.0    15.0    15.0    15.0     1.38   15.0    15.0    15.0
 15.0    15.0    15.0    15.0    15.0    15.0    15.0    15.0    15.0
 15.0     0.40    1.87    2.04   15.0    15.0    15.0    15.0    15.0
C
C VIOLA PAY 1 GROSS THICKNESS
C
2.35    0.0     2.77    3.99    5.82    8.07    6.72   10.56   17.36
5.17    3.06    5.46    8.76   11.44   12.36   11.85   15.29   17.58
15.31   14.60   12.68   13.18   12.95   20.81   18.58   20.92   14.27
15.73   14.73   13.97   15.30   15.24   19.42   16.78   17.30   14.41
18.02   16.45   16.34   16.86   16.03   19.28   15.38   15.59   17.56
17.67   19.08   18.43   17.33   17.23   15.04   19.97   23.66   21.13
20.60   21.53   19.43   18.28   18.75   17.35   14.03   15.72   19.35
18.16   19.62   18.40   19.68   20.23   17.87   15.44   18.59   22.15
16.26   17.69   19.46   20.45   20.87   18.21   19.15   21.77   23.39
13.81   14.70   18.02   21.36   19.71   19.55   22.36   24.86   25.39
11.90   11.78   16.69   21.63   23.42   22.98   24.21   26.63   27.00
C
C DEPTH TO TOPS OF GRIDBLOCKS
C
C DEPTHS WERE OBTAINED BY ADDING THE GROSS THICKNESS OF EACH GRIDBLOCK
C TO THE TOP OF THE VIOLA/MOQUOKETA SINCE WE HAD GOOD CONTROL OVER THIS
C SURFACE
C
DEPTH VALUE
C MISENER LIMESTONE
1869.7 1864.8  1871.9  1879.3  1882.2  1876.9  1872.6  1883.1  1870.7
1875.1 1867.5  1867.8  1890.3  1900.4  1878.9  1870.1  1876.5  1864.2
1880.2 1871.3  1876.4  1873.6  1877.3  1896.8  1883.8  1883.4  1894.2
```

```
1908.7 1908.3  1888.0  1877.6  1882.2  1885.8  1903.6  1915.2  1923.8
1918.4 1898.9  1905.4  1894.3  1899.5  1898.5  1897.7  1919.9  1950.9
1953.7 1951.0  1922.5  1935.3  1931.4  1928.3  1931.8  1926.3  1944.9
1971.9 1961.7  1954.9  1959.8  1961.1  1964.9  1974.0  2004.0  2057.8
2000.1 1996.5  1971.3  1972.0  1979.8  2005.1  2009.7  2009.3  2059.7
1997.9 1994.5  1987.9  1976.0  1977.3  2004.1  2018.2  2058.4  2093.3
2018.0 2003.3  1997.5  2006.5  2003.9  2016.0  2041.6  2095.8  2114.6
2036.1 2022.6  2009.5  2022.3  2028.7  2031.6  2074.6  2110.0  2130.6
C MISENER SANDSTONE LAYER 1
1869.7 1864.8  1871.9  1879.3  1882.2  1876.9  1872.6  1883.1  1870.7
1875.1 1867.5  1867.8  1890.3  1900.4  1878.9  1870.1  1876.5  1864.2
1880.2 1871.3  1876.4  1873.6  1877.3  1896.8  1883.8  1883.4  1894.2
1909.8 1908.3  1892.7  1877.6  1883.6  1885.8  1903.6  1915.2  1923.8
1929.8 1898.9  1906.0  1901.7  1907.5  1898.5  1897.7  1919.9  1950.9
1956.7 1952.7  1928.8  1949.8  1939.1  1928.3  1931.8  1926.3  1944.9
1975.5 1965.1  1978.9  1982.0  1961.1  1964.9  1974.0  2004.0  2057.8
2017.5 2004.4  1989.9  1988.3  1979.8  2005.1  2009.7  2009.3  2059.7
2025.5 2026.7  1995.8  1984.0  1977.3  2006.0  2018.2  2058.4  2093.3
2040.7 2021.0  2000.7  2013.3  2005.0  2018.0  2041.6  2095.8  2114.6
2053.5 2031.3  2022.1  2028.4  2030.6  2033.5  2074.6  2110.0  2130.6
C MISENER SANDSTONE LAYER 2
1869.7 1864.8  1874.9  1885.3  1893.2  1888.9  1885.6  1889.1  1874.7
1875.1 1867.5  1867.8  1890.3  1903.4  1895.8  1883.1  1879.5  1868.2
1880.2 1871.3  1876.4  1873.6  1879.5  1904.9  1893.1  1890.6  1899.6
1909.8 1908.3  1892.7  1877.6  1885.3  1895.4  1914.8  1921.8  1927.2
1929.8 1898.9  1906.6  1901.7  1915.3  1909.8  1907.0  1922.9  1951.9
1956.7 1954.3  1932.7  1952.1  1947.6  1940.6  1940.4  1927.7  1944.9
1975.5 1966.1  1981.7  1987.5  1973.8  1975.1  1980.7  2006.0  2057.8
2017.5 2004.4  1994.7  2001.1  1997.7  2014.0  2013.3  2012.3  2060.8
2026.4 2030.1  2007.5  2004.5  1995.0  2016.0  2023.3  2060.7  2096.0
2044.4 2025.8  2009.0  2023.3  2017.7  2026.9  2046.3  2101.9  2119.8
2056.6 2035.1  2029.1  2035.3  2037.8  2040.4  2081.0  2119.0  2135.9
C MOQUOKETA DOLOMITE
1869.7 1864.8  1874.9  1885.3  1893.2  1888.9  1891.6  1889.1  1874.7
1875.1 1867.5  1867.8  1890.3  1903.4  1895.8  1890.7  1884.8  1879.2
1889.3 1877.0  1880.8  1881.2  1890.5  1916.0  1901.3  1896.5  1904.0
1923.7 1921.3  1899.2  1888.9  1893.7  1904.0  1922.9  1925.6  1931.2
1948.3 1930.1  1927.8  1923.2  1920.4  1924.2  1917.3  1928.8  1956.6
1974.9 1981.4  1950.2  1955.0  1954.1  1952.2  1949.3  1933.0  1950.0
1993.6 1995.6  1987.6  1987.5  1979.8  1984.1  1988.7  2009.9  2062.9
2025.2 2020.2  1994.7  2005.1  1999.8  2020.1  2019.7  2015.4  2064.0
2031.2 2030.8  2007.5  2010.1  1999.7  2022.1  2026.6  2064.1  2101.2
2046.4 2026.6  2010.1  2027.6  2022.9  2031.7  2050.6  2106.5  2125.7
2056.6 2036.9  2031.7  2042.9  2044.2  2045.6  2087.3  2125.5  2142.3
C VIOLA PAY 1
1926.3 1930.2  1912.1  1917.5  1922.1  1922.5  1923.6  1914.6  1897.3
1918.8 1911.9  1918.5  1913.6  1914.5  1925.9  1926.5  1906.4  1899.7
1922.2 1920.1  1912.8  1909.8  1905.6  1934.9  1933.5  1920.1  1916.0
1936.4 1936.6  1925.7  1918.1  1904.9  1924.6  1933.4  1934.0  1929.2
1958.2 1968.3  1953.8  1943.0  1944.8  1939.8  1937.2  1936.1  1939.7
1993.2 1998.8  1984.8  1978.7  1978.0  1974.8  1968.5  1946.1  1952.0
2026.0 2019.3  2009.1  2004.4  2003.6  2002.8  1995.1  1983.8  1968.2
2037.0 2031.6  2024.6  2023.3  2024.0  2028.7  2025.1  2044.4  2050.9
2043.0 2040.1  2033.1  2028.6  2029.8  2044.2  2071.5  2091.3  2096.5
2056.8 2056.4  2050.8  2045.3  2045.7  2054.9  2099.9  2136.6  2142.2
2069.2 2073.0  2065.5  2059.1  2056.0  2083.8  2114.6  2146.6  2159.7
C
C PERMEABILITIES
C
C X-DIRECTION PERMEABILITY
C MISENER LIMESTONE PERMEABILITY
```

KX VALUE

0.0	0.0	0.0	0.0	0.0	0.0	0.0	0.0	0.0
0.0	0.0	0.0	0.0	0.0	0.0	0.0	0.0	0.0
0.68	0.68	1.03	1.60	2.21	1.58	1.67	1.48	0.0
0.58	0.84	1.17	2.50	2.42	1.30	1.31	1.53	0.0
1.11	1.61	3.41	4.91	0.66	0.68	0.80	1.20	0.0
1.90	4.99	13.21	4.25	0.80	0.52	0.52	0.94	0.0
3.92	9.35	7.44	1.32	0.56	0.53	0.49	0.60	0.0
7.63	10.61	3.34	0.77	0.65	0.47	0.70	0.69	0.0
11.41	7.04	3.07	0.62	0.68	0.60	0.85	0.73	0.0
6.64	2.06	1.13	0.69	0.77	0.88	0.92	0.0	0.0
7.65	0.85	0.80	0.79	0.74	0.95	0.96	0.0	0.0

C MISENER SANDSTONE LAYER 1 PERMEABILITY

0.0	0.0	10.0	10.0	30.0	30.0	30.0	20.0	30.0
0.0	0.0	10.0	10.0	30.0	45.0	45.0	25.0	35.0
0.0	0.0	10.0	20.0	40.0	50.0	50.0	50.0	40.0
0.0	0.0	10.0	20.0	30.0	40.0	50.0	50.0	40.0
0.0	0.0	15.0	0.0	35.0	60.0	50.0	50.0	40.0
0.0	0.0	20.0	20.0	45.0	60.0	50.0	50.0	40.0
0.0	0.0	20.0	30.0	100.0	70.0	60.0	50.0	40.0
0.0	0.0	20.0	60.0	200.0	60.0	60.0	50.0	40.0
0.0	20.0	20.0	50.0	60.0	60.0	50.0	50.0	40.0
0.0	20.0	20.0	50.0	60.0	50.0	50.0	50.0	40.0
0.0	20.0	20.0	50.0	60.0	50.0	50.0	50.0	40.0

C MISENER SANDSTONE LAYER 2 PERMEABILITY

0.0	0.0	0.0	0.0	0.0	0.0	90.0	0.0	0.0
0.0	0.0	0.0	0.0	0.0	0.0	90.0	70.0	70.0
0.0	0.0	0.0	0.0	0.0	100.0	100.0	100.0	60.0
0.0	0.0	0.0	0.0	0.0	150.0	100.0	100.0	60.0
0.0	0.0	0.0	0.0	70.0	200.0	300.0	100.0	60.0
0.0	0.0	0.0	70.0	100.0	300.0	300.0	100.0	100.0
0.0	0.0	0.0	100.0	400.0	300.0	200.0	300.0	100.0
0.0	0.0	0.0	300.0	1000.0	600.0	500.0	500.0	100.0
0.0	0.0	0.0	300.0	1200.0	900.0	150.0	300.0	100.0
0.0	0.0	0.0	300.0	400.0	300.0	300.0	300.0	100.0
0.0	0.0	0.0	300.0	300.0	300.0	300.0	300.0	100.0

C MOQUOKETA DOLOMITE/"PSEUDO" FERNVALE PERMEABILITY

0.5	0.5	0.5	0.5	0.5	0.5	0.5	0.5	0.5
0.5	0.5	0.5	0.5	0.5	0.5	0.5	0.5	0.5
0.5	0.5	0.5	0.5	0.5	0.5	0.5	0.5	0.5
0.5	0.5	3.3	10.8	11	0.5	0.5	0.5	0.5
0.5	0.5	11.5	13.6	12.1	4.8	0.5	0.5	0.5
0.5	0.5	10.9	9.5	7.8	0.5	0.5	0.5	0.5
0.5	0.5	8.7	6.5	5.1	4.1	0.5	0.5	0.5
0.5	9.1	0.5	0.5	0.5	0.5	0.5	0.5	0.5
0.5	0.5	0.5	0.5	0.5	2.6	0.5	0.5	0.5
0.5	0.5	0.5	0.5	0.5	0.5	0.5	0.5	0.5
0.5	0.5	0.5	0.5	0.5	0.5	0.5	0.5	0.5

C VIOLA PAY 1 PERMEABILITY

2.0	2.0	2.0	2.0	2.0	2.0	2.0	2.0	2.0
2.0	2.0	2.0	2.0	2.0	2.0	2.0	2.0	2.0
2.3	3.2	2.7	2.3	2.4	2.1	1.8	1.9	1.9
2.9	3.5	3.0	2.6	3.0	3.4	2.9	2.7	1.8
3.6	4.2	3.0	2.4	3.5	6.1	2.0	2.1	1.4
2.6	3.2	2.4	2.4	3.2	4.5	5.1	1.4	1.2
1.9	2.2	2.5	3.0	3.0	3.1	3.2	1.3	1.1
2.0	2.4	3.1	3.4	3.4	2.8	2.3	1.7	1.3
2.2	2.9	4.8	6.0	7.1	4.2	3.0	2.4	1.8
2.1	2.7	4.6	6.3	9.7	8.2	5.3	3.1	3.4
2.1	2.2	3.1	4.3	6.6	7.0	5.5	5.5	5.4

KY MULT

```
1.00 KX
VMOD
1  9   1  11   2  3
C MISENER SANDSTONE LAYER 1 Y-DIR PERM
 0.0      0.0    10.0    10.0    10.0    10.0    10.0     5.0     5.0
 0.0      0.0    10.0    10.0    10.0    10.0    10.0     5.0     5.0
 0.0      0.0    10.0    20.0    20.0    40.0    40.0    40.0    40.0
 0.0      0.0    10.0    20.0    30.0    60.0    50.0    40.0    40.0
 0.0      0.0    15.0     0.0    35.0    50.0    50.0    40.0    40.0
 0.0      0.0    20.0    20.0    45.0    50.0    50.0    60.0    40.0
 0.0      0.0    20.0    30.0   300.0    70.0    90.0    50.0    40.0
 0.0      0.0    20.0    60.0   300.0   200.0   150.0    50.0    40.0
 0.0     20.0    20.0    50.0   120.0   120.0    50.0    50.0    40.0
 0.0     20.0    20.0   100.0   120.0    70.0    50.0    50.0    40.0
 0.0     20.0    20.0   100.0   120.0    70.0    50.0    50.0    40.0
C MISENER SANDSTONE LAYER 2 Y-DIR PERM
0.0      0.0     0.0     0.0     0.0     0.0    60.0     0.0     0.0
0.0      0.0     0.0     0.0     0.0     0.0    60.0    70.0   100.0
0.0      0.0     0.0     0.0     0.0    50.0    70.0    70.0   100.0
0.0      0.0     0.0     0.0     0.0    80.0    80.0    70.0    70.0
0.0      0.0     0.0     0.0    40.0    90.0    90.0    70.0    70.0
0.0      0.0     0.0    70.0    90.0    90.0    90.0   100.0   300.0
0.0      0.0     0.0   100.0  1000.0   500.0   200.0   200.0   300.0
0.0      0.0     0.0   300.0  1000.0   900.0   500.0   100.0   300.0
0.0      0.0     0.0   300.0  1000.0   900.0   200.0   300.0   300.0
0.0      0.0     0.0   600.0  1000.0   500.0   300.0   300.0   300.0
0.0      0.0     0.0   600.0   800.0   500.0   300.0   300.0   300.0
KZF MULT
0.10 KX
MOD
C NO CROSSFLOW BETWEEN MISENER SANDSTONE LAYERS WHERE SHALE EXISTS
7  9   1  11   3  3  =0.0
6  6   4  9   3  3  =0.0
C DEFINE CROSSFLOW FROM MISE SAND TO LIME ACCORDING TO KGS MAP
1  9   1  11   2  2  *10.0
4  4   6  6   2  2   =0.0
5  5   5  5   2  2   =0.0
C DEFINE AREAS OF CROSSFLOW WHERE MOQUOKETA IS EXPOSED
1  9   1  11   5  5  *.1
1  9   1  11   4  4  =0.0
7  7   6  6   4  4  =0.0
6  6   6  6   4  4  =0.0
5  5   6  6   4  4  =5.0
4  4   5  5   4  4  =5.0
5  5   5  5   4  4  =1.0
6  6   5  5   4  4  =0.0
7  7   5  5   4  4  =0.0
3  3   7  7   4  4  =1.0
4  4   7  7   4  4  =5.0
5  5   7  7   4  4  =5.0
6  6   7  7   4  4  =5.0
7  7   7  7   4  4  =3.0
6  6   8  8   4  4  =0.0
6  6   9  9   4  4  =5.0
5  5   9  9   4  4  =0.5
C DEFINE AREAS OF FERNVALE CROSSFLOW
4  4   8  8   4  4  =0.1
4  4   9  9   4  4  =0.0
C
C POROSITIES
C
```

```
C MISENER LIMESTONE POROSITY
POR VALUE
 0.0     0.0     0.0     0.0     0.0     0.0     0.0     0.0     0.0
 0.0     0.0     0.0     0.0     0.0     0.0     0.0     0.0     0.0
 0.0     0.0     0.0     0.0     0.0     0.0     0.0     0.0     0.0
 0.0467  0.0     0.12    0.12    0.1176  0.0     0.0     0.0     0.0
 0.0788  0.0     0.1347  0.1528  0.0530  0.0     0.0     0.0     0.0
 0.1057  0.1536  0.2021  0.1456  0.0628  0.0     0.0     0.0     0.0
 0.1416  0.1849  0.1735  0.0874  0.0448  0.0     0.0     0.0     0.0
 0.1748  0.1912  0.1336  0.0604  0.0     0.0     0.0     0.0     0.0
 0.1948  0.1708  0.1294  0.0498  0.0547  0.0485  0.0     0.0     0.0
 0.1679  0.1095  0.0799  0.0555  0.0603  0.0672  0.0697  0.0     0.0
 0.1749  0.0653  0.0628  0.0617  0.0584  0.0713  0.0714  0.0     0.0
C MISENER SANDSTONE LAYER 1 POROSITY
0.0     0.0     0.10    0.10    0.12    0.14    0.15    0.15    0.15
0.0     0.0     0.10    0.10    0.1230  0.1412  0.1537  0.1591  0.1621
0.0     0.0     0.10    0.10    0.1230  0.1412  0.1537  0.1591  0.1621
0.0     0.0     0.10    0.10    0.1060  0.12    0.1275  0.1527  0.1490
0.0     0.0     0.0993  0.10    0.10    0.12    0.120   0.1407  0.1360
0.0     0.1345  0.1242  0.10    0.0991  0.12    0.1318  0.1209  0.12
0.0     0.1432  0.1431  0.1134  0.1001  0.10    0.09    0.0974  0.10
0.0     0.1274  0.1094  0.1066  0.1121  0.10    0.09    0.0898  0.0957
0.124   0.1198  0.0992  0.0938  0.1169  0.0957  0.0852  0.0885  0.0888
0.101   0.1203  0.1259  0.1270  0.1212  0.1071  0.1013  0.0973  0.0900
0.111   0.1130  0.1214  0.1242  0.1206  0.1122  0.0977  0.0946  0.0900
C MISENER SANDSTONE LAYER 2 POROSITY
0.0     0.0     0.0     0.0     0.0     0.0     0.10    0.10    0.10
0.0     0.0     0.0     0.0     0.0     0.0     0.1081  0.1006  0.1004
0.0     0.0     0.0     0.0     0.0     0.0     0.1081  0.1006  0.1004
0.0     0.0     0.0     0.0     0.0     0.1194  0.11    0.11    0.1032
0.0     0.0     0.0     0.08    0.09    0.1175  0.1215  0.1295  0.1152
0.0     0.0     0.0     0.08    0.09    0.1183  0.1336  0.1374  0.1225
0.0     0.0     0.0     0.08    0.09    0.11    0.11    0.1208  0.1207
0.0     0.0     0.0     0.1066  0.11    0.11    0.11    0.1085  0.1117
0.0     0.0     0.0     0.0905  0.1071  0.1007  0.1013  0.1071  0.1116
0.0     0.0897  0.0907  0.0949  0.1075  0.1054  0.1106  0.1156  0.1089
0.0     0.0914  0.0934  0.0978  0.1028  0.1037  0.1019  0.1006  0.1000
C MOQUOKETA DOLOMITE/"PSEUDO" FERNVALE  POROSITY
  .01     .01     .01     .01     .01     .01     .01     .01     .01
  .01     .01     .01     .01     .01     .01     .01     .01     .01
  .01     .01     .01     .01     .01     .01     .01     .01     .01
  .01     .01    0.033   0.108   0.11     .01     .01     .01     .01
  .01     .01    0.115   0.136   0.121   0.048    .01     .01     .01
  .01     .01    0.109   0.095   0.078    .01     .01     .01     .01
  .01     .01    0.087   0.065   0.051   0.041    .01     .01     .01
  .01    0.091    .01     .01     .01     .01     .01     .01     .01
  .01     .01     .01     .01     .01    0.026    .01     .01     .01
  .01     .01     .01     .01     .01     .01     .01     .01     .01
  .01     .01     .01     .01     .01     .01     .01     .01     .01
C VIOLA PAY 1 POROSITY
0.085   0.103   0.094   0.085   0.089   0.081   0.074   0.076   0.075
0.085   0.103   0.094   0.085   0.089   0.081   0.074   0.076   0.075
0.085   0.103   0.094   0.085   0.089   0.081   0.074   0.076   0.075
0.097   0.107   0.100   0.093   0.100   0.106   0.098   0.094   0.074
0.109   0.117   0.099   0.089   0.108   0.136   0.078   0.081   0.059
0.093   0.103   0.088   0.088   0.103   0.120   0.127   0.061   0.051
0.075   0.083   0.090   0.099   0.100   0.102   0.103   0.058   0.048
0.079   0.089   0.101   0.106   0.106   0.096   0.085   0.069   0.057
0.083   0.097   0.124   0.135   0.144   0.117   0.099   0.087   0.073
0.080   0.094   0.122   0.138   0.160   0.151   0.129   0.101   0.106
0.080   0.083   0.101   0.118   0.140   0.143   0.131   0.131   0.130
```

```
C
C ========= FRACTURE DIMENSIONS ==========
C
C FRACTURE POROSITY
PORF ZVAR
.005
0.0
0.0
.005
.005
C FRACTURE PERMEABILITY
KXFEFF ZVAR
25.
0.0
0.0
1000.
1000.
VMOD
1  5   1  11  1  1
 0    0    0    0    0
 0    0    0    0    0
 0    0   15   10   10
30    0   35   30   10
30    0   20   30   10
30   20   10   15   10
40   10   20   20   10
25   35   70   50   40
25   80  100   50   10
40  100   60   20   10
50   45  100   40   10
KYFEFF MULT
1.0   KXFEFF
KZFEFF MULT
1.0   KXFEFF
MOD
1  9   1  11   4  4   =0.0
7  7   6  6   4  4  =0.0
6  6   6  6   4  4  =0.0
5  5   6  6   4  4  =500.0
5  5   5  5   4  4  =500.0
6  6   5  5   4  4  =0.0
7  7   5  5   4  4  =0.0
4  4   7  7   4  4  =500.0
5  5   7  7   4  4  =500.0
6  6   7  7   4  4  =500.0
7  7   7  7   4  4  =500.0
6  6   8  8   4  4  =0.0
6  6   9  9   4  4  =1000.0
5  5   9  9   4  4  =100.0
C DEFINE AREAS OF FERNVALE CROSSFLOW
4  4   5  5   4  4  =200.0
4  4   8  8   4  4  =0.0
4  4   9  9   4  4  =0.0
C
C MATRIX BLOCK DIMENSIONS
LX ZVAR
1320.
2640
2640
2640.
50.
```

```
VMOD
1  9    3  11    5  5
 2778     1558     2134     1350     3294     4395     1108      665       75
 2888      197       81       69       69     2370     1360      498       76
  529      308       76       53      223     1172     1049      111      204
 5138      288      219      111      198      162      124      117      150
 6489      695      593       72       56       50       74       58      147
 1070     1204      546      121      126      104       84      111      182
  909     1029      789      123      134      105      110      115      187
  720      786     1058      173      122      117      147      153      185
  587      579      944      141      190      153      169      196      212
LY MULT
1.0 LX
LZ CON
20.0
C ======== ARRAYS TO DEFINE ROCK TYPE ==========
C
ISAT ZVAR
C MISENER LIMESTONE
     1
C MISENER SANDSTONE LAYER 1
     2
C MISENER SANDSTONE LAYER 2
     2
C MOQUOKETA DOLOMITE
     1
C VIOLA PAY 2
     1
C
C ======== FAULT DATA ========
C
FAULTS
FY  7  9  108.8  *0.0
FX  9  7   47.4  *0.6
FX  9  8   45.1  *0.6
FY  9  8   46.0  *0.6
FX  7  10   22.2  *0.8
FX  7  11   48.5  *0.6
C
C ASSIGN NO FLOW BOUNDARIES IN THE MISENER LIMESTONE
C
OVER   TX
4  4   5  5   1  1  *0.2
2  2   6  6   1  1  *0.3
3  3   6  6   1  1  *0.6
5  5   5  5   1  1  *0.5
2  2   7  7   1  1  =0.0
3  3   7  7   1  1  *0.6
3  3   10 10   1  1  *0.2
OVER   TXF
4  4   5  5   1  1  *0.2
2  2   6  6   1  1  *0.6
5  5   5  5   1  1  *0.5
2  2   7  7   1  1  =0.0
3  3   10 10   1  1  *0.2
OVER   TY
3  3   5  5   1  1  *0.4
3  3   6  6   1  1  *0.5
2  2   7  7   1  1  =0.0
3  3   10 10   1  1  *0.2
OVER  TYF
```

```
3  3   5  5   1  1  *0.4
4  4   6  6   1  1  *0.5
1  2   7  7   1  1  =0.0
3  3   10  10   1  1  *0.2
C
C ASSIGN NO FLOW BOUNDARIES IN THE MISENER SANDSTONE
C
OVER TX
8  8   6  6   2  3  *0.5
5  5   5  5   2  3  =0.0
5  5   4  4   2  3  *0.1
5  5   3  3   2  3  =0.0
6  6   5  6   2  3  *0.3
OVER TY
4  4   6  6   2  3  =0.0
8  8   6  6   2  3  *0.5
6  6   7  7   2  3  *0.3
7  7   7  7   2  3  *0.1
C
C ====== AQUIFER INFLUX DATA =========
C
INFLUX 1
WTR   CT
NBINF      BINF      TC     VISC
20        6000.    8E-04    0.7
IINF     JINF     KINF    SINF
WINDOW
1  9   11  11    5  5  YCALC
ENDAQ
C DIMENSIONLESS TIMES AND PRESSURED FOR RD = 2.5
TD     PD
.40   .565
.42   .576
.44   .587
.46   .598
.48   .608
.50   .618
.52   .682
.54   .638
.56   .647
.58   .657
.60   .666
.65   .688
.70   .710
.75   .731
.80   .752
.85   .772
.90   .792
.95   .812
1.0   .832
2.0   1.215
3.0   1.596
4.0   1.977
5.0   2.358
END
```

```
C
C This in the recurrent data file input into the VIP simulator
C that resulted in the history match of the first two years
C of primary production in the Zenith Field.

NOLIST
DIM NWMAX NPRFMX   NPRFTOT
     154      8      1232
IMPLICIT
RESTART 0 3
TITLE1
      Misener Sandstone and Limestone
TITLE2
        Primary Production Simulation
START
BLITZ
DT -1
ITNLIM 1 10 250 .25 .25 .25
C
C RUN CONTROL
C
OUTPUT TSSDAT
WPLOT  TIME
C
C INPUT ALL WELLS PRODUCING BEFORE JANUARY 1940 BECAUSE SOME OF THE
C WELLS WERE COMPLETED INTO THE VIOLA/MOQUOKETA TOP.  I WILL PERFORATE
C THE MOQUOKETA FOR A COUPLE OF FEET INTO IT, BUT I WILL LET THE
C TRANSMISSIBILITY TAKE CARE OF THE COMPLETIONS INTO THE FERNVALE
C
WELL     N   NAME   I   J
          1  NE11   5   5
          2  NE11   5   5
          3  NE11   5   5
          4  NE11   5   5
          5  NW11   4   5
          6  NW11   4   5
          7  NW11   4   5
          8  NW11   4   5
          9  NW11   4   5
         10  SW11   4   6
         11  SW11   4   6
         12  SW11   4   6
         13  SW11   4   6
         14  SW11   4   6
         15  SW11   4   6
         16  SW11   4   6
         17  SW11   4   6
         18  SE11   5   6
         19  SE11   5   6
         20  SE11   5   6
         21  SE11   5   6
         22  SE11   5   6
         23  SE11   5   6
         24  SE11   5   6
         25  SE11   5   6
         26  SE11   5   6
         27  NE12   7   5
         28  NW12   6   5
         29  SW12   6   6
         30  SW12   6   6
         31  SW12   6   6
```

32	SW12	6	6
33	SW12	6	6
34	SW12	6	6
35	SW12	6	6
36	SW12	6	6
37	SE12	7	6
38	SE12	7	6
39	NE13	7	7
40	NE13	7	7
41	NE13	7	7
42	NE13	7	7
43	NE13	7	7
44	NE13	7	7
45	NE13	7	7
46	NE13	7	7
47	NE13	7	7
48	NE13	7	7
49	NE13	7	7
50	NW13	6	7
51	NW13	6	7
52	NW13	6	7
53	NW13	6	7
54	NW13	6	7
55	NW13	6	7
56	NW13	6	7
57	NW13	6	7
58	NW13	6	7
59	NW13	6	7
60	NW13	6	7
61	SW13	6	8
62	SW13	6	8
63	SW13	6	8
64	SW13	6	8
65	SW13	6	8
66	SW13	6	8
67	SW13	6	8
68	SW13	6	8
69	SW13	6	8
70	SW13	6	8
71	SW13	6	8
72	SW13	6	8
73	SW13	6	8
74	SW13	6	8
75	SW13	6	8
76	SW13	6	8
77	SE13	7	8
78	SE13	7	8
79	SE13	7	8
80	SE13	7	8
81	SE13	7	8
82	SE13	7	8
83	SE13	7	8
84	SE13	7	8
85	SE13	7	8
86	SE13	7	8
87	NE14	5	7
88	NE14	5	7
89	NE14	5	7
90	NE14	5	7
91	NE14	5	7
92	NE14	5	7

93	NE14	5	7
94	NE14	5	7
95	NE14	5	7
96	NE14	5	7
97	NE14	5	7
98	NE14	5	7
99	NW14	4	7
100	NW14	4	7
101	NW14	4	7
102	NW14	4	7
103	NW14	4	7
104	NW14	4	7
105	NW14	4	7
106	SW14	4	8
107	SW14	4	8
108	SW14	4	8
109	SW14	4	8
110	SW14	4	8
111	SW14	4	8
112	SW14	4	8
113	SW14	4	8
114	SE14	5	8
115	SE14	5	8
116	SE14	5	8
117	SE14	5	8
118	SE14	5	8
119	SE14	5	8
120	SE14	5	8
121	SE14	5	8
122	SE14	5	8
123	SE14	5	8
124	SE14	5	8
125	SE14	5	8
126	SE14	5	8
127	SE14	5	8
128	SE14	5	8
129	SE14	5	8
130	SE15	3	8
131	NE23	5	9
132	NE23	5	9
133	NE23	5	9
134	NE23	5	9
135	NE23	5	9
136	NE23	5	9
137	NE23	5	9
138	NE23	5	9
139	NE23	5	9
140	NE23	5	9
141	NE23	5	9
142	NW23	4	9
143	NW23	4	9
144	NW23	4	9
145	NW23	4	9
146	NW23	4	9
147	NW23	4	9
148	NW23	4	9
149	NW24	6	9
150	NW24	6	9
151	NW24	6	9
152	NW24	6	9
153	NW24	6	9

```
       154  NW24   6   9
       PROD O 1 -154
FPERF
WELL   L   HTOP  HBOT
 1     1    0     1
 X     2    0     1
 X     3    0     1
 2     1    0     1
 X     2    0     1
 X     3    0     1
 3     1    0     1
 X     2    0     1
 X     3    0     1
 X     4    0    .09
 4     1    0     1
 X     2    0     1
 X     3    0     1
 X     4    0     1
 5     1    0     1
 X     2    0     1
 X     3    0     1
 X     4    0    .15
 6     1    0     1
 X     2    0     1
 X     3    0     1
 7     1    0     1
 X     2    0     1
 X     3    0     1
 8     1    0     1
 X     2    0     1
 X     3    0     1
 X     4    0    .27
 9     1    0     1
 X     2    0     1
 X     3    0     1
 X     4    0     1
10     1    0     1
 X     2    0     1
 X     3    0     1
 X     4    0    .06
11     1    0     1
 X     2    0     1
 X     3    0     1
 X     4    0    .16
12     1    0     1
 X     2    0     1
 X     3    0     1
 X     4    0    .04
13     1    0     1
 X     2    0     1
 X     3    0     1
 X     4    0    .04
14     1    0     1
 X     2    0     1
 X     3    0     1
15     1    0     1
 X     2    0     1
 X     3    0     1
16     1    0     1
 X     2    0     1
 X     3    0     1
```

X	4	0	.08
17	1	0	1
X	2	0	1
X	3	0	1
X	4	0	1
18	1	0	1
X	2	0	1
X	3	0	1
X	4	0	.47
19	1	0	1
X	2	0	1
X	3	0	1
X	4	0	.05
20	1	0	1
X	2	0	1
X	3	0	1
21	1	0	1
X	2	0	1
X	3	0	1
X	4	0	.05
22	1	0	1
X	2	0	1
X	3	0	1
X	4	0	.03
23	1	0	1
X	2	0	1
X	3	0	1
X	4	0	.05
24	1	0	1
X	2	0	1
X	3	0	1
X	4	0	.05
25	1	0	1
X	2	0	1
X	3	0	1
X	4	0	.05
26	1	0	1
X	2	0	1
X	3	0	1
27	1	0	1
X	2	0	1
X	3	0	1
28	1	0	1
X	2	0	1
X	3	0	1
X	4	0	.04
29	1	0	1
X	2	0	1
X	3	0	1
30	1	0	1
X	2	0	1
X	3	0	1
31	1	0	1
X	2	0	1
X	3	0	1
32	1	0	1
X	2	0	1
X	3	0	1
33	1	0	1
X	2	0	1
X	3	0	1

```
      34     1      0       1
       X     2      0       1
       X     3      0       1
      35     1      0       1
       X     2      0       1
       X     3      0       1
      36     1      0       1
       X     2      0       1
       X     3      0       1
      37     1      0       1
       X     2      0       1
       X     3      0       1
      38     1      0       1
       X     2      0       1
       X     3      0       1
      39     1      0       1
       X     2      0       1
       X     3      0       1
      40     1      0       1
       X     2      0       1
       X     3      0       1
      41     1      0       1
       X     2      0       1
       X     3      0       1
      42     1      0       1
       X     2      0       1
       X     3      0       1
      43     1      0       1
       X     2      0       1
       X     3      0       1
      44     1      0       1
       X     2      0       1
       X     3      0       1
      45     1      0       1
       X     2      0       1
       X     3      0       1
      46     1      0       1
       X     2      0       1
       X     3      0       1
      47     1      0       1
       X     2      0       1
       X     3      0       1
      48     1      0       1
       X     2      0       1
       X     3      0       1
      49     1      0       1
       X     2      0       1
       X     3      0       1
      50     1      0       1
       X     2      0       1
       X     3      0       1
       X     4      0      .09
      51     1      0       1
       X     2      0       1
       X     3      0       1
      52     1      0       1
       X     2      0       1
       X     3      0       1
      53     1      0       1
       X     2      0       1
       X     3      0       1
```

X	4	0	.09
54	1	0	1
X	2	0	1
X	3	0	1
55	1	0	1
X	2	0	1
X	3	0	1
56	1	0	1
X	2	0	1
X	3	0	1
57	1	0	1
X	2	0	1
X	3	0	1
X	4	0	.045
58	1	0	1
X	2	0	1
X	3	0	1
X	4	0	.045
59	1	0	1
X	2	0	1
X	3	0	1
X	4	0	.02
60	1	0	1
X	2	0	1
X	3	0	1
X	4	0	.045
61	1	0	1
X	2	0	1
X	3	0	1
62	1	0	1
X	2	0	1
X	3	0	1
63	1	0	1
X	2	0	1
X	3	0	1
64	1	0	1
X	2	0	1
X	3	0	1
65	1	0	1
X	2	0	1
X	3	0	1
66	1	0	1
X	2	0	1
X	3	0	1
67	1	0	1
X	2	0	1
X	3	0	1
68	1	0	1
X	2	0	1
X	3	0	1
69	1	0	1
X	2	0	1
X	3	0	1
70	1	0	1
X	2	0	1
X	3	0	1
71	1	0	1
X	2	0	1
X	3	0	1
72	1	0	1
X	2	0	1

```
   X      3      0       1
  73      1      0       1
   X      2      0       1
   X      3      0       1
  74      1      0       1
   X      2      0       1
   X      3      0       1
  75      1      0       1
   X      2      0       1
   X      3      0       1
  76      1      0       1
   X      2      0       1
   X      3      0       1
  77      1      0       1
   X      2      0       1
   X      3      0       1
  78      1      0       1
   X      2      0       1
   X      3      0       1
  79      1      0       1
   X      2      0       1
   X      3      0       1
  80      1      0       1
   X      2      0       1
   X      3      0       1
  81      1      0       1
   X      2      0       1
   X      3      0       1
  82      1      0       1
   X      2      0       1
   X      3      0       1
  83      1      0       1
   X      2      0       1
   X      3      0       1
  84      1      0       1
   X      2      0       1
   X      3      0       1
  85      1      0       1
   X      2      0       1
   X      3      0       1
  86      1      0       1
   X      2      0       1
   X      3      0       1
  87      1      0       1
   X      2      0       1
   X      3      0       1
   X      4      0     .32
  88      1      0       1
   X      2      0       1
   X      3      0       1
  89      1      0       1
   X      2      0       1
   X      3      0       1
   X      4      0     .23
  90      1      0       1
   X      2      0       1
   X      3      0       1
   X      4      0     .09
  91      1      0       1
   X      2      0       1
   X      3      0       1
```

X	4	0	.09
92	1	0	1
X	2	0	1
X	3	0	1
X	4	0	.09
93	1	0	1
X	2	0	1
X	3	0	1
X	4	0	.09
94	1	0	1
X	2	0	1
X	3	0	1
X	4	0	.05
95	1	0	1
X	2	0	1
X	3	0	1
96	1	0	1
X	2	0	1
X	3	0	1
97	1	0	1
X	2	0	1
X	3	0	1
X	4	0	.07
98	1	0	1
X	2	0	1
X	3	0	1
99	1	0	1
X	2	0	1
X	3	0	1
X	4	0	.21
100	1	0	1
X	2	0	1
X	3	0	1
X	4	0	.21
101	1	0	1
X	2	0	1
X	3	0	1
X	4	0	.17
102	1	0	1
X	2	0	1
X	3	0	1
X	4	0	.04
103	1	0	1
X	2	0	1
X	3	0	1
X	4	0	.08
104	1	0	1
X	2	0	1
X	3	0	1
X	4	0	.04
105	1	0	1
X	2	0	1
X	3	0	1
X	4	0	1
106	1	0	1
X	2	0	1
X	3	0	1
107	1	0	1
X	2	0	1
X	3	0	1
108	1	0	1

X	2	0	1
X	3	0	1
109	1	0	1
X	2	0	1
X	3	0	1
110	1	0	1
X	2	0	1
X	3	0	1
111	1	0	1
X	2	0	1
X	3	0	1
112	1	0	1
X	2	0	1
X	3	0	1
113	1	0	1
X	2	0	1
X	3	0	1
114	1	0	1
X	2	0	1
X	3	0	1
115	1	0	1
X	2	0	1
X	3	0	1
116	1	0	1
X	2	0	1
X	3	0	1
117	1	0	1
X	2	0	1
X	3	0	1
118	1	0	1
X	2	0	1
X	3	0	1
119	1	0	1
X	2	0	1
X	3	0	1
120	1	0	1
X	2	0	1
X	3	0	1
121	1	0	1
X	2	0	1
X	3	0	1
122	1	0	1
X	2	0	1
X	3	0	1
123	1	0	1
X	2	0	1
X	3	0	1
124	1	0	1
X	2	0	1
X	3	0	1
125	1	0	1
X	2	0	1
X	3	0	1
126	1	0	1
X	2	0	1
X	3	0	1
127	1	0	1
X	2	0	1
X	3	0	1
128	1	0	1
X	2	0	1

X	3	0	1
129	1	0	1
X	2	0	1
X	3	0	1
130	1	0	1
X	2	0	1
X	3	0	1
131	1	0	1
X	2	0	1
X	3	0	1
132	1	0	1
X	2	0	1
X	3	0	1
133	1	0	1
X	2	0	1
X	3	0	1
134	1	0	1
X	2	0	1
X	3	0	1
135	1	0	1
X	2	0	1
X	3	0	1
136	1	0	1
X	2	0	1
X	3	0	1
137	1	0	1
X	2	0	1
X	3	0	1
138	1	0	1
X	2	0	1
X	3	0	1
139	1	0	1
X	2	0	1
X	3	0	1
140	1	0	1
X	2	0	1
X	3	0	1
141	1	0	1
X	2	0	1
X	3	0	1
142	1	0	1
X	2	0	1
X	3	0	1
143	1	0	1
X	2	0	1
X	3	0	1
144	1	0	1
X	2	0	1
X	3	0	1
145	1	0	1
X	2	0	1
X	3	0	1
146	1	0	1
X	2	0	1
X	3	0	1
147	1	0	1
X	2	0	1
X	3	0	1
148	1	0	1
X	2	0	1
X	3	0	1

```
149     1     0     1
 X      2     0     1
 X      3     0     1
150     1     0     1
 X      2     0     1
 X      3     0     1
151     1     0     1
 X      2     0     1
 X      3     0     1
152     1     0     1
 X      2     0     1
 X      3     0     1
153     1     0     1
 X      2     0     1
 X      3     0     1
154     1     0     1
 X      2     0     1
 X      3     0     1
C
C WELL INDEXES FOR EACH WELL
C
RFLOW 1 -154
154*0.5
154*523.0
154*0.0
C
C BHP CONSTRAINTS
C
BHP 1 -154
154*100.0
154*1900.0
C
C ------ DECEMBER 1937 TIME BLOCK ------
DATE 1 12 1937
QMAX 142
     41.6
DATE 1 1 1938
QMAX  142 -145
   4*20.6
DATE 1 2 1938
C
C ------- MARCH 1938 TIME BLOCK --------
C
DATE 1 3 1938
C
C --------- APRIL 1938 TIME BLOCK ------------
DATE 1 4 1938
QMAX 99 -100  106 -110   114 -117
2*14.8  5*18.3  4*33.2
C
C  ---------- MAY 1938 TIME BLOCK -----------
DATE 1 5 1938
QMAX 87 -88
2*27.2
WMAP TNEXT
DATE 15  5 1938
C
C  ---------- JUNE 1938 TIME BLOCK -----------
C
DATE 1 6 1938
QMAX 149 -150
```

```
2*24.7
C
C --------- JULY 1938 TIME BLOCK ----------
C
DATE 1 7 1938
QMAX 1 10 -12 87 -93 99 -103 106 -111
20.9  3*14.2   7*8.3  5*12.4  6*22.0
QMAX 114 -125 142 -146  149 -153
  12*24.4  5*26.6  5*15.0
C
C --------- AUGUST 1938 TIME BLOCK ----------
C
DATE 1 8 1938
QMAX  5
31.1
C
C --------- SEPTEMBER 1938 TIME BLOCK ----------
C
DATE 1 9 1938
QMAX 130
13.9
C
C -------- OCTOBER 1938 TIME BLOCK ------------
C
DATE 1 10 1938
C
C ----------- NOVEMBER 1938 TIME BLOCK ---------
C
DATE 1 11 1938
QMAX 77 -78
2*23.9
C
C --------- DECEMBER 1938 TIME BLOCK
C
DATE 1 12 1938
QMAX  50  61 -76
13.2  16*23
C
C ---------- JANUARY 1939 TIME BLOCK ---------
C
DATE 1 1 1939
QMAX 1 -4 5 -9 10 -17 50 -60 61 -76  77 -86 87 -98 99 -105 106 -113
4*21.0  5*28.4 8*13.4 11*16.5 16*24.3 10*17.4 12*15.5 7*21.2 8*29.3
QMAX  114 -129  130  142 -148  149 -154
16*29.0  13.9  7*25.8  6*20.1
C
C ----------- FEBRUARY 1939 TIME BLOCK -----------
C
DATE 1 2 1939
QMAX  39 -49
11*22.8
C
C --------- MARCH 1939 TIME BLOCK ---------
C
DATE 1 3 1939
QMAX  18 -26  131 -141
 9*20.2  11*34.0
C
C --------- APRIL 1939 TIME BLOCK ----------
C
DATE 1 4 1939
```

```
C
C ----------  MAY 1939 TIME BLOCK ----------
C
DATE 1 5 1939
C
C ----------JUNE 1939 TIME BLOCK ----------
DATE 1 6 1939
QMAX  28  29 -36
35.5     8*8.5
C
WMAP  TNEXT
DATE  15  6  1939
C ---------  JULY 1939 TIME BLOCK ------------
C
DATE 1 7 1939
QMAX  37 -38
2*20.2
C
C --------  AUGUST 1939 TIME BLOCK  -----------
C
DATE 1 8 1939
C
C -------- SEPTEMBER 1939 TIME BLOCK ----------
C
DATE 1 9 1939
C
C -------- OCTOBER 1939 TIME BLOCK ----------
C
DATE 1 10 1939
C
C -------- NOVEMBER 1939 TIME BLOCK ----------
C
DATE 1 11 1939
QMAX  27
6.8
C
C -------- DECEMBER 1939 TIME BLOCK ----------
C
DATE 1 12 1939
QMAX  18 -26  39 -49  131 -141
31*0.0
WMAP TNEXT
C
C ----------- JANUARY 1940 TIME BLOCK ------------
C
DATE 15 1 1940
C
C DEFINE SEPARATOR CONDITIONS
C
SEPARATOR 1
STAGE   VFRAC VDEST LFRAC LDEST
  1       1.   VENT   1.    OIL
DLIQ  MWL
.9622 200
KVALUES
COMP  STAGE 1
1     91.14
2     .0055
C WMAP  TNEXT
DATE 15 2 1940
STOP
```

```
END
```